博士學位論文

Synthesis, Structures, and Properties of Mono- and Bi-nuclear Metals (Cu^{2+}, Ni^{2+}, Mn^{2+}, and Ln^{3+}) Complexes with 22-Membered Phenol-Based N_4O_2 Compartmental Macrocyclic Ligand

Department of Chemistry
Graduate School
Cheju National University

Chung-Hun Han

December, 2004

22-원 페놀 바탕 N_4O_2 칸막이형 거대고리 리간드의 일핵과 이핵 (Cu^{2+}, Ni^{2+}, Mn^{2+}, Ln^{3+}) 착물들의 합성, 구조 및 물성 연구

지도교수 : 변 종 철

한 충 훈

이 논문을 이학 박사학위 논문으로 제출함.

2004년 12월

한충훈의 이학 박사학위 논문을 인준함.

심사위원장 _____

위 원 _____

위 원 _____

위 원 _____

위 원 _____

제주대학교 대학원

2004년 12월

Synthesis, Structures, and Properties of Mono- and Bi-nuclear Metals (Cu^{2+}, Ni^{2+}, Mn^{2+}, and Ln^{3+}) Complexes with 22-Membered Phenol-Based N_4O_2 Compartmental Macrocyclic Ligand

Chung-Hun Han
(Supervised by professor Jong-Chul Byun)

A thesis submitted in partial fulfillment of the requirement for the degree of Doctor of Science.

2004. 12. .

This thesis has been examined and approved.

Date Approved :

Department of Chemistry
GRADUATE SCHOOL
CHEJU NATIONAL UNIVERSITY

Contents

List of Tables

List of Figures

Abstract

The 22-membered phenol-based N_4O_2 compartmental macrocycle ligand H_2[22]-HMTADO {5,5,11,17,17,23-hexamethyl-3,7,15,19-tetraazatricyclo[19,3,1,$1^{9,13}$] -hexacosa-1(25),2,7,9,11,13(26),14,19,21,23-decane-25,26-diol} · $2HClO_4$ derived from the [2+2] cyclic condensation of 2,6-diformyl-*p*-cresol and 2,2-dimethyl -1,3-propanediamine with $HClO_4$. The macrocycle ligand has relatively high thermal stability. Binuclear {Cu(II), Ni(II), and Mn(II)} and mononuclear {Ni(II), Pr(III), Sm(III), Gd(III), and Dy(III)} complexes with [2+2] symmetrical N_4O_2 compartmental macrocyclic ligand containing bridging phenolic oxygen atoms was synthesized by condensation of 2,6-diformyl-*p*-cresol and 2-dimethyl-1,3-propandiamine in the metal ions.

The reaction of $[Cu_2([22]\text{-HMTADO})(OH_2)]Cl_2 \cdot H_2O$ with L_a (ClO_4^-, CN^-, NCS^-, N_3^-, NO_3^-, NO_2^-, Br^-, and $S_2O_3^{2-}$) ligands in aqueous solution formed a new $[Cu_2([22]\text{-HMTADO})(OClO_3)(OH_2)]ClO_4 \cdot 2H_2O$, $[Cu_2([22]\text{-HMTADO})(CN)_2] \cdot 0.5H_2O$, $[Cu_2([22]\text{-HMTADO})(NCS)(OH_2)]NCS \cdot 2H_2O$, $[Cu_2([22]\text{-HMTADO})(N_3)(OH_2)]N_3 \cdot H_2O$, $[Cu_2([22]\text{-HMTADO})ONO_2]NO_3 \cdot 4H_2O$, $[Cu_2([22]\text{-HMTADO})NO_2]NO_2 \cdot 2H_2O$, $[Cu_2([22]\text{-HMTADO})]Br_2 \cdot 1.5H_2O$, and $[Cu_2([22]\text{-HMTADO})S_2O_3] \cdot 5H_2O$ complexes.

The reaction of $[Ni_2([22]\text{-HMTADO})(OH_2)_2]Cl_2 \cdot H_2O$ with L_a (ClO_4^-, CN^-, NCS^-, N_3^-, NO_3^-, NO_2^-, Br^-, and $S_2O_3^{2-}$) ligands in aqueous solution formed a new $[Ni_2([22]\text{-HMTADO})(OH_2)_2](ClO_4)_2 \cdot H_2O$, $[Ni_2([22]\text{-HMTADO})(CN)_2] \cdot 0.5H_2O$, $[Ni_2([22]\text{-HMTADO})(NCS)_2(OH_2)] \cdot 2H_2O$, $[Ni_2([22]\text{-HMTADO})(N_3)_2$

-(OH_2)], [Ni_2([22]-HMTADO)(ONO_2)(OH_2)$_2$]NO_3 · 3H_2O, [Ni_2([22]-HMTADO) -NO_2]NO_2 · H_2O, [Ni_2([22]-HMTADO)]Br_2 · 2H_2O, and [Ni_2([22]-HMTADO) (μ-S_2O_3] complexes. The mononuclear Ni(II) complex, [Ni(H_2[22]-HMTADO) -($OHCH_3$)$_2$](ClO_4)$_2$, was synthesized by condensation of 2,6-diformyl-*p*-cresol and 2-dimethyl-1,3-propandiamine in nickel perchlorate hexahydrate. The reaction of [Ni(H_2[22]-HMTADO)($OHCH_3$)$_2$](ClO_4)$_2$ with L_a (NCS^- and N_3^-) ligands in aqueous solution formed a new [Ni(H_2[22]-HMTADO)(NCS)$_2$] · H_2O and Ni(H_2[22]-HMTADO)(N_3)(OH_2)]ClO_4 · H_2O complexes.

The binonuclear Mn(II) complex, [Mn_2([22]-HMTADO)Cl_2] · H_2O, was synthesized by condensation of 2,6-diformyl-*p*-cresol and 2-dimethyl-1,3-propandiamine in manganese acetate tetrahydrate.

The mononuclear lanthanide complexes, [Pr(H_2[22]-HMTADO)O_2NO](NO_3)$_2$ · 2H_2O, [Sm(H_2[22]-HMTADO)O_2NO](NO_3)$_2$ · 2H_2O, [Gd(H_2[22]-HMTADO)O_2NO] (NO_3)$_2$ · 2H_2O, and [Dy(H_2[22]-HMTADO)O_2NO](NO_3)$_2$ · H_2O, with [2+2] symmetrical N_4O_2 compartmental macrocyclic ligand containing bridging phenolic oxygen atoms was synthesized by condensation of 2,6-diformyl-*p* -cresol and 2-dimethyl-1,3-propandiamine in the lathanide ions.

These complexes have been characterized by a combination of elemental analysis, conductivity, IR and Vis spectroscopy, mass spectrometry, thermogravimetry, and X-ray crystallography. The crystal structures of eight complexes were determined by XRD ; (1) Octahedral-Octahedral environment : [Cu_2([22]-HMTADO)(OH_2)$_4$]Cl_2 . 10H_2O, [Cu_2([22]-HMTADO)(OH_2)$_4$]Br_2 · 10H_2O, [Ni_2([22]-HMTADO)(OH_2)$_4$](ClO_4)$_2$ · 3H_2O, [Ni_2([22]-HMTADO)(OH_2)$_4$]Br_2 · 10H_2O, (2) Octahedral-Square pyramidal environment : [Ni_2([22]-HMTADO)(N_3)$_2$(OH_2)], (3)

trans-Square pyramidal-Square pyramidal environment : $[Cu_2([22]\text{-HMTADO})(OClO_3)(OH_2)]ClO_4 \cdot 2CH_3OH$, (4) *cis*-Square pyramidal-Square pyramidal environment : $[Ni_2([22]\text{-HMTADO})(\mu\text{-}S_2O_3)]$, (5) Octahedral environment : $[Ni(H_2[22]\text{-HMTADO})\text{-}(OHCH_3)_2](ClO_4)_2$.

In the crystals of $[Ni_2([22]\text{-HMTADO})(N_3)_2(OH_2)]$, the two azido groups coordinated to the nickel centers are situated trans to each other with respect to the mean $\{NiN_2O_2\}$ plane. The N_3 ligand keep their linearity, N-N-N bond angle is 179.1(5)°, whereas the Ni(1)-N(5)-N(6) linkage is slightly bent {120.4(3)°} towards Ni(2) {Ni(2)···N(7) 3.619 Å}. The Ni(1)-N(5)-N(6) basal least -trigonal plane are bent at basal least-trigonal plane for N(5)-Ni(1)-Ni(2) edge with a dihedral angle of 17.87° towards O(2)-phenolic group. The Ni(2) is displaced by 0.320 Å from the basal N_2O_2 least-squares plane towards N(8) (azido). The N_3 ligand keep their linearity, N-N-N bond angle is 177.8(4)°, whereas the Ni(2)-N(8)-N(9) linkage is slightly bent {121.3(3)°} towards the opposite Ni(1) by the repulsion of coordinated aqua of Ni(1). This complex is wholly asymmetric. The O(2)-phenolic groups of macrocycle is bent 18.6° with the basal Ni_2O_2 least-squares plane, whereas O(1)-phenolic groups of macrocycle is flat with the basal Ni_2O_2 least-squares plane. Hydrogen bonds are between water and azide molecules of octahedral of neighbor complexes. And there are a weak π-π interactions by aromatic ring of neighbor complexes ; a dihedral angle and a distance between aromatic rings are 9.4(2)° and 4.1 Å, respectively.

In the crystals of $[Ni_2([22]\text{-HMTADO})(\mu\text{-}S_2O_3)]$, the geometry about two nickel metals in the N_2O_2 site are two square-pyramid with a sulfur atom and a oxygen atom of bridged thiosulfate in cis positions. The Ni(1) is

displaced by 0.430 Å from the basal N_2O_2 least-squares plane towards S(2) (thiosulfate). The Ni(2) is displaced by 0.350 Å from the basal N_2O_2 least-squares plane towards O(3) (thiosulfate). This complex is wholly asymmetric. The bridged thiosulfate, tetragonal geometry, slants toward the Ni(2) and the O(2)-phenolic groups of macrocycle.

In the crystals of $[Ni(H_2[22]\text{-}HMTADO)(OHCH_3)_2](ClO_4)_2$, the geometry about Ni(1) in the N_2O_2 site is a octahedral with two oxygen atom of methanol molecule in trans positions, and other N_2O_2 site is vacant. The macrocyclic complex adopts a flat structure with the an octahedral nickel center bridged by the two phenoxide oxygen atoms. The two coordinated methanol molecules dihedral angle between the least-squares plan defined by Ni, O(3), and C(29) and the plane defined by Ni, O(4), and C(30) is 87.47°. This complex is wholly asymmetric. The O(1)-phenolic and O(2)-phenolic groups of macrocycle are bent 35.02° and 28.46° with the basal NiN_2O_2 least-squares plane, respectively.

These macrocyclic complexes have relatively high thermal stability.

I. Introduction

Polyamines are essential for life.[1] As a result, many studies have targeted polyamine as a potential site for chemotherapeutic intervention.[2] Macrocyclic complexes with a tetraazamacrocyclic ligand (e. g., cyclen, cyclam, and bicyclam) and their derivatives have been found utilities in antitumor[3-6] and anti-HIV[7, 8] applications.

Over the past decade, many studies have been focused upon metal complexes of cyclic triamines which cleaving carboxyester[9], phos -phoeaster[10-14], RNA[15, 16], DNA[17, 18], dipeptides and proteins[19]. To our knowledge, a few papers have been published for the cytotoxic properties and the *in vivo* antitumor effects of triazacyclic polyamines metal complexes[20, 21].

The application of designer compartmental ligands to the study of dinuclear metal complexes first occurred in the early 1970s and the term binucleating ligand was introduced by Robson[22] for polydentate chelating ligands that are capable of simultaneously binding two metal ions in close proximity. If the metal ions used are of the same type then the term homodinuclear is used and if the two metal ions are different then the complex is termed heterodinuclear.

One interest in such bimetallic complexes lies in the area of magnetochemistry. Studies on the magnetic properties of homo- and hetero-dinuclear complexes have significantly helped in advancing our understanding of spin-exchange mechanisms, relating them to the geometries and to the ground state electronic configurations of the constituting metal

ions, and to the nature of the bridging group[23]. A second area of interest is bioinorganic chemistry where dinuclear complexes can serve as synthetic analogs for bimetallobiosites and so give insight into the significance of the bimetallic cores present therein[24]. This is very topical with the recent recognition of the heterodinuclear cores at the metallobiosites in purple acid phosphatase (FeZn)[25], human calcineurin (FeZn)[26] and human protein phos -phatase 1 (MnFe)[27] stimulating a search for model complexes of unsymmetrical ligands which can bind two dissimilar metal ions in close proximity[28].

Various types of compartmental ligands including the end-off type, the side-off type and the macrocyclic type have been developed[29-32]. The macrocyclic Schiff bases **(1)**, derived from the [2+2] condensation of a 2,6-diacyl substituted phenol and a diamine, form a unique family of compartmental ligands.

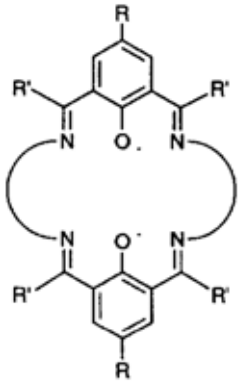

1

The symmetrical macrocycle $(L^1)^{2-}$ **(2)** was first obtained by Pilkington and Robson in 1970 as the dinuclear matal(II) complexes $M_2(L^1)X_2$, in a one pot reaction of 2,6-diformyl-*p*-cresol, 1,3-diaminopropane and a M(II) ion.[22] The "direct template reaction" has been used for providing homodinuclear complexes of $(L^1)^{2-}$ and related symmetrical macrocycles.[33~37] The N_2O_2 cavity of $(L^1)^{2-}$, formed by a trimethylene lateral chain, has an appropriate size to accommodate a wide range of metal ions within its cavity. The analogous macrocycle $(L^2)^{2-}$ **(3)**, the smallest member in this family, can accommodate only the small Cu(II) and Ni(II) ions[38~41] because the cavity derived from the ethylene lateral chain is small and the "salen" (*N,N′*-ethylenedisalicylaldiminate)-like entity embedded in the macrocyclic framework has little flexibility compared with salen itself. The synthesis of the metal-free, protonate form of $(L^1)^{2-}$ and $(L^2)^{2-}$ (and their homologs) has been described by Schroder et al.[42]

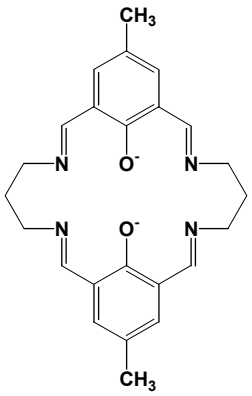

$(L^1)^{2-}$

2

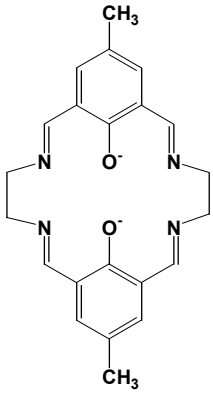

$(L^2)^{2-}$

3

Many modifications can be made to the basic structure such as the provision of different lateral chains, the introduction of an additional donor atom on one lateral chain, and partial or full saturation at the azomethine linkages. For the macrocycles which have been reduced at the azomethine groups, a potentially donating auxiliary can be introduced at the aminic nitrogen as a pendant arm. Unsymmetrical modifications of the macrocycles are of importance for providing discrete heterodinuclear core complexes. The present review is concerned with hetero-dinuclear metal complexes derived from sym -metrical and unsymmetrical phenol-based compartmental ligands of this family.

Recent attention is directed to the organization of three or more metal centers in predetermined arrays using polynucleating macrocyclic ligands. For example, tetranuclear Ni(II) and Zn(II)[43] and hexanuclear Cu(II)[44] complexes have been obtained by the [2 + 2] or [3 + 3] condensation between 2,6-diformyl-*p*-cresol and 2,6-bis(aminomethyl)-4-methylphenol in the presence of the metal ions. Furthermore, the [2 + 2] condensation product between 2,6-diformyl-*p*-cresol and 1,5-diamino-3-pentanol has been used to produce tetra-, octa-, and dodeca-nuclear Cu(II) complexes.[43, 45, 46]

This work performs synthesis, crystal X-ray diffraction studies and physicochemical characterization of dinuclear {Cu(II), Ni(II), and Mn(II)} and mononuclear {Ni(II), Pr(III), Sm(III), Gd(III), and Dy(III)} complexes with [2+2] symmetrical N_4O_2 compartmental macrocyclic ligand {H_2[22]-HMTADO ; 5,5,11,17,17,23-hexamethyl-3,7,15,19-tetraazatricyclo[19,3,1,$1^{9,13}$]hexacosa-1(25),2,7,9,11,13(26),14,19,21,23-decane-25,26-diol} containing bridging phenolic oxygen atoms synthesized by condensation, in the metal ions, of 2,6-

diformyl-*p*-cresol and 2-dimethyl-1,3-propandiamine.

II. Experimental section

1. Chemicals and Physical Measurements

All chemicals were commercial analytical reagents and were used without further purification. For the spectroscopic and physical measurements, organic solvents were dried and purified according to the literature methods[47]. Nanopure quality water was used throughout this work. Microanalyses of C, H, and N were carried out using LECO CHN-900 analyzer. NMR spectra were obtained with a JNM-LA400 FT-NMR (JEOL) Spectrophotometer. Conductance measurements of the complexes were performed at 25±1℃ using an ORION 162 conductivity temperature meter. IR spectra were recorded with a Bruker FSS66 FT-IR spectrometer in the range 4000-370 cm^{-1} using KBr pellets. Electronic absorption spectra were measured at 25℃ on a UV-3150 UV-VIS-NIR Spectrophotometer (SHIMADZU). FAB-mass spectra were obtained on a JEOL JMS-700 Mass Spectrometer using argon (6 kV, 10 mA) as the FAB gas. The accelerating voltage was 10 kV andglycerol was used as the matrix. The mass spectrometer was operated in positive ion mode and mass spectrum was calibrated by Alkali-CsI positive. TGA was carried out on a TGA 2050 thermal analyzer. The thermogravimetric curves of complexes were recorded in 30～1000℃ range under nitrogen atmosphere. The heating rate was 10℃/min.

2. Synthesis of Ligand and Complexes

1) Preparation of 2, 6-diformyl-*p*-cresol.

The synthesis of 2, 6-diformyl-*p*-cresol was prepared according to the methods previously reported.[48, 49]

2) Preparation of (H_2[22]-HMTADO)・2$HClO_4$; {5,5,11,17,17,23-hexamethyl-3,7,15,19-tetraazatricyclo[19, 3, 1, $1^{9,13}$]hexacosa-1(25),2,7,9,11,13(26),14,19,21,23-decane-25,26-diol・2$HClO_4$} ligand.

To a solution of 2,2-dimethyl-1,3-propanediamine (0.206 g) in 20 mL of ethanol was added 0.17 mL of 70% $HClO_4$. The mixture was added a solution of 2,6-diformyl-*p*-cresol (0.328 g) in 20 mL of ethanol and the resulting red solution was refluxed for 1 h, after which time a yellow-red compound separated out. The solution was cooled to room temperature and the yellow-red product was filtered, thoroughly washed with ethanol, dried under vacuum over anhydrous calcium chloride.

Yield 0.550 g (83%).

Anal. Calc. (%) for $(C_{28}H_{36}N_4O_2)(H_2ClO_4)_2$:
C, 50.84 ; H, 5.79 ; N, 8.47.
Found (%) : C, 50.71 : H, 5.65 : N, 8.47.

Solubility : DMSO, DMF, acetonitrile.

UV-Vis (DMF) [λ_{max} (nm) (ε ($M^{-1}cm^{-1}$))] :

349 (10,490), 433 (13,990), 462 sh (8,220).

Λ_M(DMF) : 245 $ohm^{-1}cm^2mol^{-1}$.

FAB-mass (*m/z*, M^+) : 461 ($C_{28}H_{36}N_4O_2$).

FT-IR (KBr, cm^{-1}) : 3437 ν(OH) ; 1662 ν(C=N) ; 1644, 1536 ν(C=C, aromatic) ; 1088, 624 $\nu(ClO_4^-)$.

3) Preparation of binuclear Cu(II) complexes.

The dinuclear Cu(II) complexes with [2+2] symmetrical N_4O_2 compartmental macrocyclic ligand {([22]-HMTADO)$^{2-}$} containing bridging phenolic oxygen atoms was synthesized by condensation, in the Cu(II) ions, of 2,6-diformyl-*p*-cresol and 2-dimethyl-1,3-propandiamine (Scheme 1).

(1) $[Cu_2([22]\text{-HMTADO})(OH_2)]Cl_2 \cdot H_2O$.

A solution of 2,6-diformyl-*p*-cresol (1.312 g) in the boiling methanol (30 mL) was added to the pale blue suspension formed by mixing 2, 2-dimethyl-1,3-propandiamine (0.824 g) with a solution of cupric chloride dihydrate (1.364 g) in methanol (30 mL). The mixture was heated under reflux whereupon the initial yellow suspended solid first turned dark green and then eventually dissolved. Methanol was removed by boiling at atmospheric pressure until precipitation had just commenced and the dark green mixture was poured into ten times its volume of tetrahydrofuran. The resulting pale green precipitate was filtered, thoroughly washed twice with

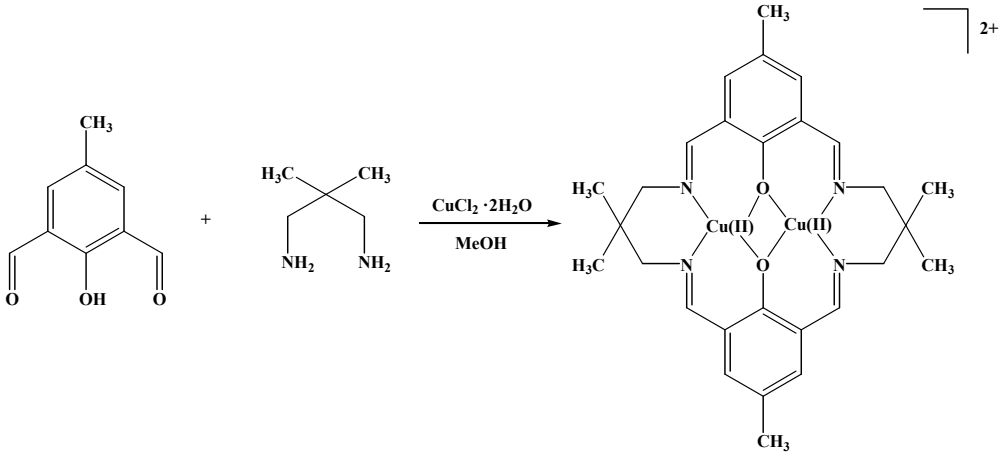

$[Cu_2([22]\text{-HMTADO})(OH_2)]Cl_2 \cdot H_2O$

sat. $NaClO_4$ → $[Cu_2([22]\text{-HMTADO})(OClO_3)(OH_2)]ClO_4$

CN^- → $[Cu_2([22]\text{-HMTADO})(CN)_2] \cdot 0.5H_2O$

NCS^- → $[Cu_2([22]\text{-HMTADO})(NCS)(OH_2)]NCS \cdot 2H_2O$

N_3^- → $[Cu_2([22]\text{-HMTADO})(N_3)(OH_2)]N_3 \cdot H_2O$

NO_3^- → $[Cu_2([22]\text{-HMTADO})ONO_2]NO_3 \cdot 4H_2O$

NO_2^- → $[Cu_2([22]\text{-HMTADO})NO_2]NO_2 \cdot 2H_2O$

Br^- → $[Cu_2([22]\text{-HMTADO})]Br_2 \cdot 1.5H_2O$

$S_2O_3^{2-}$ → $[Cu_2([22]\text{-HMTADO})S_2O_3] \cdot 5H_2O$

Scheme 1. Synthesis of the binuclear Cu(II) complexes of phenol-based macrocyclic ligand ([22]-HMTADO).

tetrahydrofuran, and dried in vacuo. Then recrystallized from hot water, yielding crystal as dark green platelets which were dried over anhydrouse calcium chloride at room temperature and atmospheric pressure. Prolonged heating in vacuum at 150℃ was required for removal of the water.

Recrystallization from water formed $[Cu_2([22]\text{-HMTADO})(OH_2)_4]Cl_2 \cdot 10H_2O$ as good crystals suitable for X-ray crystallography.

Yield 2.550 g (92%).

Anal. Calc. (%) for $Cu_2(C_{28}H_{34}N_4O_2)(Cl)_2(H_2O)_2$:

C, 48.56 ; H, 5.53 ; N, 8.09.

Found (%) : C, 48.71 ; H, 5.93 ; N, 8.23.

Solubility : water, methanol, ethanol, DMSO, DMF, acetonitrile.

Λ_M (water) : 218 $ohm^{-1}cm^2mol^{-1}$.

(2) $[Cu_2([22]\text{-HMTADO})(OClO_3)(OH_2)]ClO_4 \cdot 2H_2O$.

A solution of $[Cu_2([22]\text{-HMTADO})(OH_2)]Cl_2 \cdot H_2O$ (0.693 g) in water (50 mL) was added dropwise a saturated aqueous sodium perchlorate solution (2 mL) with stirring and a solution was refluxed for 2 h. The resulting pale green precipitate was filtered, thoroughly washed twice with water, and dried in vacuo. Then recrystallized from hot methanol, yielding crystal as pale green platelets which were dried over anhydrouse calcium chloride.

Recrystallization from methanol formed $[Cu_2([22]\text{-HMTADO})(OH_2)(OClO_3)]$ $-ClO_4 \cdot 2MeOH$ as good crystals suitable for X-ray crystallography.

Yield 0.503 g (60%).

Anal. Calc. (%) for $Cu_2(C_{28}H_{34}N_4O_2)(ClO_4)_2(H_2O)_3$:

C, 40.10 ; H, 4.81 ; N, 6.68.

Found (%) : C, 40.11 ; H, 4.43 ; N, 6.72.

Solubility : methanol, DMSO, DMF, acetonitrile, acetone.

Λ_M (methanol) : 108 $ohm^{-1}cm^2mol^{-1}$.

(3) $[Cu_2([22]\text{-HMTADO})(CN)_2] \cdot 0.5H_2O$.

A solution of $[Cu_2([22]\text{-HMTADO})(OH_2)]Cl_2 \cdot H_2O$ (0.693 g) in hot water (50 mL) was added dropwise a solution of sodium cyanide (0.245 g) in water (30 mL) with stirring and the mixture was heated under reflux whereupon the initial pale yellow-red precipitate first turned green. The resulting green precipitate was filtered, thoroughly washed twice with water, and dried in vacuo.

Yield 0.601 g (95%).

Anal. Calc. (%) for $Cu_2(C_{28}H_{34}N_4O_2)(CN)_2(H_2O)_{0.5}$:

C, 55.71 ; H, 5.45 ; N, 13.00.

Found (%) : C, 56.00 ; H, 5.06 ; N, 13.40.

Solubility : hot DMSO, hot DMF

Λ_M (DMSO) : 17 $ohm^{-1}cm^2mol^{-1}$.

(4) $[Cu_2([22]\text{-HMTADO})(NCS)(OH_2)]NCS \cdot 2H_2O$.

A solution of $[Cu_2([22]\text{-HMTADO})(OH_2)]Cl_2 \cdot H_2O$ (0.693 g) in hot water (50 mL) was added dropwise a solution of sodium thiocyanide (0.414 g) in water (30 mL) with stirring and the mixture was refluxed for 2 h. The resulting white green needles were filtered, thoroughly washed twice with water and acetone, and dried in vacuo.

Yield 0.564 g (75%).

Anal. Calc. (%) for $Cu_2(C_{28}H_{34}N_4O_2)(NCS)_2(H_2O)_3$:

C, 47.67 ; H, 5.33 ; N, 11.12.

Found (%) : C, 47.23 ; H, 4.70 ; N, 11.45

Solubility : hot DMSO, hot DMF

Λ_M (DMSO) : 63 $ohm^{-1}cm^2mol^{-1}$.

(5) $[Cu_2([22]\text{-HMTADO})(N_3)(OH_2)]N_3 \cdot H_2O$.

A solution of $[Cu_2([22]\text{-HMTADO})(OH_2)]Cl_2 \cdot H_2O$ (0.693 g) in hot water (50 mL) was added dropwise a solution of sodium azide (0.325 g) in water (30 mL) with stirring and the mixture was refluxed for 2 h. The resulting white green precipitate were filtered, thoroughly washed twice with water and acetone, and dried in vacuo.

Yield 0.542 g (77 %).

Anal. Calc. (%) for $Cu_2(C_{28}H_{34}N_4O_2)(N_3)_2(H_2O)_2$:

C, 47.65 ; H, 5.43 ; N, 19.85.

Found (%) : C, 47.53 ; H, 5.33 ; N, 19.61

Solubility : methanol, hot DMSO, hot DMF

Λ_M (methanol) : 71 $ohm^{-1}cm^2mol^{-1}$.

(6) $[Cu_2([22]\text{-HMTADO})ONO_2]NO_3 \cdot 4H_2O$.

A solution of $[Cu_2([22]\text{-HMTADO})(OH_2)]Cl_2 \cdot H_2O$ (0.693 g) in hot water (50 mL) was added dropwise a solution of sodium nitrate (0.425 g) in water (30 mL) with stirring and a solution was refluxed for 2 h. The resulting white green precipitate was filtered, thoroughly washed twice with ice-cold water, and dried in vacuo.

Yield 0.562 g (72%).

Anal. Calc. (%) for $Cu_2(C_{28}H_{34}N_4O_2)(NO_3)_2(H_2O)_4$:

C, 43.02 ; H, 5.41 ; N, 10.75.

Found (%) : C, 43.03 ; H, 4.59 ; N, 10.88.

Solubility : hot methanol, DMSO, DMF, hot acetonitrile.

Λ_M (methanol) : 57 $ohm^{-1}cm^2mol^{-1}$.

(7) $[Cu_2([22]\text{-HMTADO})NO_2]NO_2 \cdot 2H_2O$.

A solution of $[Cu_2([22]\text{-HMTADO})(OH_2)]Cl_2 \cdot H_2O$ (0.693 g) in hot water (50 mL) was added dropwise a solution of sodium nitrite (0.345 g) in water (30 mL) with stirring and a solution was refluxed for 2 h. The resulting solution was evaporated to approx. 20 mL and on standing overnight at room temperature. The green precipitate was filtered, thoroughly washed with small

portions ice-cold water, and dried in vacuo.

Yield 0.351 g (49%).

Anal. Calc. (%) for $Cu_2(C_{28}H_{34}N_4O_2)(NO_2)_2(H_2O)_2$:

C, 47.12 ; H, 5.37 ; N, 11.77.

Found (%) : C, 47.09 ; H, 5.23 ; N, 11.54.

Solubility : hot water, methanol, DMSO, DMF, hot acetonitrile.

Λ_M (methanol) : 97 $ohm^{-1}cm^2mol^{-1}$.

(8) $[Cu_2([22]\text{-HMTADO})]Br_2 \cdot 1.5H_2O$.

A solution of $[Cu_2([22]\text{-HMTADO})(OH_2)]Cl_2 \cdot H_2O$ (0.693 g) in hot water (50 mL) was added dropwise a solution of sodium bromide (0.514 g) in water (30 mL) with stirring and a solution was refluxed for 2 h. The resulting solution was evaporated to approx. 20 mL and on standing overnight at room temperature. The green precipitate was filtered, thoroughly washed with small portions ice-cold water, and dried in vacuo.

Recrystallization from water formed $[Cu_2([22]\text{-HMTADO})(OH_2)_4]Br_2 \cdot 10H_2O$ as good crystals suitable for X-ray crystallography.

Yield 0.430 g (55%).

Anal. Calc. (%) for $Cu_2(C_{28}H_{34}N_4O_2)(Br)_2(H_2O)_{1.5}$:

C, 43.53 ; H, 4.83 ; N, 7.25.

Found (%) : C, 43.56 ; H, 4.53 ; N, 7.34.

Solubility : water, methanol, DMSO, DMF.

Λ_M (methanol) : 160 $ohm^{-1}cm^2mol^{-1}$.

(9) $[Cu_2([22]\text{-HMTADO})S_2O_3] \cdot 5H_2O$.

A solution of $[Cu_2([22]\text{-HMTADO})]Cl_2 \cdot 2H_2O$ (0.693 g) in hot water (50 mL) was added dropwise a solution of sodium thiosulfate (0.620 g) in water (30 mL) with stirring and a solution was refluxed for 2 h. The dark green precipitate was filtered, thoroughly washed with ice-cold water, and dried in vacuo.

Yield 0.642 g (92 %).

Anal. Calc. (%) for $Cu_2(C_{28}H_{34}N_4O_2)(S_2O_3)(H_2O)_5$:

C, 42.68 ; H, 5.63 ; N, 7.11.

Found (%) : C, 42.73 ; H, 5.60 ; N, 7.21.

Solubility : hot DMSO, hot DMF

Λ_M (DMSO) : 29 $ohm^{-1}cm^2mol^{-1}$.

4) Preparation of bi- and mono-nuclear Ni(II) complexes.

The di- and mono-nuclear Ni(II) complexes with [2+2] symmetrical N_4O_2 compartmental macrocyclic ligand $\{([22]\text{-HMTADO})^{2-}\}$ containing bridging phenolic oxygen atoms was synthesized by condensation, in the Ni(II) ions, of 2,6-diformyl-*p*-cresol and 2-dimethyl-1,3-propandiamine (Scheme 2 and 3).

(1) $[Ni_2([22]\text{-HMTADO})(OH_2)_2]Cl_2 \cdot H_2O$.

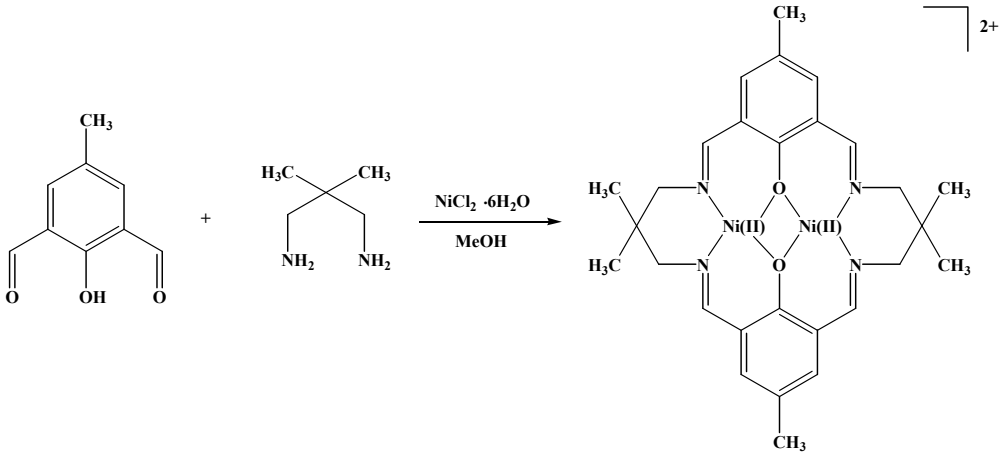

$[Ni_2([22]\text{-HMTADO})(OH_2)_2]Cl_2 \cdot H_2O$

sat. $NaClO_4$	$[Ni_2([22]\text{-HMTADO})(OH_2)_2](ClO_4)_2 \cdot H_2O$
CN^-	$[Ni_2([22]\text{-HMTADO})(CN)_2] \cdot 0.5H_2O$
NCS^-	$[Ni_2([22]\text{-HMTADO})(NCS)_2(OH_2)] \cdot 2H_2O$
N_3^-	$[Ni_2([22]\text{-HMTADO})(N_3)_2(OH_2)]$
NO_3^-	$[Ni_2([22]\text{-HMTADO})(ONO_2)(OH_2)_2]NO_3 \cdot 3H_2O$
NO_2^-	$[Ni_2([22]\text{-HMTADO})NO_2]NO_2 \cdot H_2O$
Br^-	$[Ni_2([22]\text{-HMTADO})]Br_2 \cdot 2H_2O$
$S_2O_3^{2-}$	$[Ni_2([22]\text{-HMTADO})S_2O_4]$

Scheme 2. Synthesis of the binuclear Ni(II) complexes of phenol-based macrocyclic ligand ([22]-HMTADO).

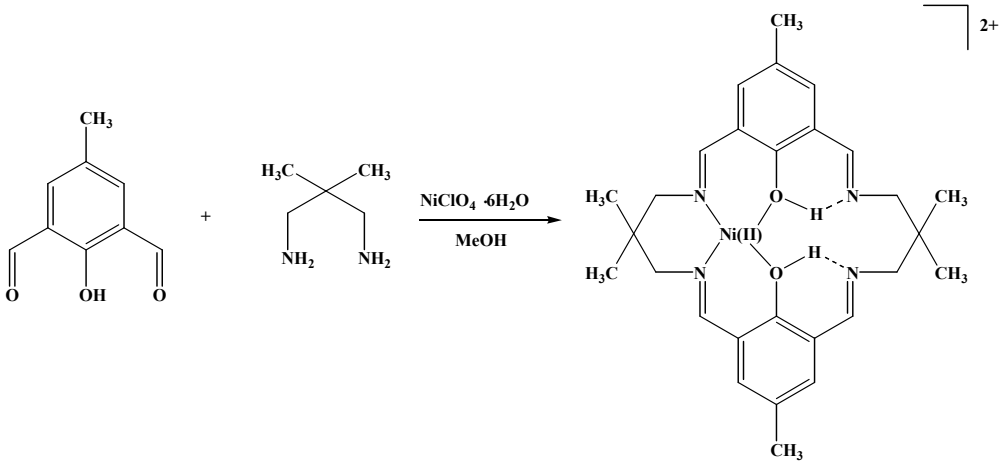

$[Ni_2(H_2[22]\text{-HMTADO})(OHCH_3)_2](ClO_4)_2$

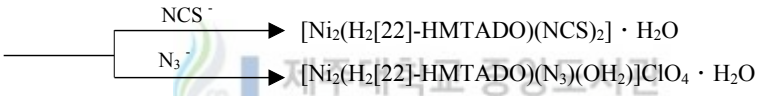

Scheme 3. Synthesis of the mononuclear Ni(II) complexes of phenol-based macrocyclic ligand (H_2[22]-HMTADO).

Nickel chloride hexahydrate (4.80 g), 2,6-diformyl-*p*-cresol (1.64 g), and 2-dimethyl-1,3-propandiamine (1.03 g) were heated under reflux in methanol (150 mL) for 4 h. The solution was cooled to room temperature and the pale green product was filtered, thoroughly washed with ice-cold methanol, dried under vacuum over anhydrouse calcium chloride.

Yield 1.462 g (42%).

Anal. Calc. (%) for $Ni_2(C_{28}H_{34}N_4O_2)(Cl)(H_2O)_3$:

C, 47.98 ; H, 5.75 ; N, 7.99.

Found (%) : C, 47.99 ; H, 5.02 ; N, 7.66.

Solubility : water, DMSO, DMF, hot acetonitrile, hot acetone, chloroform.

Λ_M (water) : 205 $ohm^{-1}cm^2mol^{-1}$.

(2) $[Ni_2([22]\text{-HMTADO})(OH_2)_2](ClO_4)_2 \cdot H_2O$.

A brown solution of $[Ni_2([22]\text{-HMTADO})(OH_2)_2]Cl_2 \cdot H_2O$ (0.701 g) in hot water (100 mL) was added dropwise a saturated aqueous sodium perchlorate solution (4 mL) with stirring and the solution was refluxed for 2 h. Then the solution stored in a refrigerator until the pale brown crystals formed on the upper part of the flask. The product was filtered off, thoroughly washed with ice-cold water, and dried in vacuo.

Recrystallization from methanol formed $[Ni_2([22]\text{-HMTADO})(OH_2)_4]ClO_4 \cdot 3H_2O$ as good crystals suitable for X-ray crystallography.

Yield 0.408 g (49%).

Anal. Calc. (%) for $Ni_2(C_{28}H_{34}N_4O_2)(ClO_4)_2(H_2O)_3$:

C, 40.57 ; H, 4.86 ; N, 6.76.

Found (%) : C, 40.95 ; H, 4.57 ; N, 6.75.

Solubility : methanol, DMSO, DMF, acetonitrile, acetone.

Λ_M (methanol) : 170 $ohm^{-1}cm^2mol^{-1}$.

(3) $[Ni_2([22]\text{-HMTADO})(CN)_2]\cdot 0.5H_2O$.

A pale brown solution of $[Ni_2([22]\text{-HMTADO})(OH_2)_2]Cl_2\cdot H_2O$ (0.701 g) in hot water (30 mL) was added dropwise a solution of sodium cyanide (0.245 g) in water (30 mL) with stirring and the solution was refluxed for 2 h. The dark green precipitate was filtered, thoroughly washed twice with water, and dried in vacuo.

Yield 0.559 g (88%).

Anal. Calc. (%) for $Ni_2(C_{28}H_{34}N_4O_2)(CN)_2(H_2O)_{0.5}$:

C, 56.56 ; H, 5.54 ; N, 13.19.

Found (%) : C, 56.33 ; H, 5.52 ; N, 13.14.

Solubility : methanol, DMSO, DMF, hot acetonitrile, chloroform.

Λ_M (methanol) : 9.5 $ohm^{-1}cm^2mol^{-1}$.

(4) $[Ni_2([22]\text{-HMTADO})(NCS)_2(OH_2)]\cdot 2H_2O$.

A pale brown solution of $[Ni_2([22]\text{-HMTADO})(OH_2)_2]Cl_2\cdot H_2O$ (0.701 g) in hot water (30 mL) was added dropwise a solution of sodium thiocyanide (0.415 g) in water (30 mL) with stirring and the solution was refluxed for 2 h. The pale green precipitate was filtered, thoroughly washed twice with water, and dried in vacuo.

Yield 0.739 g (99%).

Anal. Calc. (%) for $Ni_2(C_{28}H_{34}N_4O_2)(NCS)_2(H_2O)_3$:

C, 48.29 ; H, 5.40 ; N, 11.26.

Found (%) : C, 49.44 ; H, 5.60 ; N, 11.23.

Solubility : DMSO, DMF, acetonitrile.

Λ_M (DMSO) : 42 $ohm^{-1}cm^2mol^{-1}$.

(5) $[Ni_2([22]\text{-HMTADO})(N_3)_2(OH_2)]$.

A pale brown solution of $[Ni_2([22]\text{-HMTADO})(OH_2)_2]Cl_2 \cdot H_2O$ (0.701 g) in hot water (30 mL) was added dropwise a solution of sodium azide (0.195 g) in water (30 mL) with stirring and the solution was refluxed for 2 h. The green yellow precipitate was filtered, thoroughly washed twice with water, and dried in vacuo.

Recrystallization from acetonitrile formed $[Ni_2([22]\text{-HMTADO})(N_3)_2(OH_2)]$ as good crystals suitable for X-ray crystallography.

Yield 0.574 g (85%).

Anal. Calc. (%) for $Ni_2(C_{28}H_{34}N_4O_2)(N_3)_2(H_2O)$:

C, 49.60 ; H, 5.35 ; N, 20.66.

Found (%) : C, 49.32 ; H, 5.55 ; N, 20.61.

Solubility : DMSO, DMF, hot acetonitrile, chloroform.

Λ_M (DMSO) : 13 $ohm^{-1}cm^2mol^{-1}$.

(6) $[Ni_2([22]\text{-HMTADO})(ONO_2)(OH_2)_2]NO_3 \cdot 3H_2O$.

A pale brown solution of $[Ni_2([22]\text{-HMTADO})(OH_2)_2]Cl_2 \cdot H_2O$ (0.701 g)

in hot water (30 mL) was added dropwise a solution of sodium nitrate (0.425 g) in water (30 mL) with stirring and the solution was refluxed for 2 h. The green yellow precipitate was filtered, thoroughly washed with ice-cold water, and dried in vacuo.

Yield 0.190 g (24%).

Anal. Calc. (%) for $Ni_2(C_{28}H_{34}N_4O_2)(NO_3)_2(H_2O)_5$:

C, 42.57 ; H, 5.61 ; N, 10.64.

Found (%) : C, 42.38 ; H, 5.14 ; N, 10.42.

Solubility : methanol, DMSO, DMF, hot acetonitrile, chloroform.

Λ_M (methanol) : 47 $ohm^{-1}cm^2mol^{-1}$.

(7) $[Ni_2([22]\text{-HMTADO})NO_2]NO_2 \cdot H_2O$.

A pale brown solution of $[Ni_2([22]\text{-HMTADO})(OH_2)_2]Cl_2 \cdot H_2O$ (0.701 g) in hot water (30 mL) was added dropwise a solution of sodium nitrite (0.345 g) in water (30 mL) with stirring and the solution was refluxed for 2 h. The dark green precipitate was filtered, thoroughly washed with ice-cold water, and dried in vacuo.

Yield 0.409 g (60%).

Anal. Calc. (%) for $Ni_2(C_{28}H_{34}N_4O_2)(NO_2)_2(H_2O)$:

C, 49.02 ; H, 5.29 ; N, 12.25.

Found (%) : C, 48.93 ; H, 5.08 ; N, 12.07.

Solubility : methanol, DMSO, DMF, hot acetonitrile, chloroform.

Λ_M (methanol) : 60 $ohm^{-1}cm^2mol^{-1}$.

(8) $[Ni_2([22]\text{-HMTADO})]Br_2 \cdot 2H_2O$.

A pale brown solution of $[Ni_2([22]\text{-HMTADO})(OH_2)_2]Cl_2 \cdot H_2O$ (0.701 g) in hot water (30 mL) was added dropwise a solution of sodium bromide (0.514 g) in water (30 mL) with stirring and the solution was refluxed for 2 h. The resulting solution was evaporated to approx. 20 mL and on standing overnight at room temperature. The green precipitate was filtered, thoroughly washed with small portions ice-cold water, and dried in vacuo.

Recrystallization from water formed $[Ni_2([22]\text{-HMTADO})(OH_2)_4]Br_2 \cdot 10H_2O$ as good crystals suitable for X-ray crystallography.

Yield 0.118 g (15%).

Anal. Calc. (%) for $Ni_2(C_{28}H_{34}N_4O_2)(Br)_2(H_2O)_2$:

C, 43.57 ; H, 4.96 ; N, 7.26.

Found (%) : C, 43.85 ; H, 4.82 ; N, 7.37.

Solubility : water, methanol, DMSO, DMF, hot acetonitrile, chloroform.

Λ_M (methanol) : 142 $ohm^{-1}cm^2mol^{-1}$.

(9) $[Ni_2([22]\text{-HMTADO})S_2O_3]$.

A pale brown solution of $[Ni_2([22]\text{-HMTADO})(OH_2)_2]Cl_2 \cdot H_2O$ (0.701 g) in hot water (30 mL) was added dropwise a solution of sodium thiosulfate (1.240 g) in water (30 mL) with stirring and the solution was refluxed for 2

h. The resulting solution was evaporated to approx. 20 mL whereupon the initial pale yellow-red precipitate turned green. The green precipitate was filtered, thoroughly washed with ice-cold water, and dried in vacuo.

Yield 0.0913 g (13%).

Anal. Calc. (%) for $Ni_2(C_{28}H_{34}N_4O_2)(S_2O_3)$:

C, 48.87 ; H, 4.98 ; N, 8.14.

Found (%) : C, 48.70 ; H, 4.76 ; N, 8.15.

Solubility : hot water, hot methanol.

Λ_M (methanol) : 3.6 $ohm^{-1}cm^2mol^{-1}$.

(10) $[Ni(H_2[22]\text{-}HMTADO)(OHCH_3)_2](ClO_4)_2$.

Nickel perchlorate hexahydrate (2.194 g), 2,6-diformyl-*p*-cresol (0.657 g), and 2-dimethyl-1,3-propandiamine (0.412 g) were heated under reflux in methanol (100 mL) for 4 h. The resulting solution was evaporated to approx. 30 mL and on standing overnight at room temperature. The yellow-red product was filtered, thoroughly washed with ice-cold methanol, dried under vacuum over anhydrouse calcium chloride.

Recrystallization from acetonitrile formed $[Ni(H_2[22]\text{-}HMTADO)(OHCH_3)_2)](ClO_4)_2$ as good crystals suitable for X-ray crystallography.

Yield 0.554 g (35%).

Anal. Calc. (%) for $Ni(C_{28}H_{36}N_4O_2)(ClO_4)_2(CH_3OH)_2$:

C, 46.06 ; H, 5.67 ; N, 7.16.

Found (%) : C, 45.81 ; H, 5.61 ; N, 7.05.

Solubility : hot methanol, DMSO, DMF, acetonitrile, acetone, hot water.

Λ_M (methanol) : 113 $ohm^{-1}cm^2mol^{-1}$.

(11) $[Ni(H_2[22]\text{-}HMTADO)(NCS)_2]\cdot H_2O$.

A pale brown solution of $[Ni(H_2[22]\text{-}HMTADO)(OHCH_3)_2)](ClO_4)_2$ (0.782 g) in hot water (100 mL) was added dropwise a solution of sodium thiocyanide (0.203 g) in water (30 mL) with stirring and the solution was refluxed for 2 h whereupon the initial yellow precipitate turned pale yellow-red. The pale yellow-red precipitate was filtered, thoroughly washed with water, and dried in vacuo.

Yield 0.273 g (84%).

Anal. Calc. (%) for $Ni(C_{28}H_{36}N_4O_2)(NCS)_2(H_2O)$:

C, 55.14 ; H, 5.89 ; N, 12.86.

Found (%) : C, 55.22 ; H, 5.34 ; N, 12.68.

Solubility : hot methanol, DMSO, DMF, hot acetonitrile.

Λ_M (DMSO) : 49 $ohm^{-1}cm^2mol^{-1}$.

(12) $[Ni(H_2[22]\text{-}HMTADO)(N_3)(OH_2)]ClO_4\cdot H_2O$.

A pale brown solution of $[Ni(H_2[22]\text{-}HMTADO)(OHCH_3)_2)](ClO_4)_2$ (0.782 g) in hot water (100 mL) was added dropwise a solution of sodium azide (0.163 g) in water (30 mL) with stirring and the solution was refluxed for 2

h whereupon the initial yellow precipitate turned pale yellow-red. The pale yellow-red precipitate was filtered, thoroughly washed with water, and dried in vacuo.

Yield 0.278 g (80%).

Anal. Calc. (%) for $Ni(C_{28}H_{36}N_4O_2)(N_3)(ClO_4)(H_2O)_2$:

C, 48.47 ; H, 5.81 ; N, 14.13.

Found (%) : C, 48.98 ; H, 5.37 ; N, 13.82.

Solubility : hot methanol, DMSO, DMF, hot acetonitrile.

Λ_M (DMSO) : 62 $ohm^{-1}cm^2mol^{-1}$.

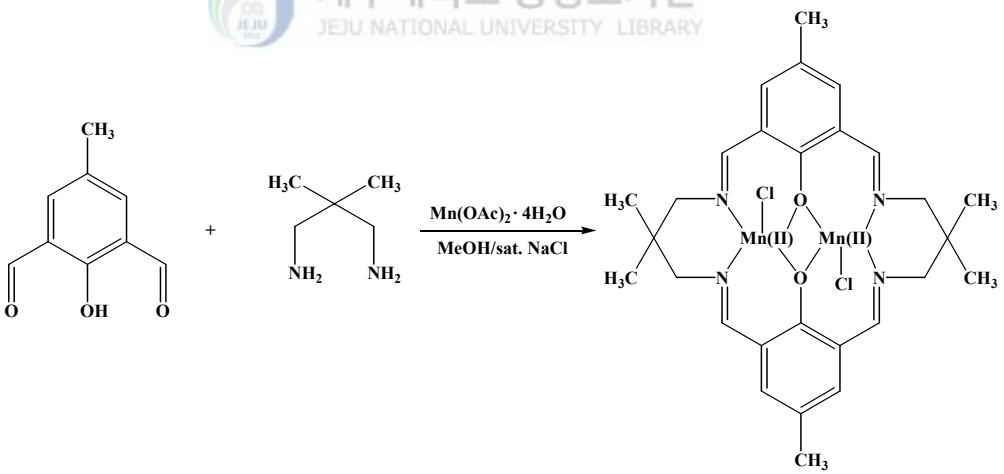

Scheme 4. Synthesis of the binuclear Mn(II) complex of phenol-based macrocyclic ligand ([22]-HMTADO).

5) Preparation of binuclear Mn(II) complex.

The dinuclear Mn(II) complexes with [2+2] symmetrical N_4O_2 compartmental macrocyclic ligand {([22]-HMTADO)$^{2-}$} containing bridging phenolic oxygen atoms was synthesized by condensation, in the Mn(II) ions, of 2,6-diformyl-*p*-cresol and 2-dimethyl-1,3-propandiamine (Scheme 4).

(1) [Mn_2([22]-HMTADO)Cl_2] · H_2O.

A solution of 2,6-diformyl-*p*-cresol (0.328 g) in the boiling methanol (30 mL) was added to the pale brown solution formed by mixing 2, 2-dimethyl-1,3-propandiamine (0.206 g) with a solution of manganese acetate tetrahydrate (0.619 g) in methanol (80 mL). The mixture was heated under reflux for 30 min, and then was dropwise added a saturated aqueous sodium chloride (1 mL). The resulting dark green mixture was stirred at the reflux temperature for 1 h to give an orange microcrystalline powder. It was collected by suction filtration, thoroughly washed with methanol and dried in vacuo.

Yield 0.290 g (44%).

Anal. Calc.(%) for $Mn_2(C_{28}H_{34}N_4O_2)(Cl)_2(H_2O)$:

C, 51.16 ; H, 5.52 ; N, 8.52.

Found(%) : C, 50.99 ; H, 5.14 ; N, 8.50.

Solubility : DMSO, DMF, chloroform.

Λ_M(chloroform) : 0.0 $ohm^{-1}cm^2mol^{-1}$.

6) Preparation of mononuclear lanthanide complexes.

The mononuclear lanthanide {Pr(III), Sm(III), Gd(III), and Dy(III)} complexes with [2+2] symmetrical N_4O_2 compartmental macrocyclic ligand containing bridging phenolic oxygen atoms was synthesized by condensation, in the lathanide ions, of 2,6-diformyl-*p*-cresol and 2-dimethyl-1,3-propandiamine (Scheme 5).

(1) [Pr(H_2[22]-HMTADO)O_2NO](NO_3)$_2$ · 2H_2O.

A solution of 2,6-diformyl-*p*-cresol (0.328 g) in the boiling acetonitrile (30 mL) was dropwise added to the yellow solution formed by mixing 2, 2-dimethyl-1,3-propandiamine (0.206 g) with a solution of $Pr(NO_3)_3 \cdot 6H_2O$ (0.435 g) in acetonitrile (50 mL).

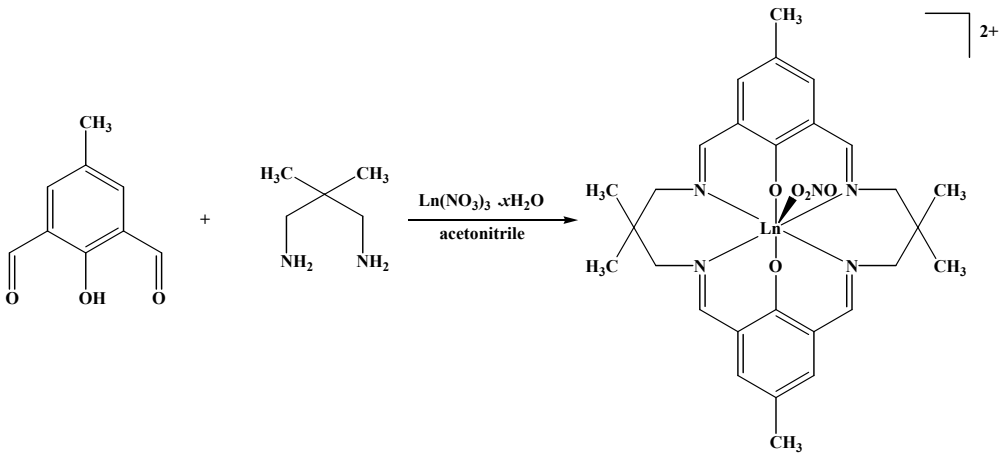

Scheme 5. Synthesis of the mononuclear lanthanide {Pr(III), Sm(III), Gd(III), and Dy(III)} complexes of phenol-based macrocyclic ligand ([22]-HMTADO).

The resulting yellow mixture was stirred at the reflux temperature for 3 h to give an yellow microcrystalline powder. It was collected by suction filtration, thoroughly washed with acetonitrile and dried in vacuo.

Yield 0.642 g (78%).

Anal. Calc. (%) for $Pr(C_{28}H_{36}N_4O_2)(NO_3)_3(H_2O)_2$:

C, 40.84 ; H, 4.90 ; N, 11.91.

Found (%) ; C, 40.82 ; H, 5.04 ; N, 11.58.

Solubility : hot methanol, DMSO, DMF.

Λ_M(methanol) : 260 ohm^{-1} cm^2mol^{-1}.

(2) $[Sm(H_2[22]\text{-}HMTADO)O_2NO](NO_3)_2 \cdot 2H_2O$.

A solution of 2,6-diformyl-*p*-cresol (0.328 g) in the boiling acetonitrile (30 mL) was dropwise added to the yellow solution formed by mixing 2, 2-dimethyl-1,3-propandiamine (0.206 g) with a solution of $Sm(NO_3)_3 \cdot 6H_2O$ (0.445 g) in acetonitrile (50 mL). The resulting yellow mixture was stirred at the reflux temperature for 3 h to give an yellow microcrystalline powder. It was collected by suction filtration, thoroughly washed with acetonitrile and dried in vacuo.

Yield 0.626 g (75%).

Anal. Calc. (%) for $Sm(C_{28}H_{36}N_4O_2)(NO_3)_3(H_2O)_2$:

C, 40.37 ; H, 4.84 ; N, 11.77.

Found (%) ; C, 40.62 ; H, 4.38 ; N, 11.45.

Solubility : hot methanol, DMSO, DMF.

Λ_M (methanol) : 258 ohm^{-1} cm^2mol^{-1}.

(3) [Gd(H_2[22]-HMTADO)O_2NO](NO_3)$_2$ · 2H_2O.

A solution of 2,6-diformyl-*p*-cresol (0.328 g) in the boiling acetonitrile (30 mL) was dropwise added to the yellow solution formed by mixing 2, 2-dimethyl-1,3-propandiamine (0.206 g) with a solution of $Gd(NO_3)_3 \cdot 6H_2O$ (0.451 g) in acetonitrile (50 mL). The resulting yellow mixture was stirred at the reflux temperature for 3 h to give an yellow microcrystalline powder. It was collected by suction filtration, thoroughly washed with acetonitrile and dried in vacuo.

Yield 0.737 g (88%).

Anal. Calc. (%) for $Gd(C_{28}H_{36}N_4O_2)(NO_3)_3(H_2O)_2$:

C, 40.14 ; H, 4.57 ; N, 11.70.

Found (%) ; C, 39.65 ; H, 4.02 ; N, 11.81.

Solubility : hot methanol, DMSO, DMF.

Λ_M (methanol) : 256 ohm^{-1} cm^2mol^{-1}.

(4) [Dy(H_2[22]-HMTADO)O_2NO](NO_3)$_2$ · H_2O.

A solution of 2,6-diformyl-*p*-cresol (0.328 g) in the boiling acetonitrile (30 mL) was dropwise added to the yellow solution formed by mixing 2, 2-dimethyl-1,3-propandiamine (0.206 g) with a solution of $Dy(NO_3)_3 \cdot 5H_2O$

(0.439 g) in acetonitrile (50 mL). The resulting yellow mixture was stirred at the reflux temperature for 3 h to give an yellow microcrystalline powder. It was collected by suction filtration, thoroughly washed with acetonitrile and dried in vacuo.

Yield 75%.

Anal. Calc. (%) for $Dy(C_{28}H_{36}N_4O_2)(NO_3)_3(H_2O)$:

C, 40.66 ; H, 4.63 ; N, 11.85.

Found (%) ; C, 41.82 ; H, 4.08 ; N, 11.99.

Solubility : hot methanol, DMSO, DMF.

Λ_M (methanol) : 326 ohm^{-1} cm^2mol^{-1}.

3. X-ray Diffraction Measurements

1) $[Cu_2([22]\text{-HMTADO})(OH_2)_4]Cl_2 \cdot 10H_2O$

Suitable crystals of $[Cu_2([22]\text{-HMTADO})(OH_2)_4]Cl_2 \cdot 10H_2O$ were obtained by slow evaporation of hot aqueous solution of $[Cu_2([22]\text{-HMTADO})(OH_2)]Cl_2 \cdot H_2O$ complex at atmospheric pressure. The dark green crystal of $[Cu_2([22]\text{-HMTADO})(OH_2)_4]Cl_2 \cdot 10H_2O$ was attached to glass fibers and mounted on a Bruker SMART diffractometer equipped with a graphite monochromated Mo Kα (= 0.71073 Å) radiation, operating at 50 kV and 30 mA and a CCD detector ; 45 frames of two-dimensional diffraction images were collected and processed to obtain the cell parameters and orientation matrix. The crystallographic data, conditions for the collection of intensity data, and some features of the structure refinements are listed in Table 1, and atomic coordinates were given in Table 2. The intensity data were corrected for Lorentz and polarization effects. Absorption correction was not made during processing. Of the 13200 unique reflections measured, 4935 reflections in the range $2.06° \leq 2\Theta \leq 28.29°$ were considered to be observed($I>2\sigma(I)$) and were used in subsequent structure analysis. The program SAINTPLUS[50] was used for integration of the diffraction profiles. The structures were solved by direct methods using the SHELXS program of the SHELXTL package[51] and refined by full matrix least squares against F^2 for all data using SHELXL. All non-H atoms were refined with anisotropic displacement parameters (Table 3). Hydrogen atoms were placed in idealized

positions [U_{iso} = 1.2U_{eq} (parent atom)]. Hydrogen coordinates and isotropic displacement parameters were given in Table 4.

Table 1. Crystal data and structure refinement for $[Cu_2([22]\text{-HMTADO})(OH_2)_4]\text{-}Cl_2 \cdot 10H_2O$

Empirical formula	$C_{28}H_{62}Cl_2Cu_2N_4O_{16}$	
Formula weight	908.80	
Temperature	173(2) K	
Wavelength	0.71073 Å	
Crystal system	Monoclinic	
Space group	C2/m	
Unit cell dimensions	a = 16.3781(6) Å	α = 90°
	b = 25.3716(9) Å	β = 96.3570(10)°
	c = 9.9589(3) Å	γ = 90°
Volume	4112.9(2) Å^3	
Z	4	
Density (calculated)	1.468 g/cm^3	
Absorption coefficient	1.233 mm^{-1}	
F(000)	1912	
Crystal size	0.50 x 0.30 x 0.20 mm^3	
Theta range for data collection	2.06 to 28.29°	
Index ranges	-21<=h<=17, -33<=k<=26, -13<=l<=13	
Reflections collected	13200	
Independent reflections	4935 [*R*(int) = 0.0393]	
Completeness to theta = 28.29°	94.3 %	
Absorption correction	None	
Refinement method	Full-matrix least-squares on F^2	
Data / restraints / parameters	4935 / 0 / 249	
Goodness-of-fit on F^2	1.094	
Final *R* indices [*I*>2sigma(*I*)]	R_1 = 0.0336, wR_2 = 0.0803	
R indices (all data)	R_1 = 0.0394, wR_2 = 0.0834	

$R = \sum \| F_0 | - | F_c \| / \sum | F_0 |$, $R_w = \left[\sum w(F_0^2 - F_c^2)^2 / \sum w(F_0^2)^2 \right]^{1/2}$

$w = 1/[\sigma^2(F_o^2)+(0.0282P)^2+7.1613P]$ where $P = (F_o^2+2F_c^2)/3$.

Table 2. Atomic coordinates ($x10^4$) and equivalent isotropic displacement parameters ($Å^2 x\ 10^3$) for $[Cu_2([22]\text{-}HMTADO)(OH_2)_4]Cl_2 \cdot 10H_2O$

atom	x	y	z	*U*(eq)
Cu(1)	2434(1)	4399(1)	7480(1)	15(1)
Cl(1)	0	2102(1)	5000	25(1)
Cl(2)	0	2769(1)	0	30(1)
O(1)	2989(1)	5000	6748(2)	16(1)
O(2)	1819(1)	5000	8100(2)	15(1)
O(3W)	1464(1)	4461(1)	5261(1)	24(1)
O(4W)	3423(1)	4456(1)	9548(1)	24(1)
N(1)	3141(1)	3892(1)	6701(2)	17(1)
N(2)	1716(1)	3896(1)	8251(2)	16(1)
C(1)	4322(2)	5000	3402(3)	20(1)
C(2)	4097(1)	4534(1)	3988(2)	20(1)
C(3)	3645(1)	4521(1)	5107(2)	17(1)
C(4)	3399(1)	5000	5673(2)	15(1)
C(5)	3542(1)	4004(1)	5701(2)	19(1)
C(6)	3226(1)	3351(1)	7247(2)	22(1)
C(7)	2416(1)	3081(1)	7488(2)	18(1)
C(8)	2004(1)	3359(1)	8605(2)	20(1)
C(9)	970(1)	4008(1)	8415(2)	18(1)
C(10)	574(1)	4522(1)	8251(2)	17(1)
C(11)	-280(1)	4536(1)	8305(2)	19(1)
C(12)	-725(2)	5000	8298(3)	20(1)
C(13)	1012(2)	5000	8178(2)	15(1)
C(14)	4823(2)	5000	2218(3)	25(1)
C(15)	2638(1)	2524(1)	8000(2)	28(1)
C(16)	1831(1)	3053(1)	6185(2)	27(1)
C(17)	-1644(2)	5000	8353(3)	26(1)
O(5W)	1910(1)	3789(1)	3271(2)	40(1)
O(6W)	507(1)	3082(1)	3158(2)	29(1)
O(7W)	3062(1)	3794(1)	11539(2)	36(1)
O(8W)	483(1)	1819(1)	8125(2)	34(1)
O(9W)	0	1072(1)	0	29(1)
O(10W)	0	3854(1)	5000	25(1)

U(eq) is defined as one third of the trace of the orthogonalized U^{ij} tensor.

Table 3. Anisotropic displacement parameters ($Å^2$ x 10^3) for $[Cu_2([22]\text{-}HMTADO)(OH_2)_4]Cl_2 \cdot 10H_2O$

atom	U^{11}	U^{22}	U^{33}	U^{23}	U^{13}	U^{12}
Cu(1)	14(1)	12(1)	21(1)	0(1)	7(1)	0(1)
Cl(1)	29(1)	24(1)	24(1)	0	5(1)	0
Cl(2)	35(1)	33(1)	23(1)	0	6(1)	0
O(1)	16(1)	12(1)	20(1)	0	7(1)	0
O(2)	13(1)	12(1)	20(1)	0	6(1)	0
O(3W)	25(1)	22(1)	26(1)	-3(1)	4(1)	-2(1)
O(4W)	24(1)	22(1)	25(1)	2(1)	2(1)	0(1)
N(1)	13(1)	14(1)	23(1)	0(1)	3(1)	0(1)
N(2)	19(1)	14(1)	17(1)	1(1)	5(1)	-1(1)
C(1)	15(1)	30(2)	14(1)	0	1(1)	0
C(2)	17(1)	24(1)	18(1)	-5(1)	2(1)	1(1)
C(3)	14(1)	19(1)	17(1)	-2(1)	3(1)	-1(1)
C(4)	11(1)	17(1)	16(1)	0	2(1)	0
C(5)	17(1)	16(1)	24(1)	-5(1)	4(1)	0(1)
C(6)	18(1)	17(1)	32(1)	4(1)	6(1)	3(1)
C(7)	21(1)	10(1)	24(1)	2(1)	4(1)	0(1)
C(8)	22(1)	16(1)	23(1)	4(1)	6(1)	1(1)
C(9)	19(1)	17(1)	18(1)	-1(1)	5(1)	-5(1)
C(10)	17(1)	18(1)	15(1)	-1(1)	5(1)	-1(1)
C(11)	17(1)	23(1)	18(1)	0(1)	5(1)	-4(1)
C(12)	14(1)	29(1)	16(1)	0	4(1)	0
C(13)	15(1)	18(1)	12(1)	0	4(1)	0
C(14)	26(1)	36(2)	14(1)	0	6(1)	0
C(15)	30(1)	16(1)	40(1)	6(1)	8(1)	4(1)
C(16)	30(1)	22(1)	28(1)	-5(1)	0(1)	-1(1)
C(17)	16(1)	31(2)	32(2)	0	5(1)	0
O(5W)	48(1)	32(1)	45(1)	-9(1)	21(1)	-8(1)
O(6W)	37(1)	26(1)	25(1)	-2(1)	5(1)	-4(1)
O(7W)	33(1)	43(1)	34(1)	5(1)	12(1)	5(1)
O(8W)	40(1)	33(1)	28(1)	6(1)	7(1)	10(1)
O(9W)	31(1)	26(1)	31(1)	0	12(1)	0
O(10W)	24(1)	26(1)	26(1)	0	6(1)	0

Table 4. Hydrogen coordinates (x 10^4) and isotropic displacement parameters ($Å^2$ x 10^3) for $[Cu_2([22]\text{-HMTADO})(OH_2)_4]Cl_2 \cdot 10H_2O$

atom	x	y	z	*U* (eq)
H(3A)	1563	4310	4606	29
H(3B)	1054	4355	5350	29
H(3C)	1388	4805	5082	29
H(4A)	3305	4336	10148	28
H(4B)	3875	4353	9529	28
H(2C)	3432	4814	9603	28
H(2A)	4253	4216	3626	23
H(5A)	3796	3723	5313	22
H(6A)	3579	3362	8096	26
H(6B)	3499	3137	6625	26
H(8A)	1540	3149	8814	24
H(8B)	2393	3375	9413	24
H(9A)	647	3732	8666	21
H(11A)	-560	4218	8348	23
H(14A)	4917	5357	1952	30
H(14B)	4530	4814	1476	30
H(14C)	5340	4830	2473	30
H(15A)	2147	2340	8166	34
H(15B)	3002	2546	8823	34
H(15C)	2905	2338	7331	34
H(16A)	1694	3404	5874	32
H(16B)	1340	2870	6353	32
H(16C)	2093	2868	5508	32
H(17A)	-1840	5357	8341	31
H(17B)	-1767	4830	9167	31
H(17C)	-1907	4814	7584	31
H(5B)	1562	3538	3036	48
H(5C)	1869	4024	3823	48
H(6C)	383	3007	2399	35
H(6D)	445	2804	3600	35
H(7A)	3541	3592	11876	43
H(7B)	2822	3769	12117	43
H(8C)	317	1919	7355	40
H(8D)	380	2126	8547	40
H(9B)	120	1267	-589	34
H(10A)	112	3678	4401	30

2) $[Cu_2([22]\text{-}HMTADO)(OClO_3)(OH_2)]ClO_4 \cdot 2CH_3OH$.

Suitable crystals of $[Cu_2([22]\text{-}HMTADO)(OClO_3)(OH_2)]ClO_4 \cdot 2CH_3OH$ were obtained by slow evaporation of hot methanol solution of $[Cu_2([22]\text{-}HMTADO)(OClO_3)(OH_2)]ClO_4 \cdot 2H_2O$ at atmospheric pressure. The green crystal of $[Cu_2([22]\text{-}HMTADO)(OClO_3)(OH_2)]ClO_4 \cdot 2CH_3OH$ was attached to glass fibers and mounted on a Bruker SMART diffractometer equipped with a graphite monochromated Mo Kα (= 0.71073 Å) radiation, operating at 50 kV and 30 mA and a CCD detector ; 45 frames of two-dimensional diffraction images were collected and processed to obtain the cell parameters and orientation matrix. The crystallographic data, conditions for the collection of intensity data, and some features of the structure refinements are listed in Table 5, and atomic coordinates were given in Table 6. The intensity data were corrected for Lorentz and polarization effects. Absorption correction was not made during processing. Of the 11949 unique reflections measured, 4537 reflections in the range $1.75° \leq 2\Theta \leq 28.26°$ were considered to be observed($I>2\sigma(I)$) and were used in subsequent structure analysis. The program SAINTPLUS[50] was used for integration of the diffraction profiles. The structures were solved by direct methods using the SHELXS program of the SHELXTL package[51] and refined by full matrix least squares against F^2 for all data using SHELXL. All non-H atoms were refined with anisotropic displacement parameters (Table 7). Hydrogen atoms were placed in idealized positions [U_{iso} = $1.2U_{eq}$(parent atom)]. Hydrogen coordinates and isotropic displacement parameters were given in Table 8.

Table 5. Crystal data and structure refinement for $[Cu_2([22]\text{-HMTADO})\text{-}(OClO_3)(OH_2)]ClO_4 \cdot 2H_2O$

Empirical formula	$C_{30}H_{44}Cl_2Cu_2N_4O_{13}$	
Formula weight	866.67	
Temperature	173(2) K	
Wavelength	0.71073 Å	
Crystal system	Monoclinic	
Space group	C2(1)/m	
Unit cell dimensions	a = 9.6501(5) Å	α = 90°
	b = 16.6054(10) Å	β = 93.5660(10)°
	c = 11.6891(7) Å	γ = 90°
Volume	1869.48(19) $Å^3$	
Z	2	
Density (calculated)	1.540 g/cm^3	
Absorption coefficient	1.347 mm^{-1}	
F(000)	896	
Crystal size	0.25 x 0.20 x 0.10 mm^3	
Theta range for data collection	1.75 to 28.26°	
Index ranges	-12<=h<=12, -21<=k<=22, -15<=l<=11	
Reflections collected	11949	
Independent reflections	4537 [*R*(int) = 0.0472]	
Completeness to theta = 28.26°	94.7 %	
Absorption correction	None	
Refinement method	Full-matrix least-squares on F^2	
Data / restraints / parameters	4537 / 59 / 271	
Goodness-of-fit on F^2	1.056	
Final *R* indices [*I*>2sigma(*I*)]	R_1 = 0.0647, wR_2 = 0.1729	
R indices (all data)	R_1 = 0.0917, wR_2 = 0.1925	

$R = \sum \| F_0 | - | F_c \| / \sum | F_0 |$, $R_w = \left[\sum w(F_0^2 - F_c^2)^2 / \sum w(F_0^2)^2 \right]^{1/2}$

$w = 1/[\sigma^2(F_o^2)+(0.0934P)^2+5.3013P]$ where $P = (F_o^2+2F_c^2)/3$.

Table 6. Atomic coordinates ($x10^4$) and equivalent isotropic displacement parameters ($Å^2 x\ 10^3$) for $[Cu_2([22]\text{-}HMTADO)(OClO_3)(OH_2)]ClO_4 \cdot 2CH_3OH$

	x	y	z	*U*(eq)
Cu(1)	5187(1)	-2500	553(1)	24(1)
Cu(2)	6628(1)	-2500	-1680(1)	29(1)
Cl(1)	8883(2)	-2500	1144(1)	32(1)
O(1)	5912(3)	-1749(2)	-552(2)	28(1)
O(2)	9607(5)	-1794(3)	1556(4)	71(1)
O(3)	8786(5)	-2500	-93(4)	35(1)
O(4)	7500(5)	-2500	1562(4)	37(1)
O(1W)	4524(8)	-2500	-2780(7)	107(3)
N(1)	4484(4)	-1624(2)	1456(3)	26(1)
N(2)	7421(4)	-1621(3)	-2534(3)	35(1)
C(1)	3525(6)	-2500	2977(5)	27(1)
C(2)	3355(4)	-1740(3)	2238(4)	30(1)
C(3)	5084(4)	-933(3)	1501(4)	29(1)
C(4)	6150(4)	-646(3)	763(4)	28(1)
C(5)	6776(5)	84(3)	1062(4)	34(1)
C(6)	7747(5)	454(3)	423(5)	37(1)
C(7)	8052(5)	76(3)	-590(4)	37(1)
C(8)	7438(5)	-654(3)	-950(4)	32(1)
C(9)	6492(4)	-1045(3)	-251(4)	27(1)
C(10)	7752(5)	-941(3)	-2074(4)	37(1)
C(11)	7734(5)	-1743(4)	-3739(4)	42(1)
C(12)	8573(6)	-2500	-3960(6)	33(2)
C(13)	2303(7)	-2500	3770(5)	32(1)
C(14)	4919(7)	-2500	3671(6)	36(2)
C(15)	8422(7)	1240(4)	788(5)	52(2)
C(16)	9942(7)	-2500	-3222(7)	38(2)
C(17)	8877(8)	-2500	-5243(6)	48(2)
Cl(2)	5490(20)	176(8)	4683(7)	352(19)
O(5)	5880(40)	225(13)	5879(9)	360(30)
O(6)	6040(20)	-561(6)	4231(13)	195(12)
O(7)	6040(30)	847(7)	4061(16)	320(20)
O(8)	4000(20)	160(20)	4500(30)	430(40)
O(9)	10539(16)	411(6)	-3285(11)	226(7)
C(18)	10745(19)	-272(10)	-3869(12)	183(8)

Table 7. Anisotropic displacement parameters ($Å^2$ x 10^3) for $[Cu_2([22]\text{-}HMTADO)(OClO_3)(OH_2)]ClO_4 \cdot 2CH_3OH$

	U^{11}	U^{22}	U^{33}	U^{23}	U^{13}	U^{12}
Cu(1)	20(1)	31(1)	20(1)	0	5(1)	0
Cu(2)	25(1)	44(1)	19(1)	0	6(1)	0
Cl(1)	21(1)	44(1)	31(1)	0	1(1)	0
O(1)	25(1)	35(2)	23(2)	5(1)	7(1)	5(1)
O(2)	66(3)	88(3)	59(3)	-25(3)	11(2)	-43(3)
O(3)	24(2)	49(3)	32(3)	0	3(2)	0
O(4)	23(2)	57(3)	31(2)	0	5(2)	0
O(1W)	59(5)	201(11)	59(5)	0	-12(4)	0
N(1)	23(2)	32(2)	25(2)	2(2)	7(1)	4(2)
N(2)	30(2)	51(3)	24(2)	11(2)	8(2)	13(2)
C(1)	20(3)	38(4)	22(3)	0	7(2)	0
C(2)	23(2)	39(3)	27(2)	0(2)	10(2)	1(2)
C(3)	28(2)	35(2)	23(2)	3(2)	6(2)	4(2)
C(4)	26(2)	32(2)	27(2)	9(2)	5(2)	3(2)
C(5)	36(2)	34(2)	33(2)	5(2)	3(2)	0(2)
C(6)	37(3)	34(3)	41(3)	11(2)	5(2)	0(2)
C(7)	34(2)	36(3)	42(3)	17(2)	10(2)	3(2)
C(8)	31(2)	35(2)	32(2)	14(2)	9(2)	10(2)
C(9)	22(2)	30(2)	28(2)	10(2)	3(2)	6(2)
C(10)	32(2)	44(3)	36(3)	20(2)	13(2)	12(2)
C(11)	35(3)	71(4)	22(2)	12(2)	10(2)	12(2)
C(12)	21(3)	57(4)	22(3)	0	7(2)	0
C(13)	29(3)	45(4)	22(3)	0	8(3)	0
C(14)	26(3)	58(5)	23(3)	0	0(3)	0
C(15)	59(4)	48(3)	49(3)	6(3)	7(3)	-20(3)
C(16)	30(3)	45(4)	40(4)	0	0(3)	0
C(17)	33(4)	87(6)	25(4)	0	10(3)	0
Cl(2)	710(40)	172(14)	136(12)	-106(11)	-230(20)	300(20)
O(5)	610(70)	300(40)	150(20)	-170(20)	-160(30)	190(40)
O(6)	360(30)	73(9)	132(14)	-49(9)	-137(17)	72(13)
O(7)	630(60)	170(20)	149(18)	-73(16)	-130(30)	260(30)
O(8)	440(50)	390(60)	430(60)	-60(50)	-110(50)	350(50)
O(9)	375(19)	107(7)	183(11)	26(7)	-90(12)	-72(10)
C(18)	300(20)	148(14)	99(10)	-15(9)	-17(12)	-63(15)

Table 8. Hydrogen coordinates (x 10^4) and isotropic displacement parameters ($Å^2$ x 10^3) for $[Cu_2([22]\text{-HMTADO})(OClO_3)(OH_2)]ClO_4 \cdot 2CH_3OH$

	x	y	z	U(eq)
H(1W)	3920	-2039	-3156	129
H(2A)	2478	-1770	1787	35
H(2B)	3319	-1275	2737	35
H(3A)	4812	-578	2061	34
H(5A)	6528	337	1729	41
H(7A)	8688	317	-1048	44
H(10A)	8252	-591	-2514	44
H(11A)	8245	-1279	-3990	50
H(11B)	6867	-1768	-4203	50
H(13A)	2357	-2974	4246	38
H(13B)	1431	-2500	3314	38
H(14A)	4995	-2974	4146	43
H(14B)	5657	-2500	3151	43
H(15A)	8094	1403	1511	62
H(15B)	8189	1645	222	62
H(15C)	9411	1171	862	62
H(16A)	10471	-2974	-3390	46
H(16B)	9753	-2500	-2423	46
H(17A)	9402	-2026	-5418	58
H(17B)	8000	-2500	-5694	58
H(9)	9790	608	-3504	272
H(18A)	10972	-141	-4636	219
H(18B)	9915	-592	-3895	219
H(18C)	11495	-569	-3494	219

3) $[Cu_2([22]\text{-}HMTADO)(OH_2)_4]Br_2 \cdot 10H_2O$

Suitable crystals of $[Cu_2([22]\text{-}HMTADO)(OH_2)_4]Br_2 \cdot 10H_2O$ were obtained by slow evaporation of hot aqueous solution of $[Cu_2([22]\text{-}HMTADO)]Br_2 \cdot 1.5H_2O$ at atmospheric pressure. The dark green crystal of $[Cu_2([22]\text{-}HMTADO)(H_2O)_4]Br_2 \cdot 10H_2O$ was attached to glass fibers and mounted on a Bruker SMART diffractometer equipped with a graphite monochromated Mo Kα (= 0.71073 Å) radiation, operating at 50 kV and 30 mA and a CCD detector ; 45 frames of two-dimensional diffraction images were collected and processed to obtain the cell parameters and orientation matrix. The crystallographic data, conditions for the collection of intensity data, and some features of the structure refinements are listed in Table 9, and atomic coordinates were given in Table 10. The intensity data were corrected for Lorentz and polarization effects. Absorption correction was not made during processing. Of the 13614 unique reflections measured, 5085 reflections in the range $1.48° \leq 2\Theta \leq 28.46°$ were considered to be observed($I>2\sigma(I)$) and were used in subsequent structure analysis. The program SAINTPLUS[50] was used for integration of the diffraction profiles. The structures were solved by direct methods using the SHELXS program of the SHELXTL package[51] and refined by full matrix least squares against F^2 for all data using SHELXL. All non-H atoms were refined with anisotropic displacement parameters (Table 11). Hydrogen atoms were placed in idealized positions [$U_{iso} = 1.2U_{eq}$ (parent atom)]. Hydrogen coordinates and isotropic displacement parameters were given in Table 12.

Table 9. Crystal data and structure refinement for $[Cu_2([22]\text{-HMTADO})(OH_2)_4]\text{-}Br_2 \cdot 10H_2O$

Empirical formula	$C_{28}H_{62}Br_2Cu_2N_4O_{16}$	
Formula weight	997.72	
Temperature	173(2) K	
Wavelength	0.71073 Å	
Crystal system	Monoclinic	
Space group	C2/m	
Unit cell dimensions	a = 16.3913(12) Å	α = 90°
	b = 25.4870(19) Å	β = 96.753(2)°
	c = 10.1814(8) Å	γ = 90°
Volume	4223.9(6) $Å^3$	
Z	4	
Density (calculated)	1.569 g/cm^3	
Absorption coefficient	2.966 mm^{-1}	
F(000)	2056	
Crystal size	0.20 x 0.16 x 0.10 mm^3	
Theta range for data collection	1.48 to 28.46°	
Index ranges	-21<=h<=18, -33<=k<=33, -13<=l<=11	
Reflections collected	13614	
Independent reflections	5085 [*R*(int) = 0.0915]	
Completeness to theta = 28.29°	93.2 %	
Absorption correction	None	
Refinement method	Full-matrix least-squares on F^2	
Data / restraints / parameters	5086 / 30 / 291	
Goodness-of-fit on F^2	1.033	
Final *R* indices [*I*>2sigma(*I*)]	R_1 = 0.0403, wR_2 = 0.1015	
R indices (all data)	R_1 = 0.0660, wR_2 = 0.1131	

$R = \sum \| F_0 | - | F_c \| / \sum | F_0 |$, $R_w = \left[\sum w(F_0^2 - F_c^2)^2 / \sum w(F_0^2)^2 \right]^{1/2}$

$w = 1/[\sigma^2(F_o^2)+(0.00475P)^2+1.0787P]$ where $P = (F_o^2+2F_c^2)/3$.

Table 10. Atomic coordinates ($x10^4$) and equivalent isotropic displacement parameters ($Å^2 x\ 10^3$) for $[Cu_2([22]\text{-}HMTADO)(OH_2)_4]Br_2 \cdot 10H_2O$

	x	y	z	*U*(eq)
Br(1)	0	2093(1)	10000	28(1)
Br(2)	0	2780(1)	5000	30(1)
Cu(1)	2552(1)	598(1)	7488(1)	16(1)
O(1)	1993(2)	0	8194(3)	17(1)
O(2)	3167(2)	0	6886(3)	16(1)
O(1W)	1584(1)	544(1)	5453(2)	25(1)
O(2W)	3514(1)	540(1)	9700(2)	25(1)
O(3W)	503(2)	1778(1)	13165(2)	35(1)
O(4W)	535(2)	3117(1)	8202(2)	30(1)
O(5W)	1959(2)	3806(1)	8350(3)	41(1)
O(6W)	3015(2)	3813(1)	6531(3)	38(1)
O(7W)	0	3875(1)	10000	26(1)
O(8W)	0	1046(2)	5000	30(1)
N(1)	1854(2)	1101(1)	8255(2)	17(1)
N(2)	3274(2)	1098(1)	6748(2)	17(1)
C(1)	728(3)	0	11532(4)	21(1)
C(2)	938(2)	461(1)	10933(3)	22(1)
C(3)	1370(2)	476(1)	9824(3)	19(1)
C(4)	1601(2)	0	9258(4)	16(1)
C(5)	1464(2)	990(1)	9236(3)	21(1)
C(6)	1769(2)	1643(1)	7724(3)	24(1)
C(7)	2579(2)	1910(1)	7513(3)	19(1)
C(8)	2985(2)	1638(1)	6412(3)	23(1)
C(9)	4016(2)	985(1)	6593(3)	21(1)
C(10)	4412(2)	475(1)	6733(3)	18(1)
C(11)	5267(2)	459(1)	6682(3)	23(1)
C(12)	5707(3)	0	6677(4)	20(1)
C(13)	3977(3)	0	6813(4)	17(1)
C(14)	257(3)	0	12709(4)	30(1)
C(15)	2364(2)	2465(1)	7015(4)	32(1)
C(16)	3161(2)	1934(1)	8789(3)	30(1)
C(17)	6628(3)	0	6638(5)	28(1)

U(eq) is defined as one third of the trace of the orthogonalized U^{ij} tensor.

Table 11. Anisotropic displacement parameters ($Å^2$ x 10^3) for $[Cu_2([22]\text{-}HMTADO)(OH_2)_4]Br_2 \cdot 10H_2O$

	U^{11}	U^{22}	U^{33}	U^{23}	U^{13}	U^{12}
Br(1)	30(1)	28(1)	29(1)	0	8(1)	0
Br(2)	32(1)	35(1)	26(1)	0	7(1)	0
Cu(1)	15(1)	11(1)	23(1)	0(1)	9(1)	0(1)
O(1)	17(2)	14(2)	20(2)	0	10(1)	0
O(2)	14(1)	15(2)	22(2)	0	7(1)	0
O(1W)	25(1)	21(1)	27(1)	0(1)	1(1)	3(1)
O(2W)	25(1)	19(1)	32(1)	-1(1)	5(1)	-5(1)
O(3W)	44(2)	34(2)	29(1)	7(1)	8(1)	11(1)
O(4W)	38(2)	28(1)	26(1)	-3(1)	7(1)	-5(1)
O(5W)	48(2)	32(2)	48(2)	-7(1)	25(1)	-8(1)
O(6W)	40(2)	39(2)	36(2)	7(1)	11(1)	6(1)
O(7W)	25(2)	25(2)	28(2)	0	7(2)	0
O(8W)	32(2)	29(2)	29(2)	0	9(2)	0
N(1)	13(1)	14(1)	24(1)	1(1)	4(1)	0(1)
N(2)	18(1)	14(1)	19(1)	1(1)	5(1)	-1(1)
C(1)	18(2)	28(3)	16(2)	0	1(2)	0
C(2)	19(2)	26(2)	20(2)	-5(1)	4(1)	0(1)
C(3)	17(2)	19(2)	19(2)	0(1)	3(1)	1(1)
C(4)	10(2)	23(2)	17(2)	0	1(2)	0
C(5)	17(2)	20(2)	28(2)	-3(1)	7(1)	0(1)
C(6)	21(2)	18(2)	35(2)	6(1)	7(1)	6(1)
C(7)	19(2)	12(2)	26(2)	-1(1)	4(1)	1(1)
C(8)	24(2)	19(2)	28(2)	7(1)	9(1)	2(1)
C(9)	24(2)	18(2)	22(2)	2(1)	8(1)	-5(1)
C(10)	17(2)	20(2)	18(2)	-2(1)	5(1)	-1(1)
C(11)	20(2)	26(2)	24(2)	-1(1)	8(1)	-4(1)
C(12)	13(2)	29(3)	20(2)	0	3(2)	0
C(13)	15(2)	18(2)	18(2)	0	6(2)	0
C(14)	31(3)	40(3)	19(2)	0	9(2)	0
C(15)	33(2)	18(2)	46(2)	9(2)	12(2)	5(2)
C(16)	31(2)	26(2)	32(2)	-2(1)	2(2)	-2(2)
C(17)	16(2)	31(3)	37(3)	0	5(2)	0

Table 12. Hydrogen coordinates (x 10^4) and isotropic displacement parameters ($Å^2$ x 10^3) for $[Cu_2([22]\text{-HMTADO})(OH_2)_4]Br_2 \cdot 10H_2O$

	x	y	z	*U*(eq)
H(1WA)	1099(8)	652(11)	5490(40)	29
H(1WB)	1604(17)	220(4)	5310(30)	29
H(2WA)	3979(9)	674(10)	9660(40)	30
H(2WB)	3517(17)	216(3)	9810(30)	30
H(3WA)	420(20)	1872(16)	12367(14)	42
H(3WB)	480(30)	2055(9)	13620(30)	42
H(4WA)	400(20)	3009(15)	7421(16)	36
H(4WB)	530(30)	2825(8)	8590(30)	36
H(5WA)	1700(20)	3519(9)	8310(40)	49
H(5WB)	1840(30)	4009(14)	8960(30)	49
H(6WA)	3120(30)	4026(13)	5930(30)	45
H(6WB)	3350(20)	3558(11)	6650(40)	45
H(7WA)	-90(20)	3664(11)	10610(30)	31
H(8WA)	-90(20)	1249(12)	5630(30)	36
H(2A)	781	784	11294	26
H(5)	1207	1275	9625	25
H(6A)	1488	1859	8340	29
H(6B)	1414	1633	6868	29
H(8A)	2586	1625	5603	28
H(8B)	3459	1852	6209	28
H(9)	4347	1268	6357	25
H(11)	5553	782	6649	27
H(14A)	167	-362	12981	35
H(14B)	-275	173	12477	35
H(14C)	570	190	13440	35
H(15A)	2105	2657	7689	38
H(15B)	1984	2445	6199	38
H(15C)	2866	2647	6840	38
H(16A)	2885	2105	9478	36
H(16B)	3652	2134	8642	36
H(16C)	3320	1577	9072	36
H(17A)	6829	-362	6656	34
H(17B)	6896	190	7407	34
H(17C)	6755	172	5826	34

4) $[Ni_2([22]\text{-}HMTADO)(OH_2)_4](ClO_4)_2 \cdot 3H_2O$.

Crystallization from water formed $[Ni_2([22]\text{-}HMTADO)(OH_2)_4](ClO_4)_2 \cdot 3H_2O$ as good crystals suitable for X-ray crystallography. The pale brown crystal of $[Ni_2([22]\text{-}HMTADO)(OH_2)_4](ClO_4)_2 \cdot 3H_2O$ was attached to glass fibers and mounted on a Bruker SMART diffractometer equipped with a graphite monochromated Mo Kα (= 0.71073 Å) radiation, operating at 50 kV and 30 mA and a CCD detector ; 45 frames of two-dimensional diffraction images were collected and processed to obtain the cell parameters and orientation matrix. The crystallographic data, conditions for the collection of intensity data, and some features of the structure refinements are listed in Table 13, and atomic coordinates were given in Table 14. The intensity data were corrected for Lorentz and polarization effects. Absorption correction was not made during processing. Of the 24087 unique reflections measured, 8863 reflections in the range $1.83° \leq 2\Theta \leq 28.27°$ were considered to be observed($I>2\sigma(I)$) and were used in subsequent structure analysis. The program SAINTPLUS[50] was used for integration of the diffraction profiles. The structures were solved by direct methods using the SHELXS program of the SHELXTL package[51] and refined by full matrix least squares against F^2 for all data using SHELXL. All non-H atoms were refined with anisotropic displacement parameters (Table 15). Hydrogen atoms were placed in idealized positions [U_{iso} = 1.2U_{eq}(parent atom)]. Hydrogen coordinates and isotropic displacement parameters were given in Table 16.

Table 13. Crystal data and structure refinement for $[Ni_2([22]\text{-}HMTADO)(OH_2)_4]\text{-}(ClO_4)_2 \cdot 3H_2O$

Empirical formula	$C_{28}H_{48}Cl_2N_4Ni_2O_{17}$	
Formula weight	901.02	
Temperature	173(2) K	
Wavelength	0.71073 Å	
Crystal system	Monoclinic	
Space group	P2(1)/c	
Unit cell dimensions	a = 9.4152(6) Å	α= 90°
	b = 22.2913(13) Å	β= 95.2790(10)°
	c = 18.2102(11) Å	γ = 90°
Volume	3805.7(4) $Å^3$	
Z	4	
Density (calculated)	1.573 g/cm^3	
Absorption coefficient	1.206 mm^{-1}	
F(000)	1880	
Crystal size	0.45 x 0.35 x 0.15 mm^3	
Theta range for data collection	1.83 to 28.27°.	
Index ranges	-12<=h<=11, -28<=k<=26, -21<=l<=23	
Reflections collected	24087	
Independent reflections	8863 [*R*(int) = 0.0659]	
Completeness to theta = 28.27°	93.8 %	
Absorption correction	None	
Refinement method	Full-matrix least-squares on F^2	
Data / restraints / parameters	8863 / 23 / 522	
Goodness-of-fit on F^2	1.046	
Final R indices [*I*>2sigma(*I*)]	R_1 = 0.0328, wR_2 = 0.0888	
R indices (all data)	R_1 = 0.0427, wR_2 = 0.0952	

$R = \sum \| F_0 | - | F_c \| / \sum | F_0 |$, $R_w = \left[\sum w(F_0^2 - F_c^2)^2 / \sum w(F_0^2)^2 \right]^{1/2}$

$w = 1/[\sigma^2(F_o^2)+(0.0451P)^2+1.7091P]$ where $P = (F_o^2+2F_c^2)/3$.

Table 14. Atomic coordinates ($x10^4$) and equivalent isotropic displacement parameters ($Å^2 x\ 10^3$) for $[Ni_2([22]\text{-}HMTADO)(OH_2)_4](ClO_4)_2 \cdot 3H_2O$

	x	y	z	*U*(eq)
Ni(1)	1797(1)	6817(1)	8813(1)	17(1)
Ni(2)	-691(1)	7442(1)	9488(1)	17(1)
Cl(1)	1276(1)	5720(1)	6193(1)	28(1)
O(3)	2415(3)	5299(1)	6206(2)	73(1)
O(4)	185(2)	5563(1)	5646(1)	55(1)
O(5)	707(2)	5714(1)	6898(1)	49(1)
O(6)	1803(2)	6309(1)	6054(1)	47(1)
Cl(2)	4328(1)	8727(1)	6524(1)	25(1)
O(7)	4578(2)	9265(1)	6943(1)	50(1)
O(8)	2905(2)	8520(1)	6568(1)	50(1)
O(9)	5307(2)	8266(1)	6814(1)	38(1)
O(10)	4553(2)	8837(1)	5765(1)	34(1)
O(1W)	3001(2)	7031(1)	9825(1)	21(1)
O(2W)	428(2)	6723(1)	7799(1)	24(1)
O(3W)	856(2)	7595(1)	10470(1)	21(1)
O(4W)	-1935(2)	7259(1)	8483(1)	24(1)
O(1)	124(1)	6606(1)	9395(1)	18(1)
O(2)	922(2)	7636(1)	8874(1)	19(1)
N(1)	2461(2)	5962(1)	8864(1)	20(1)
N(2)	-2128(2)	7129(1)	10131(1)	19(1)
N(3)	-1305(2)	8303(1)	9496(1)	20(1)
N(4)	3384(2)	7142(1)	8265(1)	20(1)
C(1)	4681(2)	6138(1)	8215(1)	23(1)
C(2)	3398(2)	5731(1)	8327(1)	24(1)
C(3)	2203(2)	5621(1)	9400(1)	21(1)
C(4)	1245(2)	5738(1)	9969(1)	20(1)
C(5)	1342(2)	5341(1)	10564(1)	24(1)
C(6)	466(2)	5374(1)	11133(1)	26(1)
C(7)	-600(2)	5804(1)	11070(1)	23(1)
C(8)	-747(2)	6219(1)	10492(1)	19(1)
C(9)	211(2)	6207(1)	9933(1)	18(1)
C(10)	-1943(2)	6641(1)	10502(1)	20(1)
C(11)	-3454(2)	7462(1)	10200(1)	23(1)
C(12)	-3253(2)	8136(1)	10360(1)	22(1)
C(13)	-2743(2)	8471(1)	9694(1)	25(1)

C(14)	-500(2)	8734(1)	9324(1)	20(1)
C(15)	933(2)	8693(1)	9080(1)	20(1)
C(16)	1679(2)	9236(1)	9068(1)	25(1)
C(17)	3045(2)	9277(1)	8841(1)	27(1)
C(18)	3635(2)	8758(1)	8586(1)	24(1)
C(19)	2954(2)	8199(1)	8587(1)	20(1)
C(20)	1584(2)	8156(1)	8853(1)	17(1)
C(21)	3710(2)	7700(1)	8273(1)	21(1)
C(22)	4243(2)	6739(1)	7842(1)	25(1)
C(23)	5557(3)	5812(1)	7668(1)	32(1)
C(24)	5588(2)	6229(1)	8946(1)	28(1)
C(25)	653(3)	4955(1)	11786(1)	37(1)
C(26)	-2257(2)	8241(1)	11059(1)	29(1)
C(27)	-4747(2)	8383(1)	10477(1)	29(1)
C(28)	3830(3)	9868(1)	8876(2)	42(1)
O(5W)	-1865(2)	8195(1)	7491(1)	33(1)
O(6W)	599(2)	7762(1)	6923(1)	29(1)
O(7W)	-2688(3)	9305(1)	7838(2)	69(1)

Table 15. Anisotropic displacement parameters ($Å^2$ x 10^3) for $[Ni_2([22]\text{-}HMTADO)(OH_2)_4](ClO_4)_2 \cdot 3H_2O$

	U^{11}	U^{22}	U^{33}	U^{23}	U^{13}	U^{12}
Ni(1)	17(1)	16(1)	17(1)	-1(1)	3(1)	-1(1)
Ni(2)	16(1)	17(1)	18(1)	0(1)	3(1)	-1(1)
Cl(1)	38(1)	20(1)	25(1)	4(1)	0(1)	1(1)
O(3)	65(2)	51(1)	106(2)	31(1)	32(1)	33(1)
O(4)	75(2)	57(1)	31(1)	6(1)	-15(1)	-27(1)
O(5)	81(2)	41(1)	26(1)	-3(1)	12(1)	-7(1)
O(6)	46(1)	28(1)	65(1)	18(1)	-6(1)	-8(1)
Cl(2)	21(1)	30(1)	23(1)	-1(1)	2(1)	0(1)
O(7)	68(1)	41(1)	39(1)	-14(1)	1(1)	1(1)
O(8)	22(1)	69(1)	58(1)	19(1)	6(1)	-7(1)
O(9)	34(1)	43(1)	37(1)	8(1)	-1(1)	9(1)
O(10)	36(1)	42(1)	25(1)	2(1)	3(1)	-2(1)
O(1W)	20(1)	25(1)	19(1)	-2(1)	2(1)	1(1)
O(2W)	31(1)	23(1)	18(1)	-2(1)	1(1)	-1(1)
O(3W)	22(1)	21(1)	19(1)	-3(1)	1(1)	-2(1)

O(4W)	24(1)	26(1)	22(1)	0(1)	0(1)	-2(1)
O(1)	20(1)	18(1)	17(1)	1(1)	3(1)	-1(1)
O(2)	20(1)	17(1)	21(1)	-1(1)	4(1)	-2(1)
N(1)	18(1)	20(1)	22(1)	-3(1)	2(1)	-2(1)
N(2)	18(1)	20(1)	19(1)	-2(1)	2(1)	-2(1)
N(3)	20(1)	21(1)	20(1)	0(1)	2(1)	1(1)
N(4)	21(1)	23(1)	19(1)	0(1)	5(1)	1(1)
C(1)	22(1)	22(1)	25(1)	-3(1)	7(1)	1(1)
C(2)	24(1)	21(1)	26(1)	-7(1)	5(1)	0(1)
C(3)	18(1)	17(1)	27(1)	-2(1)	1(1)	1(1)
C(4)	19(1)	18(1)	24(1)	0(1)	1(1)	-4(1)
C(5)	22(1)	20(1)	29(1)	3(1)	0(1)	-1(1)
C(6)	26(1)	25(1)	26(1)	6(1)	-1(1)	-5(1)
C(7)	23(1)	26(1)	21(1)	1(1)	4(1)	-6(1)
C(8)	18(1)	20(1)	19(1)	-1(1)	1(1)	-4(1)
C(9)	19(1)	16(1)	17(1)	-1(1)	-1(1)	-6(1)
C(10)	16(1)	24(1)	19(1)	-2(1)	4(1)	-3(1)
C(11)	18(1)	25(1)	28(1)	-1(1)	4(1)	0(1)
C(12)	17(1)	25(1)	25(1)	-2(1)	3(1)	1(1)
C(13)	20(1)	24(1)	31(1)	2(1)	4(1)	5(1)
C(14)	24(1)	18(1)	19(1)	0(1)	1(1)	3(1)
C(15)	23(1)	19(1)	19(1)	2(1)	2(1)	-1(1)
C(16)	32(1)	18(1)	25(1)	0(1)	6(1)	-1(1)
C(17)	32(1)	20(1)	28(1)	3(1)	4(1)	-7(1)
C(18)	23(1)	25(1)	26(1)	5(1)	3(1)	-6(1)
C(19)	21(1)	21(1)	18(1)	2(1)	2(1)	-2(1)
C(20)	20(1)	18(1)	14(1)	1(1)	0(1)	-1(1)
C(21)	20(1)	24(1)	20(1)	5(1)	4(1)	-1(1)
C(22)	27(1)	26(1)	23(1)	-1(1)	10(1)	2(1)
C(23)	32(1)	30(1)	37(1)	-5(1)	15(1)	4(1)
C(24)	22(1)	31(1)	31(1)	-1(1)	3(1)	-2(1)
C(25)	35(1)	41(1)	34(1)	17(1)	3(1)	2(1)
C(26)	24(1)	37(1)	27(1)	-8(1)	2(1)	3(1)
C(27)	21(1)	32(1)	35(1)	-3(1)	7(1)	4(1)
C(28)	45(2)	25(1)	59(2)	0(1)	19(1)	-14(1)
O(5W)	34(1)	33(1)	31(1)	3(1)	-1(1)	6(1)
O(6W)	28(1)	30(1)	28(1)	1(1)	3(1)	-2(1)
O(7W)	61(2)	44(1)	94(2)	-30(1)	-30(1)	11(1)

Table 16. Hydrogen coordinates (x 10^4) and isotropic displacement parameters ($Å^2$ x 10^3) for $[Ni_2([22]\text{- HMTADO})(H_2O)_4](ClO_4)_2 \cdot 3H_2O$

	x	y	z	*U*(eq)
H(1WA)	2450(20)	7180(11)	10110(11)	26
H(1WB)	3370(30)	6754(8)	10089(11)	26
H(2WA)	460(30)	6429(7)	7517(11)	29
H(2WB)	620(30)	7001(8)	7512(11)	29
H(3WA)	720(30)	7442(10)	10878(7)	25
H(3WB)	1120(30)	7948(6)	10574(13)	25
H(4WA)	-1970(30)	7546(8)	8187(11)	29
H(4WB)	-1460(20)	7001(9)	8281(12)	29
H(2A)	2840	5679	7856	28
H(2B)	3748	5340	8489	28
H(3A)	2680	5255	9430	25
H(5A)	2028	5040	10579	29
H(7A)	-1246	5817	11427	28
H(10A)	-2643	6544	10810	24
H(11A)	-3941	7284	10593	28
H(11B)	-4068	7416	9745	28
H(13A)	-3423	8399	9270	30
H(13B)	-2748	8898	9797	30
H(14A)	-872	9119	9357	25
H(16A)	1241	9583	9219	30
H(18A)	4526	8781	8406	29
H(21A)	4529	7801	8052	25
H(22A)	5102	6950	7738	30
H(22B)	3706	6653	7373	30
H(23A)	5867	5431	7870	38
H(23B)	6375	6050	7581	38
H(23C)	4980	5751	7212	38
H(24A)	5832	5845	9163	33
H(24B)	5058	6456	9276	33
H(24C)	6444	6441	8860	33
H(25A)	1439	4690	11730	44
H(25B)	-202	4724	11812	44

H(25C)	840	5184	12230	44
H(26A)	-2149	8664	11145	35
H(26B)	-1342	8067	11000	35
H(26C)	-2654	8058	11471	35
H(27A)	-4681	8805	10581	35
H(27B)	-5112	8179	10883	35
H(27C)	-5376	8319	10038	35
H(28A)	4752	9815	8700	51
H(28B)	3943	10007	9377	51
H(28C)	3295	10157	8574	51
H(5WA)	-2600(20)	8164(17)	7196(16)	71(12)
H(5WB)	-1930(30)	8525(7)	7708(15)	50(9)
H(6WA)	-110(30)	7954(13)	7062(15)	34
H(6WB)	1200(30)	8009(13)	6973(15)	34
H(7WA)	-2540(40)	9608(11)	8107(18)	82
H(7WB)	-3537(15)	9337(19)	7670(20)	82

5) $[Ni_2([22]\text{-}HMTADO)(OH_2)_4]Br_2 \cdot 10H_2O$

Suitable crystals of $[Ni_2([22]\text{-}HMTADO)(OH_2)_4]Br_2 \cdot 10H_2O$ were obtained by slow evaporation of hot aqueous solution of $[Ni_2([22]\text{-}HMTADO)]Br_2 \cdot 1.5H_2O$ at atmospheric pressure. The dark green crystal of $[Ni_2([22]\text{-}HMTADO)(OH_2)_4]Br_2 \cdot 10H_2O$ was attached to glass fibers and mounted on a Bruker SMART diffractometer equipped with a graphite monochromated Mo Kα (= 0.71073 Å) radiation, operating at 50 kV and 30 mA and a CCD detector ; 45 frames of two-dimensional diffraction images were collected and processed to obtain the cell parameters and orientation matrix. The crystallographic data, conditions for the collection of intensity data, and some features of the structure refinements are listed in Table 17, and atomic coordinates were given in Table 18. The intensity data were corrected for Lorentz and polarization effects. Absorption correction was not made during processing. Of the 12901 unique reflections measured, 4890 reflections in the range $1.50° \leq 2\Theta \leq 28.29°$ were considered to be observed($I>2\sigma(I)$) and were used in subsequent structure analysis. The program SAINTPLUS[50] was used for integration of the diffraction profiles. The structures were solved by direct methods using the SHELXS program of the SHELXTL package[51] and refined by full matrix least squares against F^2 for all data using SHELXL. All non-H atoms were refined with anisotropic displacement parameters (Table 19). Hydrogen atoms were placed in idealized positions [$U_{iso} = 1.2U_{eq}$ (parent atom)]. Hydrogen coordinates and isotropic displacement parameters were given in Table 20.

Table 17. Crystal data and structure refinement for $[Ni_2([22]\text{-HMTADO})O(H_2)_4]$ $-Br_2 \cdot 10H_2O$

Empirical formula	$C_{28}H_{62}Br_2Ni_2N_4O_{16}$	
Formula weight	988.06	
Temperature	173(2) K	
Wavelength	0.71073 Å	
Crystal system	Monoclinic	
Space group	C2/m	
Unit cell dimensions	a = 16.2547(11) Å	α = 90°
	b = 25.3361(18) Å	β = 99.5040(10)°
	c = 10.1334(7) Å	γ = 90°
Volume	4116.0(3) $Å^3$	
Z	4	
Density (calculated)	1.594 g/cm^3	
Absorption coefficient	2.925 mm^{-1}	
F(000)	2048	
Crystal size	0.40 x 0.25 x 0.20 mm^3	
Theta range for data collection	1.50 to 28.29°	
Index ranges	-18<=h<=21, -32<=k<=33, -12<=l<=13	
Reflections collected	12901	
Independent reflections	4890 [*R*(int) = 0.0255]	
Completeness to theta = 28.29°	93.4 %	
Absorption correction	None	
Refinement method	Full-matrix least-squares on F^2	
Data / restraints / parameters	4890 / 28 / 291	
Goodness-of-fit on F^2	1.189	
Final *R* indices [*I*>2sigma(*I*)]	R_1 = 0.0567, wR_2 = 0.1165	
R indices (all data)	R_1 = 0.0699, wR_2 = 0.1214	

$R = \sum \| F_0 | - | F_c \| / \sum | F_0 |$, $R_w = \left[\sum w(F_0^2 - F_c^2)^2 / \sum w(F_0^2)^2 \right]^{1/2}$

$w = 1/[\sigma^2(F_o^2)+(0.00350P)^2+31.2749P]$ where $P = (F_o^2+2F_c^2)/3$.

Table 18. Atomic coordinates ($x10^4$) and equivalent isotropic displacement parameters ($Å^2 x\ 10^3$) for $[Ni_2([22]\text{-}HMTADO)(OH_2)_4]Br_2 \cdot 10H_2O$

	x	y	z	*U*(eq)
Br(1)	0	2109(1)	10000	25(1)
Br(2)	0	2751(1)	5000	25(1)
Ni(1)	2534(1)	604(1)	7474(1)	12(1)
O(1)	1921(2)	0	8138(4)	14(1)
O(2)	3153(2)	0	6806(4)	13(1)
O(1W)	1672(2)	548(1)	5615(3)	17(1)
O(2W)	3406(2)	542(1)	9406(3)	16(1)
O(3W)	523(2)	1748(1)	13191(3)	30(1)
O(4W)	524(2)	3153(1)	8223(3)	25(1)
O(5W)	1964(2)	3841(1)	8406(4)	37(1)
O(6W)	2981(2)	3855(2)	6511(4)	34(1)
O(7W)	0	3940(2)	10000	21(1)
O(8W)	0	1008(2)	5000	25(1)
N(1)	1821(2)	1119(1)	8239(3)	14(1)
N(2)	3268(2)	1119(1)	6748(3)	14(1)
C(1)	755(4)	0	11518(6)	18(1)
C(2)	955(3)	466(2)	10913(4)	19(1)
C(3)	1339(2)	481(2)	9778(4)	15(1)
C(4)	1558(3)	0	9198(6)	14(1)
C(5)	1425(3)	1004(2)	9186(4)	17(1)
C(6)	1745(3)	1668(2)	7712(5)	19(1)
C(7)	2572(2)	1931(1)	7538(4)	12(1)
C(8)	2976(3)	1666(2)	6434(4)	19(1)
C(9)	3998(3)	1001(2)	6544(4)	16(1)
C(10)	4401(2)	479(2)	6692(4)	15(1)
C(11)	5258(3)	465(2)	6663(4)	18(1)
C(12)	5708(3)	0	6676(6)	17(1)
C(13)	3951(4)	0	6750(6)	15(1)
C(14)	352(4)	0	12736(6)	26(1)
C(15)	2366(3)	2495(2)	7073(5)	25(1)
C(16)	3175(3)	1939(2)	8854(4)	23(1)
C(17)	6639(4)	0	6652(7)	25(1)

U(eq) is defined as one third of the trace of the orthogonalized U^{ij} tensor.

Table 19. Anisotropic displacement parameters ($Å^2$ x 10^3) for $[Ni_2([22]\text{-}HMTADO)(OH_2)_4]Br_2 \cdot 10H_2O$

	U^{11}	U^{22}	U^{33}	U^{23}	U^{13}	U^{12}
Br(1)	26(1)	21(1)	28(1)	0	7(1)	0
Br(2)	29(1)	27(1)	21(1)	0	5(1)	0
Ni(1)	12(1)	5(1)	20(1)	0(1)	7(1)	0(1)
O(1)	14(2)	10(2)	19(2)	0	8(2)	0
O(2)	12(2)	7(2)	21(2)	0	5(2)	0
O(1W)	17(1)	16(1)	20(2)	2(1)	4(1)	1(1)
O(2W)	14(1)	15(1)	19(2)	0(1)	5(1)	0(1)
O(3W)	37(2)	27(2)	26(2)	6(1)	7(2)	10(2)
O(4W)	32(2)	23(2)	19(2)	-1(1)	3(1)	-3(1)
O(5W)	38(2)	27(2)	47(2)	2(2)	7(2)	-8(2)
O(6W)	34(2)	36(2)	33(2)	-2(2)	4(2)	8(2)
O(7W)	27(2)	17(2)	20(2)	0	4(2)	0
O(8W)	33(3)	18(2)	25(2)	0	10(2)	0
N(1)	12(2)	9(1)	20(2)	1(1)	2(1)	-1(1)
N(2)	18(2)	10(1)	14(2)	0(1)	3(1)	2(1)
C(1)	17(3)	22(3)	13(3)	0	0(2)	0
C(2)	17(2)	21(2)	18(2)	-4(2)	1(2)	-2(2)
C(3)	11(2)	15(2)	18(2)	-3(2)	2(2)	0(1)
C(4)	10(3)	11(2)	20(3)	0	1(2)	0
C(5)	18(2)	10(2)	24(2)	-3(2)	5(2)	1(1)
C(6)	17(2)	11(2)	29(2)	3(2)	7(2)	3(2)
C(7)	14(2)	2(2)	18(2)	2(1)	0(2)	-1(1)
C(8)	22(2)	13(2)	24(2)	4(2)	6(2)	0(2)
C(9)	22(2)	11(2)	17(2)	1(1)	8(2)	-3(2)
C(10)	16(2)	15(2)	16(2)	1(2)	5(2)	-1(2)
C(11)	19(2)	19(2)	16(2)	-1(2)	2(2)	-2(2)
C(12)	12(3)	23(3)	14(3)	0	-1(2)	0
C(13)	20(3)	12(2)	15(3)	0	6(2)	0
C(14)	27(3)	33(3)	20(3)	0	6(3)	0
C(15)	27(2)	13(2)	37(3)	5(2)	12(2)	4(2)
C(16)	24(2)	18(2)	26(2)	-2(2)	-1(2)	-1(2)
C(17)	13(3)	24(3)	36(4)	0	3(3)	0

Table 20. Hydrogen coordinates (x 10^4) and isotropic displacement parameters ($Å^2$ x 10^3) for $[Ni_2([22]\text{-}HMTADO)(OH_2)_4]Br_2 \cdot 10H_2O$

	x	y	z	U (eq)
H(1WA)	1840(30)	703(17)	4970(30)	21
H(1WB)	1180(12)	651(18)	5640(50)	21
H(2WA)	3150(30)	662(17)	10010(30)	19
H(2WB)	3895(12)	665(17)	9460(50)	19
H(3WA)	450(30)	2028(12)	13610(50)	36
H(3WB)	370(30)	1830(20)	12376(17)	36
H(4WA)	470(30)	2886(13)	8710(40)	30
H(4WB)	370(30)	3050(20)	7426(19)	30
H(5WA)	1650(30)	3574(15)	8300(60)	45
H(5WB)	1900(40)	4110(15)	8870(50)	45
H(6WA)	3380(20)	3637(18)	6610(60)	41
H(6WB)	2680(30)	3810(20)	7100(40)	41
H(7WA)	-100(30)	3729(15)	10610(40)	26
H(8WA)	-90(30)	1220(15)	5610(40)	30
H(2A)	823	791	11294	23
H(5)	1154	1288	9550	20
H(6A)	1474	1887	8326	23
H(6B)	1373	1665	6834	23
H(8A)	2565	1661	5595	23
H(8B)	3456	1882	6272	23
H(9)	4319	1281	6266	19
H(11)	5545	790	6633	22
H(14A)	264	-365	13004	32
H(14B)	-186	182	12542	32
H(14C)	714	182	13465	32
H(15A)	2109	2682	7748	30
H(15B)	1977	2488	6224	30
H(15C)	2879	2677	6947	30
H(16A)	2909	2108	9544	28
H(16B)	3677	2136	8742	28
H(16C)	3330	1576	9126	28
H(17A)	6842	-365	6669	30
H(17B)	6928	190	7435	30
H(17C)	6747	174	5835	30

6) [Ni_2([22]-HMTADO)$(N_3)_2(OH_2)$].

Crystallization from acetonitrile formed [Ni_2([22]-HMTADO)$(N_3)_2(OH_2)$] as good crystals suitable for X-ray crystallography. The pale green crystal of [Ni_2([22]-HMTADO)$(N_3)_2(OH_2)$] was attached to glass fibers and mounted on a Bruker SMART diffractometer equipped with a graphite monochromated Mo Kα (= 0.71073 Å) radiation, operating at 50 kV and 30 mA and a CCD detector ; 45 frames of two-dimensional diffraction images were collected and processed to obtain the cell parameters and orientation matrix. The crystallographic data, conditions for the collection of intensity data, and some features of the structure refinements are listed in Table 21, and atomic coordinates were given in Table 22. The intensity data were corrected for Lorentz and polarization effects. Absorption correction was not made during processing. Of the 18991 unique reflections measured, 6954 reflections in the range $1.89° \leq 2\Theta \leq 28.26°$ were considered to be observed($I>2\sigma(I)$) and were used in subsequent structure analysis. The program SAINTPLUS[50] was used for integration of the diffraction profiles. The structures were solved by direct methods using the SHELXS program of the SHELXTL package[51] and refined by full matrix least squares against F^2 for all data using SHELXL. All non-H atoms were refined with anisotropic displacement parameters (Table 23). Hydrogen atoms were placed in idealized positions [U_{iso} = 1.2U_{eq}(parent atom)]. Hydrogen coordinates and isotropic displacement parameters were given in Table 24.

Table 21. Crystal data and structure refinement for $[Ni_2([22]\text{-HMTADO})(N_3)_2(OH_2)]$

Empirical formula	$C_{28}H_{36}Ni_2N_{10}O_3$	
Formula weight	678.09	
Temperature	173(2) K	
Wavelength	0.71073 Å	
Crystal system	Orthorhombic	
Space group	$P_{2(1)2(1)2(1)}$	
Unit cell dimensions	a = 8.3219(5) Å	α = 90°
	b = 16.6230(10) Å	β = 90°
	c = 21.4994(13) Å	γ = 90°
Volume	2974.1(3) $Å^3$	
Z	4	
Density (calculated)	1.514 g/cm^3	
Absorption coefficient	1.315 mm^{-1}	
F(000)	1416	
Crystal size	0.40 x 0.25 x 0.02 mm^3	
Theta range for data collection	1.89 to 28.26°	
Index ranges	-10<=h<=11, -21<=k<=21, -28<=l<=21	
Reflections collected	18991	
Independent reflections	6954 [*R*(int) = 0.0535]	
Completeness to theta = 28.29°	96.6 %	
Absorption correction	None	
Refinement method	Full-matrix least-squares on F^2	
Data / restraints / parameters	6954 / 5 / 394	
Goodness-of-fit on F^2	1.041	
Final *R* indices [*I*>2sigma(*I*)]	R_1 = 0.0487, wR_2 = 0.1124	
R indices (all data)	R_1 = 0.0623, wR_2 = 0.1200	

$R = \sum \| F_0 | - | F_c \| / \sum | F_0 |$, $R_w = \left[\sum w(F_0^2 - F_c^2)^2 / \sum w(F_0^2)^2 \right]^{1/2}$

$w = 1/[\sigma^2(F_o^2)+(0.0742P)^2+0.0000P]$ where $P = (F_o^2+2F_c^2)/3$.

Table 22. Atomic coordinates ($x10^4$) and equivalent isotropic displacement parameters ($Å^2 x\ 10^3$) for $[Ni_2([22]\text{-}HMTADO)(N_3)_2(OH_2)]$

	x	y	z	*U*(eq)
Ni(1)	3925(1)	7878(1)	3018(1)	18(1)
Ni(2)	2408(1)	7086(1)	1843(1)	19(1)
O(1)	3062(3)	6810(2)	2718(1)	21(1)
O(2)	3067(3)	8176(2)	2167(1)	20(1)
O(1W)	6109(3)	7518(2)	2551(1)	32(1)
N(1)	4851(4)	7389(2)	3796(2)	22(1)
N(2)	1423(4)	5984(2)	1741(2)	22(1)
N(3)	1304(4)	7604(2)	1123(2)	21(1)
N(4)	4671(4)	9009(2)	3180(1)	20(1)
N(5)	1585(4)	8117(2)	3393(2)	31(1)
N(6)	448(4)	8103(2)	3070(2)	32(1)
N(7)	-668(5)	8093(3)	2743(3)	73(2)
N(8)	4522(4)	6818(2)	1435(2)	38(1)
N(9)	4573(4)	6502(2)	935(2)	25(1)
N(10)	4667(4)	6182(3)	458(2)	38(1)
C(1)	5586(5)	8737(2)	4286(2)	25(1)
C(2)	5954(5)	7840(2)	4206(2)	29(1)
C(3)	4677(5)	6641(2)	3937(2)	22(1)
C(4)	3821(5)	6017(2)	3592(2)	22(1)
C(5)	3830(5)	5259(2)	3878(2)	25(1)
C(6)	3121(5)	4585(2)	3619(2)	29(1)
C(7)	2346(5)	4689(2)	3057(2)	26(1)
C(8)	2310(4)	5432(2)	2745(2)	22(1)
C(9)	3071(4)	6120(2)	3008(2)	19(1)
C(10)	1494(4)	5428(2)	2153(2)	23(1)
C(11)	702(5)	5743(2)	1145(2)	26(1)
C(12)	-361(4)	6382(2)	847(2)	22(1)
C(13)	647(4)	7100(3)	618(2)	25(1)
C(14)	1131(5)	8363(2)	1042(2)	22(1)
C(15)	1699(4)	9015(2)	1445(2)	20(1)
C(16)	1233(5)	9793(2)	1263(2)	23(1)
C(17)	1631(5)	10475(2)	1599(2)	23(1)

C(18)	2584(4)	10365(2)	2122(2)	22(1)
C(19)	3092(4)	9606(2)	2330(2)	19(1)
C(20)	2638(4)	8899(2)	1988(2)	18(1)
C(21)	4149(4)	9611(2)	2867(2)	21(1)
C(22)	5840(5)	9194(2)	3675(2)	25(1)
C(23)	6830(5)	9061(3)	4753(2)	33(1)
C(24)	3885(6)	8869(3)	4540(2)	35(1)
C(25)	3164(6)	3767(3)	3929(2)	40(1)
C(26)	-1140(5)	5998(3)	269(2)	31(1)
C(27)	-1666(5)	6651(2)	1295(2)	29(1)
C(28)	1051(5)	11297(2)	1409(2)	29(1)

U(eq) is defined as one third of the trace of the orthogonalized U^{ij} tensor.

Table 23. Anisotropic displacement parameters ($Å^2$ x 10^3) for [Ni_2([22]-HMTADO)$(N_3)_2(OH_2)$]

	U_{11}	U_{22}	U_{33}	U_{23}	U_{13}	U_{12}
Ni(1)	16(1)	16(1)	22(1)	-2(1)	-3(1)	-1(1)
Ni(2)	15(1)	19(1)	22(1)	-4(1)	-1(1)	-1(1)
O(1)	21(1)	18(1)	25(1)	0(1)	-5(1)	-1(1)
O(2)	22(1)	15(1)	25(1)	-3(1)	-4(1)	0(1)
O(1W)	18(1)	47(2)	31(2)	-10(1)	-1(1)	-2(1)
N(1)	21(2)	18(2)	28(2)	-2(1)	-3(1)	0(1)
N(2)	17(2)	20(2)	28(2)	-7(1)	-2(1)	3(1)
N(3)	16(2)	24(2)	23(2)	-4(1)	-2(1)	-4(1)
N(4)	18(1)	21(2)	22(2)	-2(1)	-1(1)	-2(1)
N(5)	19(2)	41(2)	31(2)	-12(2)	0(1)	-5(1)
N(6)	21(2)	23(2)	51(2)	11(2)	1(2)	-1(1)
N(7)	35(2)	81(4)	105(4)	63(3)	-36(3)	-25(2)
N(8)	21(2)	48(2)	45(2)	-21(2)	3(2)	-2(2)
N(9)	13(1)	28(2)	34(2)	-1(2)	4(1)	-1(1)
N(10)	27(2)	54(3)	33(2)	-9(2)	5(2)	0(2)
C(1)	27(2)	20(2)	28(2)	-4(2)	-9(2)	-4(2)
C(2)	29(2)	24(2)	33(2)	0(2)	-14(2)	-1(2)

C(3)	23(2)	21(2)	22(2)	2(2)	-1(2)	-1(2)
C(4)	17(2)	20(2)	29(2)	-2(2)	4(2)	1(2)
C(5)	26(2)	23(2)	25(2)	2(2)	2(2)	-2(2)
C(6)	32(2)	21(2)	33(2)	5(2)	7(2)	-5(2)
C(7)	26(2)	19(2)	33(2)	-3(2)	3(2)	-6(2)
C(8)	17(2)	19(2)	30(2)	-2(2)	3(2)	-1(1)
C(9)	16(2)	17(2)	24(2)	-1(2)	6(2)	-1(1)
C(10)	20(2)	17(2)	32(2)	-9(2)	-1(2)	-1(1)
C(11)	25(2)	21(2)	34(2)	-8(2)	0(2)	-1(2)
C(12)	14(2)	23(2)	28(2)	-8(2)	-3(2)	-2(2)
C(13)	29(2)	25(2)	22(2)	-5(2)	-2(2)	-3(2)
C(14)	18(2)	29(2)	21(2)	0(2)	-4(2)	-3(2)
C(15)	17(2)	21(2)	23(2)	-3(2)	-1(2)	0(1)
C(16)	19(2)	24(2)	25(2)	4(2)	0(2)	-2(2)
C(17)	21(2)	19(2)	28(2)	0(2)	2(2)	1(2)
C(18)	19(2)	20(2)	26(2)	-3(2)	2(2)	-1(2)
C(19)	17(2)	17(2)	22(2)	0(1)	1(1)	-2(1)
C(20)	16(2)	18(2)	20(2)	1(1)	3(2)	0(1)
C(21)	22(2)	20(2)	22(2)	-4(1)	0(2)	-3(1)
C(22)	24(2)	21(2)	30(2)	0(2)	-8(2)	-7(2)
C(23)	36(2)	31(2)	31(2)	1(2)	-13(2)	-9(2)
C(24)	35(2)	42(3)	29(2)	-11(2)	0(2)	-1(2)
C(25)	53(3)	24(2)	42(3)	9(2)	-6(2)	-10(2)
C(26)	30(2)	29(2)	35(2)	-9(2)	-10(2)	-3(2)
C(27)	17(2)	25(2)	44(3)	-5(2)	1(2)	-2(2)
C(28)	31(2)	22(2)	34(2)	5(2)	-5(2)	3(2)

Table 24. Hydrogen coordinates (x 10^4) and isotropic displacement parameters ($Å^2$ x 10^3) for $[Ni_2([22]\text{-HMTADO})(N_3)_2(H_2O)]$

	x	y	z	*U*(eq)
H(1WA)	7030(30)	7740(30)	2580(17)	39
H(1WB)	5950(40)	7370(30)	2180(7)	39
H(2A)	7058	7786	4039	34
H(2B)	5941	7584	4622	34

H(3)	5169	6474	4314	26
H(5)	4348	5206	4270	30
H(7)	1816	4242	2874	31
H(10)	932	4947	2055	28
H(11A)	52	5252	1213	32
H(11B)	1575	5604	851	32
H(13A)	1549	6894	364	30
H(13B)	-31	7440	346	30
H(14)	570	8523	677	27
H(16)	618	9853	894	27
H(18)	2909	10826	2351	26
H(21)	4496	10126	3004	25
H(22A)	5795	9778	3763	30
H(22B)	6932	9072	3518	30
H(23A)	6703	8783	5152	39
H(23B)	6663	9640	4812	39
H(23C)	7915	8967	4592	39
H(24A)	3755	8570	4930	42
H(24B)	3097	8678	4235	42
H(24C)	3716	9444	4618	42
H(25A)	2581	3377	3672	47
H(25B)	2655	3801	4340	47
H(25C)	4282	3592	3977	47
H(26A)	-1791	5535	396	38
H(26B)	-299	5820	-19	38
H(26C)	-1827	6395	61	38
H(27A)	-1172	6895	1663	34
H(27B)	-2309	6185	1421	34
H(27C)	-2360	7046	1089	34
H(28A)	1456	11699	1703	35
H(28B)	-127	11305	1409	35
H(28C)	1445	11421	990	35

7) [Ni_2([22]-HMTADO)(μ-S_2O_3)].

Crystallization from hot water formed [Ni_2([22]-HMTADO)(μ-S_2O_3)] as good crystals suitable for X-ray crystallography. The pale green crystal of [Ni_2([22]-HMTADO)(μ-S_2O_3)] was attached to glass fibers and mounted on a Bruker SMART diffractometer equipped with a graphite monochromated Mo Kα (= 0.71073 Å) radiation, operating at 50 kV and 30 mA and a CCD detector ; 45 frames of two-dimensional diffraction images were collected and processed to obtain the cell parameters and orientation matrix. The crystallographic data, conditions for the collection of intensity data, and some features of the structure refinements are listed in Table 25, and atomic coordinates were given in Table 26. The intensity data were corrected for Lorentz and polarization effects. Absorption correction was not made during processing. Of the 18648 unique reflections measured, 6987 reflections in the range $2.09° \leq 2\Theta \leq 28.29°$ were considered to be observed($I>2\sigma(I)$) and were used in subsequent structure analysis. The program SAINTPLUS[50] was used for integration of the diffraction profiles. The structures were solved by direct methods using the SHELXS program of the SHELXTL package[51] and refined by full matrix least squares against F^2 for all data using SHELXL. All non-H atoms were refined with anisotropic displacement parameters (Table 27). Hydrogen atoms were placed in idealized positions [U_{iso} = 1.2U_{eq}(parent atom)]. Hydrogen coordinates and isotropic displacement parameters were given in Table 28.

Table 25. Crystal data and structure refinement for [Ni_2([22]-HMTADO)(μ-S_2O_3)]

Empirical formula	$C_{28}H_{34}N_4Ni_2O_5S_2$	
Formula weight	688.13	
Temperature	173(2) K	
Wavelength	0.71073 Å	
Crystal system	Monoclinic	
Space group	P2(1)/n	
Unit cell dimensions	a = 15.4796(11) Å	α = 90°
	b = 13.0076(9) Å	β = 112.4380(10)°
	c = 15.9632(12) Å	γ = 90°
Volume	2970.9(4) $Å^3$	
Z	4	
Density (calculated)	1.538 g/cm^3	
Absorption coefficient	1.453 mm^{-1}	
F(000)	1432	
Crystal size	0.35 x 0.20 x 0.15 mm^3	
Theta range for data collection	2.09 to 28.29°.	
Index ranges	-20<=h<=15, -16<=k<=15, -20<=l<=20	
Reflections collected	18648	
Independent reflections	6987 [*R*(int) = 0.0513]	
Completeness to theta = 28.29°	94.7 %	
Absorption correction	None	
Refinement method	Full-matrix least-squares on F^2	
Data / restraints / parameters	6987 / 0 / 370	
Goodness-of-fit on F^2	1.021	
Final *R* indices [*I*>2sigma(*I*)]	R_1 = 0.0395, wR_2 = 0.0889	
R indices (all data)	R_1 = 0.0700, wR_2 = 0.1009	

$R = \sum \| F_0 | - | F_c \| / \sum | F_0 |$, $R_w = \left[\sum w(F_0^2 - F_c^2)^2 / \sum w(F_0^2)^2 \right]^{1/2}$

$w = 1/[\sigma^2(F_o^2)+(0.0428P)^2+1.4855P]$ where $P = (F_o^2+2F_c^2)/3$.

Table 26. Atomic coordinates ($x10^4$) and equivalent isotropic displacement parameters ($Å^2 x\ 10^3$) for [Ni_2([22]-HMTADO)(μ-S_2O_3)]

	x	y	z	*U*(eq)
Ni(1)	2492(1)	10089(1)	1240(1)	16(1)
Ni(2)	3399(1)	8814(1)	204(1)	16(1)
S(1)	2192(1)	10637(1)	-942(1)	21(1)
S(2)	2325(1)	11422(1)	213(1)	24(1)
O(1)	3779(1)	9602(2)	1371(1)	19(1)
O(2)	2252(1)	8798(2)	494(1)	18(1)
O(3)	3029(2)	9942(2)	-702(1)	22(1)
O(4)	1328(2)	10052(2)	-1246(2)	35(1)
O(5)	2243(2)	11403(2)	-1584(2)	30(1)
N(1)	3062(2)	10993(2)	2331(2)	20(1)
N(2)	4740(2)	8627(2)	373(2)	17(1)
N(3)	2895(2)	7678(2)	-694(2)	19(1)
N(4)	1236(2)	9964(2)	1322(2)	17(1)
C(1)	1600(2)	11154(2)	2669(2)	21(1)
C(2)	2442(2)	11684(3)	2581(2)	26(1)
C(3)	3948(2)	11116(2)	2778(2)	21(1)
C(4)	4719(2)	10628(2)	2627(2)	19(1)
C(5)	5619(2)	10926(2)	3211(2)	23(1)
C(6)	6422(2)	10554(2)	3135(2)	23(1)
C(7)	6312(2)	9862(2)	2443(2)	20(1)
C(8)	5431(2)	9532(2)	1837(2)	16(1)
C(9)	4614(2)	9907(2)	1926(2)	17(1)
C(10)	5443(2)	8898(2)	1089(2)	19(1)
C(11)	4980(2)	8153(2)	-350(2)	23(1)
C(12)	4440(2)	7173(2)	-771(2)	21(1)
C(13)	3395(2)	7410(3)	-1290(2)	24(1)
C(14)	2122(2)	7205(2)	-840(2)	23(1)
C(15)	1454(2)	7372(2)	-418(2)	20(1)
C(16)	686(2)	6706(2)	-676(2)	21(1)
C(17)	-44(2)	6820(2)	-381(2)	21(1)
C(18)	-8(2)	7659(2)	167(2)	19(1)
C(19)	749(2)	8352(2)	454(2)	16(1)
C(20)	1509(2)	8201(2)	187(2)	16(1)

C(21)	650(2)	9228(2)	980(2)	19(1)
C(22)	898(2)	10800(2)	1746(2)	23(1)
C(23)	1088(2)	11984(3)	2993(2)	31(1)
C(24)	1890(3)	10274(3)	3344(2)	33(1)
C(25)	7392(2)	10901(3)	3780(2)	33(1)
C(26)	4575(3)	6354(3)	-53(2)	34(1)
C(27)	4822(3)	6800(3)	-1478(2)	35(1)
C(28)	-882(2)	6099(2)	-693(2)	30(1)

U(eq) is defined as one third of the trace of the orthogonalized U^{ij} tensor.

Table 27. Anisotropic displacement parameters ($Å^2$ x 10^3) for [Ni_2([22]-HMTADO) -(μ-S_2O_3)]

	U^{11}	U^{22}	U^{33}	U^{23}	U^{13}	U^{12}
Ni(1)	14(1)	17(1)	18(1)	-3(1)	7(1)	0(1)
Ni(2)	14(1)	16(1)	18(1)	-2(1)	7(1)	1(1)
S(1)	17(1)	27(1)	22(1)	4(1)	9(1)	3(1)
S(2)	28(1)	20(1)	28(1)	3(1)	16(1)	5(1)
O(1)	13(1)	21(1)	21(1)	-4(1)	6(1)	1(1)
O(2)	16(1)	18(1)	22(1)	-5(1)	9(1)	-3(1)
O(3)	22(1)	23(1)	24(1)	5(1)	13(1)	7(1)
O(4)	19(1)	47(2)	37(1)	-4(1)	8(1)	-7(1)
O(5)	30(1)	35(1)	29(1)	14(1)	15(1)	14(1)
N(1)	19(1)	21(1)	21(1)	-5(1)	9(1)	-1(1)
N(2)	16(1)	14(1)	23(1)	-1(1)	11(1)	0(1)
N(3)	19(1)	19(1)	21(1)	-3(1)	9(1)	2(1)
N(4)	17(1)	19(1)	16(1)	-1(1)	7(1)	3(1)
C(1)	22(2)	24(2)	19(2)	-4(1)	10(1)	3(1)
C(2)	21(2)	27(2)	31(2)	-11(1)	11(1)	1(1)
C(3)	22(2)	21(2)	19(2)	-9(1)	7(1)	-2(1)
C(4)	17(2)	20(2)	19(2)	-1(1)	5(1)	-1(1)
C(5)	23(2)	22(2)	21(2)	-3(1)	5(1)	-1(1)
C(6)	16(2)	21(2)	26(2)	2(1)	2(1)	-4(1)
C(7)	15(2)	21(2)	23(2)	5(1)	6(1)	3(1)

C(8)	15(2)	13(1)	18(1)	4(1)	6(1)	0(1)
C(9)	17(2)	15(1)	18(1)	2(1)	6(1)	-1(1)
C(10)	14(2)	16(1)	28(2)	6(1)	8(1)	2(1)
C(11)	20(2)	27(2)	25(2)	-3(1)	13(1)	-2(1)
C(12)	22(2)	19(2)	24(2)	-2(1)	12(1)	4(1)
C(13)	21(2)	31(2)	20(2)	-6(1)	8(1)	1(1)
C(14)	23(2)	19(2)	23(2)	-6(1)	7(1)	-1(1)
C(15)	20(2)	18(2)	22(2)	-2(1)	8(1)	1(1)
C(16)	22(2)	15(2)	23(2)	-4(1)	4(1)	-1(1)
C(17)	17(2)	19(2)	25(2)	3(1)	4(1)	-3(1)
C(18)	13(2)	23(2)	19(2)	5(1)	4(1)	0(1)
C(19)	15(2)	15(1)	16(1)	3(1)	4(1)	1(1)
C(20)	14(2)	17(2)	14(1)	2(1)	3(1)	0(1)
C(21)	16(2)	23(2)	20(2)	2(1)	7(1)	4(1)
C(22)	17(2)	22(2)	26(2)	-4(1)	6(1)	5(1)
C(23)	26(2)	35(2)	33(2)	-14(2)	13(2)	2(2)
C(24)	37(2)	40(2)	25(2)	7(2)	14(2)	9(2)
C(25)	18(2)	39(2)	35(2)	-7(2)	1(2)	-1(2)
C(26)	39(2)	21(2)	43(2)	3(2)	17(2)	8(2)
C(27)	30(2)	40(2)	39(2)	-15(2)	18(2)	2(2)
C(28)	24(2)	25(2)	42(2)	-5(2)	11(2)	-8(1)

Table 28. Hydrogen coordinates (x 10^4) and isotropic displacement parameters ($Å^2$ x 10^3) for [Ni_2([22]-HMTADO)(μ-S_2O_3)]

	x	y	z	*U*(eq)
H(2A)	2213	12231	2117	31
H(2B)	2812	12018	3165	31
H(3)	4116	11588	3269	25
H(5)	5679	11405	3680	28
H(7)	6855	9599	2376	24
H(10)	6038	8655	1134	23
H(11A)	5656	7990	-99	27
H(11B)	4871	8666	-839	27
H(13A)	3336	7989	-1711	29

H(13B)	3090	6803	-1658	29
H(14)	1968	6676	-1284	27
H(16)	663	6152	-1072	25
H(18)	-513	7771	355	23
H(21)	85	9260	1082	23
H(22A)	322	10565	1819	27
H(22B)	729	11397	1329	27
H(23A)	540	11680	3062	37
H(23B)	888	12540	2546	37
H(23C)	1511	12260	3577	37
H(24A)	2213	9748	3132	40
H(24B)	1333	9972	3399	40
H(24C)	2310	10532	3936	40
H(25A)	7329	11389	4221	40
H(25B)	7716	11236	3432	40
H(25C)	7753	10303	4099	40
H(26A)	4329	6605	391	41
H(26B)	5243	6202	253	41
H(26C)	4241	5728	-340	41
H(27A)	5488	6635	-1176	42
H(27B)	4742	7342	-1928	42
H(27C)	4481	6184	-1782	42
H(28A)	-783	5554	-1071	36
H(28B)	-1447	6486	-1046	36
H(28C)	-955	5793	-163	36

8) [Ni(H_2[22]-HMTADO)($OHCH_3$)$_2$](ClO_4)$_2$.

Crystallization from methanol formed [Ni(H_2[22]-HMTADO)($OHCH_3$)$_2$] -(ClO_4)$_2$ as good crystals suitable for X-ray crystallography. The pale green crystal of [Ni(H_2[22]-HMTADO)($OHCH_3$)$_2$](ClO_4)$_2$ was attached to glass fibers and mounted on a Bruker SMART diffractometer equipped with a graphite monochromated Mo Kα (= 0.71073 Å) radiation, operating at 50 kV and 30 mA and a CCD detector ; 45 frames of two-dimensional diffraction images were collected and processed to obtain the cell parameters and orientation matrix. The crystallographic data, conditions for the collection of intensity data, and some features of the structure refinements are listed in Table 29, and atomic coordinates were given in Table 30. The intensity data were corrected for Lorentz and polarization effects. Absorption correction was not made during processing. Of the 11147 unique reflections measured, 7790 reflections in the range 1.38° ≤ 2Θ ≤ 28.33° were considered to be observed(I>2σ(I)) and were used in subsequent structure analysis. The program SAINTPLUS[50] was used for integration of the diffraction profiles. The structures were solved by direct methods using the SHELXS program of the SHELXTL package[51] and refined by full matrix least squares against F^2 for all data using SHELXL. All non-H atoms were refined with anisotropic displacement parameters (Table 31). Hydrogen atoms were placed in idealized positions [U_{iso} = 1.2U_{eq}(parent atom)]. Hydrogen coordinates and isotropic displacement parameters were given in Table 32.

Table 29. Crystal data and structure refinement for [Ni(H_2[22]-HMTADO)-($OHCH_3$)$_2$](ClO_4)$_2$

Empirical formula	$C_{30}H_{44}Cl_2N_4NiO_{12}$	
Formula weight	782.3	
Temperature	173(2) K	
Wavelength	0.71073 Å	
Crystal system	Triclinic	
Space group	P-1	
Unit cell dimensions	a = 9.5874(11) Å	α = 94.056(2)°
	b = 12.5956(14) Å	β = 92.061(2)°
	c = 14.8087(17) Å	γ = 102.497(2)°
Volume	1739.1(3) Å^3	
Z	2	
Density (calculated)	1.494 g/cm^3	
Absorption coefficient	0.778 mm^{-1}	
F(000)	820	
Crystal size	0.30 x 0.30 x 0.05 mm^3	
Theta range for data collection	1.38 to 28.33°.	
Index ranges	-12<=h<=6, -14<=k<=16, -19<=l<=19	
Reflections collected	11147	
Independent reflections	7790 [*R*(int) = 0.0585]	
Completeness to theta = 28.33°	90.0 %	
Absorption correction	None	
Refinement method	Full-matrix least-squares on F^2	
Data / restraints / parameters	7790 / 0 / 442	
Goodness-of-fit on F^2	1.031	
Final *R* indices [*I*>2sigma(*I*)]	R_1 = 0.0726, wR_2 = 0.1908	
R indices (all data)	R_1 = 0.1260, wR_2 = 0.2224	

$R = \sum \| F_0 | - | F_c \| / \sum | F_0 |$, $R_w = \left[\sum w(F_0^2 - F_c^2)^2 / \sum w(F_0^2)^2 \right]^{1/2}$

$w = 1/[\sigma^2(F_o^2)+(0.1147P)^2+1.2294P]$ where $P = (F_o^2+2F_c^2)/3$.

Table 30. Atomic coordinates ($x10^4$) and equivalent isotropic displacement parameters ($Å^2 x\ 10^3$) for $[Ni(H_2[22]\text{-}HMTADO)(OHCH_3)_2](ClO_4)_2$

	x	y	z	*U*(eq)
Ni(1)	7686(1)	6897(1)	7215(1)	21(1)
Cl(1)	10866(2)	7689(2)	10632(1)	45(1)
Cl(2)	3890(2)	7656(1)	5171(1)	38(1)
O(1)	6009(4)	6905(3)	8002(2)	22(1)
O(2)	7406(3)	8304(3)	6757(2)	20(1)
O(3)	9070(4)	7904(3)	8318(2)	29(1)
O(4)	6312(4)	6055(3)	6133(2)	26(1)
O(5)	11944(6)	7371(4)	11130(4)	66(2)
O(6)	10500(6)	7073(5)	9781(4)	70(2)
O(7)	9696(6)	7788(7)	11108(5)	109(3)
O(8)	11560(7)	8800(4)	10347(4)	76(2)
O(9)	2652(6)	7011(7)	4714(4)	125(3)
O(10)	5069(5)	7224(4)	4906(3)	52(1)
O(11)	3756(5)	7605(4)	6141(3)	46(1)
O(12)	4121(11)	8760(5)	4961(4)	121(3)
N(1)	7962(4)	5524(3)	7802(3)	22(1)
N(2)	4032(4)	8009(3)	8351(3)	22(1)
N(3)	5833(4)	9798(4)	6959(3)	24(1)
N(4)	9343(4)	6915(3)	6391(3)	19(1)
C(1)	10043(5)	5217(4)	6892(3)	22(1)
C(2)	8633(6)	4715(4)	7315(3)	23(1)
C(3)	7703(5)	5383(4)	8627(3)	24(1)
C(4)	6900(5)	5988(4)	9195(3)	22(1)
C(5)	6891(6)	5826(4)	10123(3)	26(1)
C(6)	6051(6)	6255(4)	10720(3)	25(1)
C(7)	5128(6)	6829(4)	10373(3)	24(1)
C(8)	5080(5)	7044(4)	9450(3)	20(1)
C(9)	6018(5)	6655(4)	8836(3)	21(1)
C(10)	4154(5)	7702(4)	9156(3)	22(1)
C(11)	3099(5)	8738(4)	8125(4)	25(1)
C(12)	3871(6)	9940(4)	8046(3)	23(1)
C(13)	4480(5)	10126(4)	7100(3)	25(1)
C(14)	6998(6)	10469(4)	6812(3)	25(1)
C(15)	8319(5)	10182(4)	6596(3)	21(1)
C(16)	9448(6)	11032(4)	6389(3)	24(1)

C(17)	10716(5)	10833(4)	6086(3)	23(1)
C(18)	10820(5)	9743(4)	5991(3)	21(1)
C(19)	9773(5)	8871(4)	6237(3)	18(1)
C(20)	8451(5)	9072(4)	6545(3)	18(1)
C(21)	10060(5)	7786(4)	6088(3)	19(1)
C(22)	9773(6)	5896(4)	6105(3)	23(1)
C(23)	10614(6)	4255(4)	6478(4)	30(1)
C(24)	11121(6)	5889(4)	7600(4)	27(1)
C(25)	6150(7)	6081(5)	11723(3)	34(1)
C(26)	5030(6)	10340(4)	8788(4)	31(1)
C(27)	2703(6)	10600(5)	8148(4)	31(1)
C(28)	11950(6)	11739(4)	5883(4)	28(1)
C(29)	8733(6)	8848(5)	8784(4)	34(1)
C(30)	5047(7)	5245(5)	6269(4)	37(1)

U(eq) is defined as one third of the trace of the orthogonalized U^{ij} tensor.

Table 31. Anisotropic displacement parameters ($Å^2$ x 10^3) for [Ni(H_2[22]-HMTADO)-$(OHCH_3)_2$]$(ClO_4)_2$

	U^{11}	U^{22}	U^{33}	U^{23}	U^{13}	U^{12}
Ni(1)	22(1)	21(1)	20(1)	5(1)	5(1)	5(1)
Cl(1)	31(1)	61(1)	43(1)	-6(1)	2(1)	15(1)
Cl(2)	30(1)	50(1)	36(1)	-3(1)	-1(1)	15(1)
O(1)	22(2)	24(2)	18(2)	2(1)	6(1)	2(2)
O(2)	16(2)	22(2)	22(2)	5(1)	5(1)	2(1)
O(3)	31(2)	27(2)	30(2)	3(2)	-2(2)	8(2)
O(4)	26(2)	28(2)	21(2)	6(2)	4(2)	2(2)
O(5)	57(3)	68(4)	74(4)	28(3)	-6(3)	10(3)
O(6)	69(4)	79(4)	61(3)	-20(3)	-6(3)	19(3)
O(7)	47(4)	181(8)	92(5)	-35(5)	35(3)	21(4)
O(8)	89(5)	56(3)	80(4)	9(3)	-5(3)	14(3)
O(9)	28(3)	249(9)	67(4)	-85(5)	0(3)	-4(4)
O(10)	36(3)	85(4)	43(3)	18(2)	17(2)	26(3)
O(11)	50(3)	54(3)	33(2)	1(2)	10(2)	11(2)
O(12)	262(11)	69(4)	60(4)	27(3)	16(5)	89(6)
N(1)	19(2)	19(2)	27(2)	0(2)	2(2)	4(2)

N(2)	22(2)	22(2)	24(2)	4(2)	9(2)	7(2)
N(3)	21(2)	25(2)	28(2)	1(2)	3(2)	6(2)
N(4)	22(2)	20(2)	16(2)	3(2)	4(2)	6(2)
C(1)	21(3)	21(3)	28(3)	6(2)	4(2)	12(2)
C(2)	29(3)	20(3)	22(3)	2(2)	6(2)	8(2)
C(3)	23(3)	20(3)	28(3)	7(2)	4(2)	3(2)
C(4)	24(3)	21(2)	20(2)	2(2)	5(2)	0(2)
C(5)	26(3)	22(3)	29(3)	10(2)	0(2)	0(2)
C(6)	34(3)	21(3)	17(2)	5(2)	6(2)	-1(2)
C(7)	30(3)	19(2)	20(2)	0(2)	9(2)	-1(2)
C(8)	22(3)	19(2)	19(2)	1(2)	6(2)	2(2)
C(9)	20(3)	14(2)	25(3)	-1(2)	4(2)	-5(2)
C(10)	22(3)	16(2)	26(3)	-1(2)	5(2)	1(2)
C(11)	17(3)	29(3)	27(3)	1(2)	0(2)	4(2)
C(12)	26(3)	26(3)	19(2)	1(2)	0(2)	11(2)
C(13)	18(3)	31(3)	28(3)	5(2)	0(2)	11(2)
C(14)	28(3)	23(3)	26(3)	4(2)	0(2)	7(2)
C(15)	20(3)	21(3)	22(3)	3(2)	4(2)	4(2)
C(16)	28(3)	19(3)	24(3)	3(2)	1(2)	4(2)
C(17)	22(3)	24(3)	20(2)	5(2)	0(2)	-1(2)
C(18)	18(3)	26(3)	18(2)	5(2)	2(2)	4(2)
C(19)	19(2)	20(2)	16(2)	7(2)	1(2)	4(2)
C(20)	17(2)	23(2)	13(2)	4(2)	0(2)	4(2)
C(21)	19(2)	23(3)	15(2)	4(2)	3(2)	6(2)
C(22)	26(3)	23(3)	21(3)	3(2)	7(2)	9(2)
C(23)	33(3)	27(3)	33(3)	4(2)	7(2)	13(2)
C(24)	30(3)	23(3)	30(3)	-3(2)	-3(2)	10(2)
C(25)	45(4)	36(3)	20(3)	7(2)	3(2)	6(3)
C(26)	33(3)	25(3)	31(3)	-4(2)	-8(2)	6(2)
C(27)	33(3)	37(3)	28(3)	0(2)	0(2)	22(3)
C(28)	26(3)	26(3)	30(3)	9(2)	4(2)	-2(2)
C(29)	37(3)	30(3)	34(3)	-1(2)	4(3)	5(3)
C(30)	38(3)	37(3)	28(3)	4(2)	0(3)	-7(3)

Table 32. Hydrogen coordinates (x 10^4) and isotropic displacement parameters ($Å^2$ x 10^3) for $[Ni(H_2[22]\text{-}HMTADO)(OHCH_3)_2](ClO_4)_2$

	x	y	z	*U*(eq)
H(3)	9440	7558	8690	35
H(4)	6116	6482	5761	31
H(2)	4528	7771	7923	26
H(3)	5849	9104	6977	29
H(2A)	7950	4306	6828	27
H(2B)	8820	4186	7743	27
H(3B)	8071	4829	8894	28
H(5B)	7502	5395	10353	31
H(7B)	4497	7094	10766	29
H(10B)	3566	7941	9596	26
H(11B)	2387	8722	8594	29
H(11C)	2569	8452	7541	29
H(13A)	3760	9718	6633	30
H(13B)	4616	10911	7004	30
H(14A)	6983	11223	6850	30
H(16A)	9332	11764	6459	29
H(18A)	11659	9583	5744	25
H(21A)	10849	7717	5735	22
H(22A)	10657	6076	5769	27
H(22B)	9016	5446	5683	27
H(23A)	11519	4531	6200	44
H(23B)	9915	3834	6016	44
H(23C)	10771	3786	6955	44
H(24A)	12005	6199	7311	41
H(24B)	11329	5422	8066	41
H(24C)	10726	6480	7880	41
H(25A)	5481	6441	12043	50
H(25B)	7127	6391	11970	50
H(25C)	5907	5297	11803	50
H(26A)	5493	11100	8714	46
H(26B)	5742	9888	8750	46
H(26C)	4605	10292	9380	46

H(27A)	3125	11376	8106	37
H(27B)	2285	10498	8738	37
H(27C)	1956	10348	7664	37
H(28A)	11683	12443	5991	34
H(28B)	12182	11637	5248	34
H(28C)	12786	11723	6279	34
H(29A)	9492	9167	9247	41
H(29B)	7822	8635	9074	41
H(29C)	8654	9387	8349	41
H(30A)	4560	4958	5681	44
H(30B)	4405	5575	6642	44
H(30C)	5314	4649	6578	44

III. Results and Discussion

1. Synthesis and characterization of the hexamethyl tetraazadioxa macrocyclic ligand (H_2[22]-HMTADO · 2$HClO_4$)

The Schiff base condensation of 2,6-diformyl-*p*-cresol and 2,2-dimethyl-1,3-propanediamine in a 1:1 mole ratio in ethanol and $HClO_4$ yields the 22-membered N_4O_2 tetraimine macrocycle H_2[22]-HMTADO · 2$HClO_4$ in 83% yield.

The 400 MHz ^{1}H NMR spectrum of the ligand, depicted in Fig. 1, consists of a singlet at 1.268 ppm and 2.117 ppm due to the lattice dimethyl and cresol CH_3 protons, respectively. The singlets at 8.594 and 3.879 ppm are due to the azomethine N=CH- and propylene CH_2 protons, respectively. The singlets at 7.327 and 13.599 ppm are due to the benzene and phenolic protons, respectively. The 100 MHz ^{13}C NMR spectrum of the ligand, depicted in Fig. 2, consists of nine peaks. The infrared spectra of the ligand recorded at room temperature are presented in Fig. 3. Infrared spectra of the ligand show ν(C=N) stretching vibration bands at around 1645 cm^{-1} and the absence of any carbonyl bands associated with the diformyl-phenol starting materials or nonmarcrocyclic intermediates. The IR spectra displayed C-H stretching vibrations from 3000 to 2800 cm^{-1}. Three C-H deformation bands exhibited at 1440, 1390, and 1370 cm^{-1} and two weak out-of-plan vibration bands at 815 and 781 cm^{-1}, respectively. The bands of the strong ionic ClO_4^- exhibited at near 1090 cm^{-1} and 624 cm^{-1}. The broad absorption band at

3429 cm^{-1} is attributed to ν(O-H). In the FAB mass spectrum the peak at m/z 461 corresponds to the molecular ion $(H_2[22]\text{-HMTADO})^+$. The FAB mass spectrum of this ligand is shown in Fig. 4. The UV-Visble spectrum of the free ligand H_2[22]-HMTADO exhibits four bands at 272 nm (ε = 24,238 $M^{-1}cm^{-1}$), 349 nm(ε = 10,490 $M^{-1}cm^{-1}$), 433 nm (ε = 13,990 $M^{-1}cm^{-1}$), and 462 nm(sh) (ε = 8,220 $M^{-1}cm^{-1}$) in Fig. 5, which are assigned to the π-π* and n-π * transitions. Thermogravimetry analysis have been carried out simultaneously for the H_2[22]-HMTADO · $2HClO_4$ ligand (Fig. 6). The result indicate that the macrocycle has relatively high thermal stability. Perchlorate ions are lost in the 275～347℃ range. The macrocyclic entity remains unchanged up to 350℃. Finally, the ligand is wholly decomposed above 678℃.

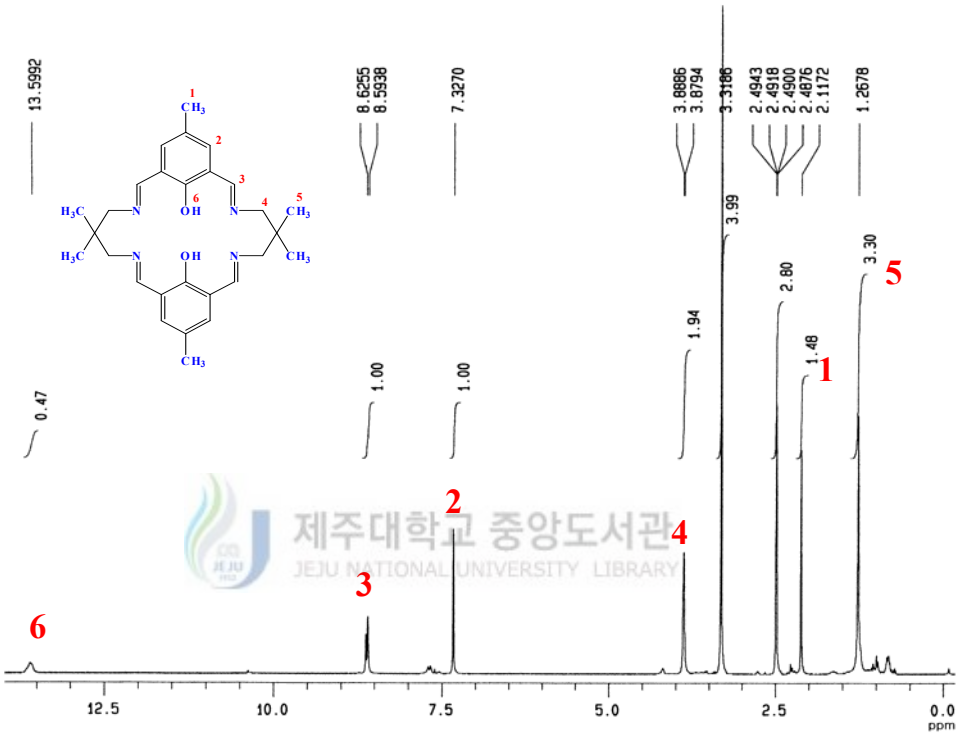

Fig. 1. ^{1}H-NMR spectrum of the H_2[22]-HMTADO · 2$HClO_4$ ligand (solvent : DMSO-d_6).

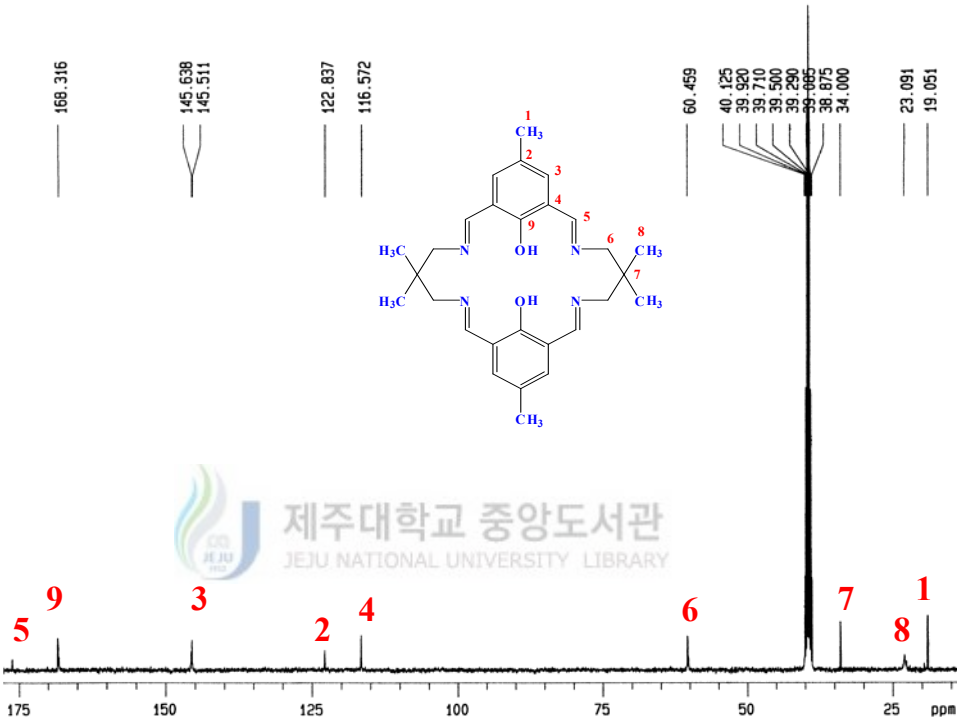

Fig. 2. ^{13}C-NMR spectrum of the H_2[22]-HMTADO · 2$HClO_4$ ligand (solvent : DMSO-d_6).

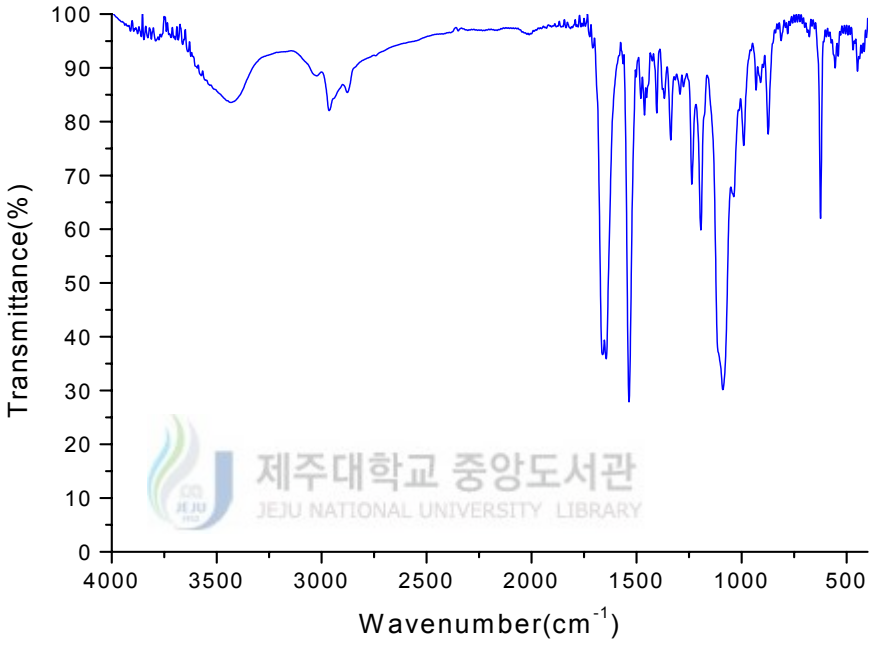

Fig. 3. IR spectrum of the $H_2HMTADO{\cdot}2HClO_4$ ligand.

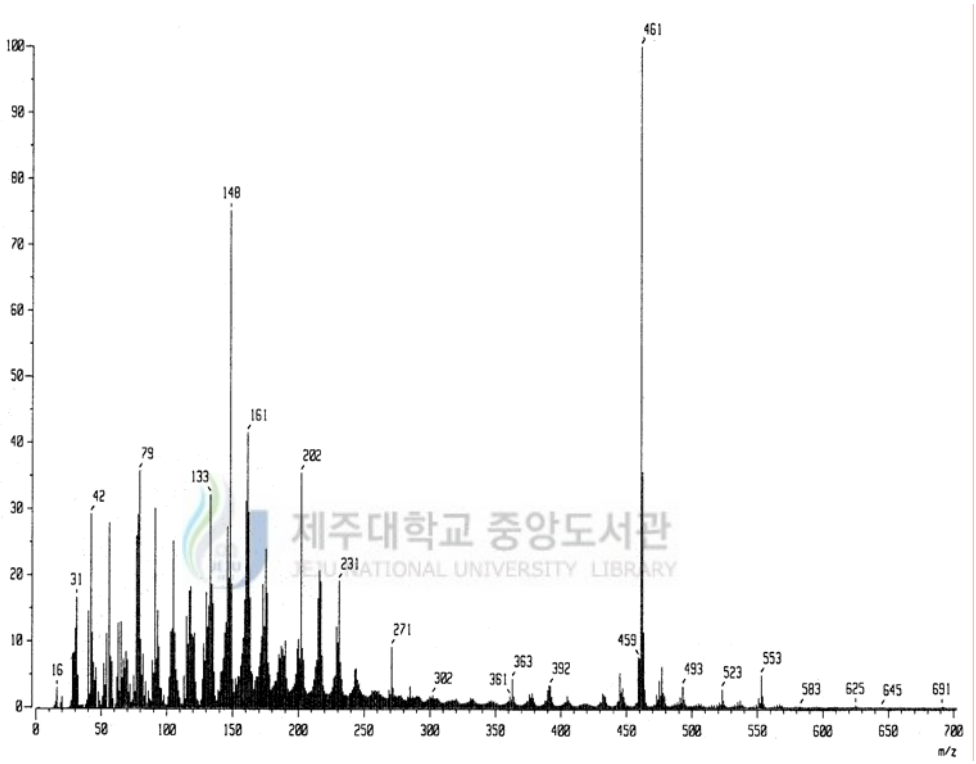

Fig. 4. FAB-mass spectrum of the $H_2HMTADO{\cdot}2HClO_4$ ligand.

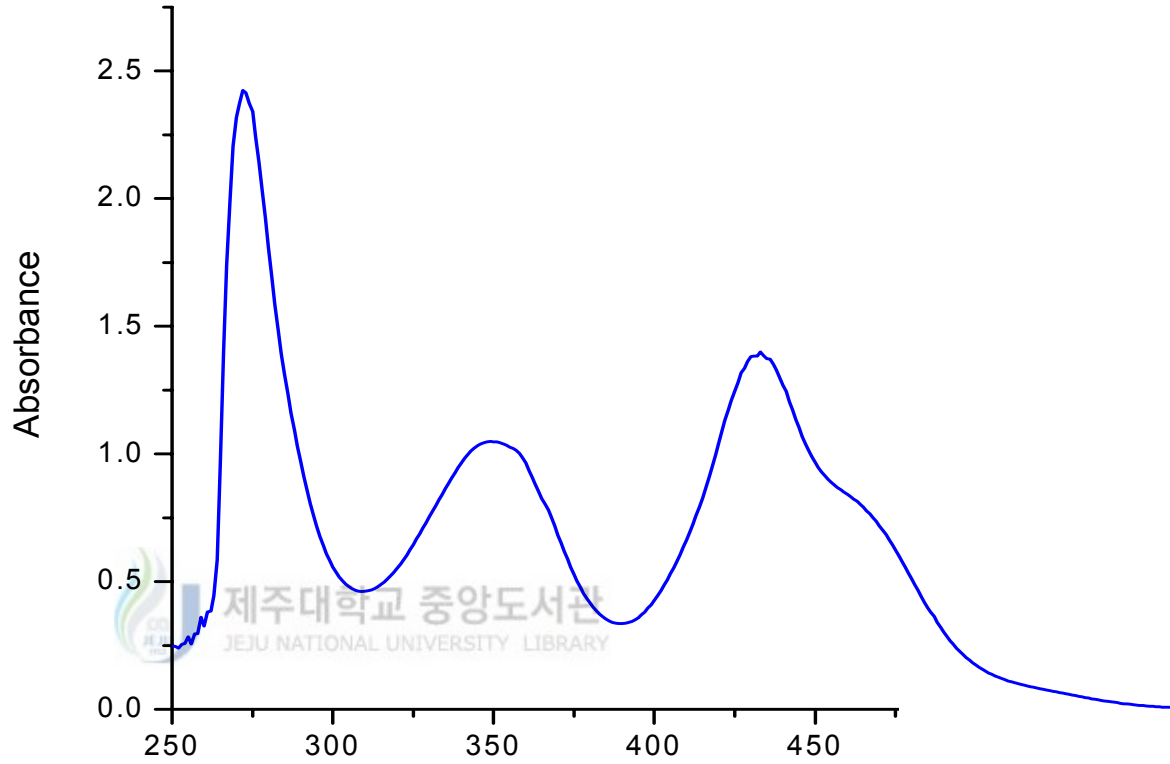

Fig. 5. Electronic absorption spectrum of H_2[22]-HMTADO · 2$HClO_4$ ligand in DMF.

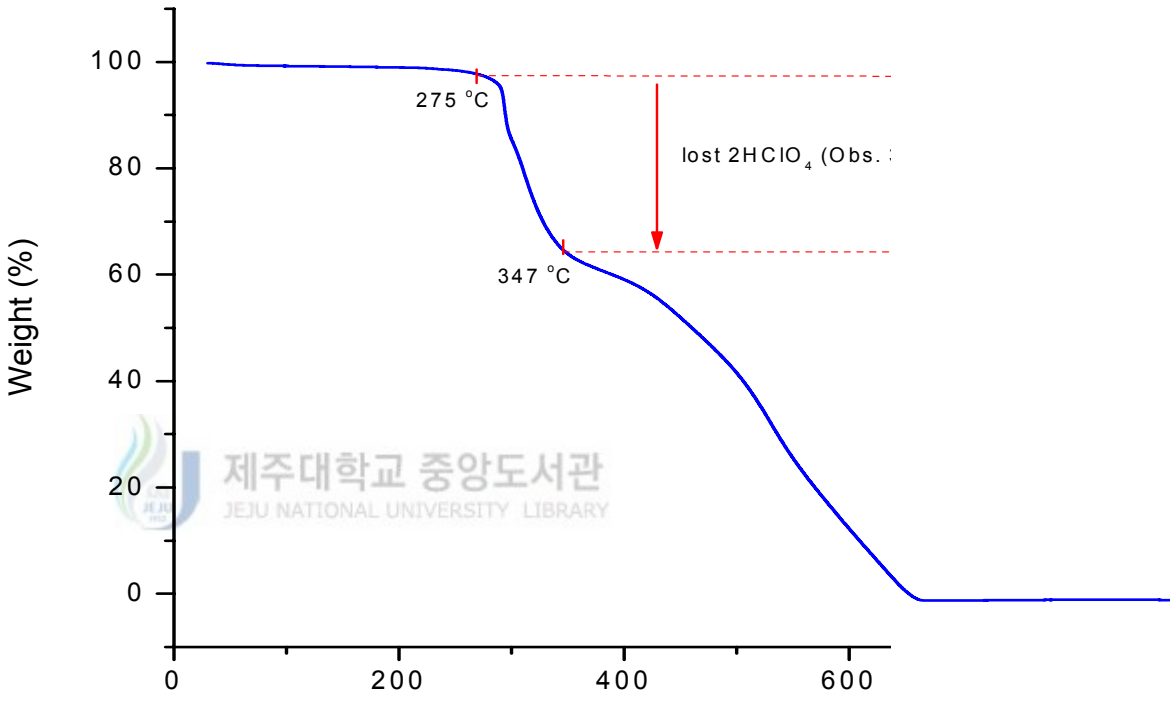

Fig. 6. TGA curve of H_2[22]-HMTADO · $2HClO_4$ ligand.

2. IR spectra of the complexes

1) Cu(II) complexes

IR spectra of the Cu(II) complexes were presented in Fig. 7 ~ 15. The characteristics of the complexes were listed in Table 33 and 34. The strong and sharp absorption bands occurring at 1635 - 1640 cm^{-1} are attributed to ν(C=N) of the coordinated [22]-HMTADO ligand[52, 53], and the absence of any carbonyl bands associated with the diformyl-phenol starting materials or nonmarcrocyclic intermediates. The IR spectra displayed C-H stretching vibrations from 3000 to 2800 cm^{-1}. The present complexes exhibited three C-H deformation bands at 1440, 1390, and 1370 cm^{-1} regions and two out-of-plan vibration bands at 820 and 765 cm^{-1} regions. The bands occurring in the IR spectra of the complexes in the 3300-3500 cm^{-1} regions may probably be due to the ν(OH) vibration of the coordinated and/or lattice water. A strong ionic ClO_4^- band at near 1095 cm^{-1} and 625 cm^{-1} in $[Cu_2([22]\text{-HMTADO})(OClO_3)(OH_2)]ClO_4 \cdot 2H_2O$ complex.

In metal-cyano complexes, the C≡N group may act as a terminal or bridging group. Terminal C≡N groups exhibit a sharp band in the region 2250-2000 cm^{-1} whereas bridging C≡N groups absorb near 2130 cm^{-1}.[54] Absorption bands are also observed in the ranges of 570-180 cm^{-1} and 450-295 cm^{-1}. Cyano complexes exhibit bands due to M-C stretching in the region 600-350 cm^{-1}, due to M-CN deformation in the region 130-60 cm^{-1}. In aqueous solution, the free CN^- ion absorbs near 2080 cm^{-1} (general range,

2250-2000 cm^{-1}, covalently bonded cyanide compounds absorb in the region 2250-2170 cm^{-1}). The CN^- ion may coordinate to a metal atom by σ -donation, which increases the frequency of the CN stretching vibration, or by π-donation from the metal, which reduces the CN stretching frequency. Since CN^- is a good σ-donor and a poor π-acceptor, the CN stretching frequency generally increases on coordination. The absorption peak at 2116 cm^{-1} in the $[Cu_2([22]\text{-HMTADO})(CN)_2] \cdot 0.5H_2O$ is assigned to the stretching frequency of CN.

Thiocyanates ions show several toxic effects towards vertebrates and for the last several years many papers have reported the results of such studies. For example, potassium thiocyanate accelerates the production of large DNA fragments, as well as the induction of trace amounts of internucleosomal DNA cleavage in human peripheral blood polymorphonuclear leukocytes.[55-57] The thiocyanate ion may act as an ambidentate ligand, bonding may occur either through the nitrogen or the sulphur atom. The bonding mode may easily be distinguished by examining the band due to the C-S stretching vibration which occurs at 730-690 cm^{-1} when the bonding occurs through the sulphur atom and at 860-780 cm^{-1} when it is through the nitrogen atom.[58] The C≡N stretching vibration of thiocyanato-complexes (sulphur-bound, i.e. M-SCN) gives rise to a sharp band at about 2100 cm^{-1} and Ga-NCS (i.e. nitrogen bound), the resulting band is often broad and occurs near and below 2050 cm^{-1}. The absorption vibrations due to the N-coordinated bonded NCS^- and ionic NCS^- groups in $[Cu_2([22]\text{-HMTADO})(NCS)(OH_2)]NCS \cdot 2H_2O$ appear 2085-1054 and 820 cm^{-1}.

The coordination chemistry of azido metal complexes has been a revival in

recent years, due to the interest for biologists and bioinorganic chemists investigating the structure and the role of the active site in copper proteins, as well as for physical chemists seeking to design new magnetic materials.[59-62] In general, for azides the band due to the asymmetric N_3 stretching vibration is strong and occurs in the region 2195-2030 cm^{-1}, while that due to the symmetric vibration is much weaker and occurs in the region 1375-1175 cm^{-1} and the band due to the deformation vibration is also weak and occurs at 680-410 cm^{-1}.[63] The absorption peak at 2034 cm^{-1} in the $[Cu_2([22]\text{-HMTADO})(N_3)(OH_2)]N_3 \cdot H_2O$ is assigned to the asymmetric stretching mode of coordinated and/or ionic azide. The symmetric stretching frequencies of coordinated and ionic azide are observed at 1329 and 1275 cm^{-1}, respectively. And deformation band of coordinated and/or ionic azide is observed at 635 cm^{-1}.

The absorption bands of coordinate nitrate occurring in the IR spectra of $[Cu_2([22]\text{-HMTADO})ONO_2]NO_3 \cdot 4H_2O$ in the 1442, 1325 and 1009 cm^{-1} regions are assignable to the ν(N=O) (ν_1), $\nu_a(NO_2)$ (ν_5) and $\nu_s(NO_2)$ (ν_2) vibrations, respectively. The absorption band at 1384 cm^{-1} is characteristic of ionic nitrate present in the outer-coordination sphere.[53, 64]

Linkage isomerism is possible in the case of metal complexes containing the unit NO_2. Coordination to the metal atom may occur through the nitrogen atom, resulting in a nitro-complex, or through an oxygen atom, resulting in a nitrito-complex. Nitro-complexes exhibit bands due to asymmetric and symmetric -NO_2 stretching vibration and, in addition, one due to a NO_2 deformation vibration.[58] The nitrito-complexes exhibit bands due to asymmetric and symmetric -ONO stretching vibrations which are well separated and occur

at 1485-1400 cm^{-1} and 1110-1050 cm^{-1}, respectively. Nitro-groups in metal coordination complexes may exist as bridging or as end groups. Terminal nitro-groups absorb at 1485-1370 cm^{-1} and 1340-1315 cm^{-1} due to the asymmetric and symmetric stretching vibrations of the NO_2 group, respectively.[58] Nitrito-complexes do not have a band near 620cm^{-1} which is present for all nitro-complexes. Nitro- groups acting as bridging units between two metal atoms absorb at 1485-1470cm^{-1} and at about 1200cm^{-1}, these bands being broader than those for terminal nitro- groups. The absorption peaks at 1383 and 1325 cm^{-1} in the $[Cu_2([22]\text{-}HMTADO)NO_2]NO_2 \cdot 2H_2O$ are assigned to the antisymmetric and symmetric stretching mode of N-bonded NO_2, respectively. And deformation band of N-bonded NO_2, is observed at 640 cm^{-1}. The absorption band at 1271 cm^{-1} is characteristic of ionic nitro present in the outer-coordination sphere.

Enzymes that metabolize small molecular compounds of nitrogen and sulfur play an important role in the biosynthesis of amino acids by plants or as a bacterial source of energy.[65] In particular, interest has grown substantially in microbial sulfur metabolism. The sulfate and thiosulfate ion may coordinate to a metal atom as a unidentate ligand and as a chelating bidentate ligand. Free ion with tetrahedral symmetry, T_d, have four fundamental vibrations, only tow of which are infrared active (one stretching mode and bending mode). For unidentate coordination, the symmetry is reduced to C_{3v}, each of the bands for the free ion being split into two bands with, in addition, the two previously only Raman active vibrations now becoming infrared active. Therefore, three bands due to stretching vibrations and three due to bending vibrations are expected. For bidentate coordination, the symmetry is reduced

to C_{2v} and each of the bands due to the two modes of vibration of the free ion is now split into three, so that, taking into account the bands which were inactive for the free ion, four bands due to stretching vibrations and four due to bending vibrations are observed. The absorption peaks at 1232-1221 and 1124-1105 cm^{-1} in the $[Cu_2([22]\text{-HMTADO})S_2O_3] \cdot 5H_2O$ are assigned to the antisymmetric and symmetric stretching mode of bidentate $S_2O_3^{2-}$, respectively. And deformation bands of bidentate O-bonded $S_2O_3^{2-}$ are observed at 1016, 644, and 607 cm^{-1} regions.

2) Ni(II) complexes of [22]-HMTADO.

IR spectra of the bi- and mono-nuclear Ni(II) complexes were presented Fig. 16 ~ 27, and contain absorption bands characteristic of the complexes (Table 35 and 36). The strong and sharp absorption band occurring at 1630 - 1640 cm^{-1} in the IR spectra of the complexes is attributed to ν(C=N) of the coordinated [22]-HMTADO ligand[52, 53], and the absence of any carbonyl bands associated with the diformyl-phenol starting materials or nonmarcrocyclic intermediates. The IR spectra displayed C-H stretching vibrations from 3000 to 2800 cm^{-1}. The present complexes exhibited three C-H deformation bands at 1440, 1390, and 1370 cm^{-1} regions and two out-of-plan vibration bands at 820 and 765 cm^{-1} regions. The absorption bands occurring in the IR spectra of the complexes in the 3300-3500 cm^{-1} regions may probably be due to the ν(OH) vibration of the coordinated and/or lattice water. The absorption peak at 2127 cm^{-1} in the $[Ni_2([22]\text{-HMTADO})(CN)_2] \cdot 0.5H_2O$ is assigned to the stretching frequency of CN. The absorption vibrations due to the

N-coordinated bonded NCS^- and ionic NCS^- groups in $[Ni_2([22]\text{-HMTADO})(NCS)_2(OH_2)] \cdot 2H_2O$ appear 2060 and 824 cm^{-1}. The absorption peak at 2043 cm^{-1} in the $[Ni_2([22]\text{-HMTADO})(N_3)_2(OH_2)]$ is assigned to the anti-symmetric stretching mode of coordinated azide. The symmetric stretching frequency of coordinated azide is observed at 1236 cm^{-1}, and deformation band of coordinated is observed at 621 cm^{-1}. The absorption bands of coordinate nitrate occurring in the IR spectra of $[Ni_2([22]\text{-HMTADO})(ONO_2)(OH_2)_2]NO_3 \cdot 3H_2O$ in the 1437, 1331 and 1005 cm^{-1} regions are assignable to the ν(N=O) (ν_1), $\nu_a(NO_2)$ (ν_5) and $\nu_s(NO_2)$ (ν_2) vibrations, respectively. The absorption band at 1385 cm^{-1} is characteristic of ionic nitrate present in the outer-coordination sphere.[53, 64] The absorption peaks at 1333 and 1310 cm^{-1} in the $[Ni_2([22]\text{-HMTADO})NO_2]NO_2 \cdot H_2O$ are assigned to the antisymmetric and symmetric stretching mode of N-bonded NO_2, respectively. And deformation band of N-bonded NO_2, is observed at 617 cm^{-1}. The absorption band at 1285 cm^{-1} is characteristic of ionic nitro present in the outer-coordination sphere. The $[Ni_2([22]\text{-HMTADO})SO_4] \cdot H_2O$ was obtaind in the reaction of sodium thiosulfate and starting binuclear Ni(II) macrocyclic complex. The absorption peaks at 1225-1193 and 1121-1093 cm^{-1} in the $[Ni_2([22]\text{-HMTADO})S_2O_3]$ are assigned to the antisymmetric and symmetric stretching mode of bidentate $S_2O_3^{2-}$, respectively. And deformation band of bidentate $S_2O_3^{2-}$ is observed at 1016, 644, and 652 cm^{-1} regions. A strong ionic ClO_4^- band at near 1090 cm^{-1} and 625 cm^{-1} in the $[[Ni_2([22]\text{-HMTADO})(OH_2)_2](ClO_4)_2 \cdot H_2O$ and $[Ni(H_2[22]\text{-HMTADO})(OHCH_3)_2](ClO_4)_2$ complex.

The absorption peaks at 3323 and 3285 cm^{-1} in the $[Ni(H_2[22]\text{-HMTADO})$

-$(OHCH_3)_2](ClO_4)_2$ are assigned to the ν(OH) vibration of the coordinated methanol. The absorption vibrations due to the N-coordinated bonded NCS^- and ionic NCS^- groups in $[Ni(H_2[22]\text{-HMTADO})(NCS)_2] \cdot H_2O$ appear 2098 and 868 cm^{-1}. The absorption peak at 2044 cm^{-1} in the $[Ni(H_2[22]\text{-HMTADO})$ -$(N_3)(OH_2)]ClO_4 \cdot H_2O$ is assigned to the antisymmetric stretching mode of coordinated azide. The symmetric stretching frequency of coordinated azide is observed at 1284 cm^{-1}, and deformation band of coordinated is observed at 667 cm^{-1}. And a strong ionic ClO_4^- band is observed at near 1088 cm^{-1} and 625 cm^{-1}.

3) Mn(II) complex of [22]-HMTADO.

IR spectra of the $[Mn_2([22]\text{-HMTADO})Cl_2]\cdot H_2O$ complex was presented Fig. 28, and contain absorption bands characteristic of the complexes (Table 37). The strong and sharp absorption band occurring at 1632 cm^{-1} in the IR spectra of the complexes is attributed to ν(C=N) of the coordinated [22]-HMTADO ligand[52, 53], and the absence of any carbonyl bands associated with the diformyl-phenol starting materials or nonmarcrocyclic intermediates. The IR spectra displayed C-H stretching vibrations at 2953 and 2890 cm^{-1}. The present complexes exhibited three C-H deformation bands at 1431, 1400, and 1364 cm^{-1} regions and two out-of-plan vibration bands at 816 and 771 cm^{-1} regions. The absorption bands in the 3433 cm^{-1} region is assigned to the ν(OH) vibration of the lattice water. A number of 500 cm^{-1} region may probably be due to the Mn-Cl vibration.

4) lanthanide(III) complexes of [22]-HMTADO.

IR spectra of the lanthanide(III) complexes were presented Fig. 29 ~ 32, and contain absorption bands characteristic of the complexes (Table 37). The strong and sharp absorption band occurring at 1645 cm^{-1} in the IR spectra of the complexes is attributed to ν(C=N) of the coordinated [22]-HMTADO ligand[52, 53], and the absence of any carbonyl bands associated with the diformyl-phenol starting materials or nonmarcrocyclic intermediates. The IR spectra displayed C-H stretching vibrations from 3000 to 2800 cm^{-1}. The present complexes exhibited three C-H deformation bands at 1478, 1390, and 1317 cm^{-1} regions and two out-of-plan vibration bands at 825 and 781 cm^{-1} regions. The absorption bands occurring in the IR spectra of the complexes in the 3430 cm^{-1} region may probably be due to the ν(OH) vibration of the lattice water.

The absorption bands occurring in the IR spectra of the complexes in the 1458-1462, 1283-1285 and 1035-1055 cm^{-1} regions are assignable to the ν(N=O) (ν_1), $\nu_a(NO_2)$ (ν_5) and $\nu_s(NO_2)$ (ν_2) vibrations, respectively, of the chelating bidentate nitrate ion.[53, 64, 67] The absorption band observed at 815 cm^{-1} in the complexes is also characteristic of chelating bidentate nitrate.[64] The larger separation of 177-177 cm^{-1} between the two higher frequency bands (ν_1 and ν_5) indicates strong interaction of the oxygen atoms of the nitrate with the lanthanide ions and is typical of bidentate coordination.[67, 68] The absorption band at 1385 cm^{-1} is characteristic of ionic nitrate present in the outer-coordination sphere.[64]

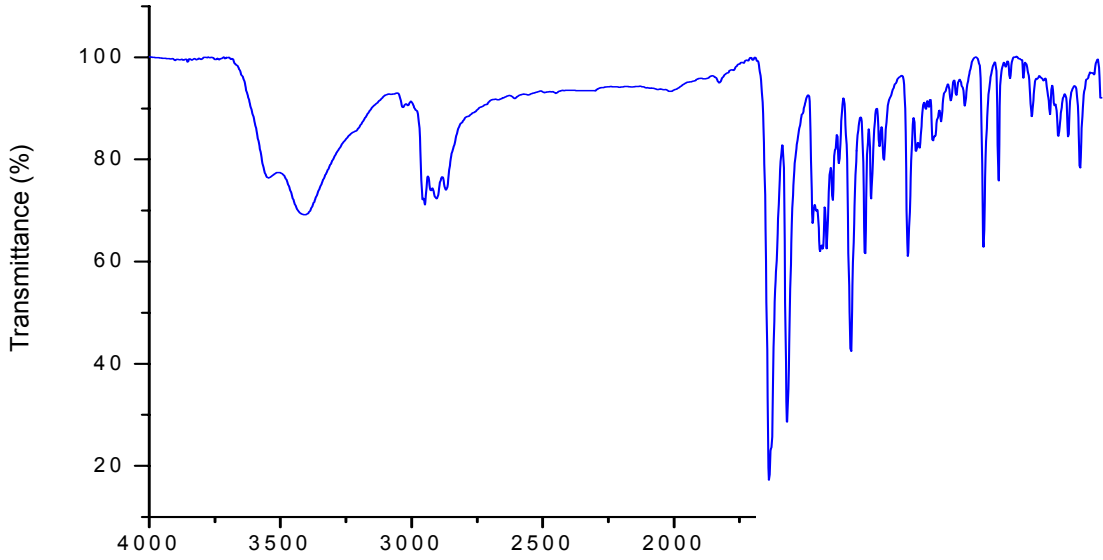

Fig. 7. FT-IR spectrum of $[Cu_2([22]\text{-HMTADO})(OH_2)]Cl_2 \cdot H_2O$.

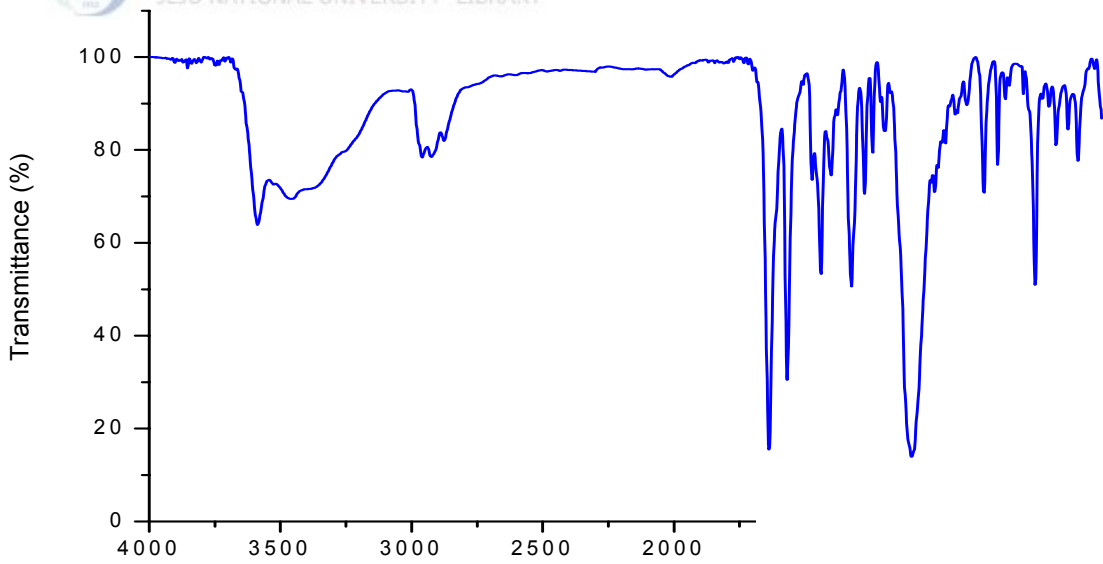

Fig. 8. FT-IR spectrum of $[Cu_2([22]\text{-HMTADO})(OClO_3)(OH_2)]ClO_4 \cdot 2H_2O$.

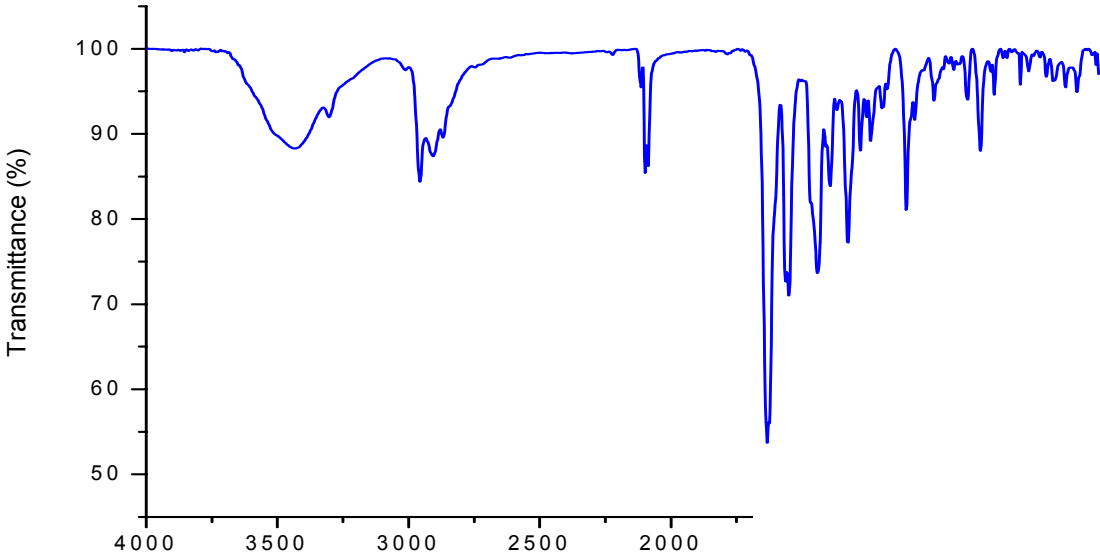

Fig. 9. FT-IR spectrum of $[Cu_2([22]\text{-HMTADO})(CN)_2] \cdot 0.5H_2O$.

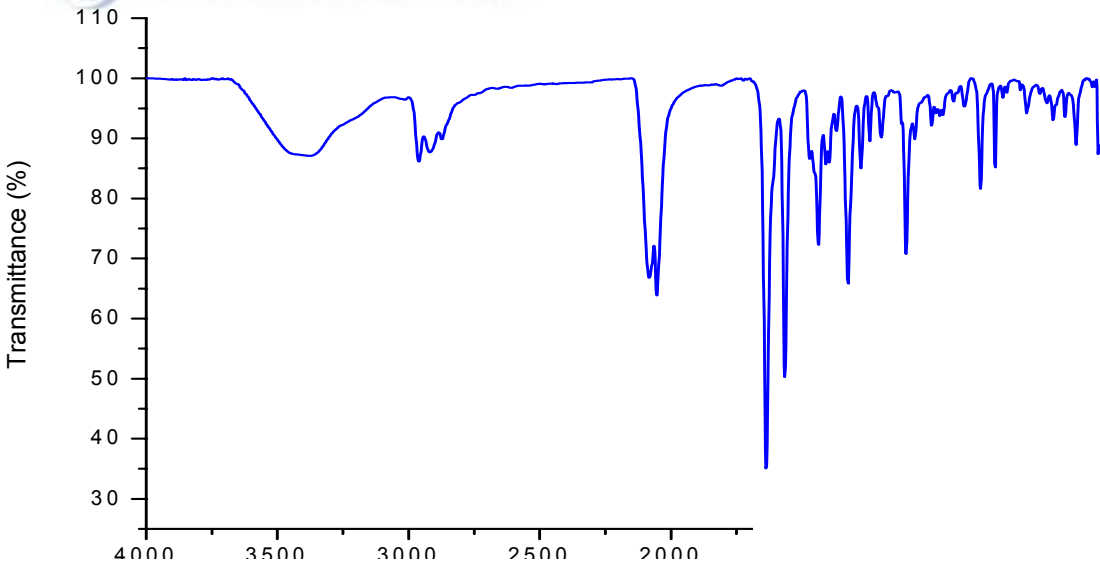

Fig. 10. FT-IR spectrum of $[Cu_2([22]\text{-HMTADO})(NCS)(OH_2)]NCS \cdot 2H_2O$.

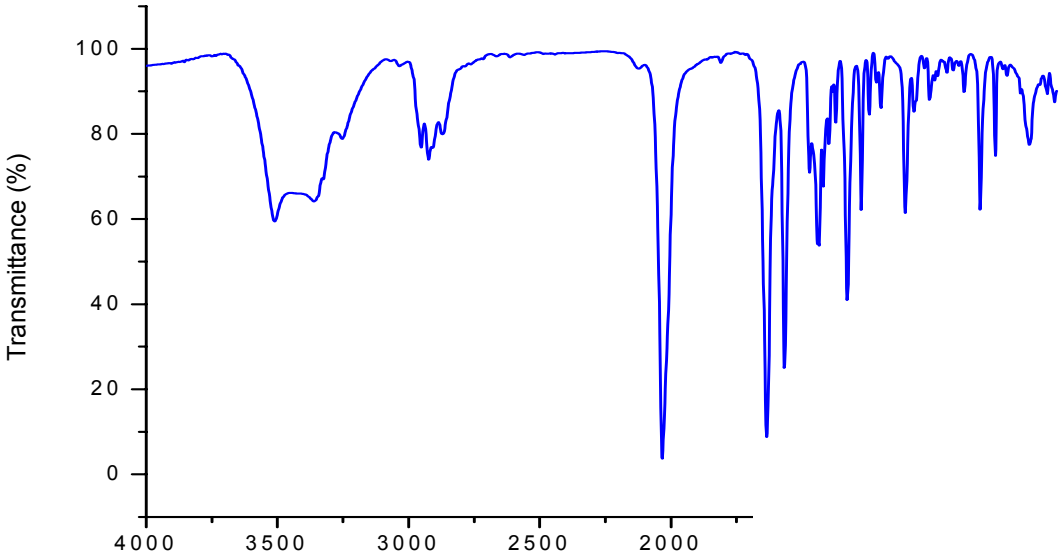

Fig. 11. FT-IR spectrum of $[Cu_2([22]\text{-HMTADO})(N_3)(OH_2)]N_3 \cdot H_2O$.

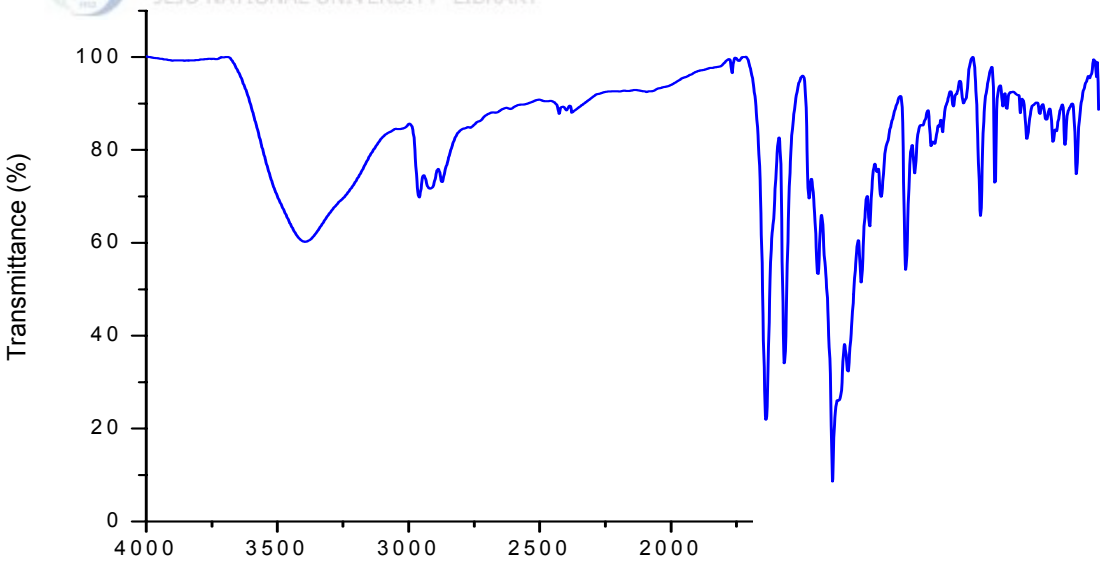

Fig. 12. FT-IR spectrum of $[Cu_2([22]\text{-HMTADO})ONO_2]NO_3 \cdot 4H_2O$.

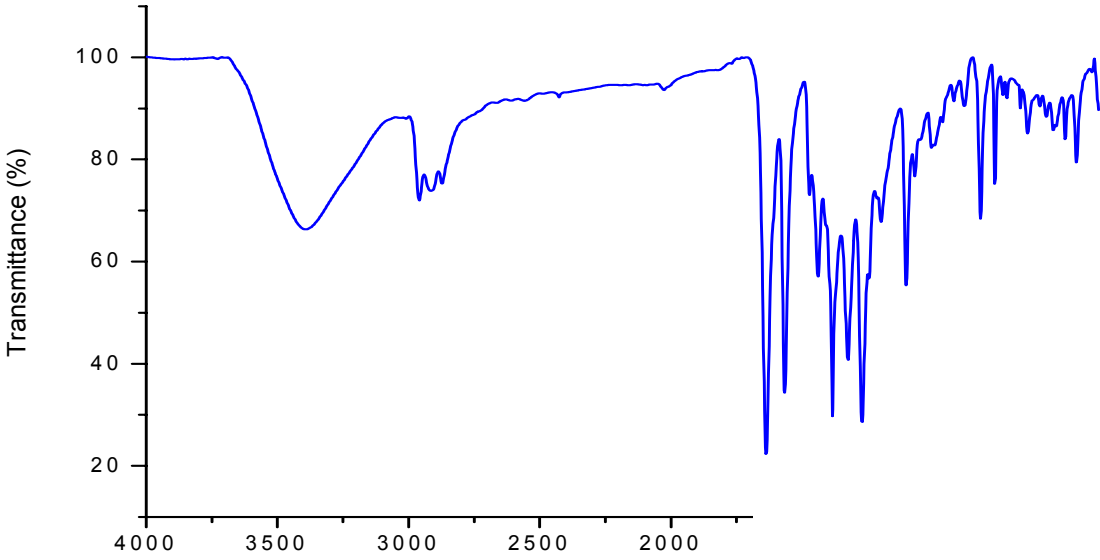

Fig. 13. FT-IR spectrum of $[Cu_2([22]\text{-HMTADO})NO_2]NO_2 \cdot 2H_2O$.

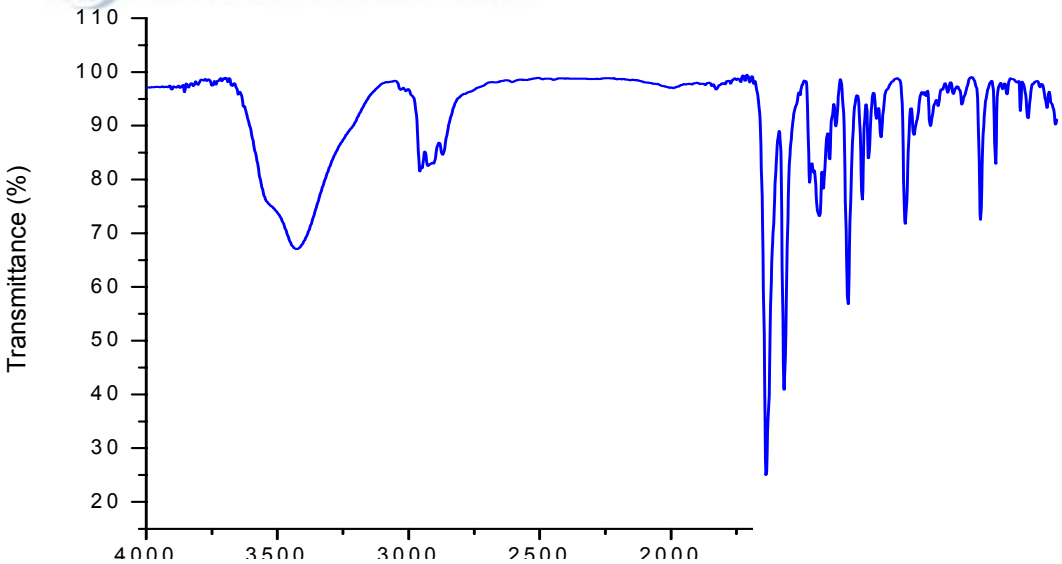

Fig. 14. FT-IR spectrum of $[Cu_2([22]\text{-HMTADO})]Br_2 \cdot 1.5H_2O$.

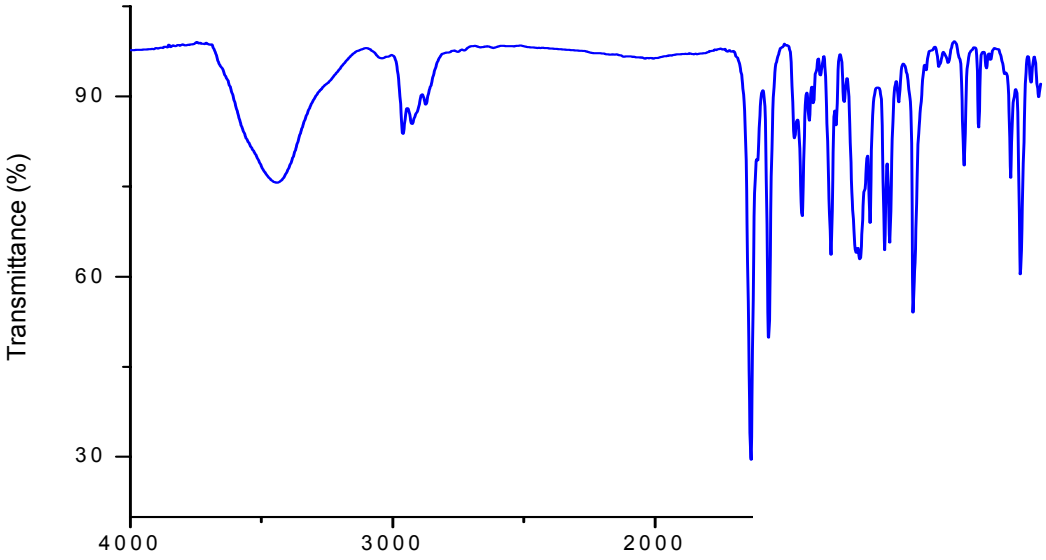

Fig. 15. FT-IR spectrum of $[Cu_2([22]\text{-HMTADO})SO_4] \cdot 6H_2O$.

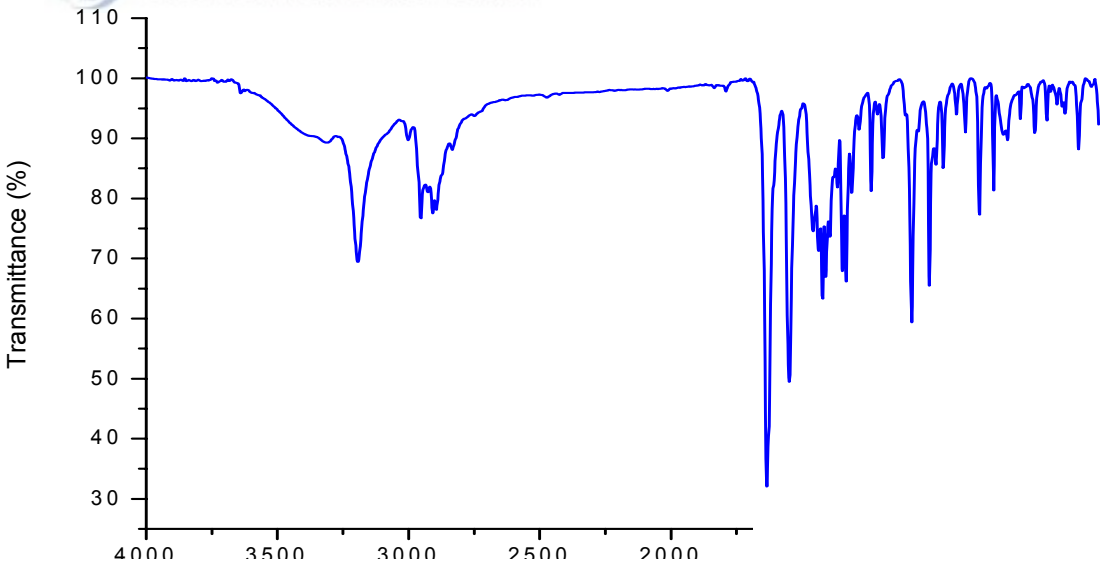

Fig. 16. FT-IR spectrum of $[[Ni_2([22]\text{-HMTADO})(OH_2)_2]Cl_2 \cdot H_2O$.

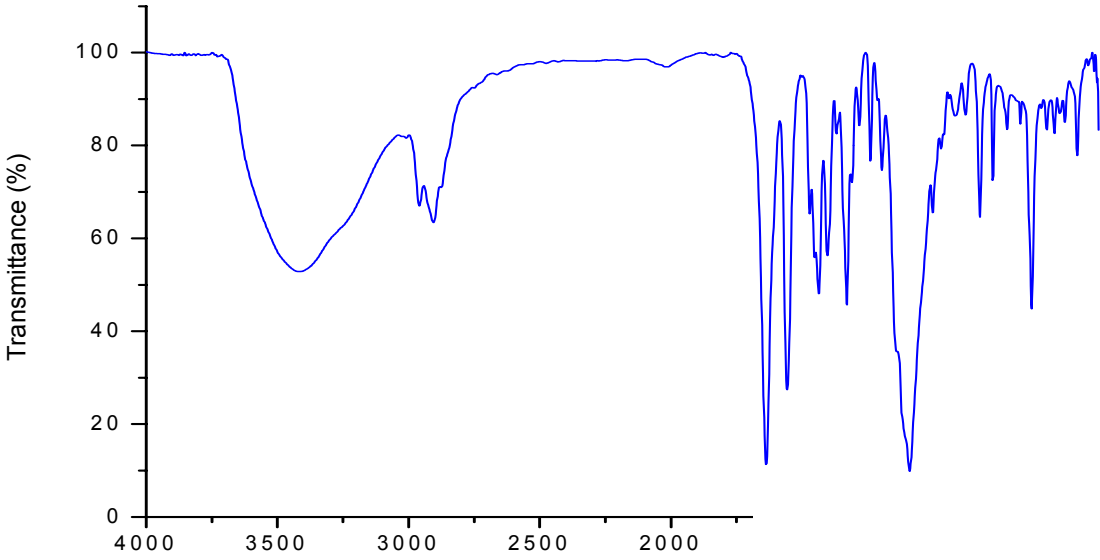

Fig. 17. FT-IR spectrum of $[Ni_2([22]\text{-HMTADO})(OH_2)_2](ClO_4)_2 \cdot H_2O$.

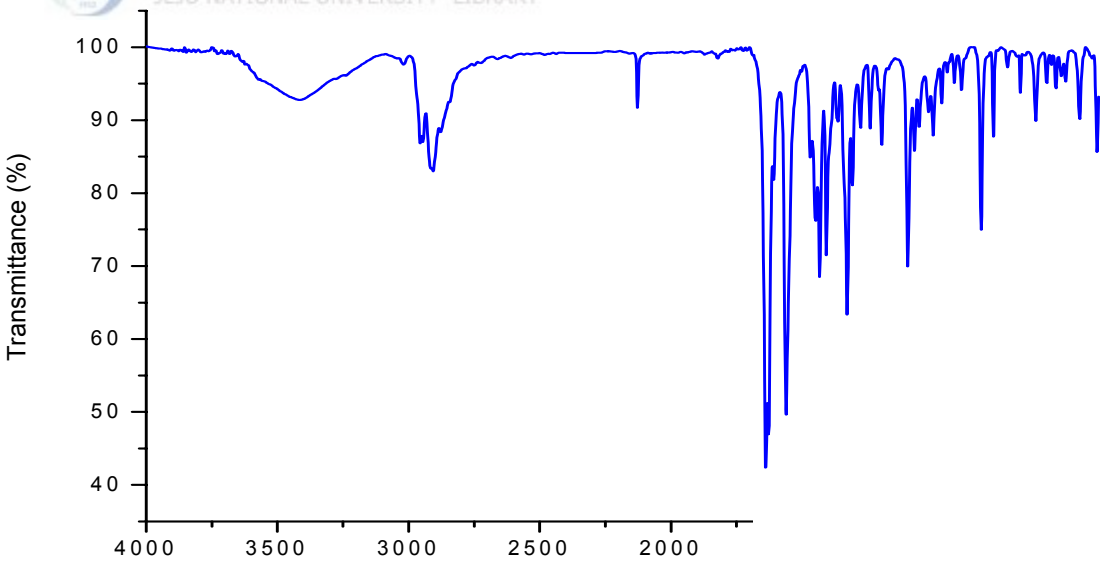

Fig. 18. FT-IR spectrum of $[Ni_2([22]\text{-HMTADO})(CN)_2] \cdot 0.5H_2O$.

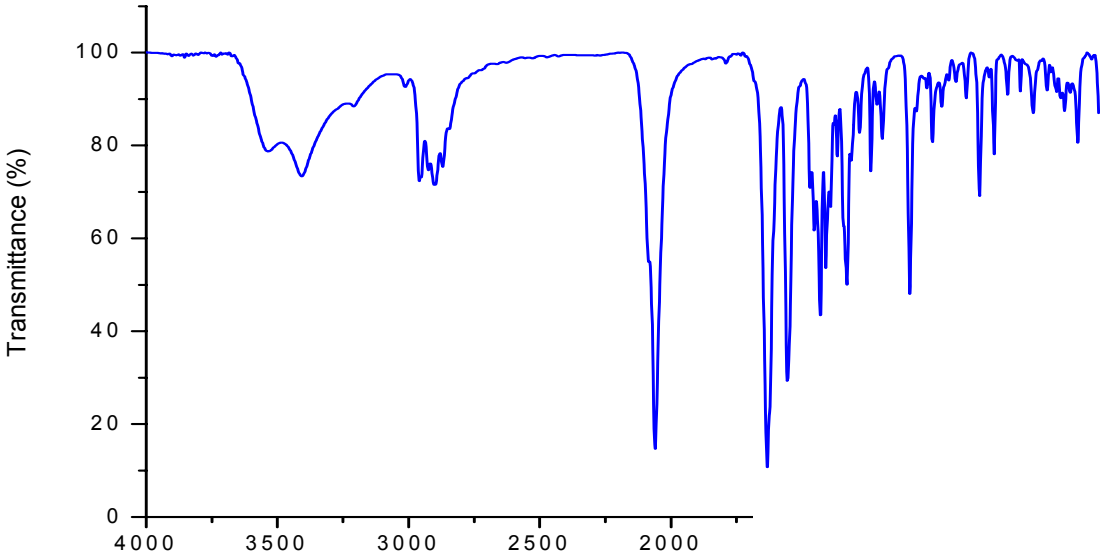

Fig. 19. FT-IR spectrum of $[Ni_2([22]\text{-HMTADO})(NCS)_2(OH_2)] \cdot 2H_2O$.

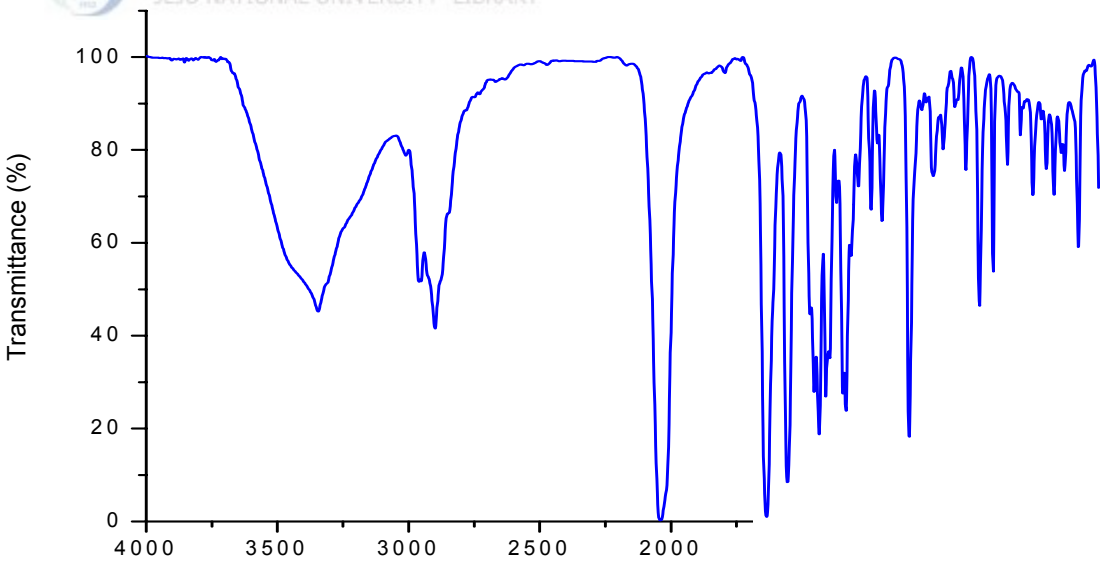

Fig. 20. FT-IR spectrum of $[Ni_2([22]\text{-HMTADO})(N_3)_2(OH_2)]$.

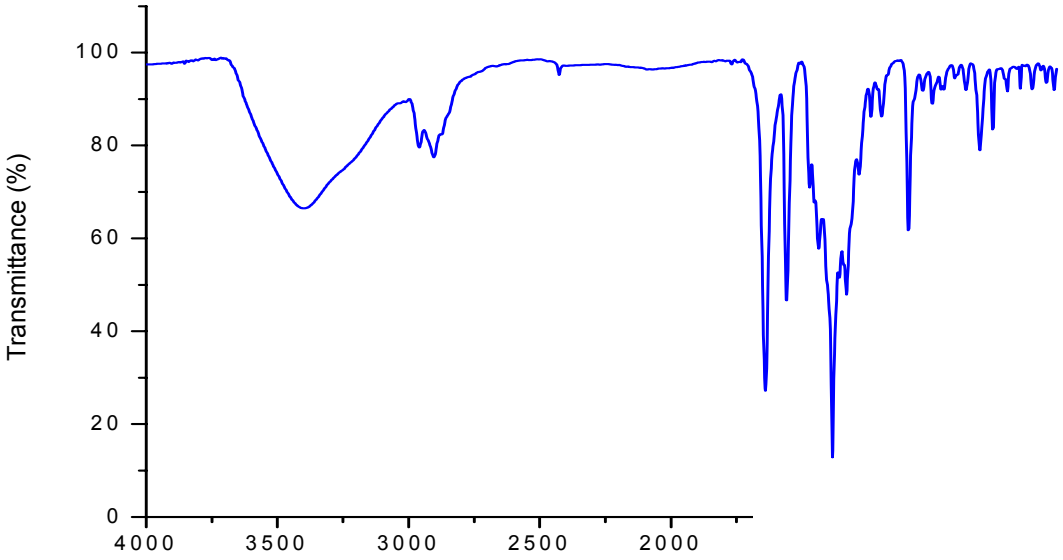

Fig. 21. FT-IR spectrum of $[Ni_2([22]\text{-HMTADO})(ONO_2)(OH_2)_2]NO_3 \cdot 3H_2O$.

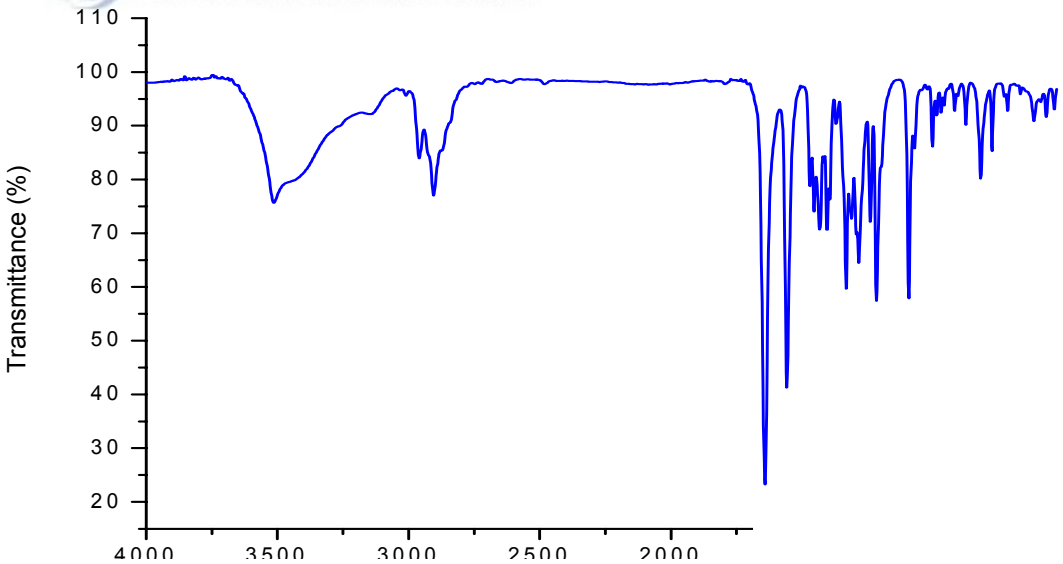

Fig. 22. FT-IR spectrum of $[Ni_2([22]\text{-HMTADO})NO_2]NO_2 \cdot H_2O$.

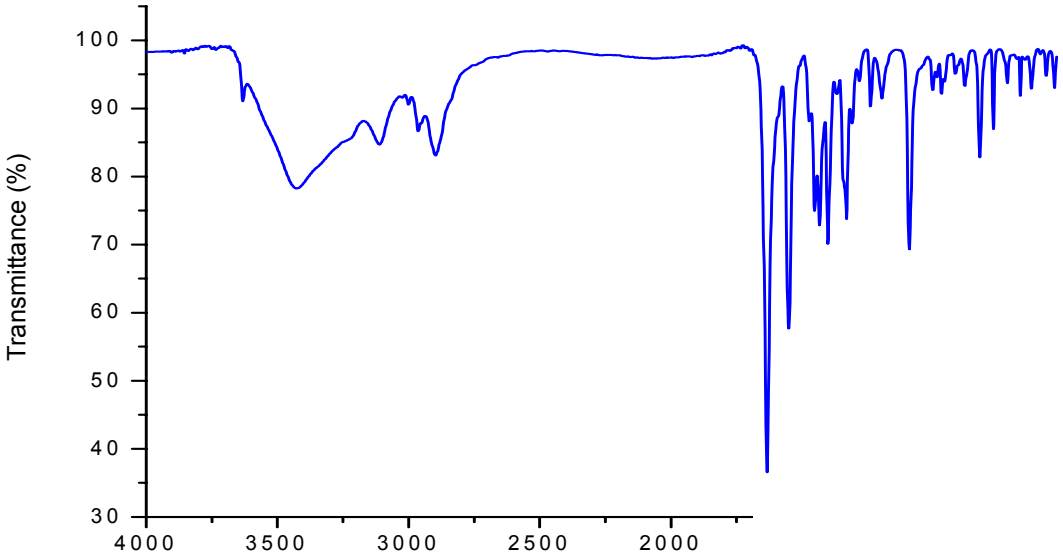

Fig. 23. FT-IR spectrum of $[Ni_2([22]\text{-HMTADO})]Br_2 \cdot 2H_2O$.

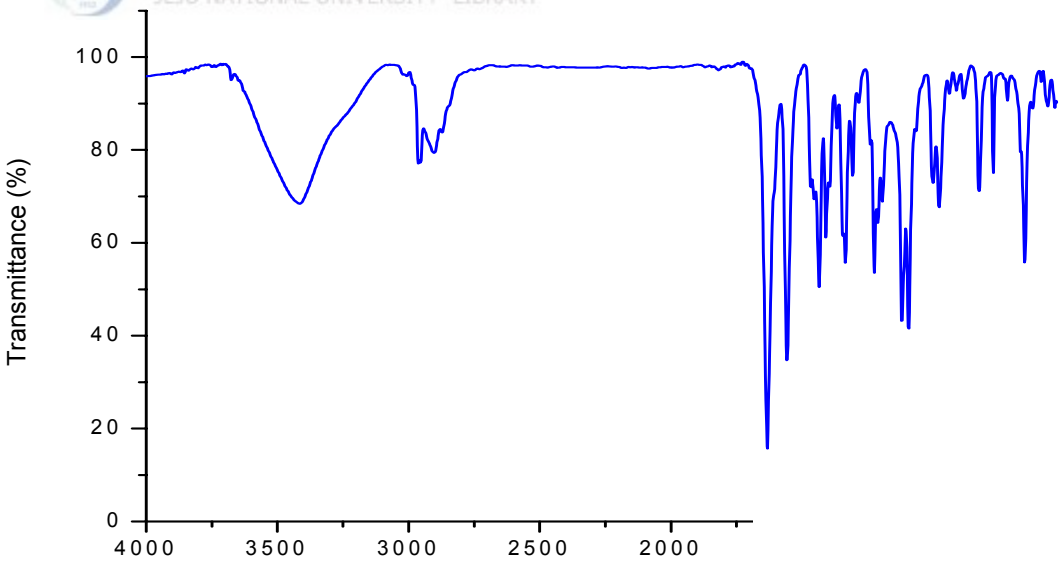

Fig. 24. FT-IR spectrum of $[Ni_2([22]\text{-HMTADO})SO_4] \cdot H_2O$.

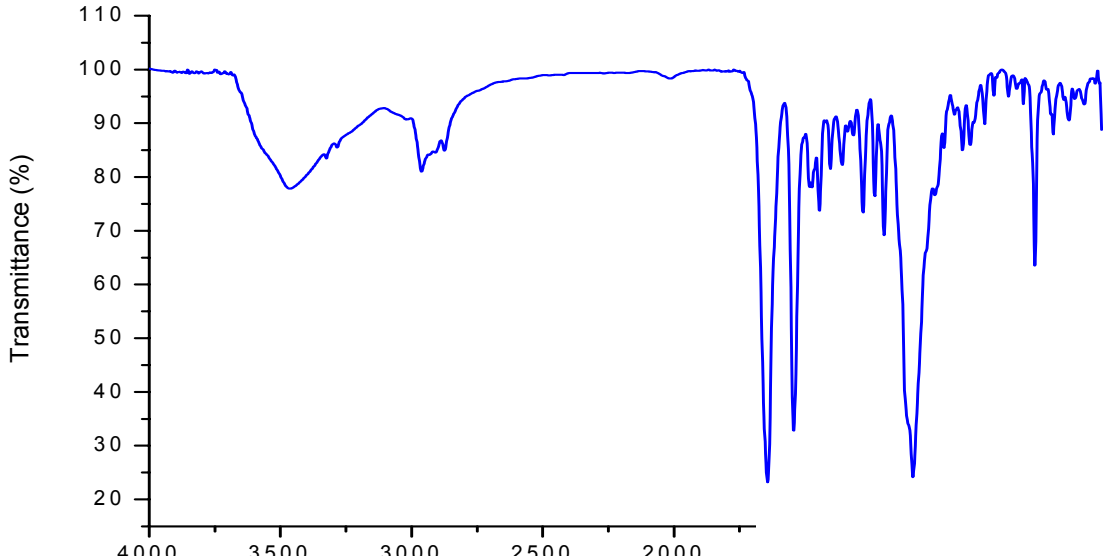

Fig. 25. FT-IR spectrum of $[Ni(H_2[22]\text{-}HMTADO)(OHCH_3)_2](ClO_4)_2$.

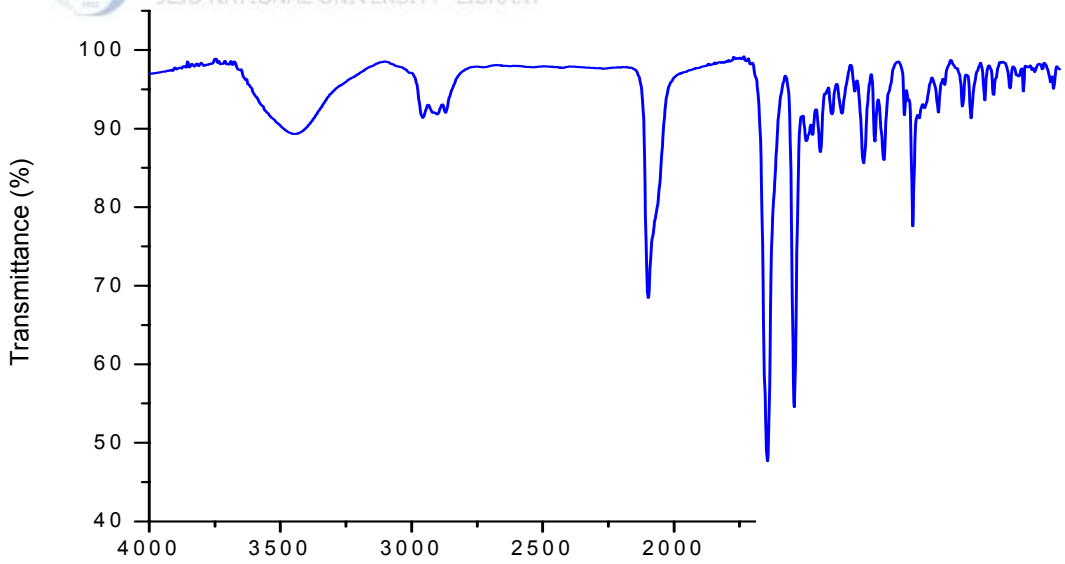

Fig. 26. FT-IR spectrum of $[Ni(H_2[22]\text{-}HMTADO)(NCS)_2] \cdot H_2O$.

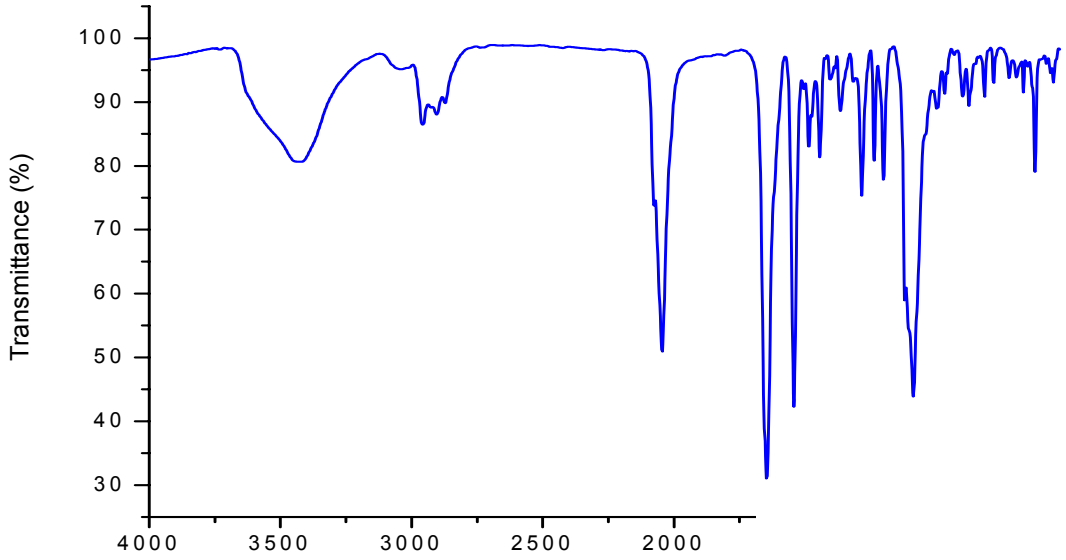

Fig. 27. FT-IR spectrum of [Ni(H_2[22]-HMTADO)(N_3)(OH_2)]ClO_4 · H_2O.

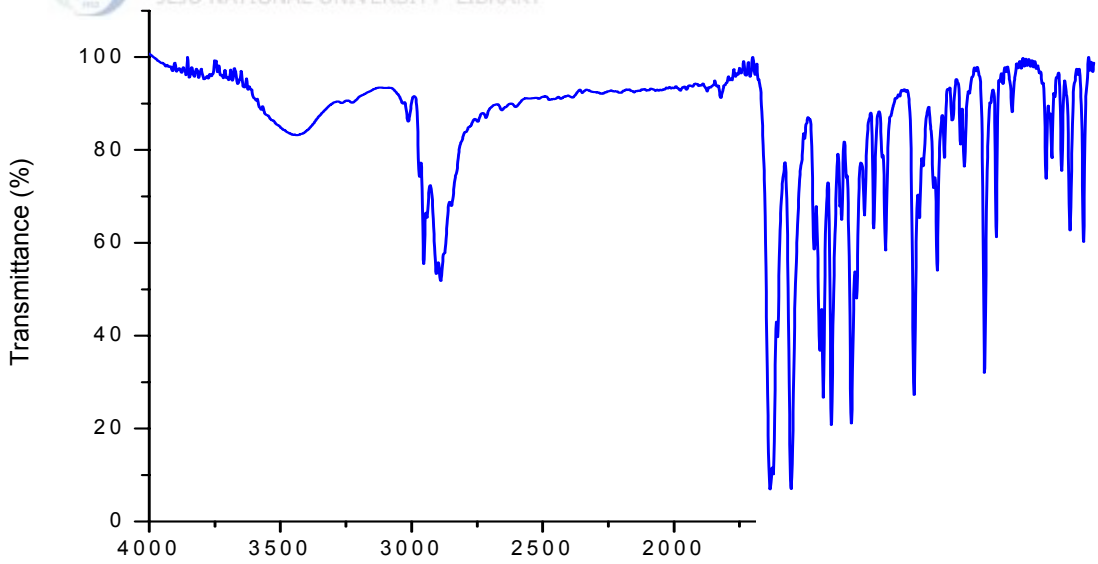

Fig. 28. FT-IR spectrum of [Mn([22]-HMTADO)Cl_2] · H_2O.

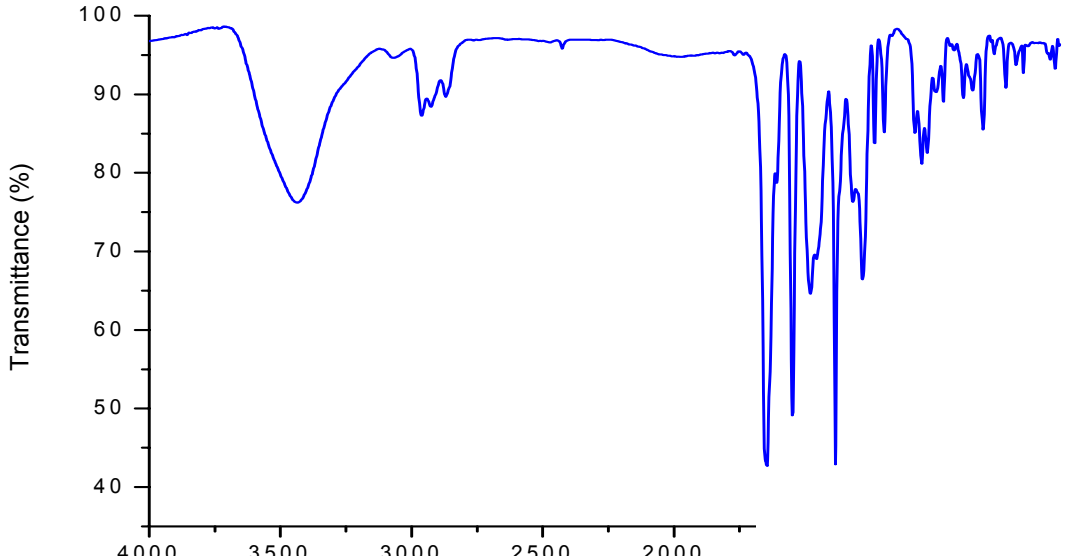

Fig. 29. FT-IR spectrum of $[Pr(H_2[22]\text{-}HMTADO)O_2NO](NO_3)_2 \cdot 2H_2O$.

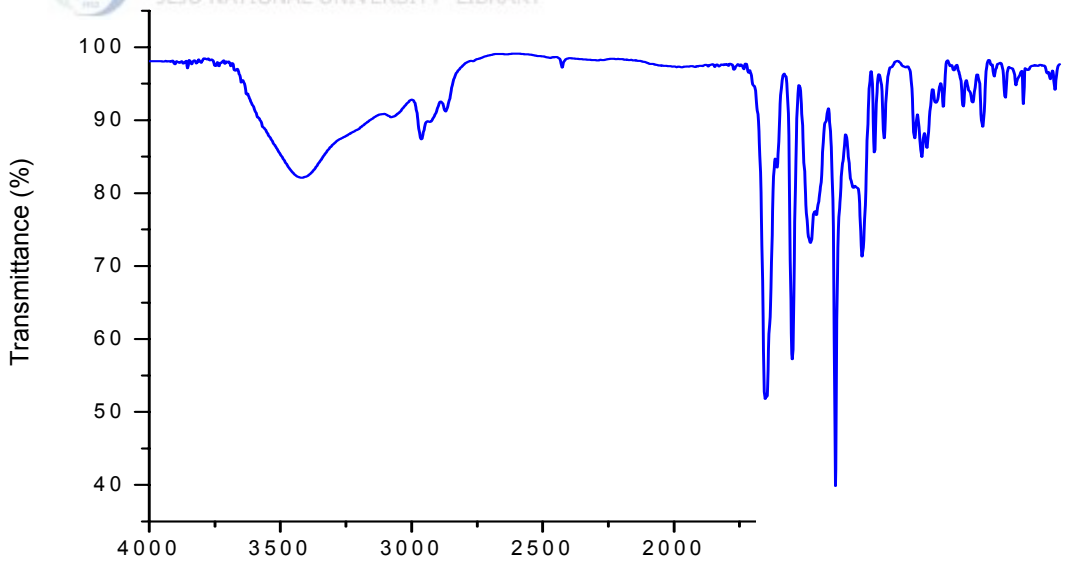

Fig. 30. FT-IR spectrum of $[Sm(H_2[22]\text{-}HMTADO)O_2NO](NO_3)_2 \cdot 2H_2O$.

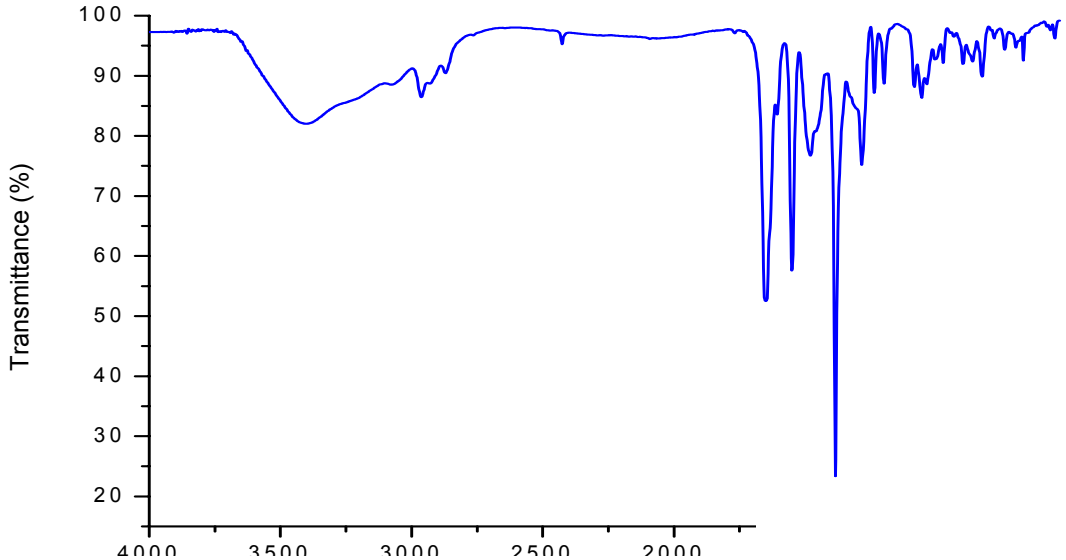

Fig. 31. FT-IR spectrum of $[Gd(H_2[22]\text{-}HMTADO)O_2NO](NO_3)_2 \cdot 2H_2O$.

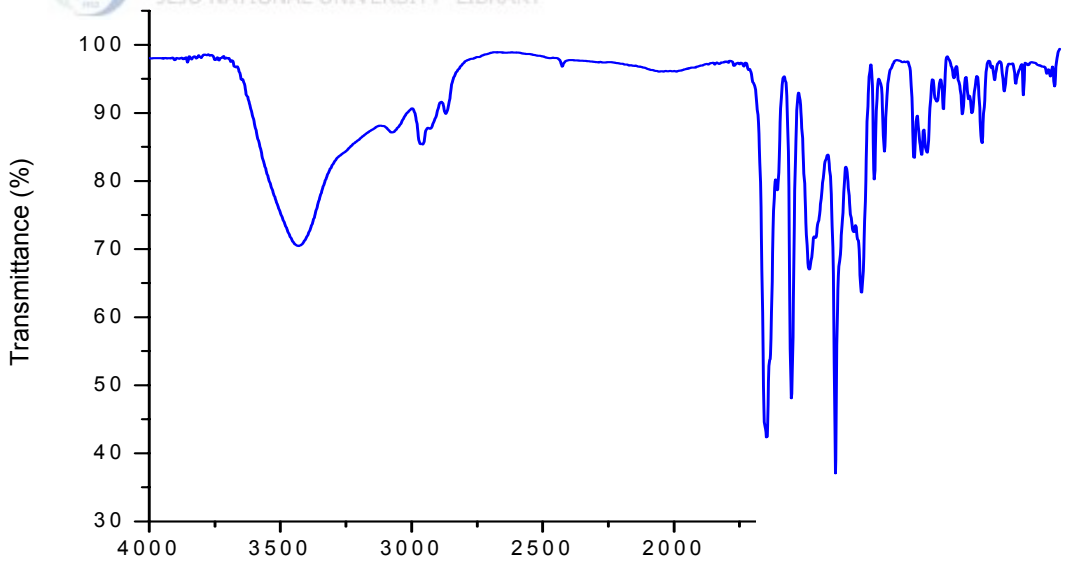

Fig. 32. FT-IR spectrum of $[Dy(H_2[22]\text{-}HMTADO)O_2NO](NO_3)_2 \cdot H_2O$.

Table 33. Characteristic IR absorptions (cm^{-1}) of macrocyclic ligand (H_2[22]-HMTADO) for the binuclear Cu(II) complexes

Compounds	Assignments										
	Macrocycle										
	ν(CH)		ν(C=N)	ν(C=C)		δ(CH)			ν(C-O)	δ_{oop}(CH)	
$[Cu_2([22]\text{-HMTADO})(OH_2)]Cl_2 \cdot H_2O$	2949	2866	1638	1570	1472	1443	1394	1371	1109	820	764
$[Cu_2([22]\text{-HMTADO})(OClO_3)(OH_2)]ClO_4 \cdot 2H_2O$	2960	2875	1637	1570	1475	1439	1399	1375	1005	819	766
$[Cu_2([22]\text{-HMTADO})(CN)_2] \cdot 0.5H_2O$	2957	2867	1639	1565	1471	1442	1392	1367	1103	820	768
$[Cu_2([22]\text{-HMTADO})(NCS)(OH_2)]NCS \cdot 2H_2O$	2963	2872	1637	1566	1474	1437	396	1369	1103	820	764
$[Cu_2([22]\text{-HMTADO})(N_3)(OH_2)]N_3 \cdot H_2O$	2952	2867	1635	1567	1473	1436	1397	1371	1107	821	764
$[Cu_2([22]\text{-HMTADO})ONO_2]NO_3 \cdot 4H_2O$	2961	2872	1638	1569	1476	1439	1385	1351	1105	820	766
$[Cu_2([22]\text{-HMTADO})NO_2]NO_2 \cdot 2H_2O$	2961	2870	1637	1568	1473	1436	1396	1370	1103	820	766
$[Cu_2([22]\text{-HMTADO})]Br_2 \cdot 1.5H_2O$	2959	2870	1638	1570	1472	1442	1395	1370	1109	820	762
$[Cu_2([22]\text{-HMTADO})S_2O_3] \cdot 5H_2O$	2962	2873	1635	1567	1470	1439	1396	1369	1105	822	766

Table 34. Characteristic IR absorptions (cm^{-1}) of exocycle molecules for the binuclear Cu(II) complexes

Compounds	Assignments
$[Cu_2([22]\text{-HMTADO})(OH_2)]Cl_2 \cdot H_2O$	3549 ν(OH) lattice H_2O, 3412 ν(OH) coord. H_2O
$[Cu_2([22]\text{-HMTADO})(OClO_3)(OH_2)]ClO_4 \cdot 2H_2O$	3589 ν(OH) lattice H_2O, 3456 ν(OH) coord. H_2O ; 1095 (br), 625 $\nu(ClO_4^-$ ionic and coord.)
$[Cu_2([22]\text{-HMTADO})(CN)_2] \cdot 0.5H_2O$	2116 ν(CN) coord. CN^-
$[Cu_2([22]\text{-HMTADO})(NCS)(OH_2)]NCS \cdot 2H_2O$	3454 ν(OH) lattice H_2O, 3379 ν(OH) coord. H_2O ; 2085 ν(C=N)ionic NCS^-,2054 ν(C=N) N-bonded NCS^- ; 820 ν(C-S) N-bonded NCS^-
$[Cu_2([22]\text{-HMTADO})(N_3)(OH_2)]N_3 \cdot H_2O$	3514 ν(OH) lattice H_2O, 3364 ν(OH) coord. H_2O ; 2034 ν_{as}(NNN) coord. and ionic N_3^- ; 1329, ν_s(NNN) ionic N_3^- ; 1275 ν_s(NNN) coord. N_3^- ; 635 δ(NNN) coord. and ionic N_3^- ;
$[Cu_2([22]\text{-HMTADO})ONO_2]NO_3 \cdot 4H_2O$	3400 ν(OH) H_2O ; 1442 ν(N=O), 1325 $\nu_{as}(NO_2)$, 1009 $\nu_s(NO_2)$ monodentate NO_3^- ; 1384 ionic NO_3^-

$[Cu_2([22]\text{-HMTADO})NO_2]NO_2 \cdot 2H_2O$	3395 ν(OH) H_2O ; 1383 $\nu_a(NO_2)$, 1325 $\nu_s(NO_2)$, 640 $\delta(NO_2)$ N-bonded NO_2^- ; 1271 ionic NO_2^-
$[Cu_2([22]\text{-HMTADO})]Br_2 \cdot 1.5H_2O$	3547(sh, br), 3433(br) ν(OH) H_2O
$[Cu_2([22]\text{-HMTADO})S_2O_3] \cdot 5H_2O$	3441 ν(OH) H_2O ; 1232-1221(two bands), 1124-1105(two bands) bidentated $S_2O_3^{2-}$; 1016, 644, 607 deformation bidentated $S_2O_3^{2-}$

Table 35. Characteristic IR absorptions (cm^{-1}) of macrocyclic ligand (H_2[22]-HMTADO) for the mono- and bi-nuclear Ni(II) complexes

Compounds	Assignments										
	Macrocycle										
	ν(CH)		ν(C=N)	ν(C=C)		δ(CH)			ν(C-O)	δ_{oop}(CH)	
$[Ni_2([22]\text{-HMTADO})(OH_2)_2]Cl_2 \cdot H_2O$	2953	2893	1636	1550	1460	1438	1393	1366	1082	824	770
$[Ni_2([22]\text{-HMTADO})(OH_2)_2](ClO_4)_2 \cdot H_2O$	2960	2901	1634	1561	1473	1435	1395	1369	1003	822	773
$[Ni_2([22]\text{-HMTADO})(CN)_2] \cdot 0.5H_2O$	2957	2904	1631	1562	1470	1432	1407	1365	1097	818	771
$[Ni_2([22]\text{-HMTADO})(NCS)_2(OH_2)] \cdot 2H_2O$	2961	2869	1634	1558	1471	1430	1391	1366	1089	823	768
$[Ni_2([22]\text{-HMTADO})(N_3)_2(OH_2)]$	2951	2898	1631	1561	1473	1434	1393	1369	1093	824	771
$[Ni_2([22]\text{-HMTADO})(ONO_2)(OH_2)_2]NO_3 \cdot 3H_2O$	2959	2902	1639	1560	1473	1437	1384	1357	1095	823	771
$[Ni_2([22]\text{-HMTADO})NO_2]NO_2 \cdot H_2O$	2960	2868	1641	1559	1471	1432	1393	1369	1094	819	775
$[Ni_2([22]\text{-HMTADO})]Br_2 \cdot 2H_2O$	2964	2898	1633	1552	1474	1433	1401	1368	1092	823	770
$[Ni_2([22]\text{-HMTADO})S_2O_3]$	2955	2903	1631	1558	1465	1434	1409	1367	1093	825	766
$[Ni(H_2[22]\text{-HMTADO})(OHCH_3)_2](ClO_4)_2$	2963	2874	1639	1546	1485	1445	1403	1358	1089	816	781
$[Ni(H_2[22]\text{-HMTADO})(NCS)_2] \cdot H_2O$	2960	2870	1643	1541	1470	1443	1398	1362	1090	816	781
$[Ni(H_2[22]\text{-HMTADO})(N_3)(OH_2)]ClO_4 \cdot H_2O$	2961	2872	1647	1543	1487	1445	1404	1367	1001	816	781

Table 36. Characteristic IR absorptions (cm^{-1}) of exocycle molecules for the mono- and bi-nuclear Ni(II) complexes

Compounds	Assignments
$[Ni_2([22]\text{-HMTADO})(OH_2)_2]Cl_2 \cdot H_2O$	3313 ν(OH) lattice H_2O, 3196 ν(OH) coord. H_2O ;
$[Ni_2([22]\text{-HMTADO})(OH_2)_2](ClO_4)_2 \cdot H_2O$	3420(br) ν(OH) lattic and coord. H_2O ; 1092 (br), 625 $\nu(ClO_4^-$ ionic)
$[Ni_2([22]\text{-HMTADO})(CN)_2] \cdot 0.5H_2O$	3420 ν(OH) lattice H_2O ; 2127 ν(CN) coord. CN^- ;
$[Ni_2([22]\text{-HMTADO})(NCS)_2(OH_2)] \cdot 2H_2O$	3533 ν(OH) lattice H_2O, 3408 ν(OH) coord. H_2O ; 2060 ν(C=N) N-bonded NCS^- ; 824 ν(C-S) N-bonded NCS^-
.$[Ni_2([22]\text{-HMTADO})(N_3)_2(OH_2)]$	3452(sh), 3348 ν(OH) coord. H_2O ; 2043 ν_{as}(NNN) coord. and ionic N_3^- ; 1236 ν_s(NNN) coord. N_3^- ; 621 δ(NNN) coord. and ionic N_3^-
$[Ni_2([22]\text{-HMTADO})(ONO_2)(OH_2)_2]NO_3 \cdot 3H_2O$	3396 ν(OH) lattice H_2O, 3209(sh) ν(OH) coord. H_2O ; 1437 ν(N=O), 1331 $\nu_{as}(NO_2)$, 1005 $\nu_s(NO_2)$ monodentate NO_3^- ; 1385 ionic NO_3^-

$[Ni_2([22]\text{-HMTADO})NO_2]NO_2 \cdot H_2O$	3516 ν(OH) H_2O ; 1333 $\nu_a(NO_2)$, 1310 $\nu_s(NO_2)$, 617 $\delta(NO_2)$ N-bonded NO_2^- ; 1285 ionic NO_2^-
$[Ni_2([22]\text{-HMTADO})]Br_2 \cdot 2H_2O$	3632, 3431(br) ν(OH) H_2O
$[Ni_2([22]\text{-HMTADO})S_2O_3]$	3418 ν(OH) H_2O ; 1225-1193(three bands), 1121-1093(three bands) bidentated $S_2O_3^{2-}$; 652 bidentated $S_2O_3^{2-}$
$[Ni(H_2[22]\text{-HMTADO})(OHCH_3)_2](ClO_4)_2$	3467 ν(OH) MeOH ; 1090, 625 $\nu(ClO_4^-$ ionic)
$[Ni(H_2[22]\text{-HMTADO})(NCS)_2] \cdot H_2O$	3443 ν(OH) H_2O ; 2098 ν(C=N) N-bonded NCS^- ; 868 ν(C-S) N-bonded NCS^-
$[Ni(H_2[22]\text{-HMTADO})(N_3)(OH_2)]ClO_4 \cdot H_2O$	3595(sh) ν(OH) lattice H_2O, 3433 ν(OH) coord. H_2O ; 2044 ν_{as}(NNN) coord. N_3^- ; 1284 ν_s(NNN) coord. N_3^- ; 667 δ(NNN) coord. N_3^- ; 1088, 625 $\nu(ClO_4^-$ ionic)

Table 37. Characteristic IR absorptions (cm^{-1}) for the binuclear Mn(II) and the mononuclear lanthanide(III) complexes

compounds	Assignments										
	Macrocycle										
	ν(CH)		ν(C=N)	ν(C=C)		δ(CH)			ν(C-O)	δ_{oop}(CH)	
$[Mn_2([22]\text{-HMTADO})Cl_2] \cdot H_2O$	2953	2890	1632	1553	1460	1431	1400	1364	1085	816	771
$[Pr(H_2[22]\text{-HMTADO})(O_2NO)](NO_3)_2 \cdot 2H_2O$	2964	2870	1645	1548	1479	1458	1399	1319	1083	821	781
$[Sm(H_2[22]\text{-HMTADO})(O_2NO)](NO_3)_2 \cdot 2H_2O$	2964	2870	1645	1549	1477	1458	1392	1317	1083	824	781
$[Gd(H_2[22]\text{-HMTADO})(O_2NO)](NO_3)_2 \cdot 2H_2O$	2964	2870	1645	1550	1478	1458	396	1317	1085	825	781
$[Dy(H_2[22]\text{-HMTADO})(O_2NO)](NO_3)_2 \cdot H_2O$	2970	2870	1646	1553	1487	1460	1397	1315	1085	827	779

compounds	Assignments
$[Mn_2([22]\text{-HMTADO})Cl_2] \cdot H_2O$	3433 ν(OH) ; ~500 Mn-Cl
$[Pr(H_2[22]\text{-HMTADO})(O_2NO)](NO_3)_2 \cdot 2H_2O$	3437 ν(OH) lattice H_2O ; 1458 ν(N=O), 1283 $\nu_{as}(NO_2)$, 1055 $\nu_s(NO_2)$ bidentate NO_3^- ; 1385 ionic NO_3^-
$[Sm(H_2[22]\text{-HMTADO})(O_2NO)](NO_3)_2 \cdot 2H_2O$	3420 ν(OH) lattice H_2O ; 1460 ν(N=O), 1284 $\nu_{as}(NO_2)$, 1035 $\nu_s(NO_2)$ bidentate NO_3^- ; 1385 ionic NO_3^-
$[Gd(H_2[22]\text{-HMTADO})(O_2NO)](NO_3)_2 \cdot 2H_2O$	3437 ν(OH) lattice H_2O ; 1460 ν(N=O), 1284 $\nu_{as}(NO_2)$, 1035 $\nu_s(NO_2)$ bidentate NO_3^- ; 1385 ionic NO_3^-
$[Dy(H_2[22]\text{-HMTADO})(O_2NO)](NO_3)_2 \cdot H_2O$	3437 ν(OH) lattice H_2O ; 1462 ν(N=O), 1285 $\nu_{as}(NO_2)$, 1035 $\nu_s(NO_2)$ bidentate NO_3^- ; 1385 ionic NO_3^-

3. FAB-mass spectra of the complexes

1) Cu(II) complexes

The FAB mass spectra of the Cu(II) complexes were shown in Fig. 33～41, and summarized at Table 38. The FAB mass spectra of all the complexes contain peaks corresponding to the $[Cu_2([22]\text{-HMTADO})]^+$ and $[Cu([22]\text{-HMTADO})]^+$ ions at m/z 585 and 522, respectively. These major peaks are associated with peaks of mass one or two greater or less, which are attributed to protonated/deprotonated forms. This also accounts for the slight ambiguities in making assignments. The molecular ions of the $[Cu_2([22]\text{-HMTADO})ClO_4]^+$, $[Cu_2([22]\text{-HMTADO})NCS]^+$, and $[Cu_2([22]\text{-HMTADO})ONO_2]^+$ are observed at m/z 684.7, 643.7, and 647.7, respectively. In the mass spectrum of $[Cu_2([22]\text{-HMTADO})(OH_2)]Cl_2 \cdot H_2O$, the peak observed at m/z 620 is due to fragment $[Cu_2([22]\text{-HMTADO})(Cl)]^+$. In the mass spectrum of $[Cu_2([22]\text{-HMTADO})NO_2]NO_2 \cdot 2H_2O$ the peak observed at m/z 675.8 is due to fragments $[Cu_2([22]\text{-HMTADO})(NO_2)_2]^+$. In the mass spectrum of $[Cu_2([22]\text{-HMTADO})S_2O_3] \cdot 5H_2O$ the peak observed at m/z 680.5 is due to the molecular ion $[Cu_2([22]\text{-HMTADO})SO_4]^+$, that is, sulfate ion may coordinate to the copper atom. The rearrangement reactions and oxidation by Fe^{3+} and O_2 from thiosulfate to sulfate has been described by Drushel et al. (see Scheme 6).[66] In the FAB-mass spectrum, this complex is not appeared to vibration bands by thiosulfate ion, but appeared to vibration bands by coordinated sulfate.

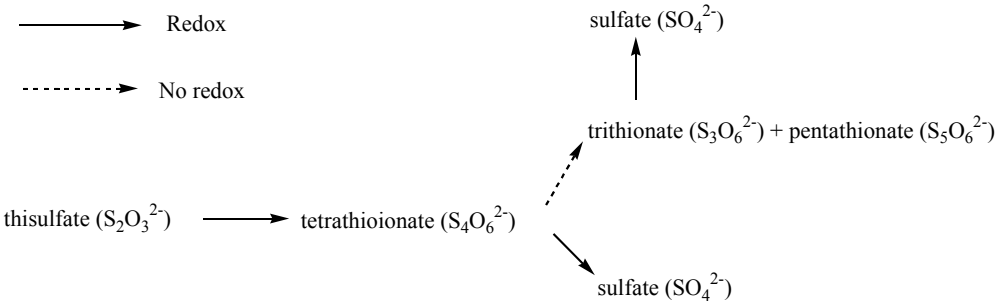

Scheme. 6. The rearrangement reactions and oxidation from thiosulfate to sulfate.

2) bi- and mono-nuclear Ni(II) complexes

The FAB mass spectra of the binuclear Ni(II) complexes were shown in Fig. 42～50, and summarized at Table 39. The FAB mass spectra of all the complexes contain peaks corresponding to the $[Ni_2([22]\text{-HMTADO})]^+$ and $[Ni([22]\text{-HMTADO})]^+$ ions at m/z 575 and 517, respectively. These major peaks are associated with peaks of mass one or two greater or less, which are attributed to protonated/deprotonated forms. This also accounts for the slight ambiguities in making assignments. In the mass spectrum of $[Ni_2([22]\text{-HMTADO})(OH_2)_2]Cl_2 \cdot H_2O$, the peaks observed at m/z 620.7 and 648.8 are due to fragments $[Ni_2([22]\text{-HMTADO})(Cl)]^+$ and $[Ni_2([22]\text{-HMTADO})\text{-}(Cl)_2]^+$, respectively. In the mass spectrum of $[Ni_2([22]\text{-HMTADO})(OH_2)_2]\text{-}(ClO_4)_2 \cdot H_2O$ the peak observed at m/z 675.6 is due to fragment $[Ni_2([22]\text{-HMTADO})(ClO_4)]^+$. In the mass spectrum of $[Ni_2([22]\text{-HMTADO})\text{-}(CN)_2] \cdot 0.5H_2O$, the peaks observed at m/z 599.3 and 618.3 are due to fragments $[Ni_2([22]\text{-HMTADO})(CN)]^+$ and $[Ni_2([22]\text{-HMTADO})(CN)(H_2O)]^+$,

respectively. In the mass spectrum of $[Ni_2([22]\text{-HMTADO})(NCS)_2(OH_2)] \cdot 2H_2O$ the peak observed at m/z 533.7 is due to fragment $[Ni_2([22]\text{-HMTADO})(NCS)]^+$. In the mass spectrum of $[Ni_2([22]\text{-HMTADO})(N_3)_2(OH_2)]$ the peak observed at m/z 618.7 is due to fragment $[Ni_2([22]\text{-HMTADO})(N_3)]^+$. The molecular ions of the $[Ni_2([22]\text{-HMTADO})NO_3]^+$ and $[Ni_2([22]\text{-HMTADO})NO_2]^+$ are observed at m/z 635.4 and 618.5, respectively. In the mass spectrum of $[Ni_2([22]\text{-HMTADO})]Br_2 \cdot 2H_2O$ the peak observed at m/z 654.5 is due to fragment $[Ni_2([22]\text{-HMTADO})Br]^+$. In the mass spectrum of $[Ni_2([22]\text{-HMTADO})S_2O_3]$ the peak observed at m/z 616.8 is due to the molecular ions $[Ni_2([22]\text{-HMTADO})SO_4]^+$, that is, sulfate ion may coordinate to the nickel atom.

The FAB mass spectra of the mononuclear Ni(II) complexes were shown in Fig. 51～53, and summarized at Table 39. The FAB mass spectra of all the complexes contain peaks corresponding to the $[Ni([22]\text{-HMTADO})]^+$ ion at m/z 516.5. These major peaks are associated with peaks of mass one or two greater or less, which are attributed to protonated/deprotonated forms. This also accounts for the slight ambiguities in making assignments. In the FAB mass spectra of the $[Ni(H_2[22]\text{-HMTADO})(OHCH_3)_2](ClO_4)_2$ complex there is an intense peak at m/z 460.8 corresponding to the species $[H_2[22]\text{-HMTADO}]^+$. This indicates that the species $[Ni([22]\text{-HMTADO})]^+$ undergoes demetallation to give the tetraazadioxa macrocycle $H_2[22]$-HMTADO under FAB conditions.

3) Mn(II) complex

The FAB mass spectra of the $[Mn_2([22]\text{-HMTADO})Cl_2] \cdot H_2O$ complex was

shown in Fig. 54, and summarized at Table 40. The FAB mass spectra of the complex contain peaks corresponding to the $[Mn_2([22]\text{-HMTADO}) + H]^+$ and $[Mn([22]\text{-HMTADO})]^+$ ions at m/z 569 and 514, respectively. And there is an intense peak at m/z 461 corresponding to the species $[H_2[22]\text{-HMTADO}]^+$. This indicates that the species $[Mn([22]\text{-HMTADO})]^+$ undergoes demetallation under FAB conditions. The peak observed at m/z 603 and 659 are due to the fragments $[Mn_2([22]\text{-HMTADO})Cl]^+$ and $[Mn_2([22]\text{-HMTADO})(Cl)_2(H_2O)]^+$, respectively.

4) Lanthanide(III) complexes

The FAB mass spectra of the lanthanide(III) complexes were shown in Fig. 55～58, and summarized at Table 40. The FAB mass spectra of all the complexes contain peaks corresponding to the molecular ion $[Ln(H_2[22]\text{-HMTADO})(NO_3)]^+$ for Ln = Pr^{3+} (m/z 661.8), Sm^{3+} (m/z 672.3), Gd^{3+} (m/z 677.7) and Dy^{3+} (m/z 683.8). The molecular ion loses the exocyclic nitrate ligand resulting in the formation of the fragment $[Ln(H_2[22]\text{-HMTADO})]^+$. All these species are well observed in the FAB mass spectra. Removal of nitrate ion from the molecular ion is observed with a mass loss of 63 as HNO_3. For each metal containing species there is a set of peaks due to the different isotopes of the metal. In the FAB mass spectra of all the complexes there is a peak at m/z 460.8 corresponding to the species $[H_2[22]\text{-HMTADO}]^+$. This indicates that the species $[Ln(H_2[22]\text{-HMTADO})]^+$ undergoes demetallation to give the tetraazadioxa macrocycle $H_2[22]$-HMTADO under FAB conditions. Peaks corresponding to sandwich complexes of the type $[Ln(H_2[22]\text{-HMTADO})_2]^+$

for Ln = Sm^{3+} (m/z 1069.2), Gd^{3+} (m/z 1075.7) and Dy^{3+} (m/z 1081.6) ; and $[\{Ln(H_2[22]\text{-}HMTADO)\}_2(NO_3)]^+$ for Ln = Pr^{3+} (m/z 1259.4) are observed in FAB mass spectra. These sandwich complexes might gave been formed during the FAB fragmentation process.[53]

Table 38. FAB-mass spectra for the binuclear Cu(II) complexes of phenol-based macrocyclic ligand (H_2[22]-HMTADO)

complex	m/z	Assignment
$[Cu_2([22]\text{-HMTADO})(OH_2)]Cl_2 \cdot H_2O$	522.5	$[Cu([22]\text{-HMTADO})]^+$
	583.7	$[Cu_2([22]\text{-HMTADO})\text{-}2H]^+$
	585.7	$[Cu_2([22]\text{-HMTADO})]^+$
	620.7	$[Cu_2([22]\text{-HMTADO})(Cl)]^+$
$[Cu_2([22]\text{-HMTADO})(OClO_3)(OH_2)]ClO_4 \cdot 2H_2O$	522.5	$[Cu([22]\text{-HMTADO})]^+$
	583.7	$[Cu_2([22]\text{-HMTADO})\text{-}2H]^+$
	585.7	$[Cu_2([22]\text{-HMTADO})]^+$
	684.7	$[Cu_2([22]\text{-HMTADO})(ClO_4)]^+$
$[Cu_2([22]\text{-HMTADO})(CN)_2] \cdot 0.5H_2O$	523.3	$[Cu([22]\text{-HMTADO})+H]^+$
	583.6	$[Cu_2([22]\text{-HMTADO})\text{-}2H]^+$
	585.6	$[Cu_2([22]\text{-HMTADO})]^+$
$[Cu_2([22]\text{-HMTADO})(NCS)(OH_2)]NCS \cdot 2H_2O$	522.7	$[Cu([22]\text{-HMTADO})]^+$
	583.5	$[Cu_2([22]\text{-HMTADO})\text{-}2H]^+$
	585.5	$[Cu_2([22]\text{-HMTADO})]^+$
	643.7	$[Cu_2([22]\text{-HMTADO})(NCS)]^+$
$[Cu_2([22]\text{-HMTADO})(N_3)(OH_2)]N_3 \cdot H_2O$	522.7	$[Cu([22]\text{-HMTADO})]^+$
	583.5	$[Cu_2([22]\text{-HMTADO})\text{-}2H]^+$
	585.5	$[Cu_2([22]\text{-HMTADO})]^+$
$[Cu_2([22]\text{-HMTADO})ONO_2]NO_3 \cdot 4H_2O$	522.7	$[Cu([22]\text{-HMTADO})]^+$
	583.6	$[Cu_2([22]\text{-HMTADO})\text{-}2H]^+$
	585.6	$[Cu_2([22]\text{-HMTADO})]^+$
	647.7	$[Cu_2([22]\text{-HMTADO})(NO_3)]^+$
$[Cu_2([22]\text{-HMTADO})NO_2]NO_2 \cdot 2H_2O$	522.3	$[Cu([22]\text{-HMTADO})]^+$
	583.7	$[Cu_2([22]\text{-HMTADO})\text{-}2H]^+$
	585.7	$[Cu_2([22]\text{-HMTADO})]^+$
	675.8	$[Cu_2([22]\text{-HMTADO})(NO_2)_2]^+$

$[Cu_2([22]\text{-HMTADO})]Br_2 \cdot 1.5H_2O$	521.5	$[Cu([22]\text{-HMTADO})]^+$
	583.4	$[Cu_2([22]\text{-HMTADO})\text{-}2H]^+$
	585.4	$[Cu_2([22]\text{-HMTADO})]^+$
	666.4	$[Cu_2([22]\text{-HMTADO})(Br)]^+$
$[Cu_2([22]\text{-HMTADO})S_2O_3] \cdot 5H_2O$	522.4	$[Cu([22]\text{-HMTADO})]^+$
	583.4	$[Cu_2([22]\text{-HMTADO})\text{-}2H]^+$
	585.4	$[Cu_2([22]\text{-HMTADO})]^+$
	680.5	$[Cu_2([22]\text{-HMTADO})(SO_4)]^+$

Table 39. FAB-mass spectra for the mono- and bi-nuclear Ni(II) complexes of phenol-based macrocyclic ligand (H_2[22]-HMTADO)

complex	m/z	Assignment
$[Ni_2([22]\text{-HMTADO})(OH_2)_2]Cl_2 \cdot H_2O$	518.5	$[Ni([22]\text{-HMTADO})+H]^+$
	573.6	$[Ni_2([22]\text{-HMTADO})\text{-}2H]^+$
	575.6	$[Ni_2([22]\text{-HMTADO})]^+$
	610.7	$[Ni_2([22]\text{-HMTADO})(Cl)\text{-}H]^+$
	648.8	$[Ni_2([22]\text{-HMTADO})(Cl)_2]^+$
$[Ni_2([22]\text{-HMTADO})(OH_2)_2](ClO_4)_2 \cdot H_2O$	518.5	$[Ni([22]\text{-HMTADO})+H]^+$
	573.6	$[Ni_2([22]\text{-HMTADO})\text{-}2H]^+$
	575.6	$[Ni_2([22]\text{-HMTADO})]^+$
	675.6	$[Ni_2([22]\text{-HMTADO})(ClO_4)]^+$
$[Ni_2([22]\text{-HMTADO})(CN)_2] \cdot 0.5H_2O$	518.2	$[Ni([22]\text{-HMTADO})+H]^+$
	573.2	$[Ni_2([22]\text{-HMTADO})\text{-}2H]^+$
	575.2	$[Ni_2([22]\text{-HMTADO})]^+$
	599.3	$[Ni_2([22]\text{-HMTADO})(CN)]^+$
	618.3	$[Ni_2([22]\text{-HMTADO})(CN)(H_2O)]^+$

$[Ni_2([22]\text{-HMTADO})(NCS)_2(OH_2)] \cdot 2H_2O$	517.2	$[Ni([22]\text{-HMTADO})]^+$
	573.5	$[Ni_2([22]\text{-HMTADO})\text{-}2H]^+$
	575.5	$[Ni_2([22]\text{-HMTADO})]^+$
	533.7	$[Ni_2([22]\text{-HMTADO})(NCS)]^+$
$[Ni_2([22]\text{-HMTADO})(N_3)_2(OH_2)]$	517.5	$[Ni([22]\text{-HMTADO})]^+$
	573.5	$[Ni_2([22]\text{-HMTADO})\text{-}2H]^+$
	575.5	$[Ni_2([22]\text{-HMTADO})]^+$
	618.7	$[Ni_2([22]\text{-HMTADO})(N_3)]^+$
$[Ni_2([22]\text{-HMTADO})(ONO_2)(OH_2)_2]NO_3 \cdot 3H_2O$	517.3	$[Ni([22]\text{-HMTADO})]^+$
	573.3	$[Ni_2([22]\text{-HMTADO})\text{-}2H]^+$
	575.3	$[Ni_2([22]\text{-HMTADO})]^+$
	635.4	$[Ni_2([22]\text{-HMTADO})(NO_3)]^+$
$[Ni_2([22]\text{-HMTADO})NO_2]NO_2 \cdot H_2O$	517.3	$[Ni([22]\text{-HMTADO})]^+$
	573.4	$[Ni_2([22]\text{-HMTADO})\text{-}2H]^+$
	575.4	$[Ni_2([22]\text{-HMTADO})]^+$
	618.5	$[Ni_2([22]\text{-HMTADO})(NO_2)]^+$
$[Ni_2([22]\text{-HMTADO})]Br_2 \cdot 2H_2O$	517.3	$[Ni([22]\text{-HMTADO})]^+$
	573.3	$[Ni_2([22]\text{-HMTADO})\text{-}2H]^+$
	575.3	$[Ni_2([22]\text{-HMTADO})]^+$
	654.5	$[Ni_2([22]\text{-HMTADO})(Br)]^+$
$[Ni_2([22]\text{-HMTADO})S_2O_3]$	517.3	$[Ni([22]\text{-HMTADO})]^+$
	573.3	$[Ni_2([22]\text{-HMTADO})\text{-}2H]^+$
	575.3	$[Ni_2([22]\text{-HMTADO})]^+$
	664.5	$[Ni_2([22]\text{-HMTADO})(SO_4)]^+$
$[Ni(H_2[22]\text{-HMTADO})(OHCH_3)_2](ClO_4)_2$	460.8	$[H_2[22]\text{-HMTADO}]^+$
	516.7	$[Ni(H_2[22]\text{-HMTADO})\text{-}2H]^+$
	517.7	$[Ni(H_2[22]\text{-HMTADO})\text{-}H]^+$
	616.8	$[Ni([22]\text{-HMTADO})(ClO_4)]^+$
$[Ni(H_2[22]\text{-HMTADO})(NCS)_2] \cdot H_2O$	516.5	$[Ni(H_2[22]\text{-HMTADO})\text{-}2H]^+$
$[Ni(H_2[22]\text{-HMTADO})(N_3)(OH_2)]ClO_4 \cdot H_2O$	516.5	$[Ni(H_2[22]\text{-HMTADO})\text{-}2H]^+$

Table 40. FAB-mass spectra for the binuclear Mn(II) and mononuclear Ln(III) complexes of phenol-based macrocyclic ligand (H_2[22]-HMTADO)

complex	m/z	Assignment
[Mn_2([22]-HMTADO)Cl_2] · H_2O	461	[H_2[22]-HMTADO]$^+$
	514	[Mn(H_2[22]-HMTADO)]$^+$
	569	[Mn_2(H_2[22]-HMTADO)+H]$^+$
	585	[Mn_2(H_2[22]-HMTADO)(H_2O)+H]$^+$
	603	[Mn_2(H_2[22]-HMTADO)(Cl)]$^+$
	659	[Mn_2(H_2[22]-HMTADO)$(Cl)_2$(H_2O)]$^+$
[Pr(H_2[22]-HMTADO)O_2NO]$(NO_3)_2$ · $2H_2O$	460.8	[H_2[22]-HMTADO]$^+$
	598.7	[Pr(H_2[22]-HMTADO)]$^+$
	661.8	[Pr(H_2[22]-HMTADO)(NO_3)]$^+$
	1259.4	[{Pr(H_2[22]-HMTADO)}$_2$$(NO_3)$]$^+$
[Sm(H_2[22]-HMTADO)O_2NO]$(NO_3)_2$ · $2H_2O$	460.5	[H_2[22]-HMTADO]$^+$
	609.3	[Sm(H_2[22]-HMTADO)]$^+$
	672.3	[Sm(H_2[22]-HMTADO)(NO_3)]$^+$
	1069.2	[Sm(H_2[22]-HMTADO)$_2$]$^+$
[Gd(H_2[22]-HMTADO)O_2NO]$(NO_3)_2$ · $2H_2O$	460.8	[H_2[22]-HMTADO]$^+$
	615.7	[Gd(H_2[22]-HMTADO)]$^+$
	677.7	[Gd(H_2[22]-HMTADO)(NO_3)]$^+$
	1075.7	[Gd(H_2[22]-HMTADO)$_2$]$^+$
[Dy(H_2[22]-HMTADO)O_2NO]$(NO_3)_2$ · H_2O	460.8	[H_2[22]-HMTADO]$^+$
	621.8	[Dy(H_2[22]-HMTADO)]$^+$
	683.8	[Dy(H_2[22]-HMTADO)(NO_3)]$^+$
	1081.6	[Dy(H_2[22]-HMTADO)$_2$]$^+$

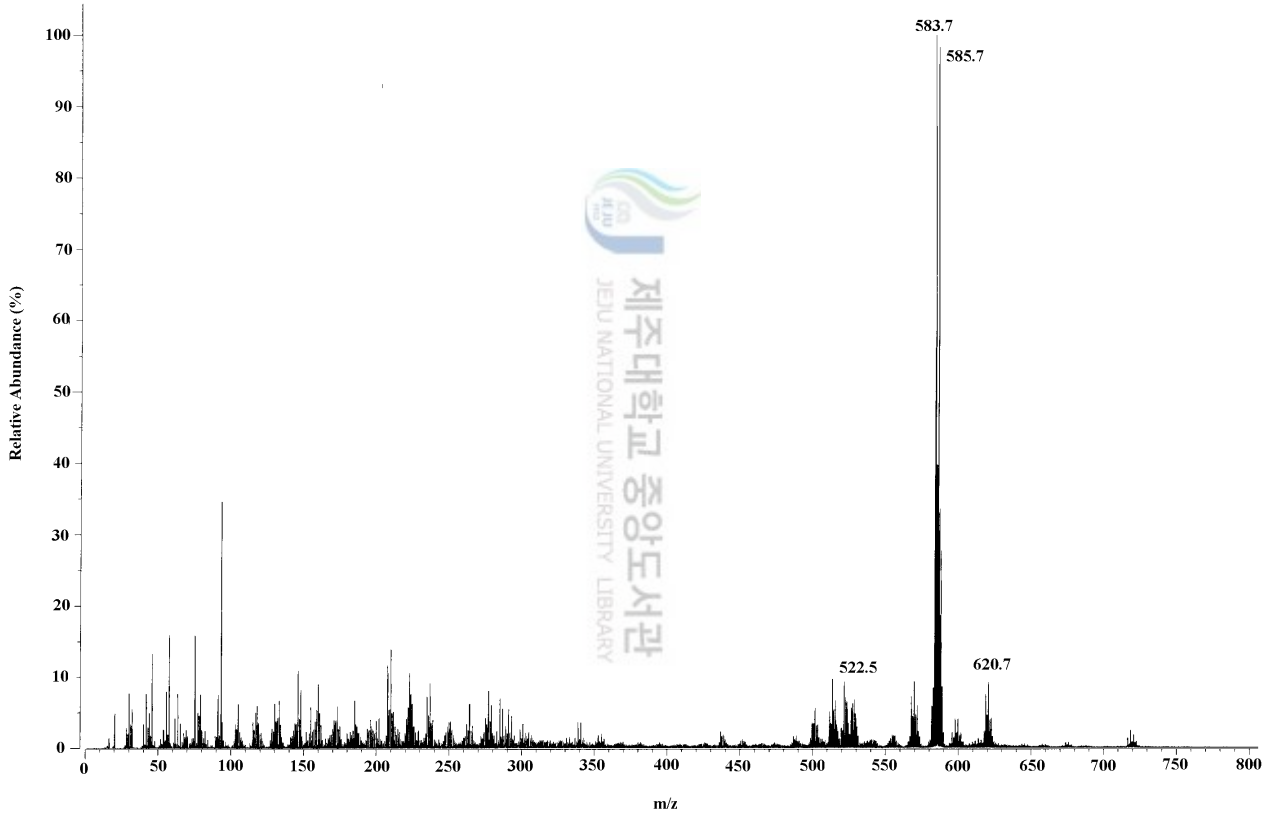

Fig. 33. FAB mass spectrum of the $[Cu_2([22]\text{-HMTADO})(OH_2)]Cl_2 \cdot H_2O$.

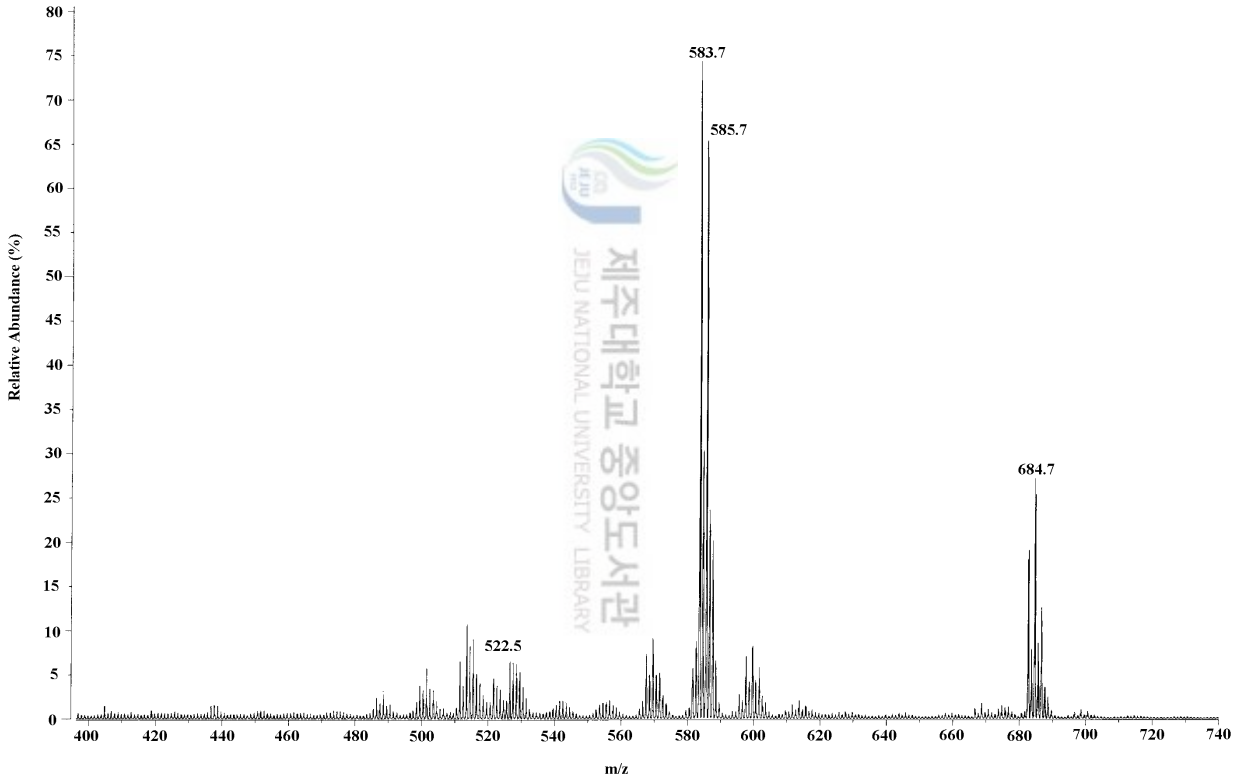

Fig. 34. FAB mass spectrum of the $[Cu_2([22]\text{-}HMTADO)(OClO_3)(OH_2)]ClO_4{\cdot}2H_2O$.

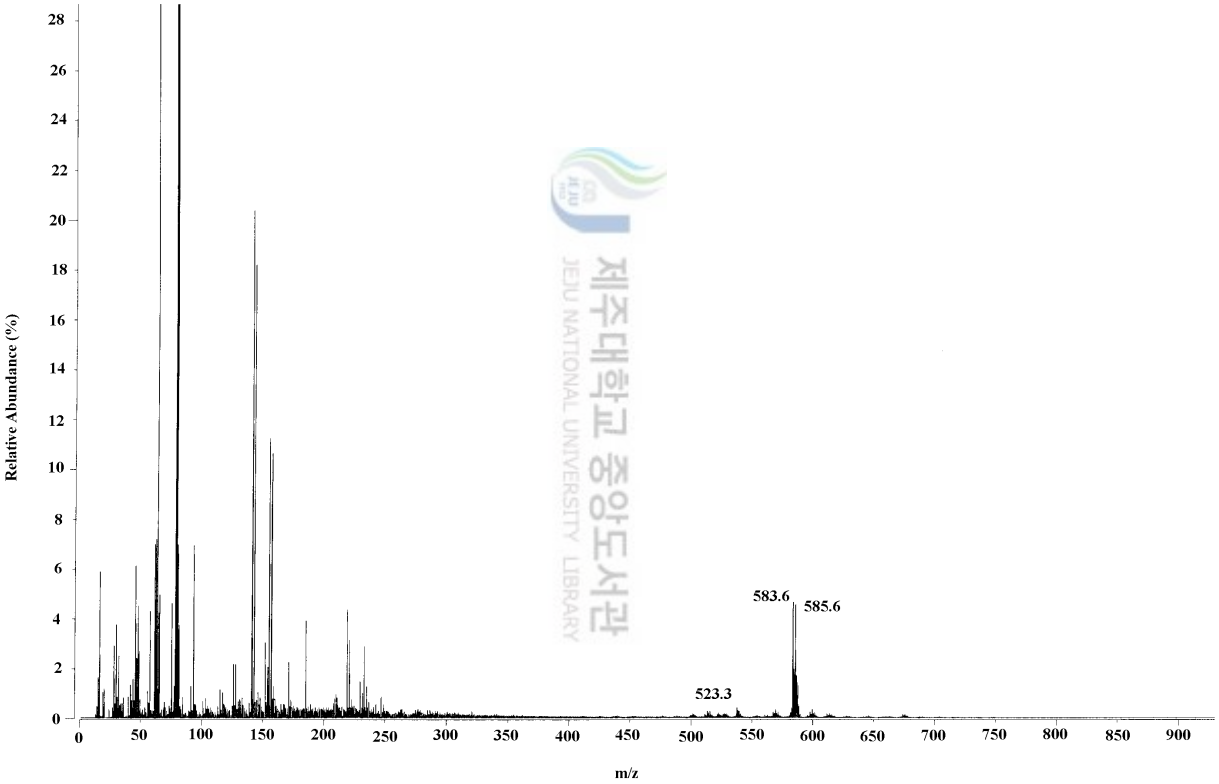

Fig. 35. FAB mass spectrum of the $[Cu_2([22]\text{-HMTADO})(CN)_2]\cdot 0.5H_2O$.

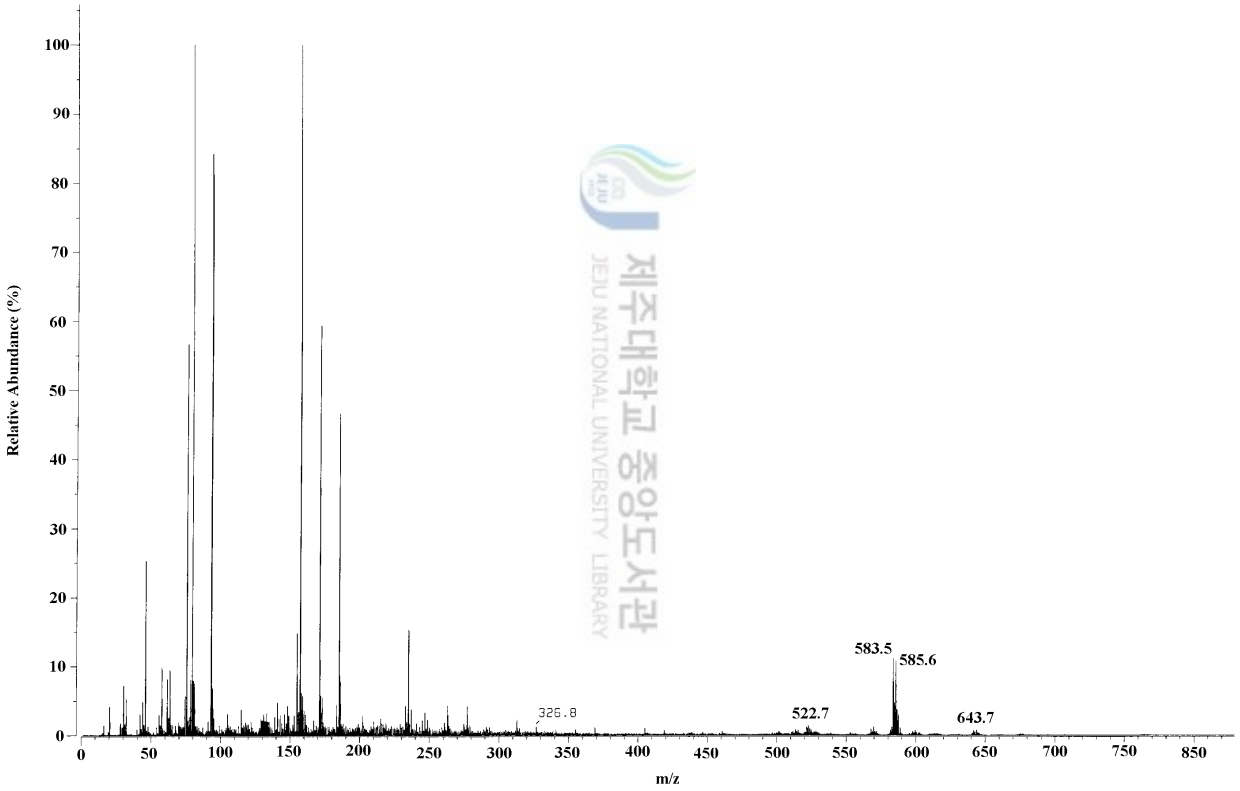

Fig. 36. FAB mass spectrum of the $[Cu_2([22]\text{-HMTADO})(NCS)(OH_2)]NCS{\cdot}2H_2O$.

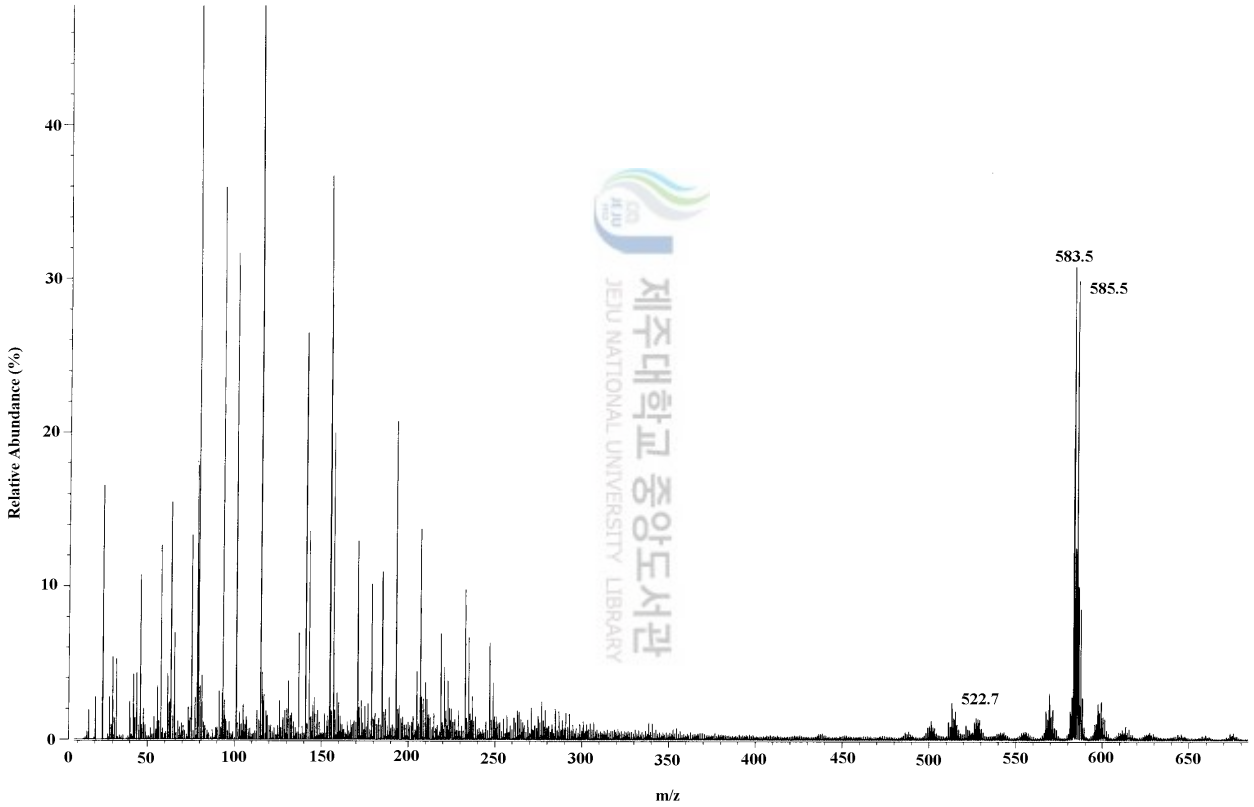

Fig. 37. FAB mass spectrum of the $[Cu_2([22]\text{-HMTADO})(N_3)(OH_2)]N_3{\cdot}H_2O$.

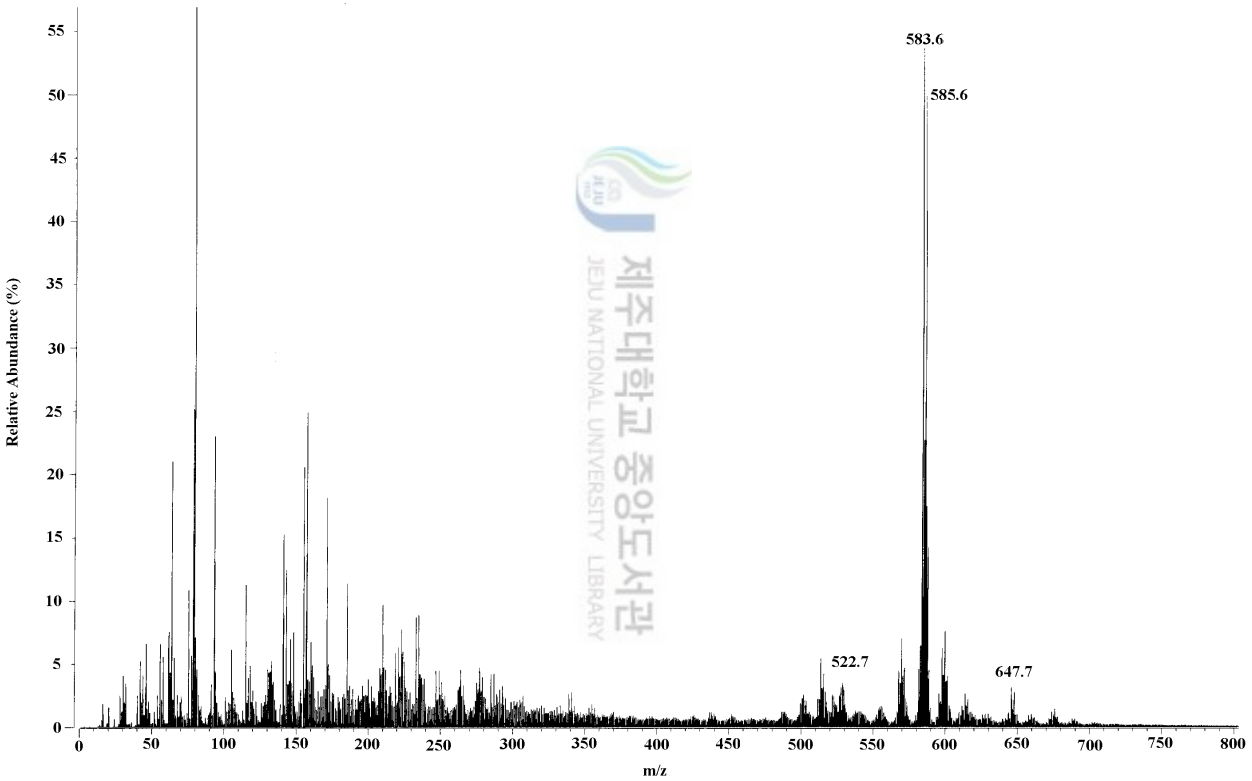

Fig. 38. FAB mass spectrum of the $[[Cu_2([22]\text{-HMTADO})ONO_2]NO_3 \cdot 4H_2O$.

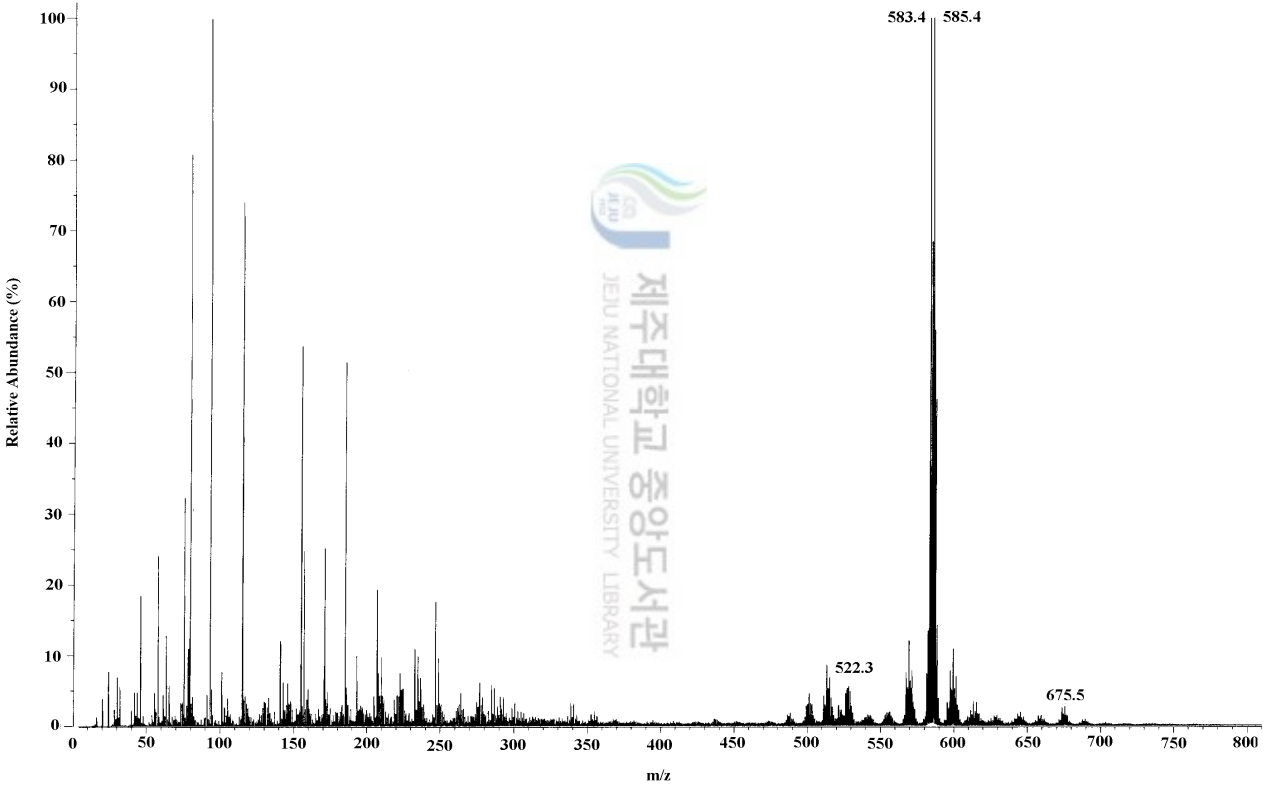

Fig. 39. FAB mass spectrum of the $[Cu_2([22]\text{-HMTADO})NO_2]NO_2 \cdot 2H_2O$.

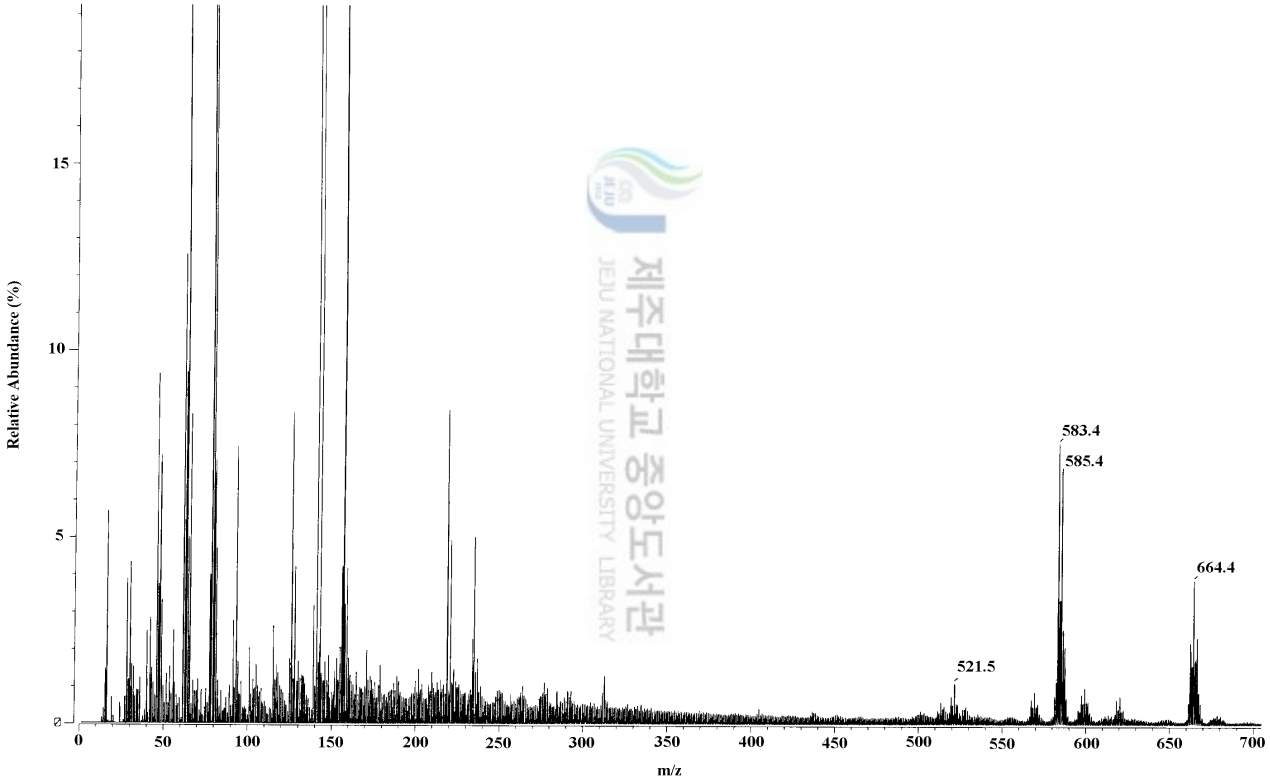

Fig. 40. FAB mass spectrum of the $[Cu_2([22]\text{-HMTADO})]Br_2 \cdot 1.5H_2O$.

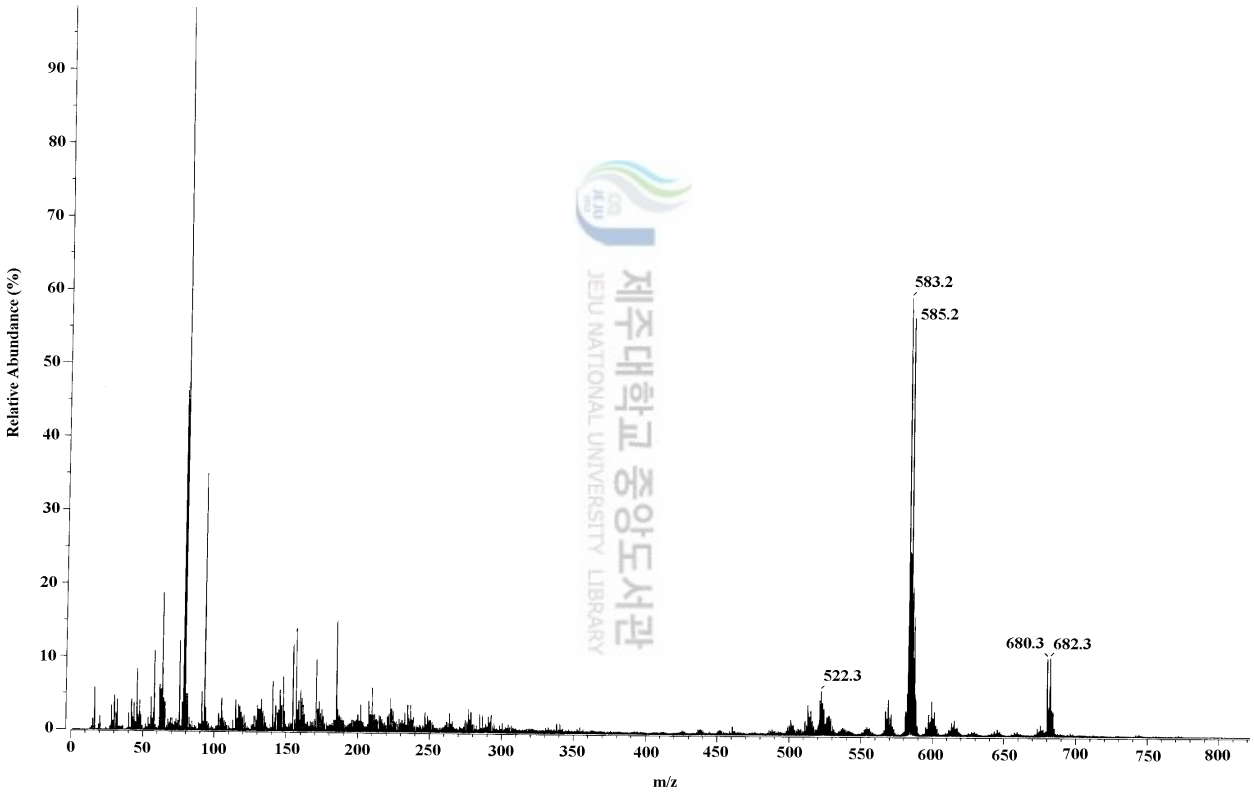

Fig. 41. FAB mass spectrum of the $[Cu_2([22]\text{-HMTADO})S_2O_3]\cdot 5H_2O$.

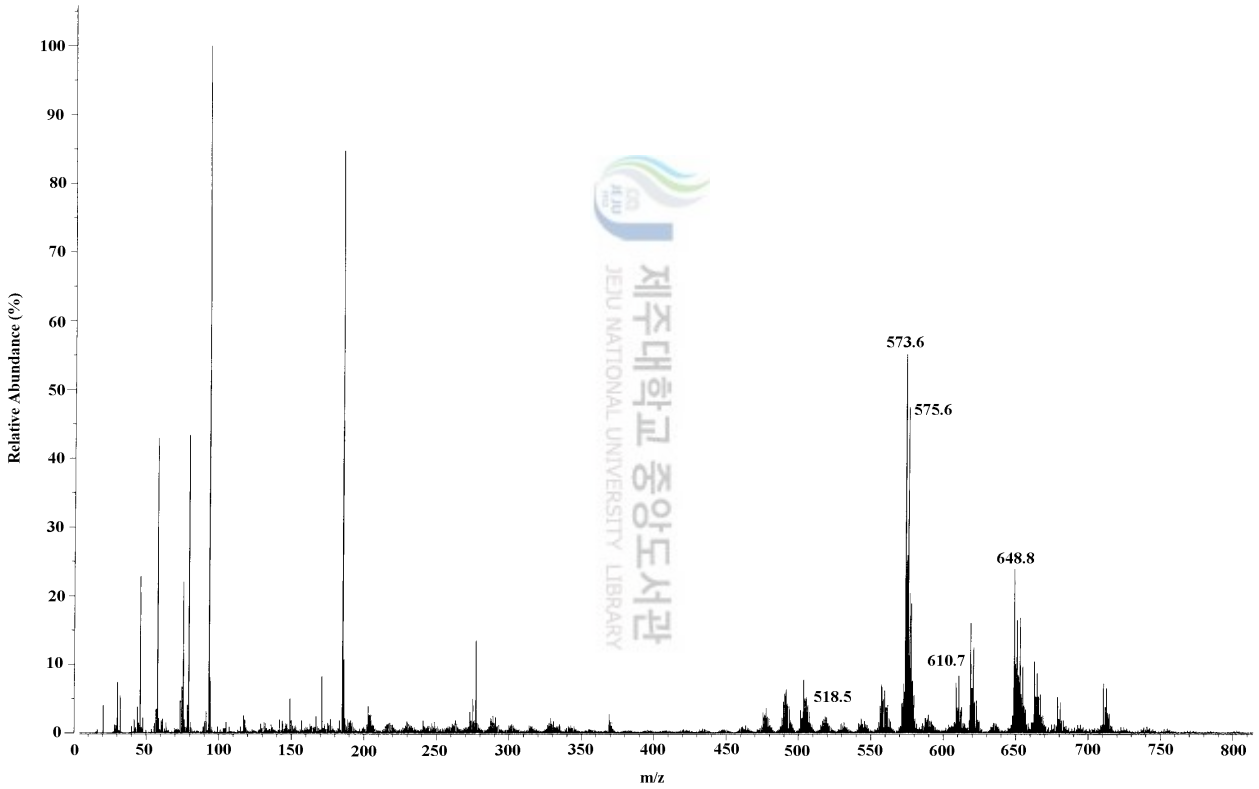

Fig. 42. FAB mass spectrum of the $[Ni_2([22]\text{-HMTADO})(OH_2)_2]Cl_2 \cdot H_2O$.

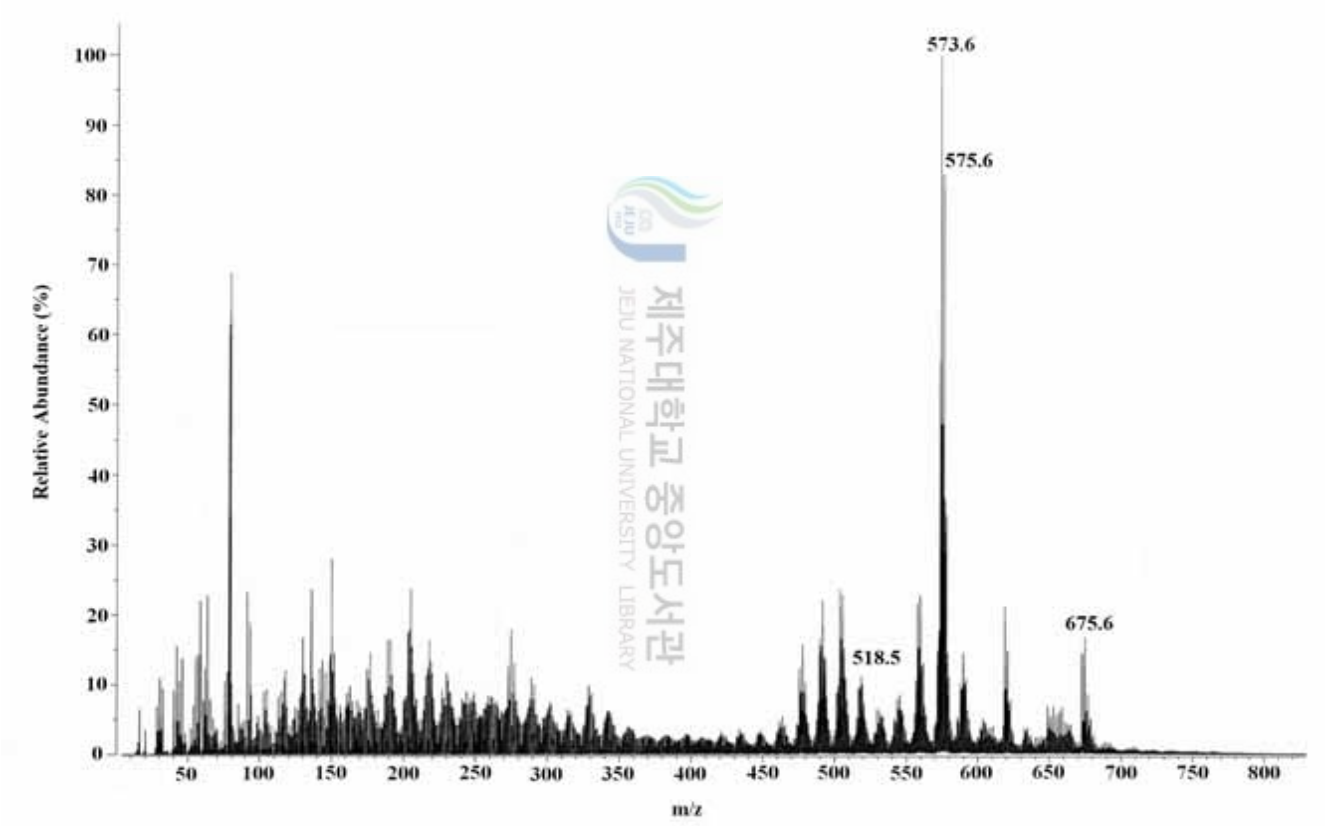

Fig. 43. FAB mass spectrum of the $[Ni_2([22]\text{-HMTADO})(OH_2)_2](ClO_4)_2 \cdot H_2O$.

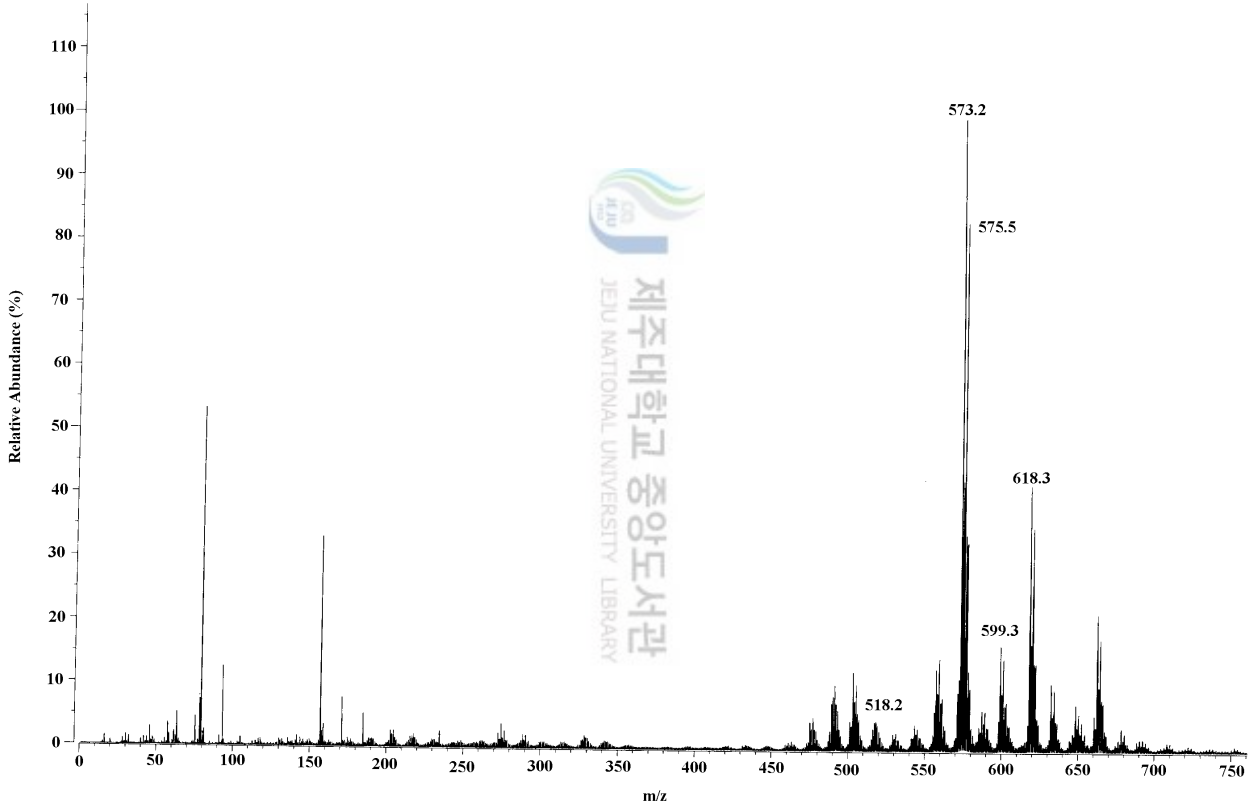

Fig. 44. FAB mass spectrum of the $[Ni_2([22]\text{-HMTADO})(CN)_2]\cdot 0.5H_2O$.

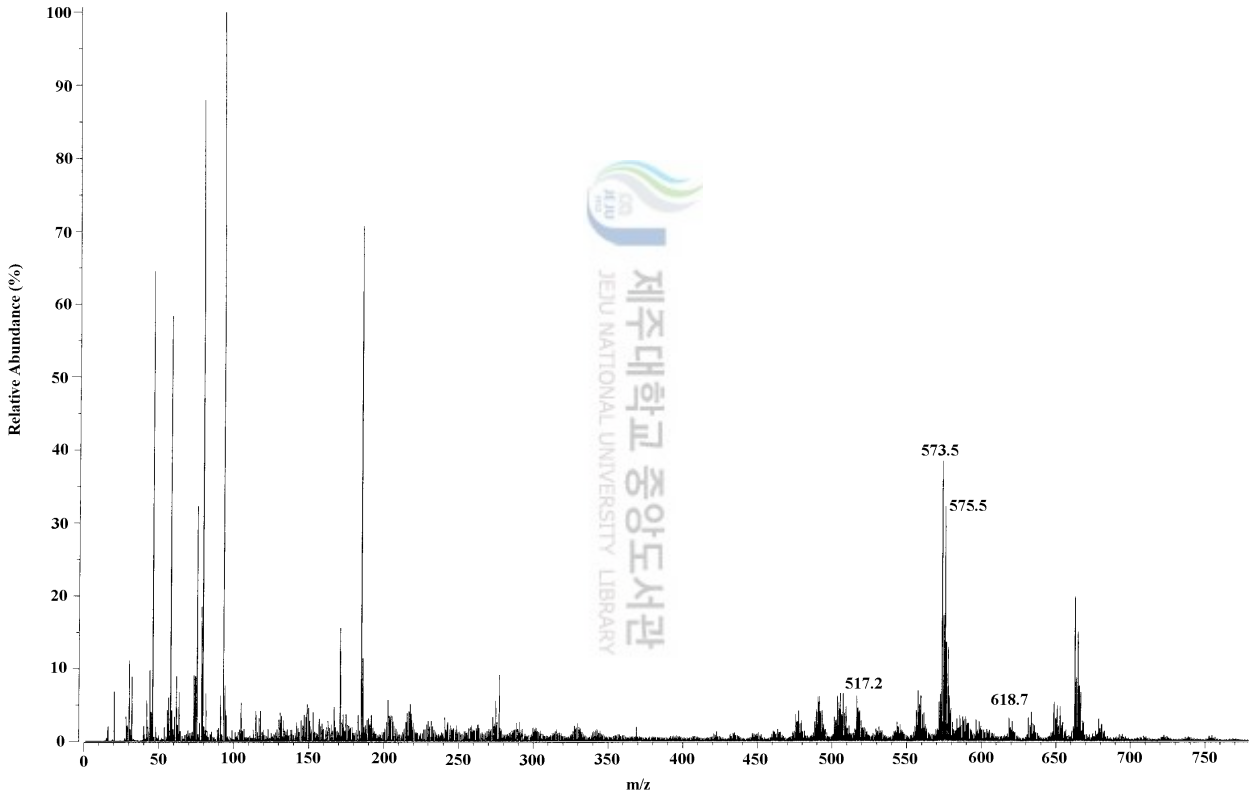

Fig. 45. FAB mass spectrum of the $[Ni_2([22]\text{-HMTADO})(NCS)_2(OH_2)]\cdot 2H_2O$.

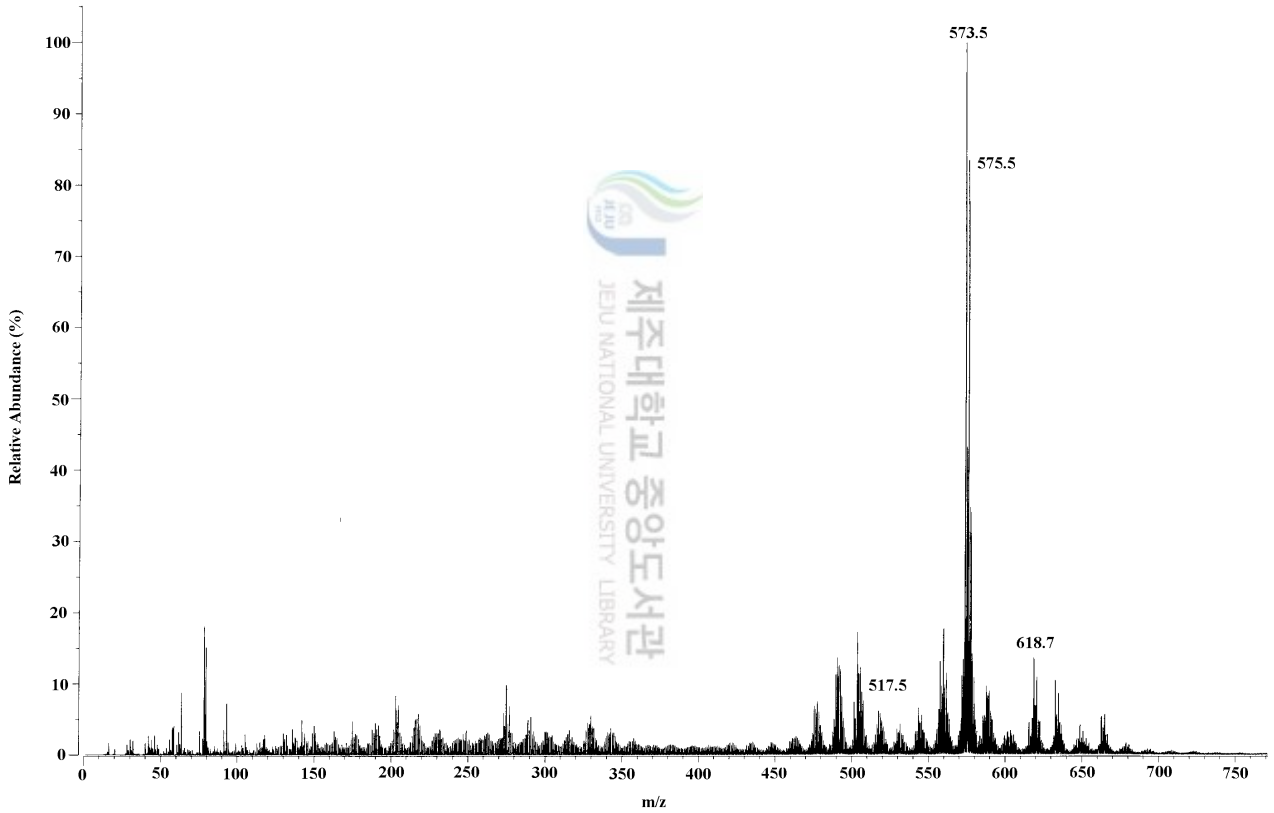

Fig. 46. FAB mass spectrum of the $[Ni_2([22]\text{-HMTADO})(N_3)_2(OH_2)]$.

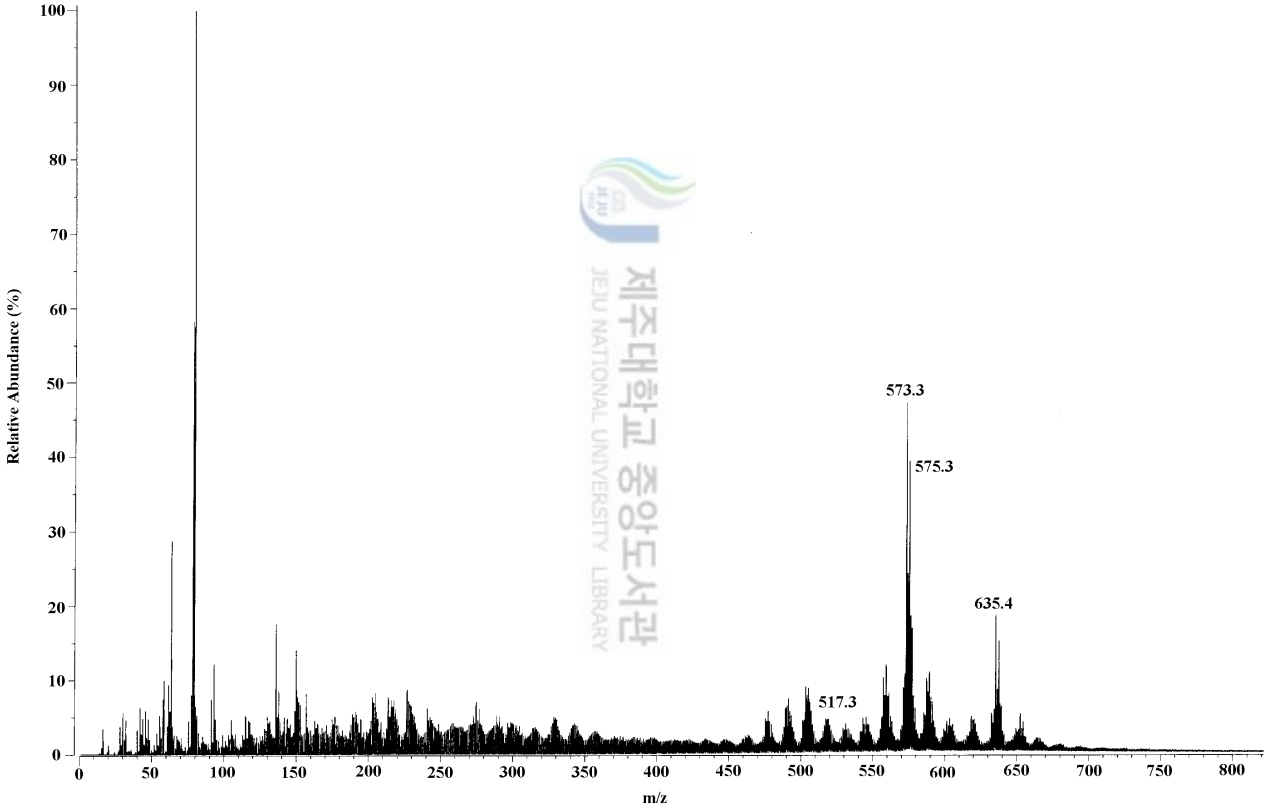

Fig. 47. FAB mass spectrum of the $[Ni_2([22]\text{-HMTADO})(ONO_2)(OH_2)_2]NO_3{\cdot}3H_2O$.

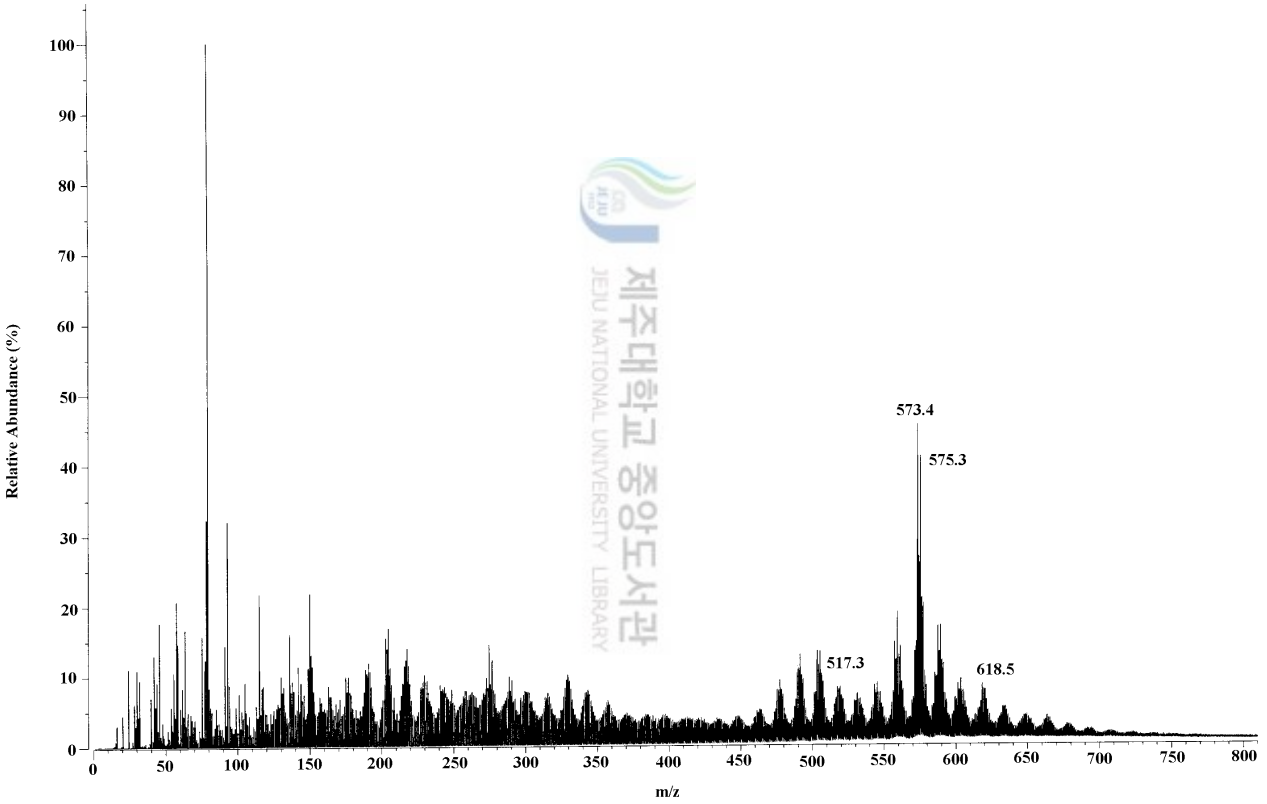

Fig. 48. FAB mass spectrum of the $[Ni_2([22]\text{-HMTADO})NO_2]NO_2{\cdot}H_2O$.

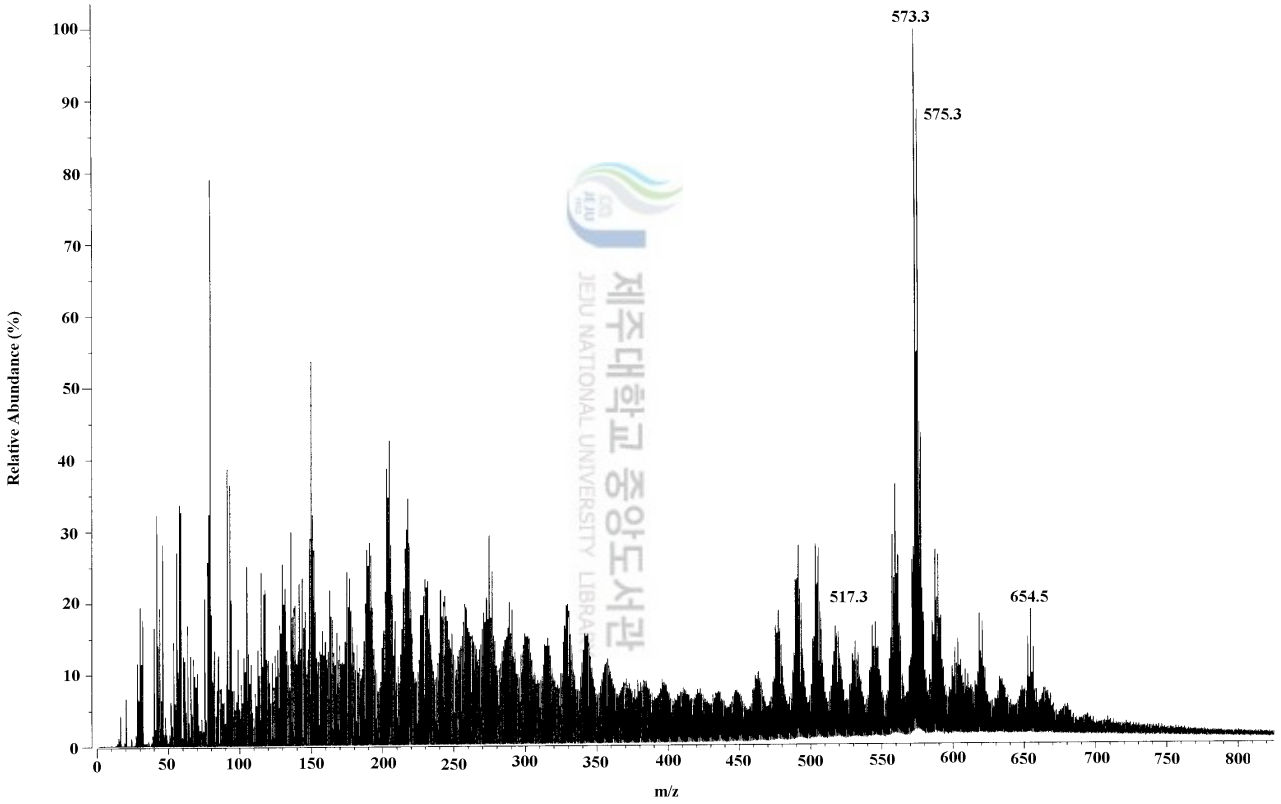

Fig. 49. FAB mass spectrum of the $[Ni_2([22]\text{-HMTADO})]Br_2 \cdot 2H_2O$.

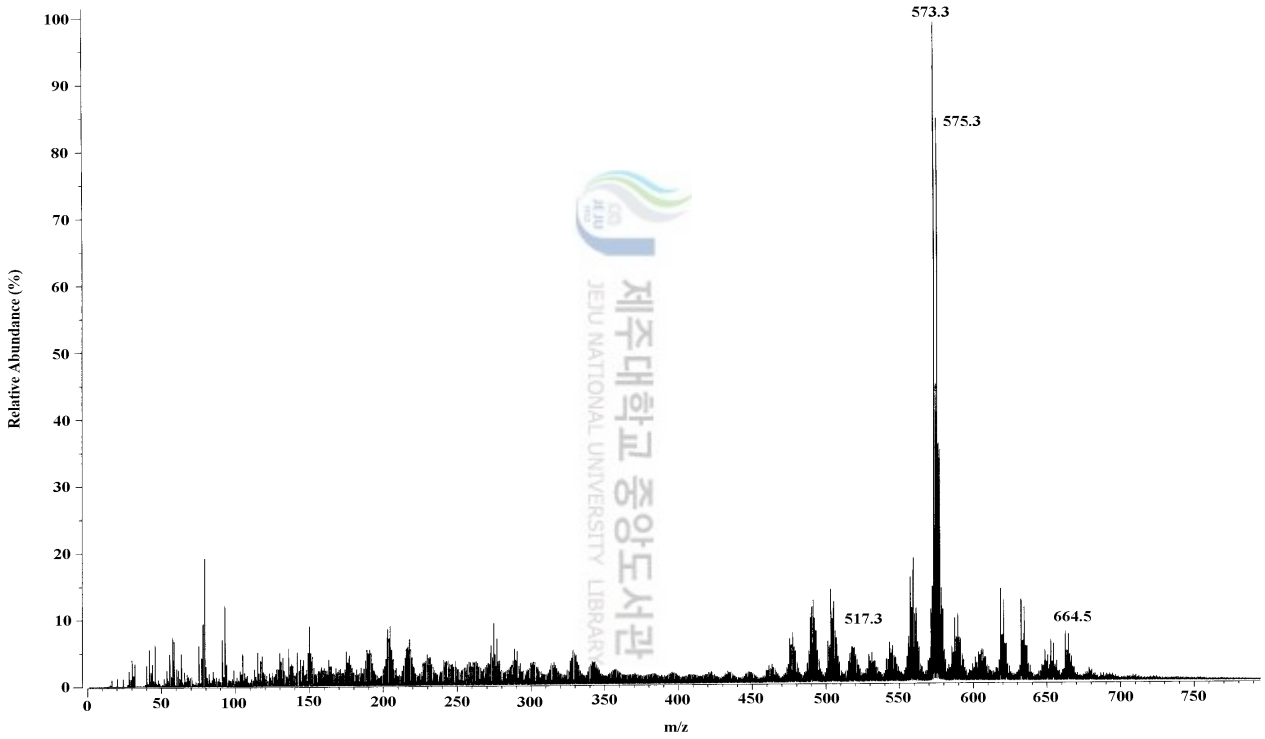

Fig. 50. FAB mass spectrum of the $[Ni_2([22]\text{-HMTADO})S_2O_3]$.

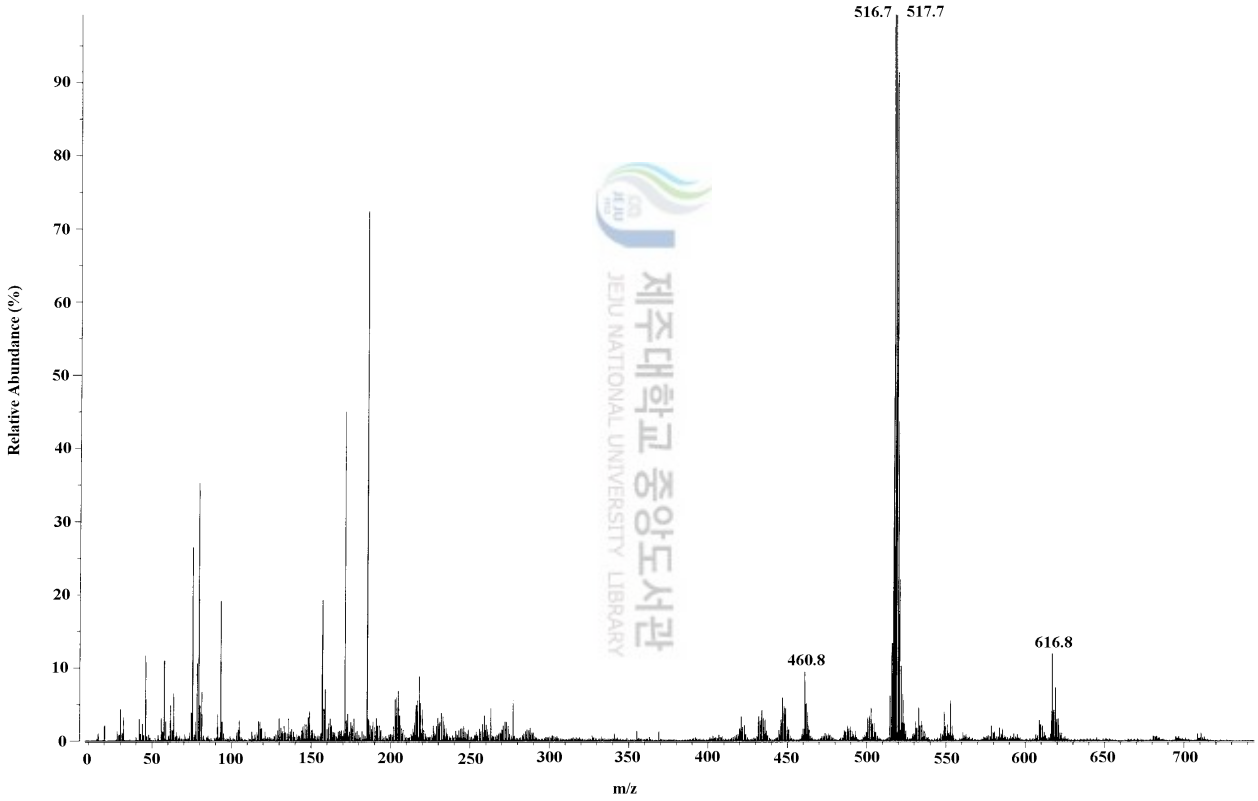

Fig. 51. FAB mass spectrum of the $[Ni(H_2[22]\text{-}HMTADO)(OHCH_3)_2](ClO_4)_2$.

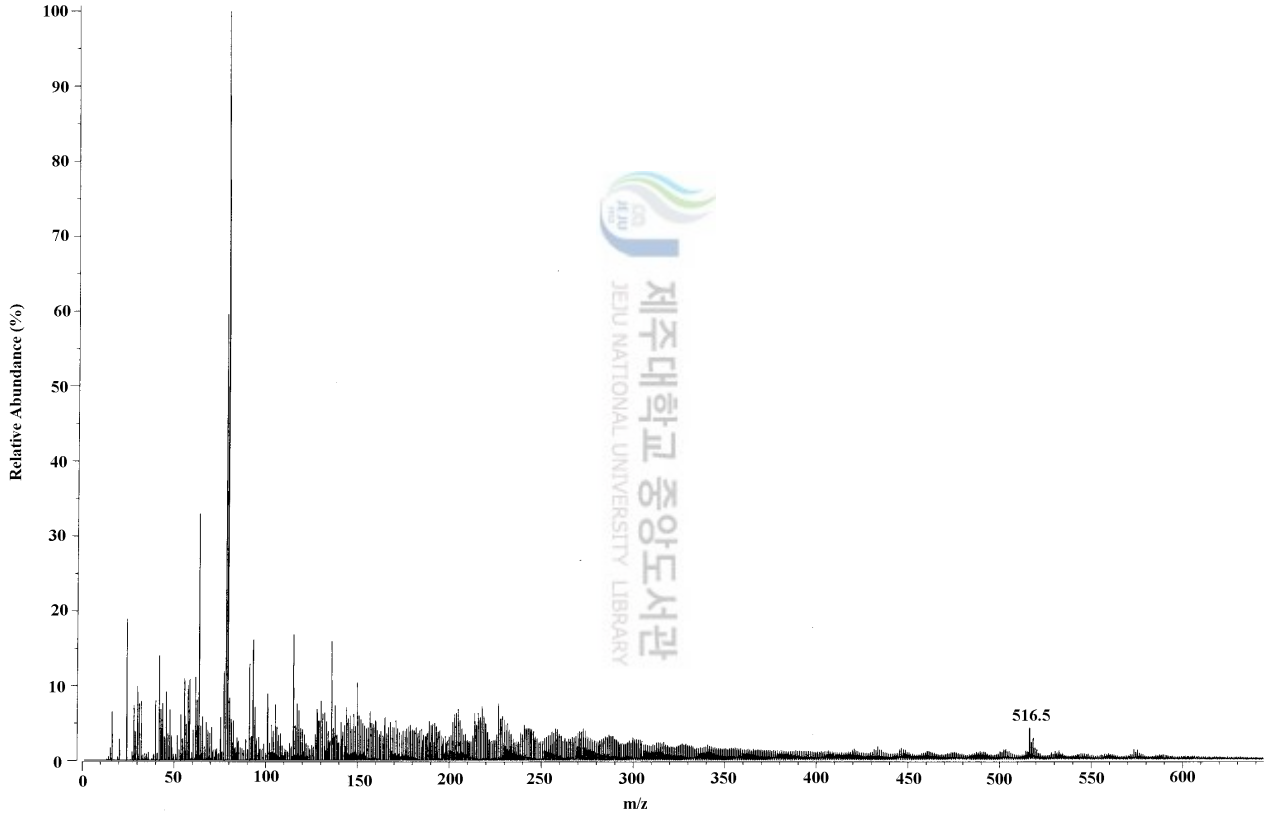

Fig. 52. FAB mass spectrum of the $[Ni(H_2[22]\text{-}HMTADO)(NCS)_2]\cdot H_2O$.

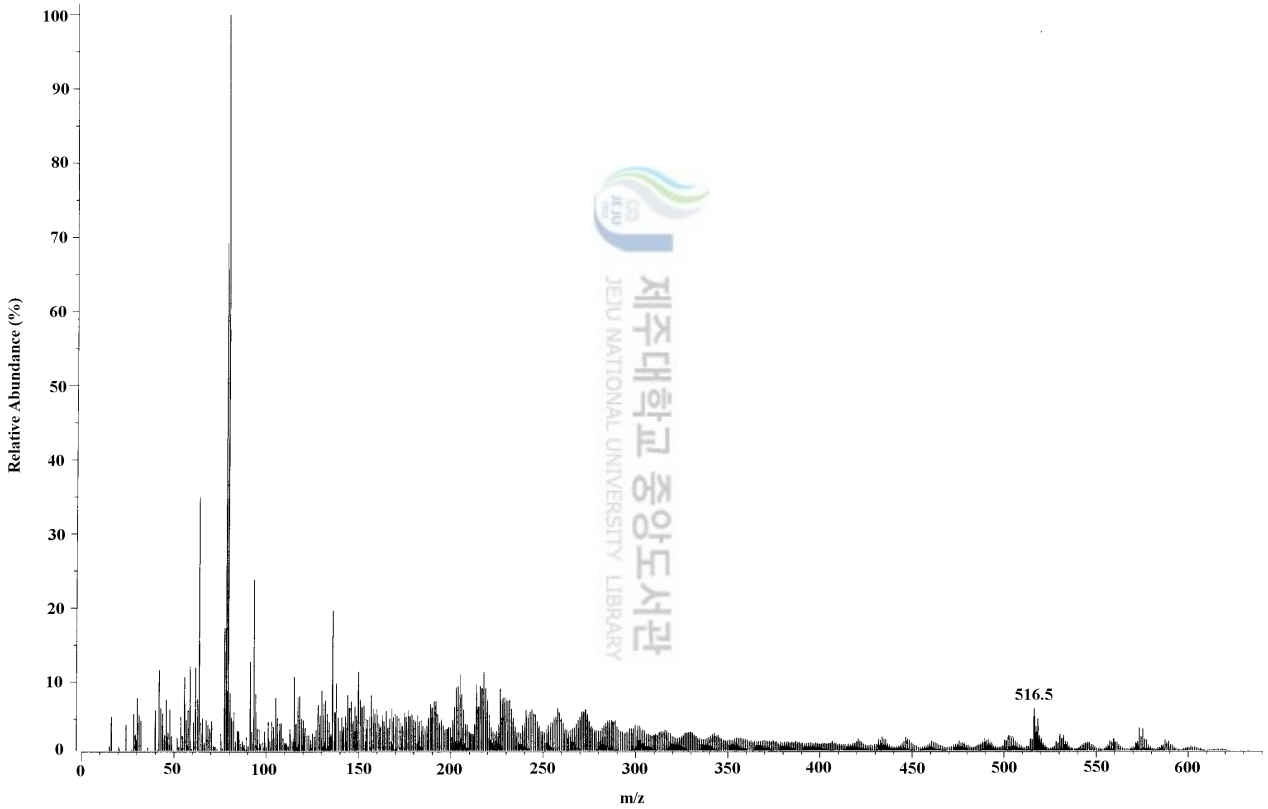

Fig. 53. FAB mass spectrum of the $[Ni(H_2[22]\text{-}HMTADO)(N_3)(OH_2)]ClO_4{\cdot}H_2O$.

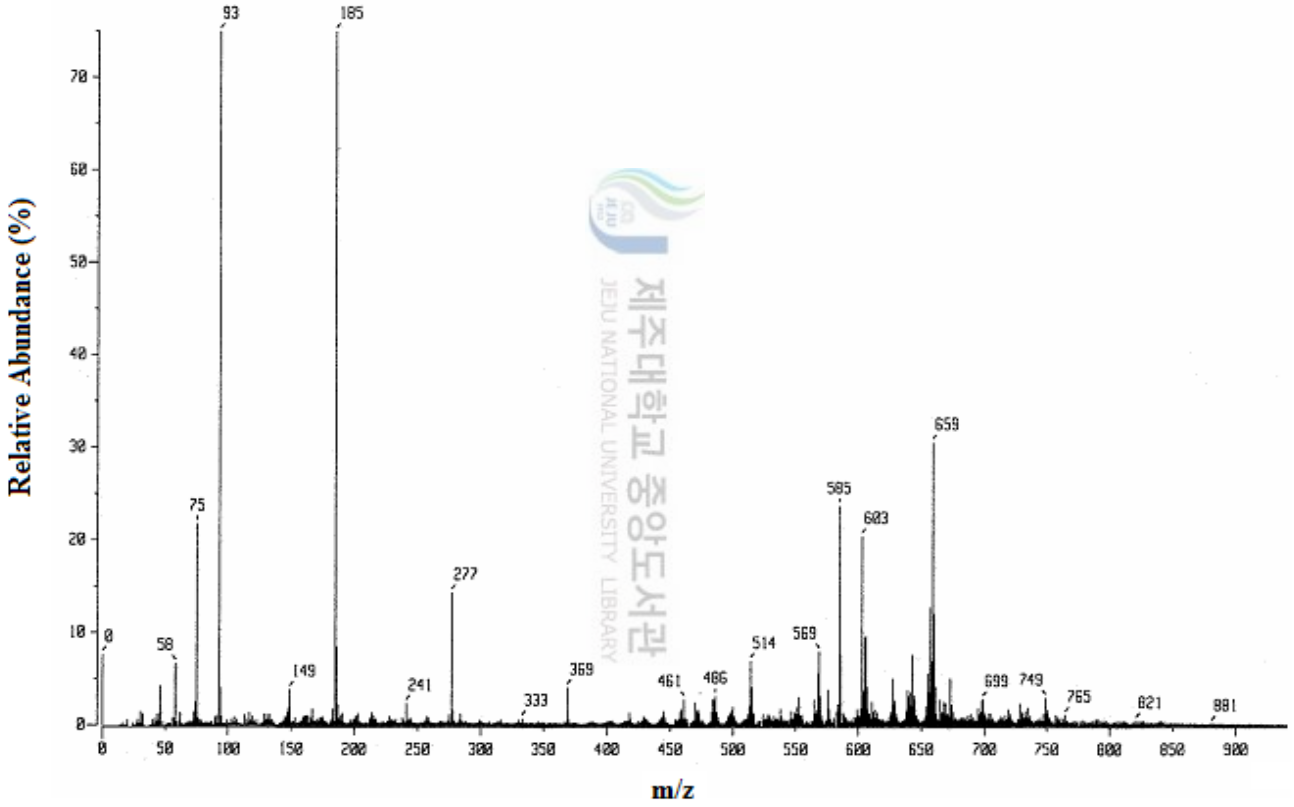

Fig. 54. FAB mass spectrum of the $[Mn_2([22]\text{-}HMTADO)Cl_2]\cdot H_2O$.

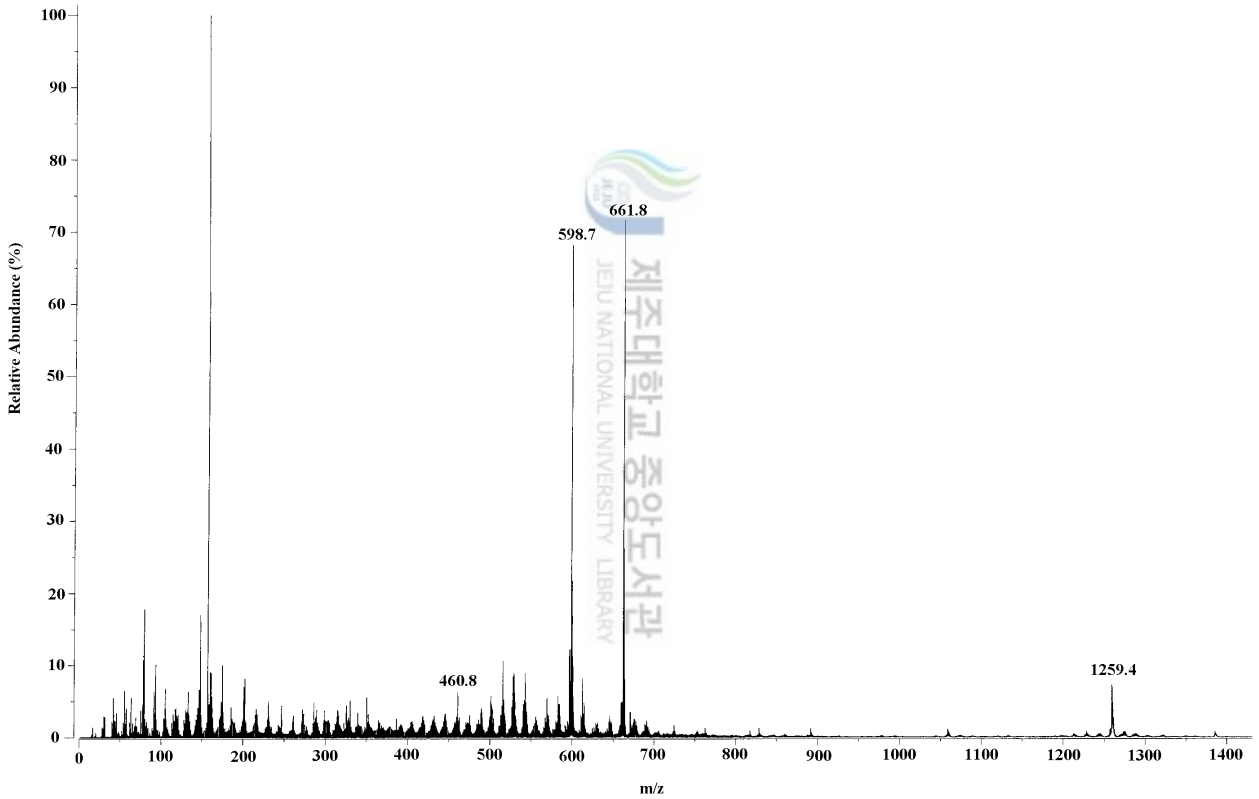

Fig. 55. FAB mass spectrum of the $[Pr(H_2[22]\text{-}HMTADO)O_2NO](NO_3)_2{\cdot}2H_2O$.

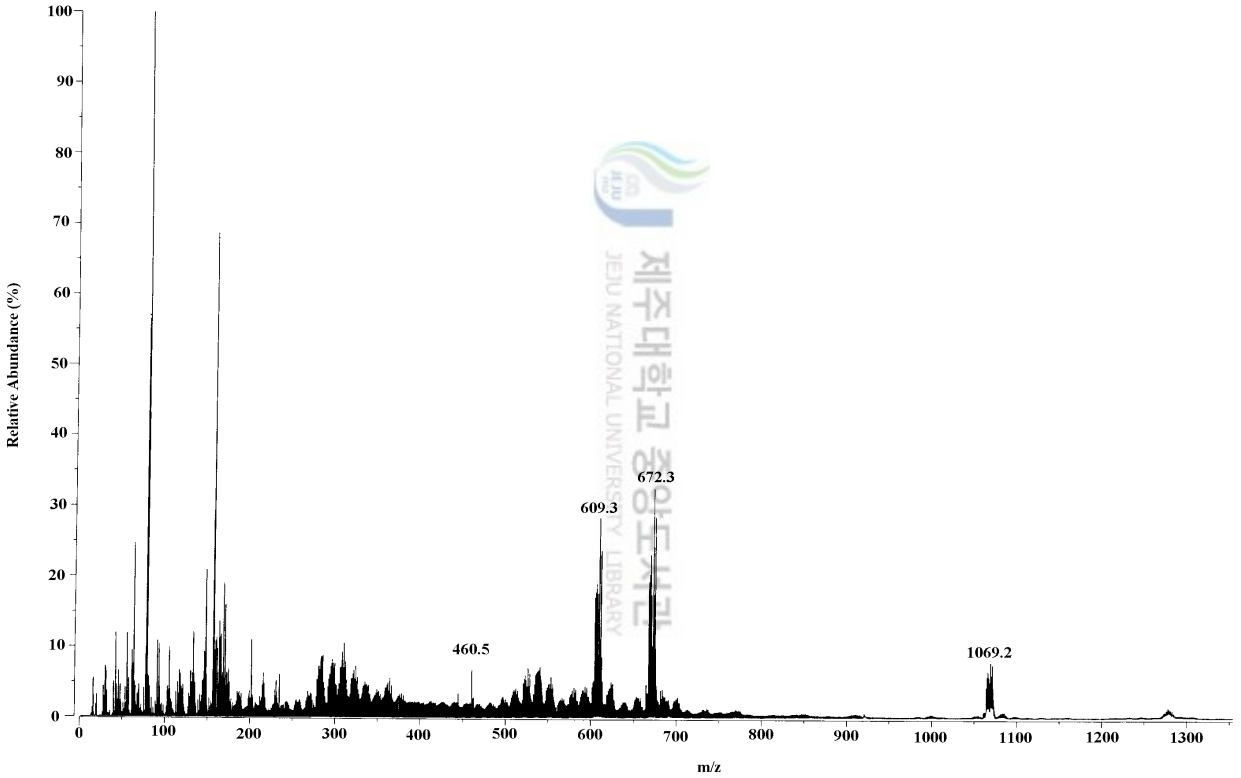

Fig. 56. FAB mass spectrum of the $[Sm(H_2[22]\text{-}HMTADO)O_2NO](NO_3)_2{\cdot}2H_2O$.

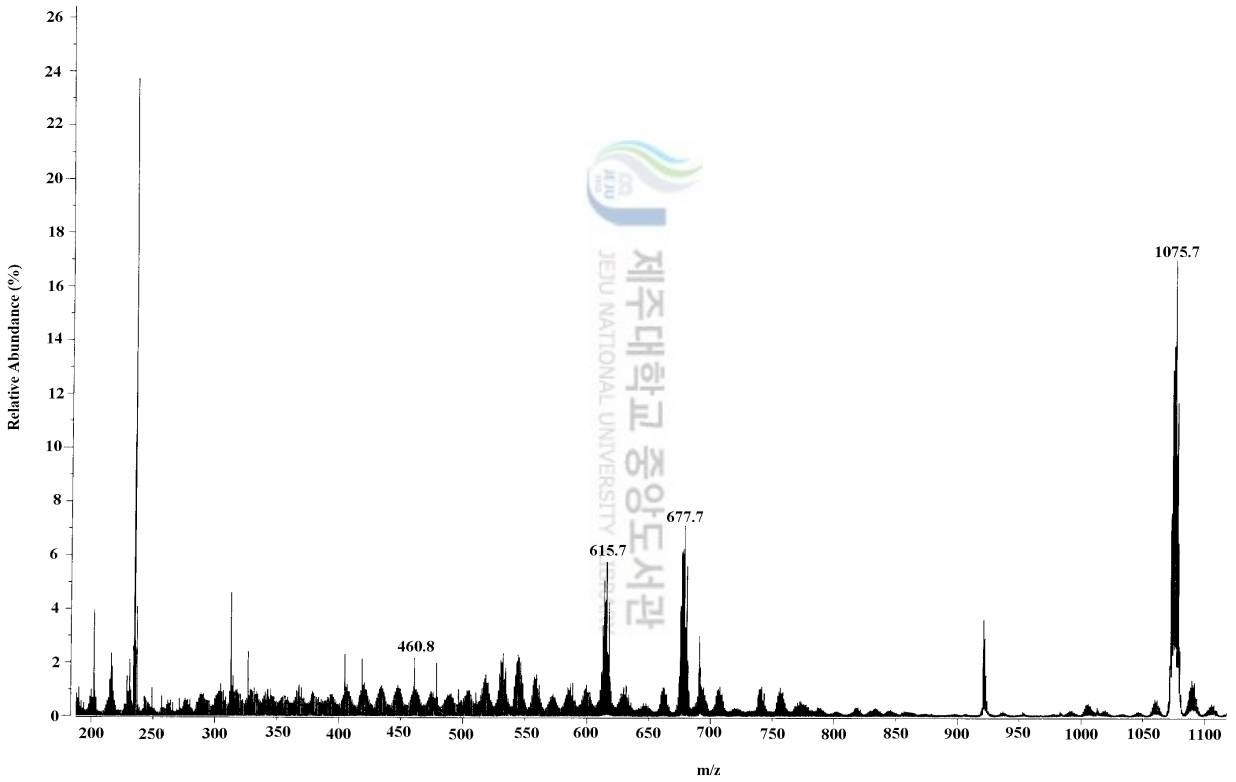

Fig. 57. FAB mass spectrum of the $[Gd(H_2[22]\text{-}HMTADO)O_2NO](NO_3)_2{\cdot}2H_2O$.

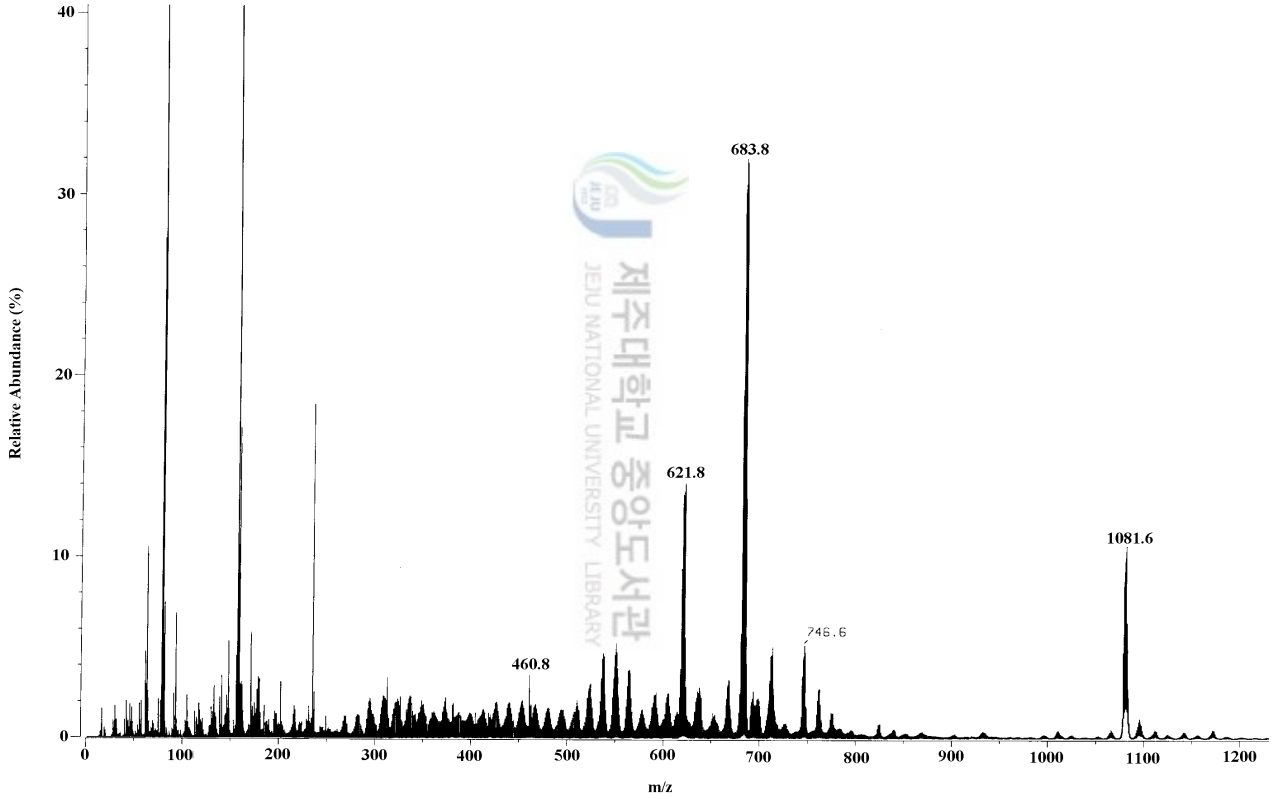

Fig. 58. FAB mass spectrum of the $[Dy(H_2[22]\text{-}HMTADO)O_2NO](NO_3)_2{\cdot}H_2O$.

4. Electronic absorption spectrum

1) Cu(II) complexes

The electronic absorption spectra of Cu(II) complexes at room temperature were represented in Fig. 59～67 and summarized Table 41. As shown these spectra exhibited one band at 584～641 nm due to the $^2E_g \rightarrow {}^2T_{2g}$ (O_h) transitions. The dark green $[Cu_2([22]\text{-HMTADO})]Cl_2 \cdot 2H_2O$ complex become green in water. The electronic absorption spectrum of this solution are typical of six-coordinate copper(II) complex indicating that species existing in solution is solvated $[Cu_2([22]\text{-HMTADO})(H_2O)_4]^{2+}$. The symmetry of the octahedron, elongated or squashed along one axis, is D_{4h}, exactly that of the square plane. For tetragonal Cu^{2+} (d^9) complexes the octahedral doublet ^2E_g and $^2T_{2g}$ are seen to split as

$$^2E_g \rightarrow {}^2A_{1g} + {}^2B_{1g}$$
$$^2T_{2g} \rightarrow {}^2E_g + {}^2B_{2g}$$

The relative energies of the tetragonal components depend upon whether the octahedron is elongated or squashed, for ground state of elongated form is $^2B_{1g}$.[69] Instead of the single $^2E_g \rightarrow {}^2T_{2g}$ transition which occurs for the regular octahedron, the tetragonally distorted molecule will exhibit two transitions $^2B_{1g} \rightarrow {}^2B_{2g}$ and $^2B_{1g} \rightarrow {}^2E_g$ at about the octahedral frequency.[69]

A further band at much lower energy is expected from $^2B_{1g} \rightarrow {}^2A_{1g}$ transition.[69]

The one *d-d* band of title complexes observed at 15,600 ~ 17,123 cm^{-1} can be related to the spin-allowed transition, $^2E_g \rightarrow {}^2T_{2g}$. Copper complexes in tetragonal symmetry are expected to have three absorption bands in *d-d* region, but title spectra apparently have one major component. Thus, we fitted the spectrum roughly with Gaussian functions first and then added a minor component to reproduce the more suitable shape of the spectrum in the region of interest. Finally, we performed least-squares fitting procedures, and the dotted lines in Fig. 59 ~ 66 are Gaussian bands representing the approximate deconvolution of the spectrum yielded by the calculations. The two peak positions calculated at 14,320 - 15,117 (ε = 32 - 111 $M^{-1}cm^{-1}$) and 16,653 - 17,762 cm^{-1} (ε = 42 - 112 $M^{-1}cm^{-1}$) can be assigned to the $^2B_{1g} \rightarrow {}^2B_{2g}$ and $^2B_{1g} \rightarrow {}^2E_g$, respectively. The $^2B_{1g} \rightarrow {}^2A_{1g}$ transition bands have expected at much lower energy. The 23,386 - 23,929 cm^{-1} (ε = 195 - 313 $M^{-1}cm^{-1}$) bands are clearly associated with ligand to metal charge transfer transitions.

2) Ni(II) complexes

The electronic absorption spectra of Ni(II) complexes at room temperature were represented in Fig. 68～79 and summarized Table 42. The pale green crystals of complex $[Ni_2([22]\text{-HMTADO})(OH_2)_2]Cl_2 \cdot H_2O$ become pale yellow-green in water. The electronic absorption spectrum of this solution is typical of six-coordinate nickel(II) complex indicating that species existing in

solution is $[Ni_2([22]\text{-HMTADO})(H_2O)_4]^{2+}$. Much weaker bands are found at lower energy, associated with *d-d* transitions. However, strong absorptions at 300 - 450 nm are clearly associated with ligand to metal charge transfer transitions, which reflect the presence of highly delocalized π marcrocyclic framework. The ground state of d^8 in an octahedral coordination is $^3A_{2g}$. Two *d-d* bands observed for the complex at 13,717 cm^{-1} (ε = 8.4 $M^{-1}cm^{-1}$), 18,051 cm^{-1} (ε = 19.2 M^1cm^{-1}) can be attributed to the transition in an octahedral model. Thus, these bands may be assigned to the spin allowed transitions $^3A_{2g} \rightarrow {}^3T_{2g}(F)$ and $^3A_{2g} \rightarrow {}^3T_{1g}(F)$, respectively. $^3A_{2g} \rightarrow {}^3T_{1g}(P)$ transition is not separated by the transfer effect to visible range of charge transfer transitions and absorptions of marcrocycle ligand.

3) Mn(II) and Ln(III) complexes

The electronic absorption spectra of Mn(II) and Ln(III) complexes at room temperature were represented in Fig. 80～84 and summarized Table 43. The absorption band at around 368 nm (ε = 15,600 M^1cm^{-1}) of Mn(II) complex are associated with ligand to metal charge transfer transitions. All lanthanide complexes exhibit one absorptions at around 398 nm (ε = 16,820 - 18,520 M^1cm^{-1}) region.

Table 41. Electronic spectral data for the Cu(II) complexes

Complexes	Solvent	λ_{max}, nm (ε, M^{-1} cm^{-1})	Spin-allowed transition, cm^{-1} (ε, M^{-1} cm^{-1})		
			$^2B_{1g} \rightarrow {}^2B_{2g}$	$^2B_{1g} \rightarrow {}^2E_g$	MLCT
$[Cu_2([22]\text{-HMTADO})(OH_2)]Cl_2 \cdot H_2O$	water	584 (95)	15,506 (61)	17,559 (42)	23,386 (195)
$[Cu_2([22]\text{-HMTADO})(OClO_3)(OH_2)]ClO_4 \cdot 2H_2O$	MeOH	544 (109)	15,117 (69)	17,182 (52)	23,403 (215)
$[Cu_2([22]\text{-HMTADO})(CN)_2] \cdot 0.5H_2O$	DMSO	597 (159)	14,073 (32)	16,762 (112)	
$[Cu_2([22]\text{-HMTADO})(NCS)(OH_2)]NCS \cdot 2H_2O$	DMSO	618 (144)	14,320 (108)	16,653 (77)	23,414 (294)
$[Cu_2([22]\text{-HMTADO})(N_3)(OH_2)]N_3 \cdot H_2O$	MeOH	606 (110)	14,573 (80)	16,895 (61)	23,929 (291)
$[Cu_2([22]\text{-HMTADO})ONO_2]NO_3 \cdot 4H_2O$	DMSO	613 (144)	14,366 (111)	16,742 (85)	23,524 (313)
$[Cu_2([22]\text{-HMTADO})NO_2]NO_2 \cdot 2H_2O$	MeOH	597 (119)	14,943 (77)	17,112 (60)	23,895 (290)
$[Cu_2([22]\text{-HMTADO})]Br_2 \cdot 1.5H_2O$	MeOH	602 (123)	14,932 (84)	17,085 (56)	23,641 (255)
$[Cu_2([22]\text{-HMTADO})S_2O_3] \cdot 5H_2O$	DMSO	641 (202)			

Table 42. Electronic spectral data for the Ni(II) complexes

Complexes	Solvent	λ_{max}, nm (ε, M^{-1} cm^{-1})
$[Ni_2([22]\text{-HMTADO})(OH_2)_2]Cl_2 \cdot H_2O$	water	554 (19.2), 729 (8.4)
$[Ni_2([22]\text{-HMTADO})(OH_2)_2](ClO_4)_2 \cdot H_2O$	MeOH	575 (21.6)
$[Ni_2([22]\text{-HMTADO})(CN)_2] \cdot 0.5H_2O$	MeOH	607 (74.8)
$[Ni_2([22]\text{-HMTADO})(NCS)_2(OH_2)] \cdot 2H_2O$	DMSO	638 (49.0)
$[Ni_2([22]\text{-HMTADO})(N_3)_2(OH_2)]$	DMSO	594 (44.5)
$[Ni_2([22]\text{-HMTADO})(ONO_2)(OH_2)_2]NO_3 \cdot 3H_2O$	MeOH	577 (33.0), 752 (13.4)
$[Ni_2([22]\text{-HMTADO})NO_2]NO_2 \cdot H_2O$	MeOH	574 (27.2), 763 (13.2)
$[Ni_2([22]\text{-HMTADO})]Br_2 \cdot 2H_2O$	MeOH	576 (22.0)
$[Ni_2([22]\text{-HMTADO})S_2O_3]$	MeOH	649 (35.6)
$[Ni(H_2[22]\text{-HMTADO})(OHCH_3)_2](ClO_4)_2$	MeOH	750 (8.4)
$[Ni(H_2[22]\text{-HMTADO})(NCS)_2] \cdot H_2O$	DMSO	586(sh) (61.0)
$[Ni(H_2[22]\text{-HMTADO})(N_3)(OH_2)]ClO_4 \cdot H_2O$	DMSO	590(sh) (28.8)

Table 43. Electronic spectral data for the Mn(II) and Ln(III) complexes

Complexes	Solvent	λ_{max}, nm (ε, M^{-1} cm^{-1})
$[Mn_2([22]\text{-HMTADO})Cl_2] \cdot H_2O$	$CHCl_3$	368 (15,600)
$[Pr(H_2[22]\text{-HMTADO})O_2NO](NO_3)_2 \cdot 2H_2O$	MeOH	398 (18,520)
$[Sm(H_2[22]\text{-HMTADO})O_2NO](NO_3)_2 \cdot 2H_2O$	MeOH	398 (17,120)
$[Gd(H_2[22]\text{-HMTADO})O_2NO](NO_3)_2 \cdot 2H_2O$	MeOH	398 (17,910)
$[Dy(H_2[22]\text{-HMTADO})O_2NO](NO_3)_2 \cdot H_2O$	DMF	398 (16,820)

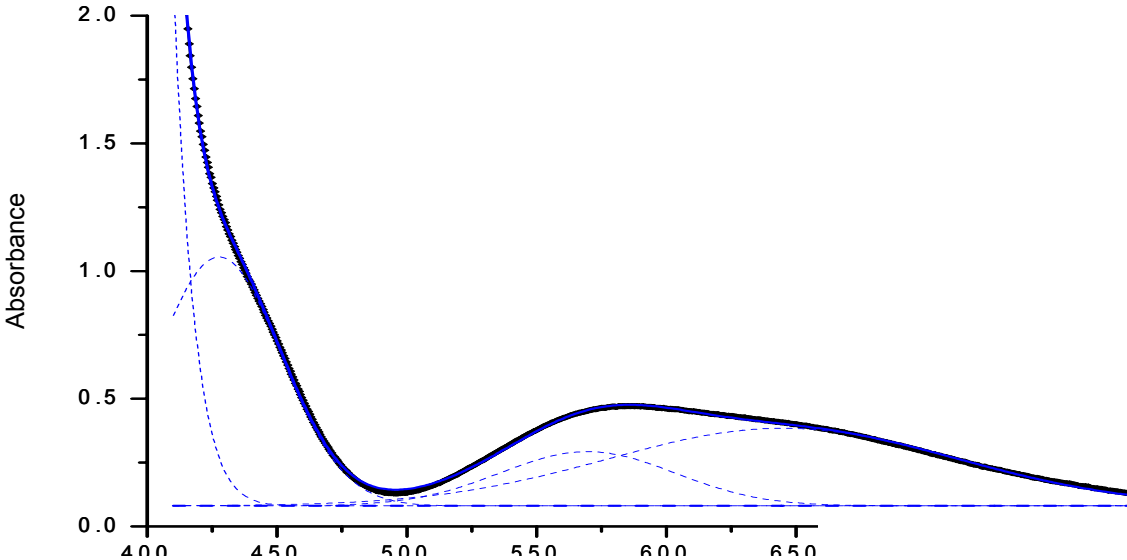

Fig. 59. Electronic absorption spectrum of $[Cu_2([22]\text{-HMTADO})(OH_2)]Cl_2 \cdot H_2O$ in water.

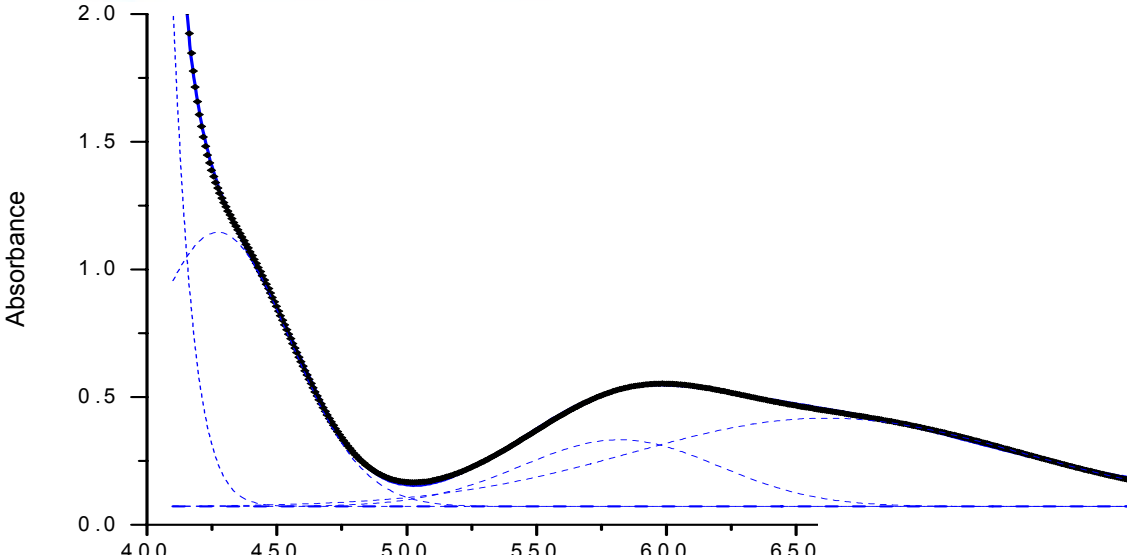

Fig. 60. Electronic absorption spectrum of $[Cu_2([22]\text{-HMTADO})(OClO_3)(OH_2)]ClO_4 \cdot 2H_2O$ in MeOH.

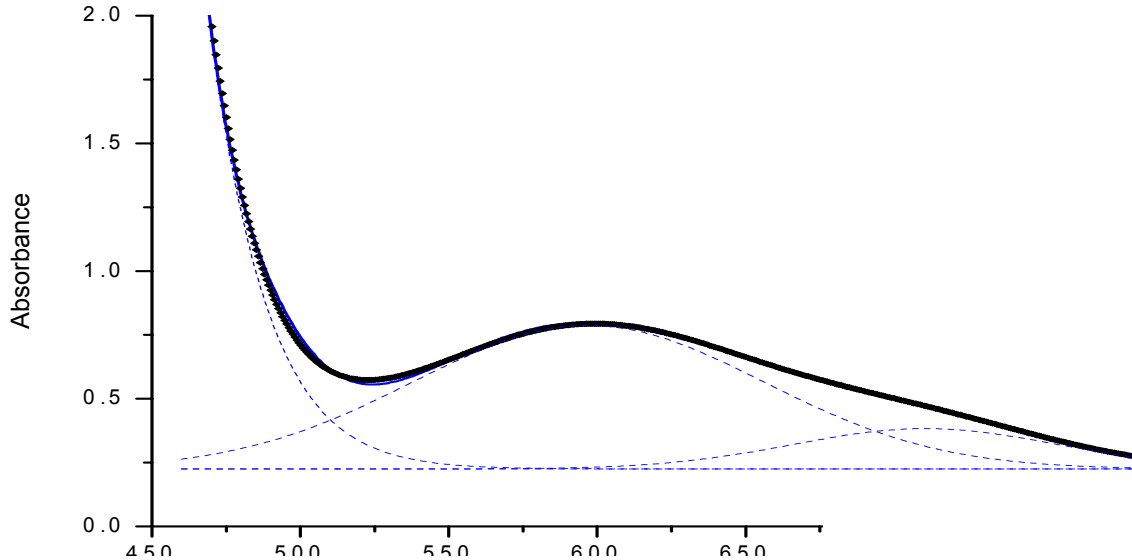

Fig. 61. Electronic absorption spectrum of $[Cu_2([22]\text{-HMTADO})(CN)_2] \cdot 0.5H_2O$ in DMSO.

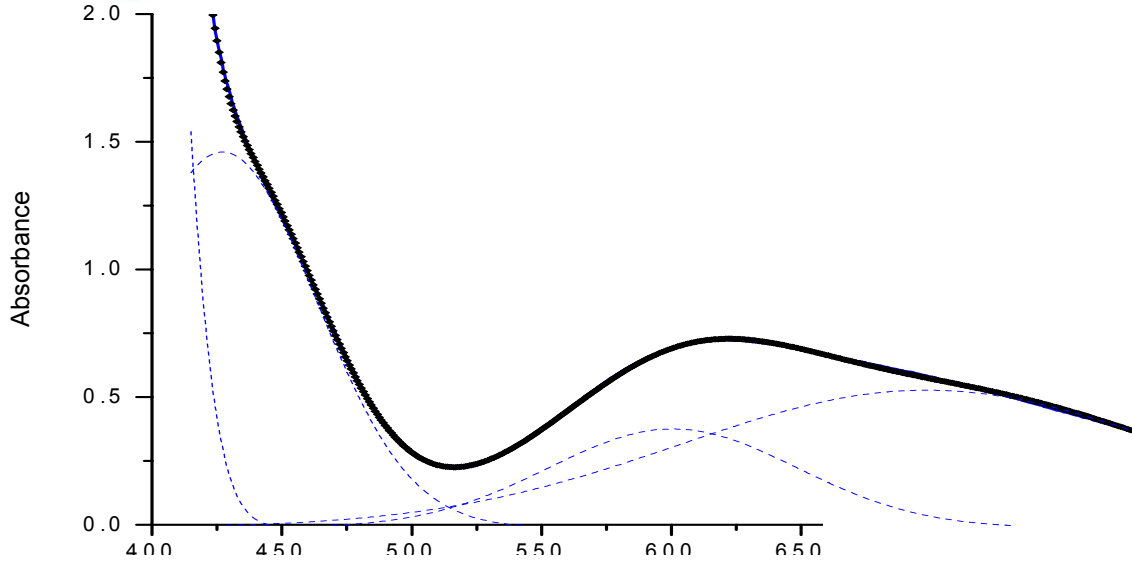

Fig. 62. Electronic absorption spectrum of $[Cu_2([22]\text{-HMTADO})(NCS)(OH_2)]NCS \cdot 2H_2O$ in DMSO.

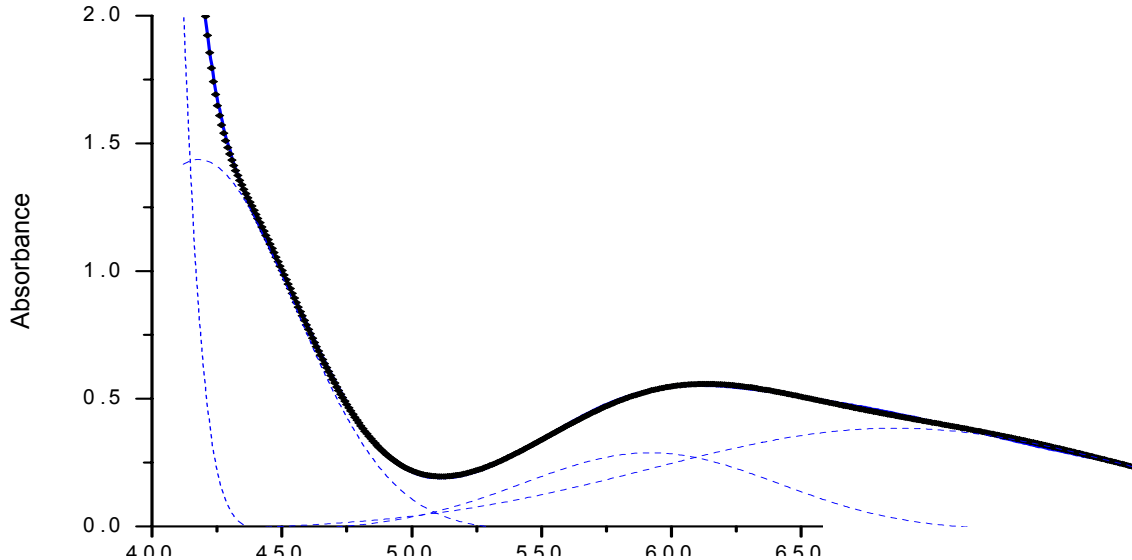

Fig. 63. Electronic absorption spectrum of $[Cu_2([22]\text{-HMTADO})(N_3)(OH_2)]N_3 \cdot H_2O$ in MeOH.

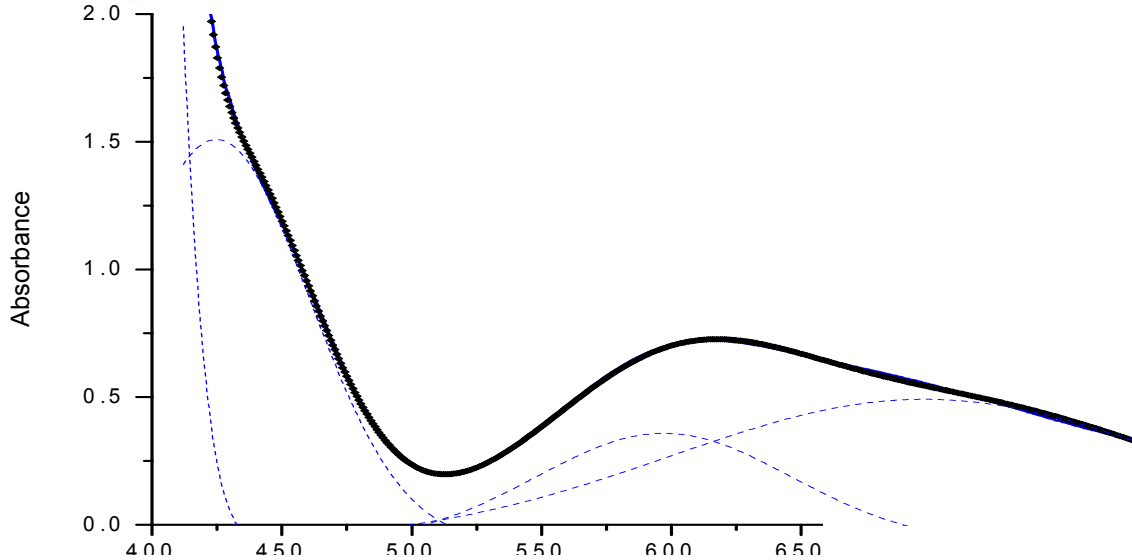

Fig. 64. Electronic absorption spectrum of $[Cu_2([22]\text{-HMTADO})ONO_2]NO_3 \cdot 4H_2O$ in MeOH.

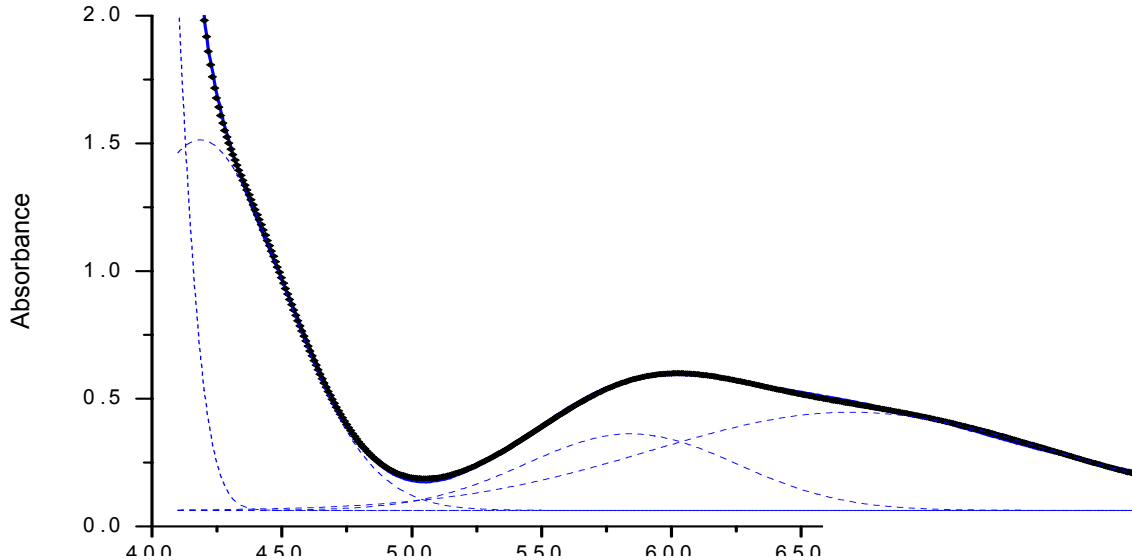

Fig. 65. Electronic absorption spectrum of $[Cu_2([22]\text{-HMTADO})NO_2]NO_2 \cdot 2H_2O$ in MeOH.

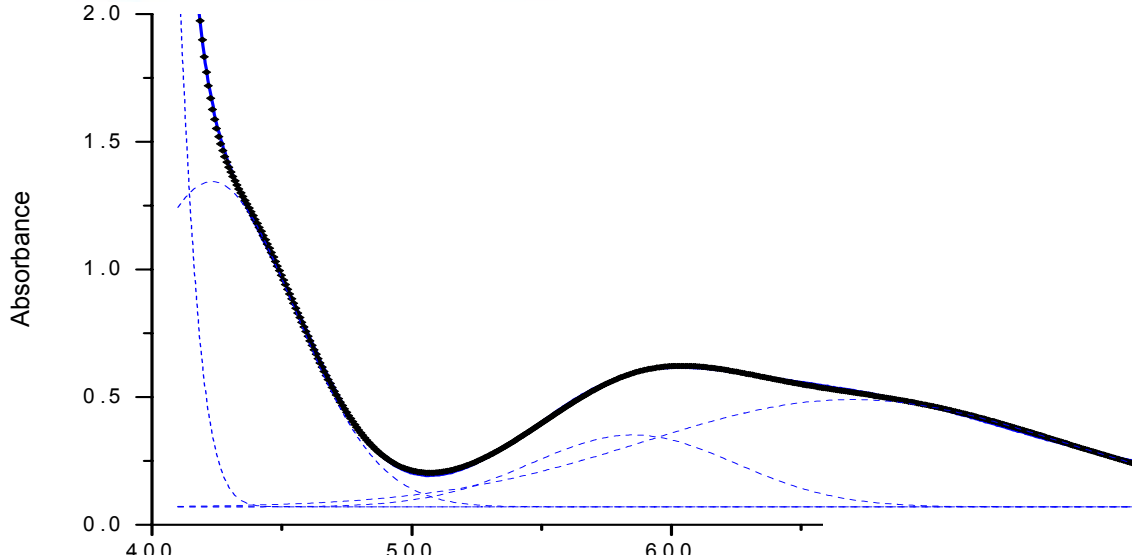

Fig. 66. Electronic absorption spectrum of $[Cu_2([22]\text{-HMTADO})]Br_2 \cdot 1.5H_2O$ in MeOH.

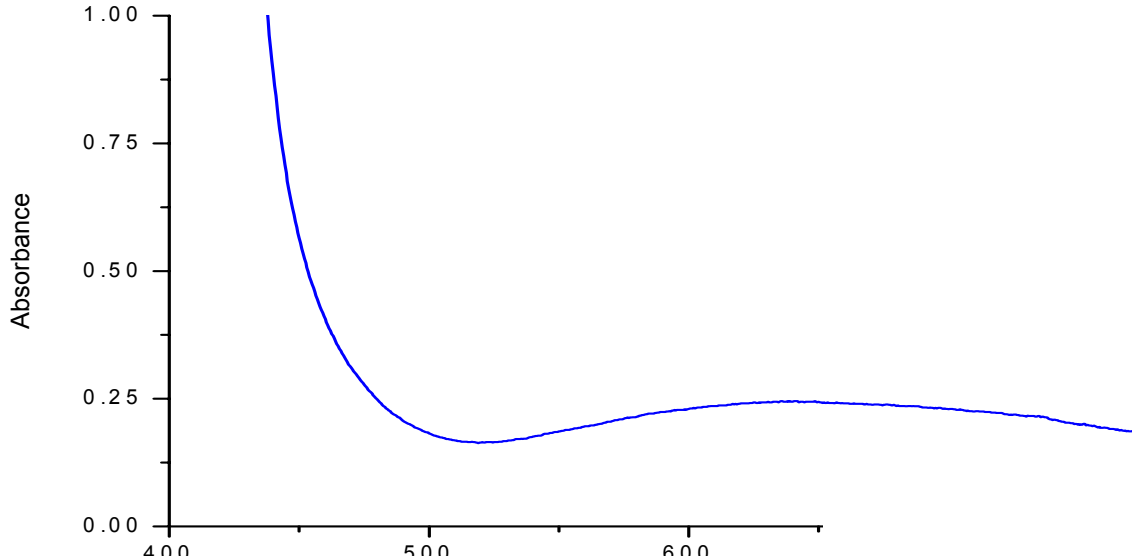

Fig. 67. Electronic absorption spectrum of $[Cu_2([22]\text{-HMTADO})S_2O_3]\cdot 5H_2O$ in DMSO.

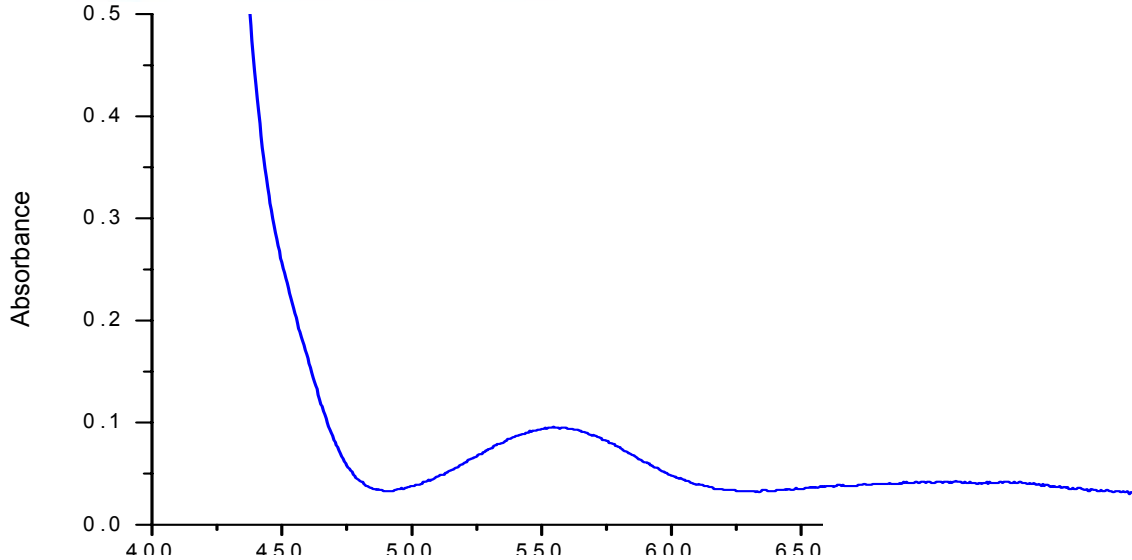

Fig. 68. Electronic absorption spectrum of $[Ni_2([22]\text{-HMTADO})(OH_2)_2]Cl_2 \cdot H_2O$ in water.

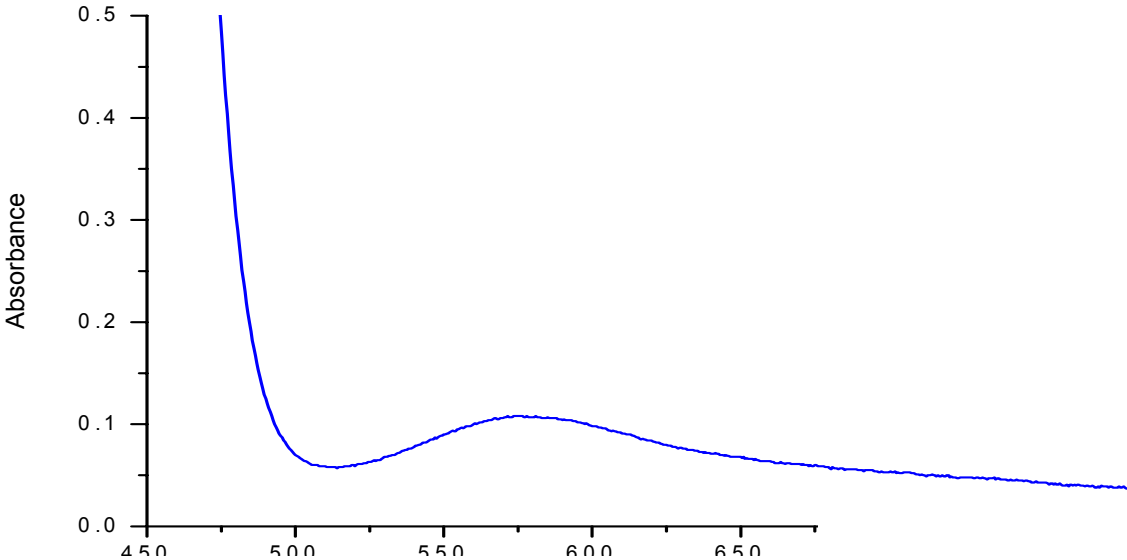

Fig. 69. Electronic absorption spectrum of $[Ni_2([22]\text{-HMTADO})(OH_2)_2](ClO_4)_2 \cdot H_2O$ in MeOH.

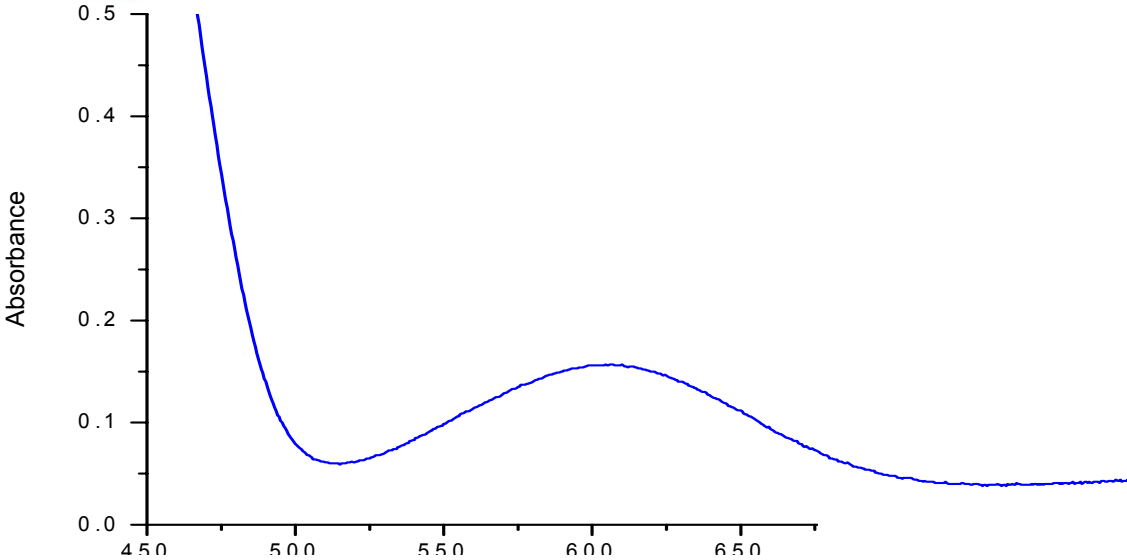

Fig. 70. Electronic absorption spectrum of $[Ni_2([22]\text{-HMTADO})(CN)_2] \cdot 0.5H_2O$ in MeOH.

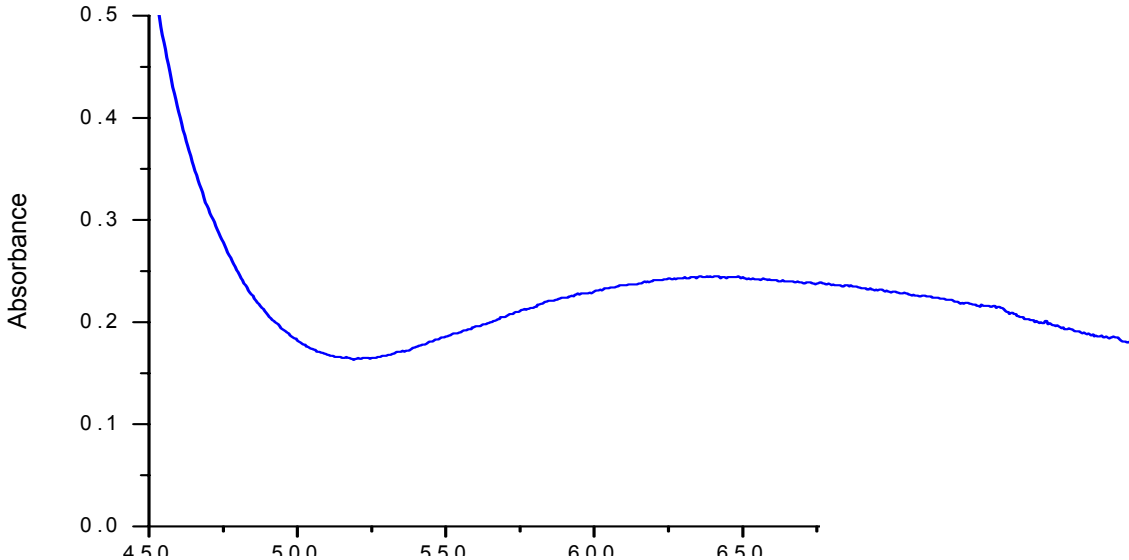

Fig. 71. Electronic absorption spectrum of $[Ni_2([22]\text{-HMTADO})(NCS)_2(OH_2)] \cdot 2H_2O$ in DMSO.

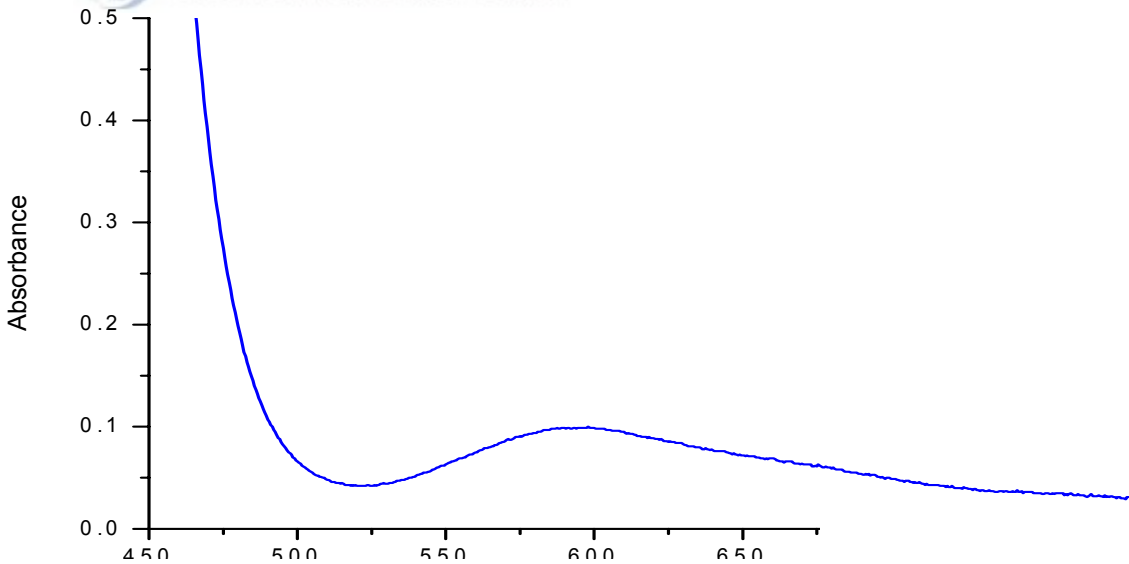

Fig. 72. Electronic absorption spectrum of $[Ni_2([22]\text{-HMTADO})(N_3)_2(OH_2)]$ in DMSO.

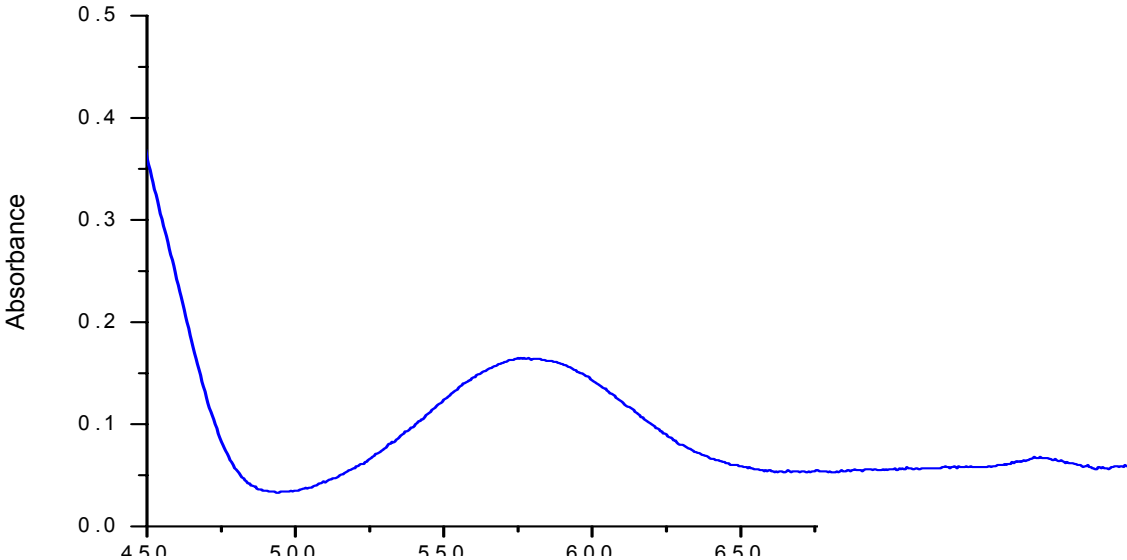

Fig. 73. Electronic absorption spectrum of $[Ni_2([22]\text{-HMTADO})(ONO_2)(OH_2)_2]NO_3 \cdot 3H_2O$ in MeOH.

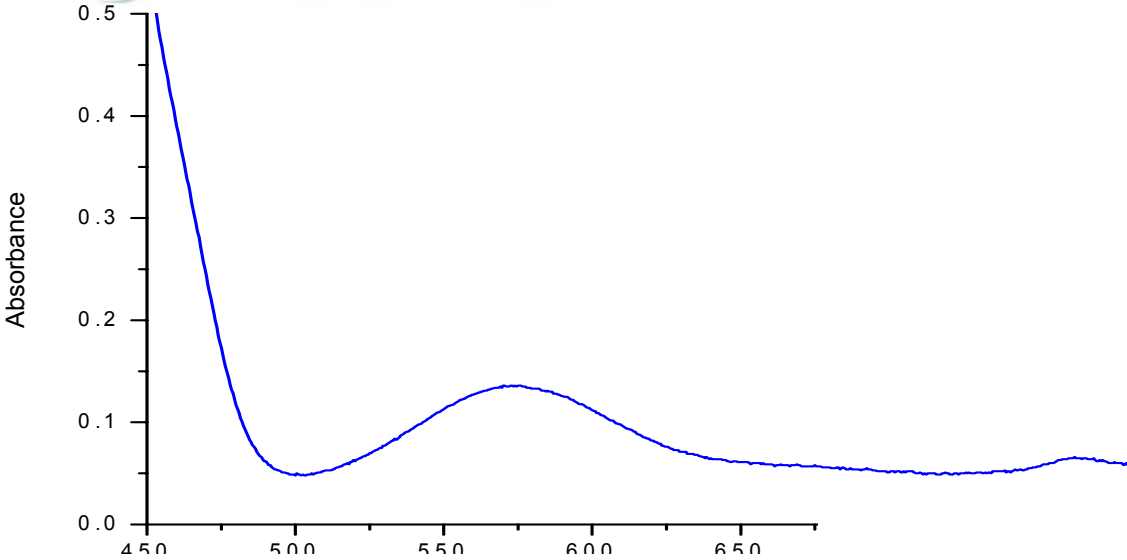

Fig. 74. Electronic absorption spectrum of $[Ni_2([22]\text{-HMTADO})NO_2]NO_2 \cdot H_2O$ in MeOH.

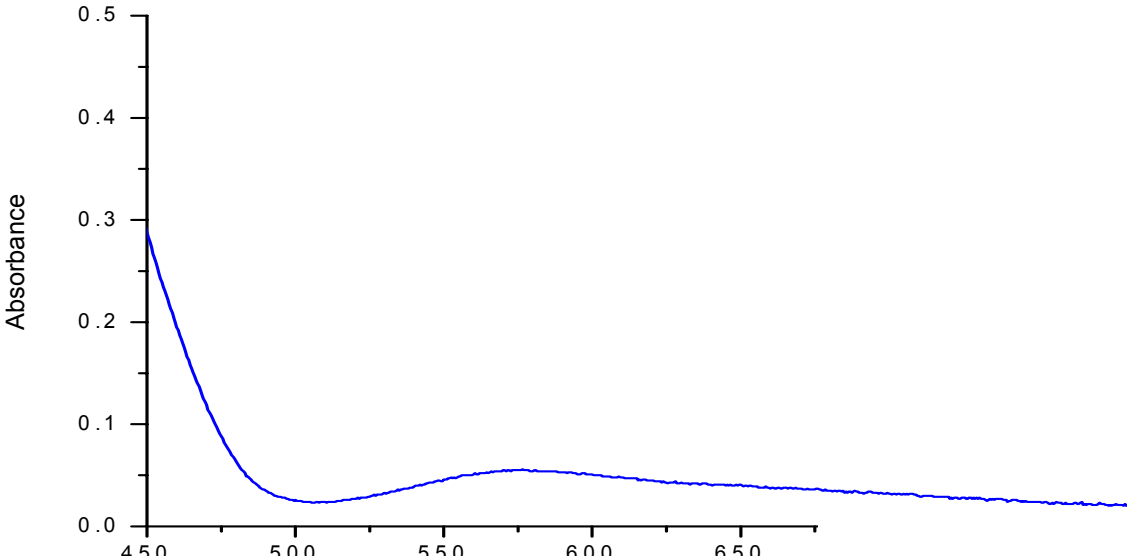

Fig. 75. Electronic absorption spectrum of $[Ni_2([22]\text{-HMTADO})]Br_2{\cdot}2H_2O$ in MeOH.

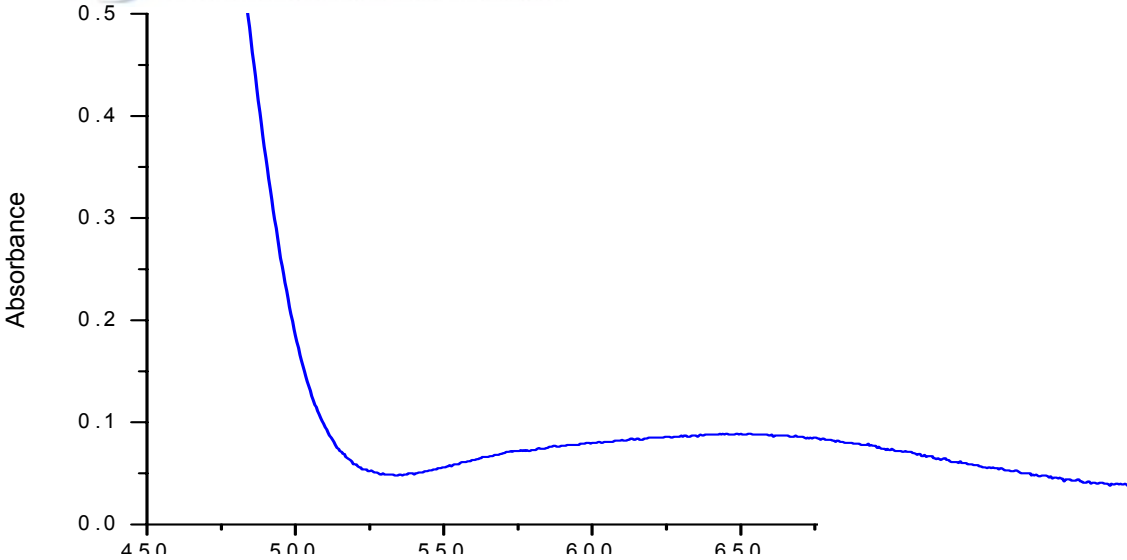

Fig. 76. Electronic absorption spectrum of $[Ni_2([22]\text{-HMTADO})S_2O_3]$ in MeOH.

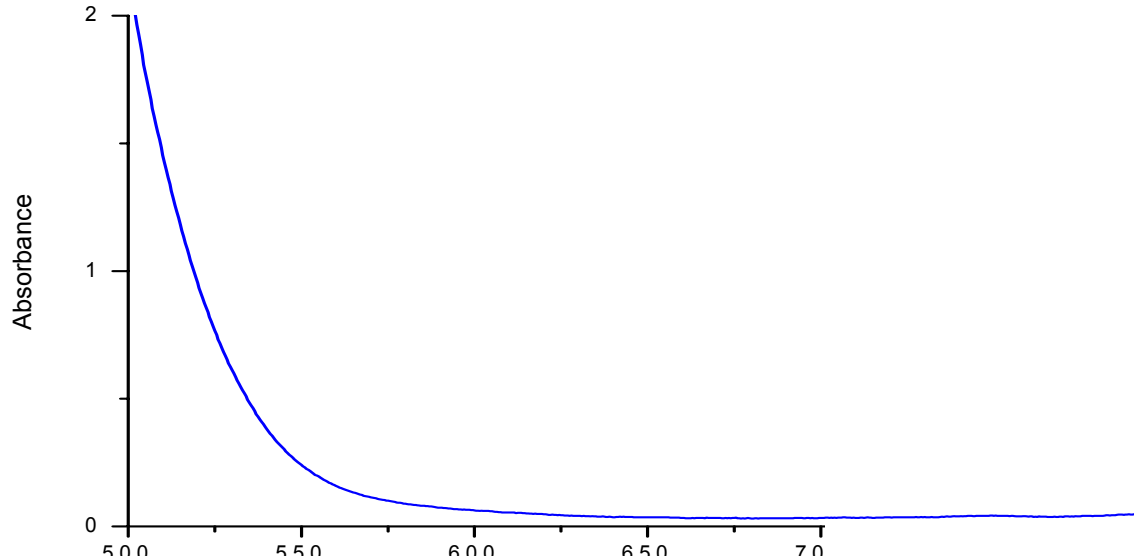

Fig. 77. Electronic absorption spectrum of $[Ni(H_2[22]\text{-}HMTADO)(OHCH_3)_2](ClO_4)_2$ in MeOH.

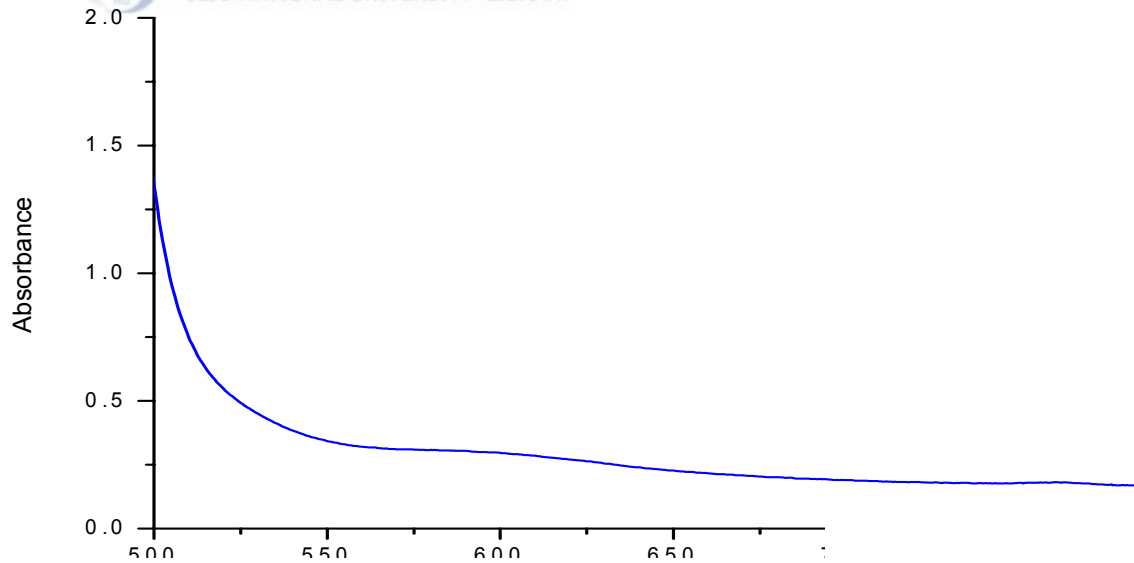

Fig. 78. Electronic absorption spectrum of $[Ni(H_2[22]\text{-}HMTADO)(NCS)_2] \cdot H_2O$ in DMSO.

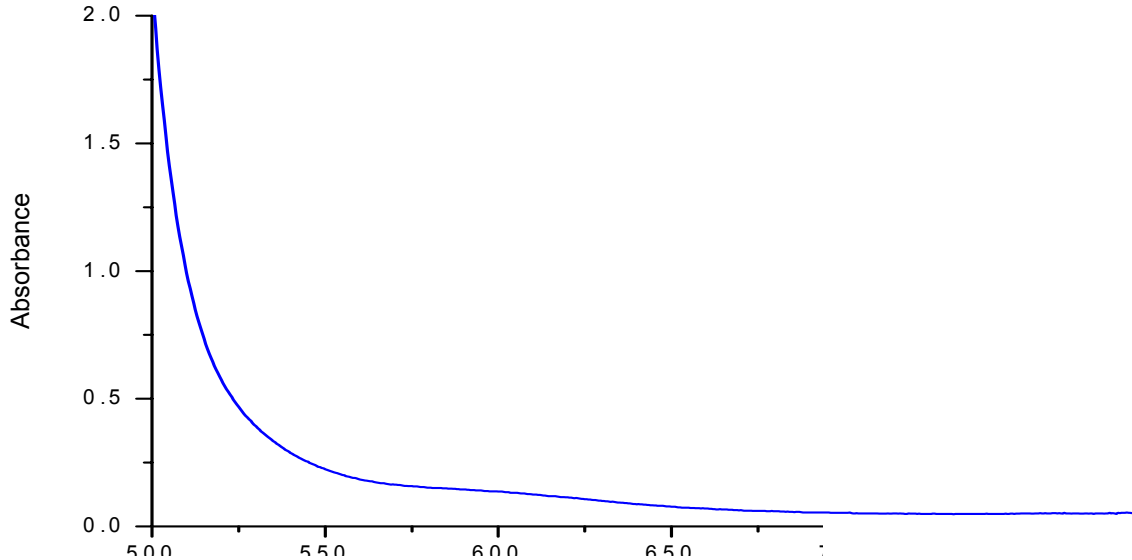

Fig. 79. Electronic absorption spectrum of $[Ni(H_2[22]\text{-}HMTADO)(N_3)(OH_2)]ClO_4 \cdot H_2O$ in DMSO.

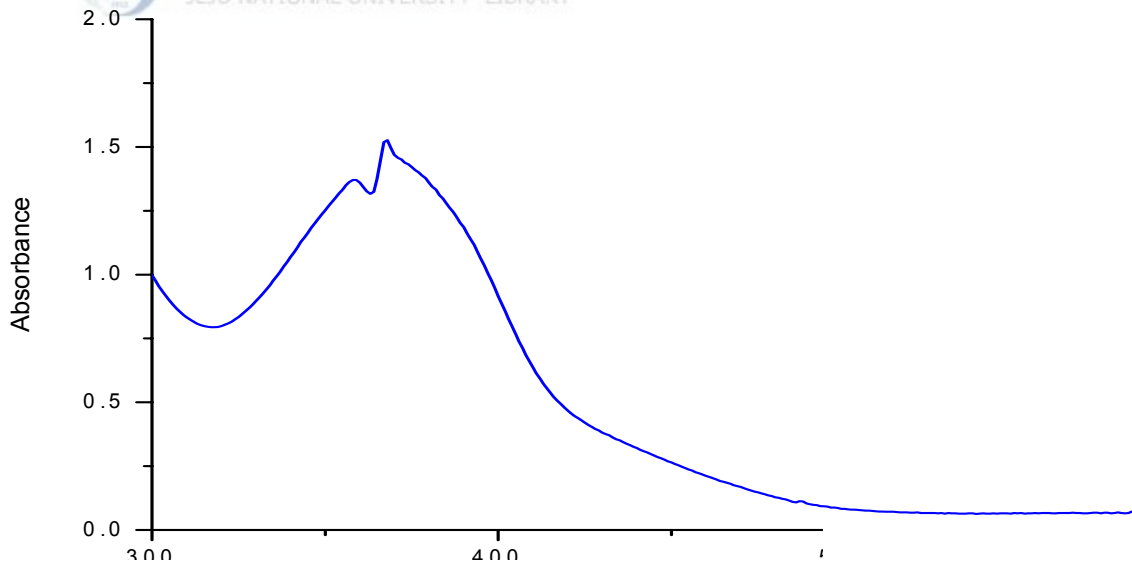

Fig. 80. Electronic absorption spectrum of $[Mn_2([22]\text{-}HMTADO)Cl_2] \cdot H_2O$ in chloroform.

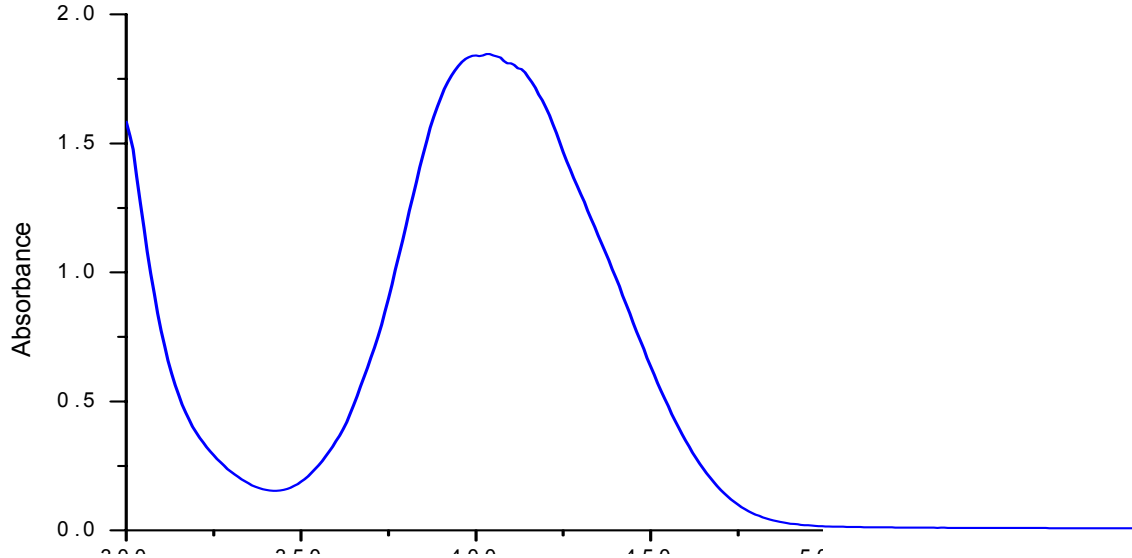

Fig. 81. Electronic absorption spectrum of [[Pr(H_2[22]-HMTADO)O_2NO]$(NO_3)_2 \cdot 2H_2O$ in MeOH.

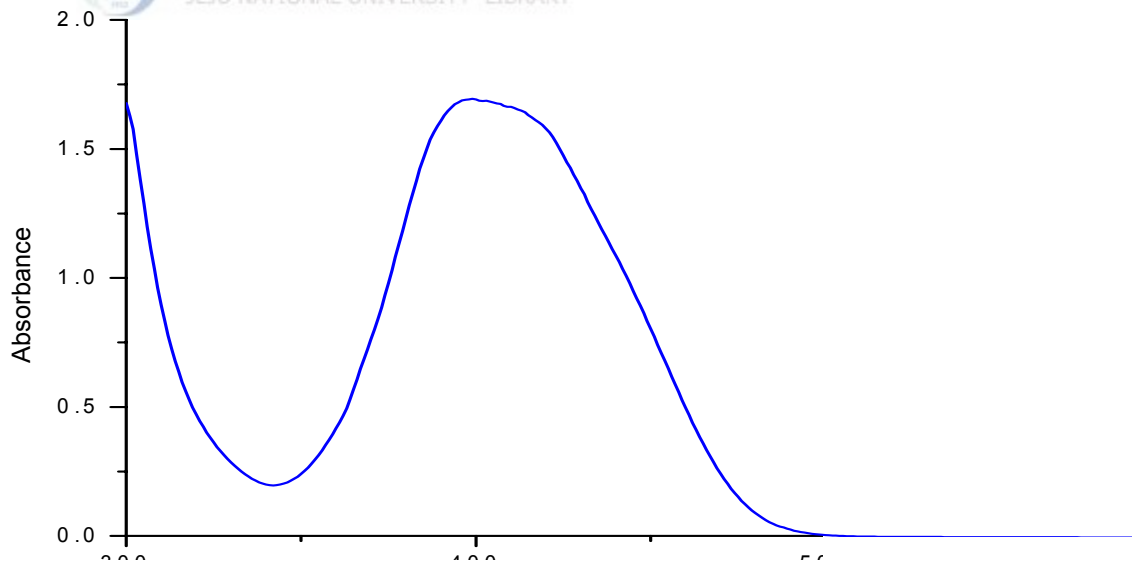

Fig. 82. Electronic absorption spectrum of [Sm(H_2[22]-HMTADO)O_2NO]$(NO_3)_2 \cdot 2H_2O$ in MeOH.

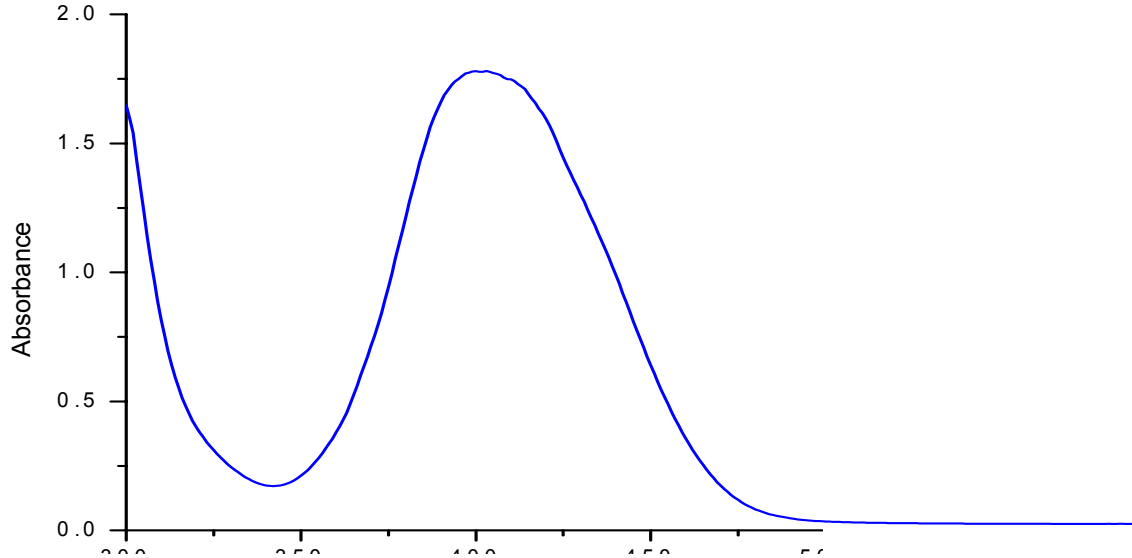

Fig. 83. Electronic absorption spectrum of $[Gd(H_2[22]\text{-}HMTADO)O_2NO](NO_3)_2 \cdot 2H_2O$ in MeOH.

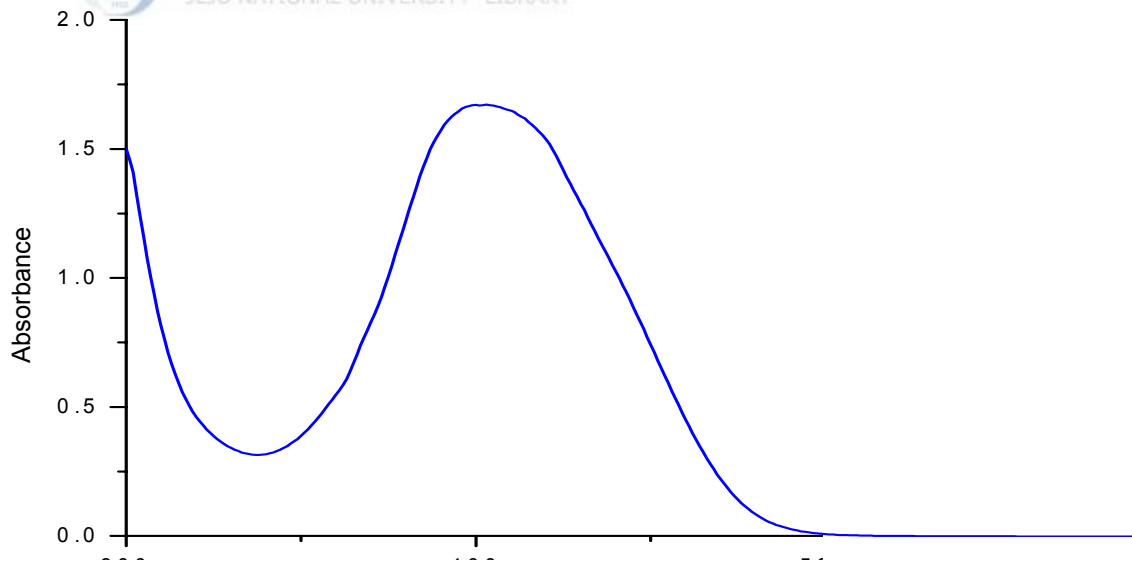

Fig. 84. Electronic absorption spectrum of $[Dy(H_2[22]\text{-}HMTADO)O_2NO](NO_3)_2 \cdot H_2O$ in DMF.

5. Thermal stability

1) Cu(II) complexes

Thermogravimetry analysis(TGA) have been carried out simultaneously for the Cu(II) complexes (Fig. 85 ~ 92). Thermogravimetric details were given in Table 44. It was found out from the results that the prepared macrocycle compounds have relatively high thermal stability. The lattice and coordinated water molecules were lost at ~ 200℃ range. The exocyclic anions were lost at 200 ~ 350℃ range. The macrocyclic entity changed slowly up to 350℃, and then those complexes were changed to CuO.

2) Ni(II) complexes

Thermogravimetry analysis(TGA) have been carried out simultaneously for the Ni(II) complexes (Fig. 93 ~ 103). Thermogravimetric details were given in Table 44. It was found out from the results that the prepared macrocycle compounds have relatively high thermal stability. The lattice and coordinated water molecules were lost at ~ 200℃ range. The exocyclic anions were lost at 270 ~ 350℃ range. The macrocyclic entity changed slowly up to 350℃, and then those complexes have been changed to NiO.

3) Lanthanide(III) complexes

Thermogravimetry analysis(TGA) have been carried out simultaneously for the lanthanide complexes (Fig. 104 ~ 107). Thermogravimetric details were given in Table 46. It was found out from the results that the prepared macrocycle compounds have relatively high thermal stability. The lattice water molecules were lost at ~ 306℃ range. The two nitrate ions were lost at 276 ~ 347℃ range. The coordinated nitrate ion was lost at 238 ~ 368℃ range. The macrocyclic entity changed slowly up to 360℃, and then those complexes have been changed to M_2O_3 {M = Pr^{3+}, Sm^{3+}, Gd^{3+}, and Dy^{3+}}.

Table 44. Thermogravimetric data of the Cu(II) complexes

Complexes	Temperature range (℃)	Moieties lost
$[Cu_2([22]\text{-HMTADO})(OH_2)]Cl_2 \cdot H_2O$	~ 154	$2H_2O$
	298 ~ 352	$2Cl^-$
	352 ~	macrocycle
$[Cu_2([22]\text{-HMTADO})(OClO_3)(OH_2)]ClO_4 \cdot 2H_2O$	~ 50	$3H_2O$
	328 ~ 366	$2ClO_4^-$
	366 ~ 708	macrocycle
$[Cu_2([22]\text{-HMTADO})(CN)_2] \cdot 0.5H_2O$	~ 202	$0.5H_2O + CN^-$
	275 ~ 720	$CN^- +$ macrocycle
$[Cu_2([22]\text{-HMTADO})(NCS)(OH_2)]NCS \cdot 2H_2O$	~ 84	$2H_2O$
	263 ~ 305	$H_2O + NCS^-$
	305 ~ 769	$NCS^- +$ macrocycle
$[Cu_2([22]\text{-HMTADO})(N_3)(OH_2)]N_3 \cdot H_2O$	~ 136	$2H_2O$
	223 ~ 235	N_3^-
	262 ~ 575	$N_3^- +$ macrocycle
$[Cu_2([22]\text{-HMTADO})ONO_2]NO_3 \cdot 4H_2O$	~ 136	$4H_2O$
	285 ~ 306	$2NO_3^-$
	306 ~ 790	macrocycle
$[Cu_2([22]\text{-HMTADO})NO_2]NO_2 \cdot 2H_2O$	~ 184	$2H_2O$
	184 ~ 213	NO_2^-
	213 ~ 654	$NO_2^- +$ macrocycle
$[Cu_2([22]\text{-HMTADO})]Br_2 \cdot 1.5H_2O$	~ 91	$1.5H_2O$
	305 ~ 329	Br^-
	329 ~	$Br^- +$ macrocycle

Table 45. Thermogravimetric data of the Ni(II) complexes

Complexes	Temperature range (℃)	Moieties lost
$[Ni_2([22]\text{-HMTADO})(OH_2)_2]Cl_2 \cdot H_2O$	~ 185	$3H_2O$
	375 ~ 673	$2Cl^-$ + macrocycle
$[Ni_2([22]\text{-HMTADO})(OH_2)_2](ClO_4)_2 \cdot H_2O$	~ 158	$3H_2O$
	305 ~ 379	$2ClO_4^-$
	379 ~ 816	macrocycle
$[Ni_2([22]\text{-HMTADO})(CN)_2] \cdot 0.5H_2O$	~ 332	$0.5H_2O$
	332 ~ 353	$2CN^-$
	353 ~ 476	macrocycle
$[Ni_2([22]\text{-HMTADO})(NCS)_2(OH_2)] \cdot 2H_2O$	~ 61	$2H_2O$
	61 ~ 335	H_2O
	335 ~ 358	NCS^-
	358 ~ 630	NCS^- + macrocycle
$[Ni_2([22]\text{-HMTADO})(N_3)_2(OH_2)]$	~ 147	H_2O
	285 ~ 296	$2N_3^-$
	296 ~ 598	macrocycle
$[Ni_2([22]\text{-HMTADO})(ONO_2)(OH_2)_2]NO_3 \cdot 3H_2O$	~ 304	$3H_2O$
	304 ~ 330	$2H_2O$ + NO_3^-
	330 ~	NO_3^- + macrocycle
$[Ni_2([22]\text{-HMTADO})NO_2]NO_2 \cdot H_2O$	~ 150	H_2O
	277 ~ 297	NO_2^-
	297 ~ 656	NO_2^- + macrocycle
$[Ni_2([22]\text{-HMTADO})]Br_2 \cdot 2H_2O$	~ 63	$2H_2O$
	399 ~ 832	$2Br^-$ + macrocycle

Complexes	Temperature range (℃)	Moieties lost
$[Ni(H_2[22]\text{-}HMTADO)(OHCH_3)_2](ClO_4)_2$	~ 104	$2CH_3OH$
	291 ~ 353	$2ClO_4^-$
	351 ~ 958	macrocycle
$[Ni(H_2[22]\text{-}HMTADO)(NCS)_2] \cdot H_2O$	254 ~ 307	$H_2O + NCS^-$
	307 ~	$NCS^- +$ macrocycle
$[Ni(H_2[22]\text{-}HMTADO)(N_3)(OH_2)]ClO_4 \cdot H_2O$	~ 137	H_2O
	137 ~ 285	N_3^-
	268 ~ 302	H_2O
	302 ~ 395	ClO_4^-
	395 ~	macrocycle

Table 46. Thermogravimetric data of the Ln(III) complexes

Complexes	Temperature range (℃)	Moieties lost
$[Pr(H_2[22]\text{-}HMTADO)O_2NO](NO_3)_2 \cdot 2H_2O$	~ 306	$2H_2O$
	306 ~ 347	$2NO_3^-$
	347 ~ 365	NO_3^-
	365 ~	macrocycle
$[Sm(H_2[22]\text{-}HMTADO)O_2NO](NO_3)_2 \cdot 2H_2O$	~ 295	$2H_2O$
	295 ~ 343	$2NO_3^-$
	343 ~ 368	NO_3^-
	368 ~	macrocycle
$[Gd(H_2[22]\text{-}HMTADO)O_2NO](NO_3)_2 \cdot 2H_2O$	~ 280	$2H_2O$
	280 ~ 338	$2NO_3^-$
	338 ~ 364	NO_3^-
	364 ~	macrocycle
$[Dy(H_2[22]\text{-}HMTADO)O_2NO](NO_3)_2 \cdot H_2O$	~ 276	$2H_2O$
	276 ~ 338	$2NO_3^-$
	338 ~ 360	NO_3^-
	360 ~	macrocycle

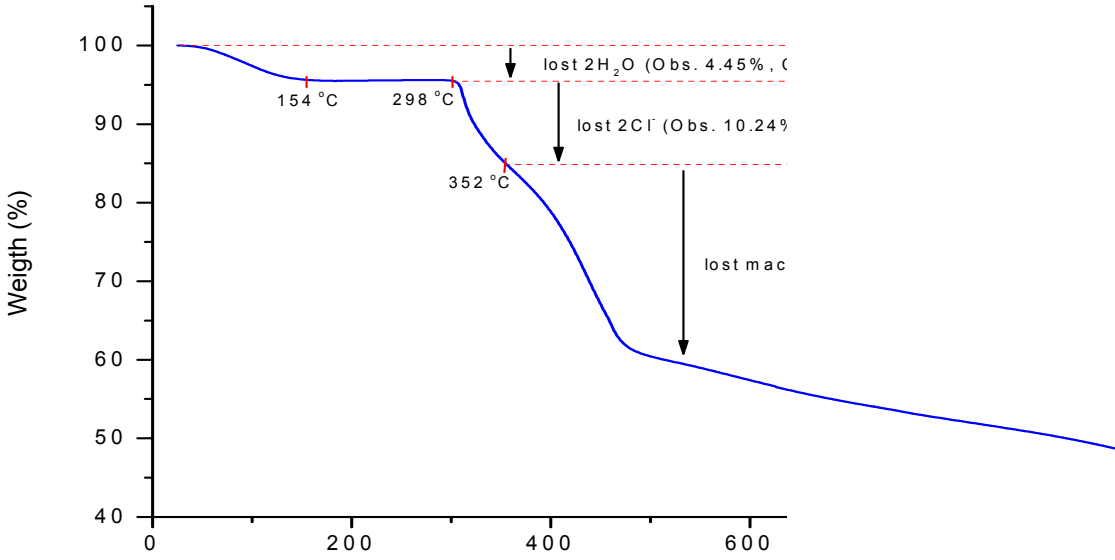

Fig. 85. TGA curve of $[Cu_2([22]\text{-HMTADO})(OH_2)]Cl_2 \cdot H_2O$.

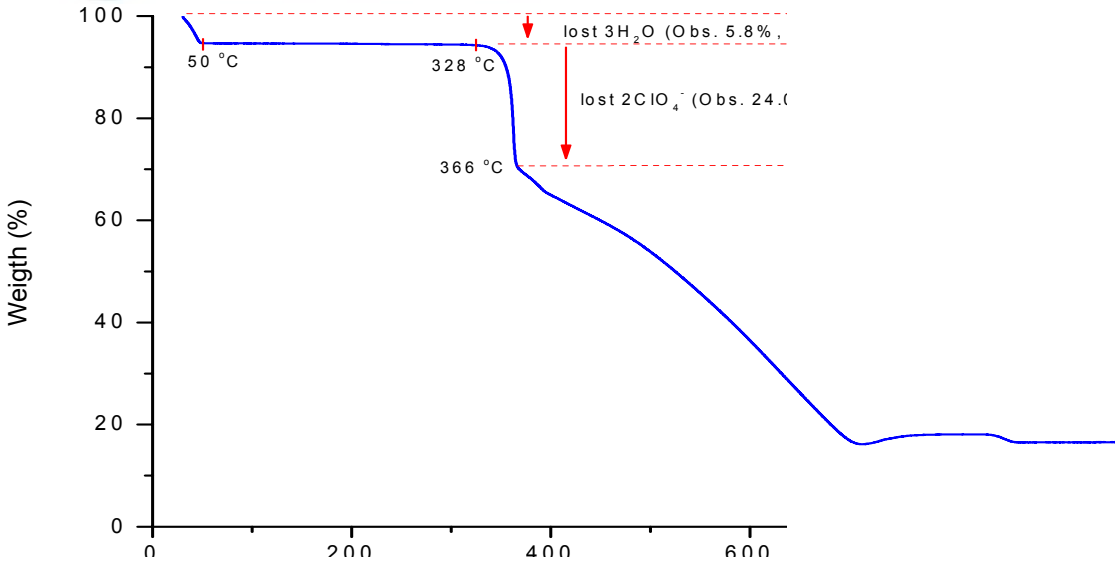

Fig. 86. TGA curve of $[Cu_2([22]\text{-HMTADO})(OClO_3)(OH_2)]ClO_4 \cdot 2H_2O$.

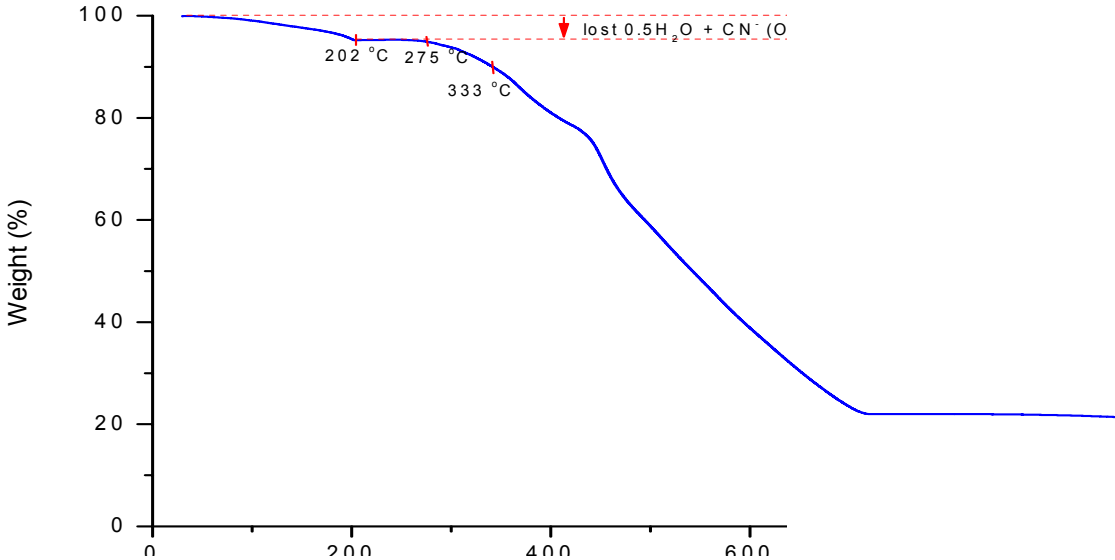

Fig. 87. TGA curve of $[Cu_2([22]\text{-HMTADO})(CN)_2]\cdot 0.5H_2O$.

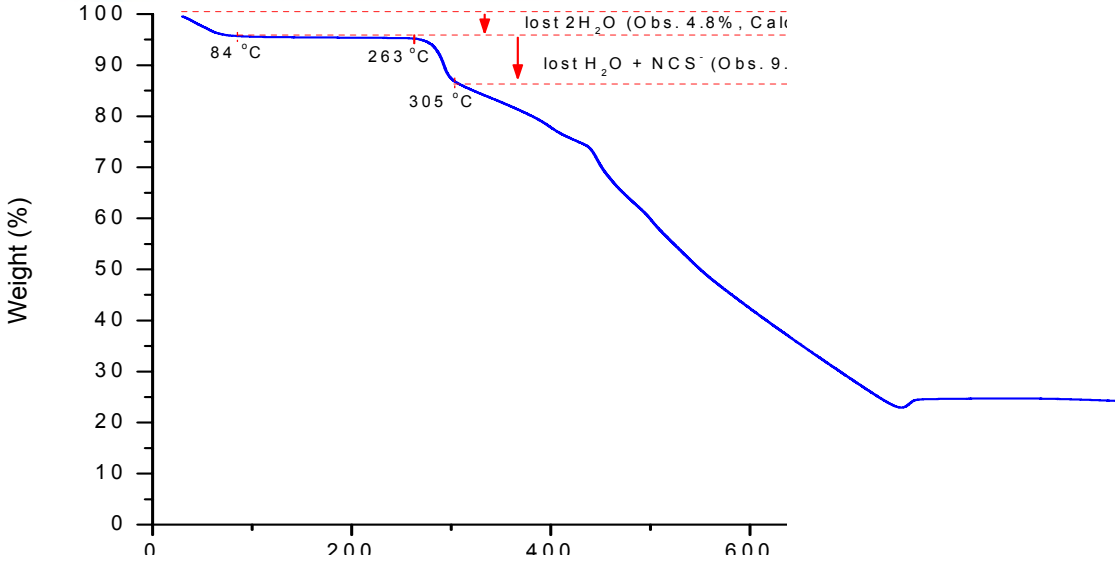

Fig. 88. TGA curve of $[Cu_2([22]\text{-HMTADO})(NCS)(OH_2)]NCS\cdot 2H_2O$.

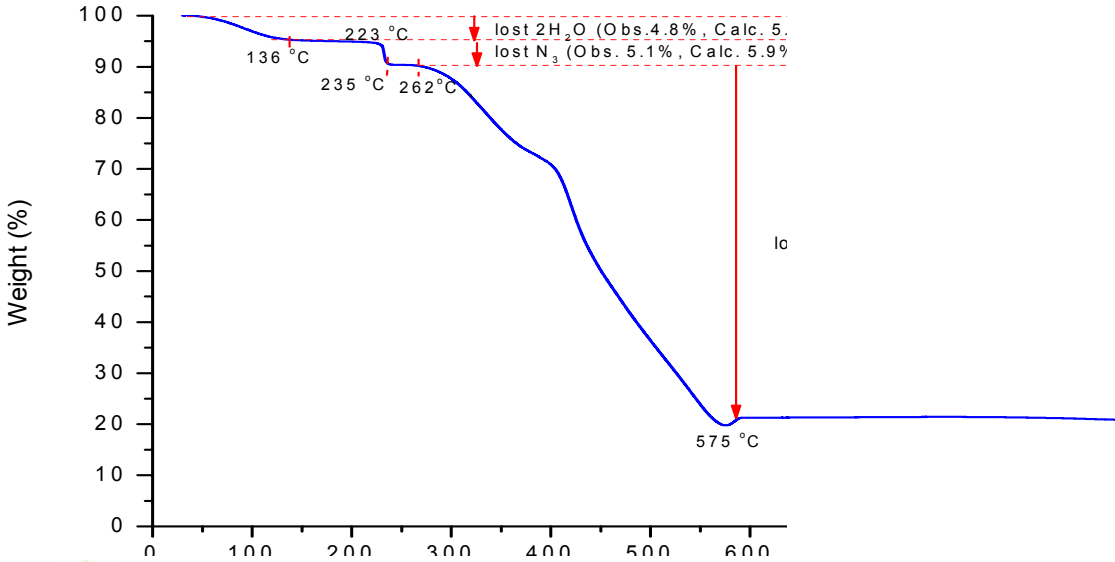

Fig. 89. TGA curve of $[Cu_2([22]\text{-HMTADO})(N_3)(OH_2)]N_3{\cdot}H_2O$.

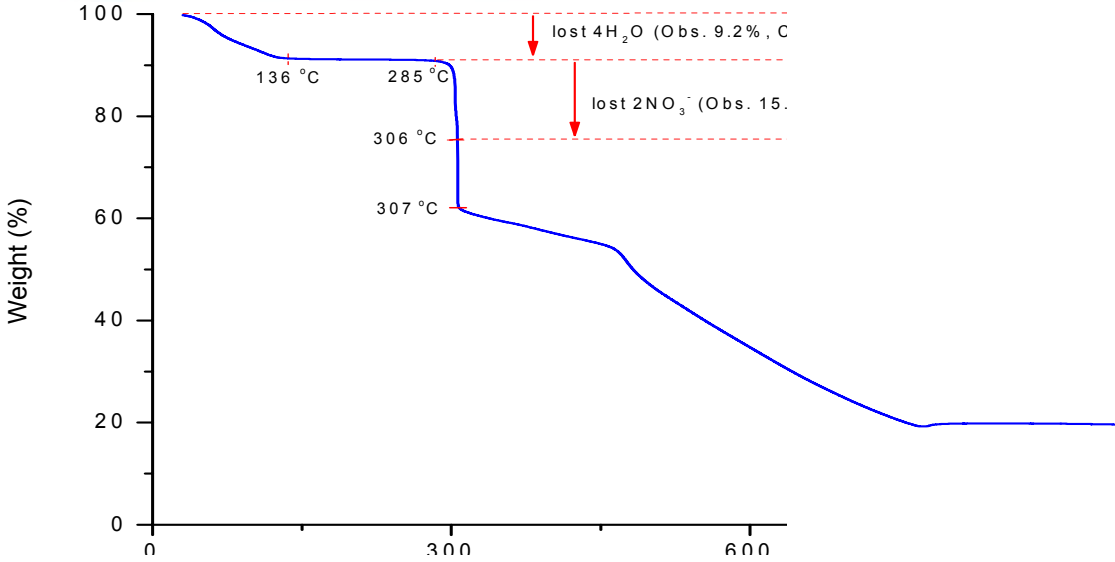

Fig. 90. TGA curve of $[Cu_2([22]\text{-HMTADO})(ONO_2)]NO_3{\cdot}4H_2O$.

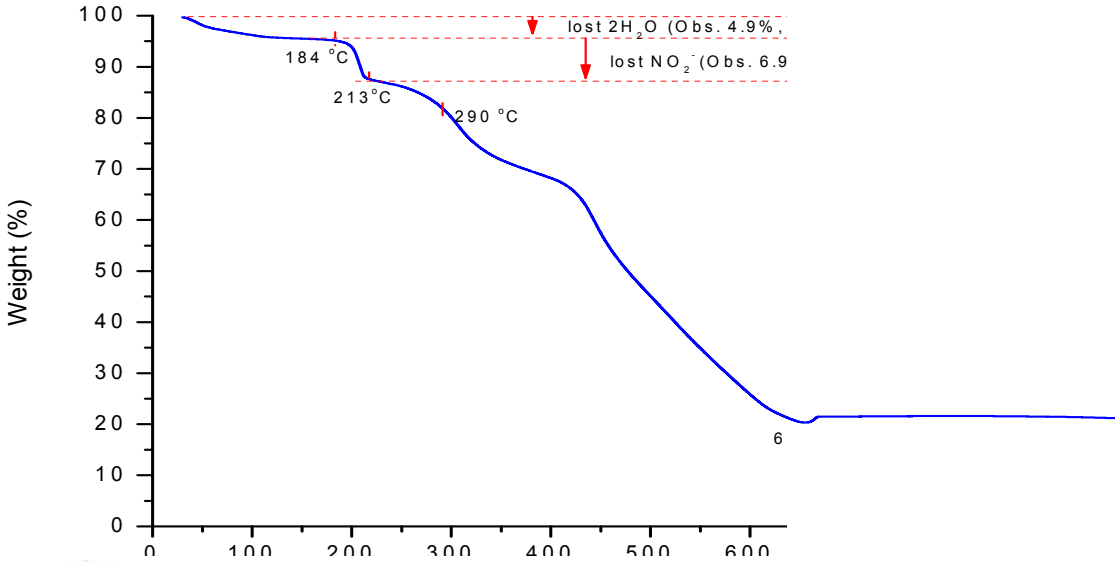

Fig. 91. TGA curve of $[Cu_2([22]\text{-HMTADO})NO_2]NO_2{\cdot}2H_2O$.

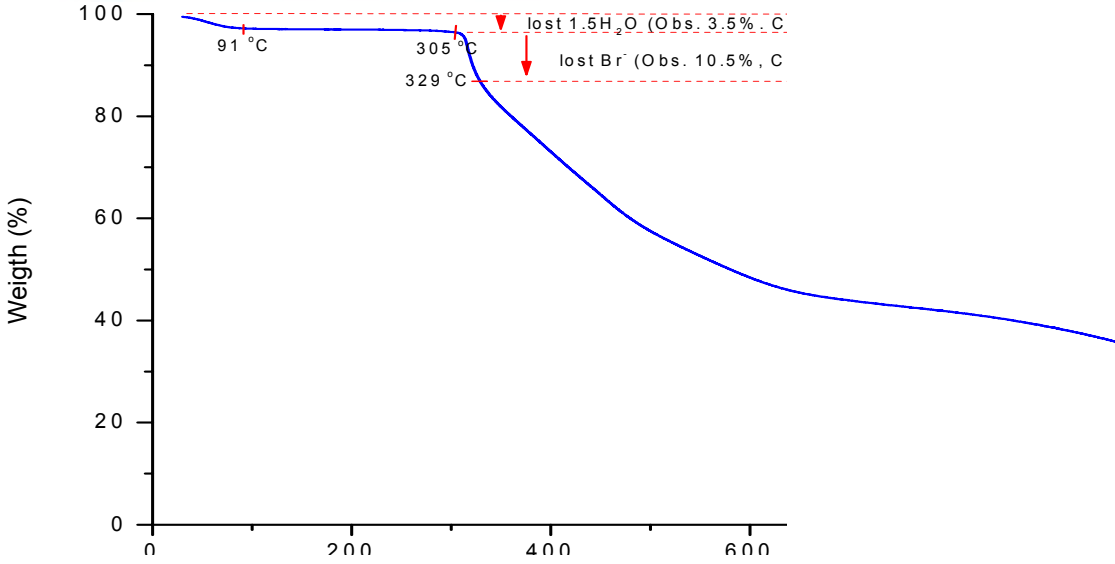

Fig. 92. TGA curve of $[Cu_2([22]\text{-HMTADO})]Br_2{\cdot}1.5H_2O$.

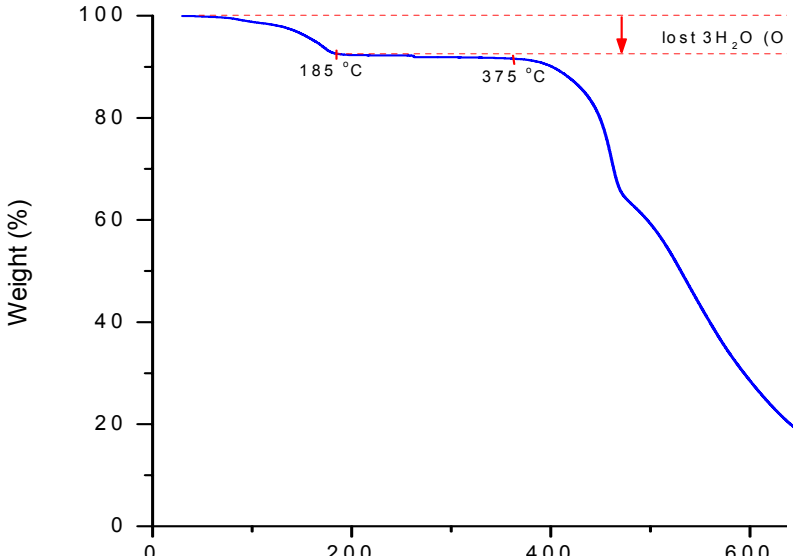

Fig. 93. TGA curve of $[Ni_2([22]\text{-HMTADO})(OH_2)_2]Cl_2{\cdot}H_2O$.

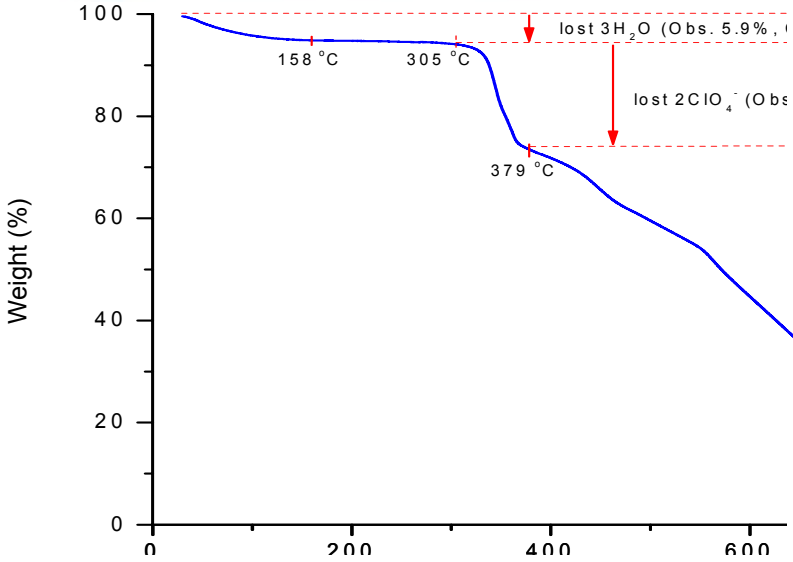

Fig. 94. TGA curve of $[Ni_2([22]\text{-HMTADO})(OH_2)_2](ClO_4)_2{\cdot}H_2O$.

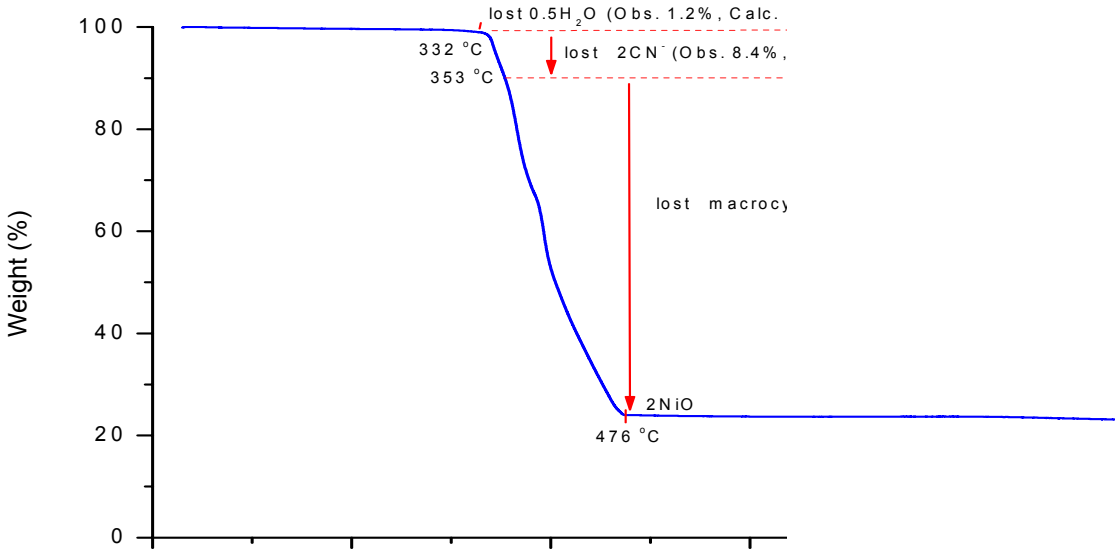

Fig. 95. TGA curve of $[Ni_2([22]\text{-HMTADO})(CN)_2]\cdot 0.5H_2O$.

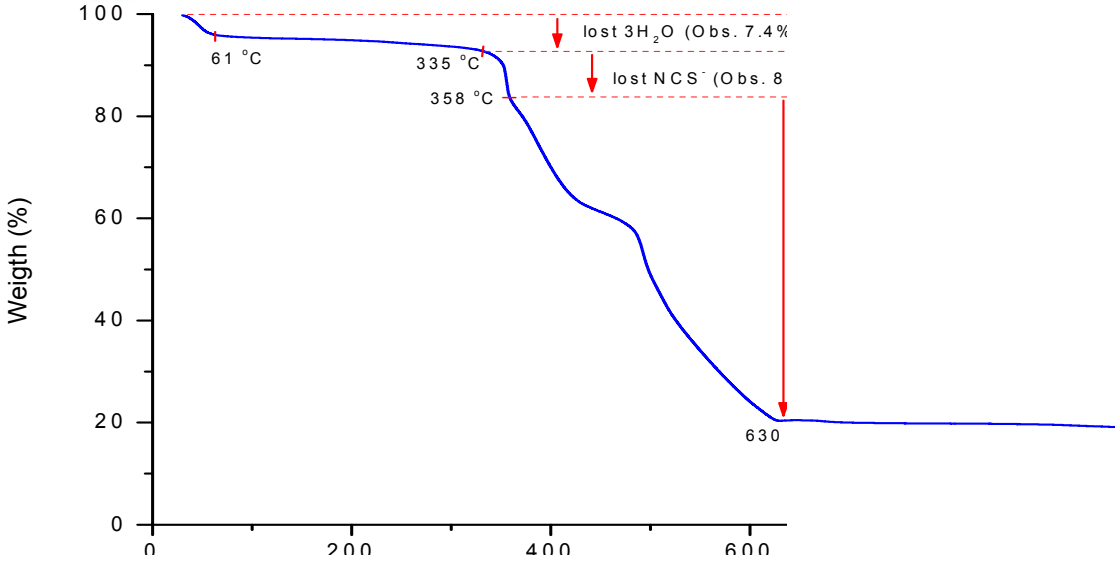

Fig. 96. TGA curve of $[Ni_2([22]\text{-HMTADO})(NCS)_2(OH_2)]\cdot 2H_2O$.

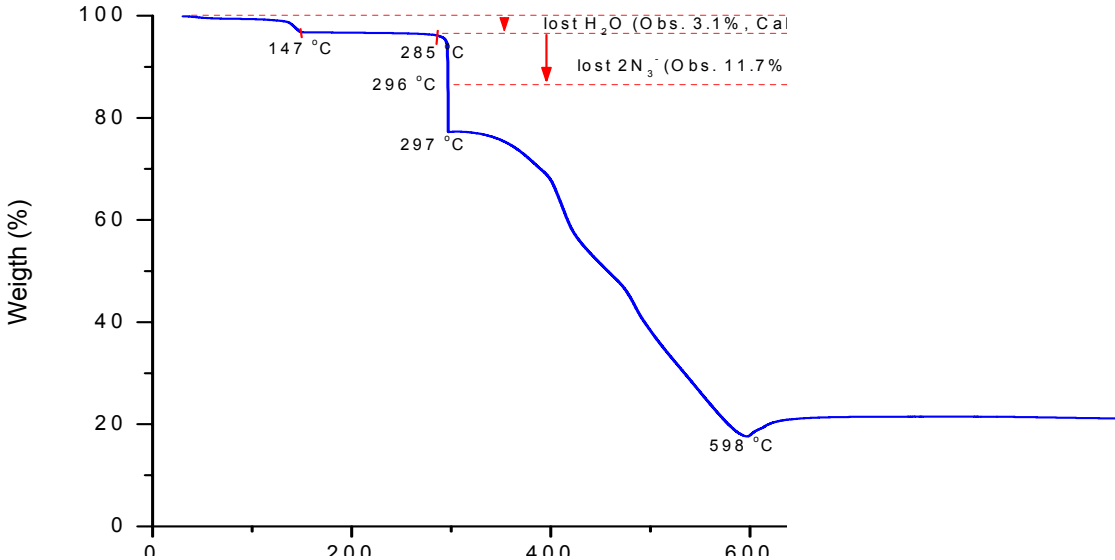

Fig. 97. TGA curve of $[Ni_2([22]\text{-HMTADO})(N_3)_2(OH_2)]$.

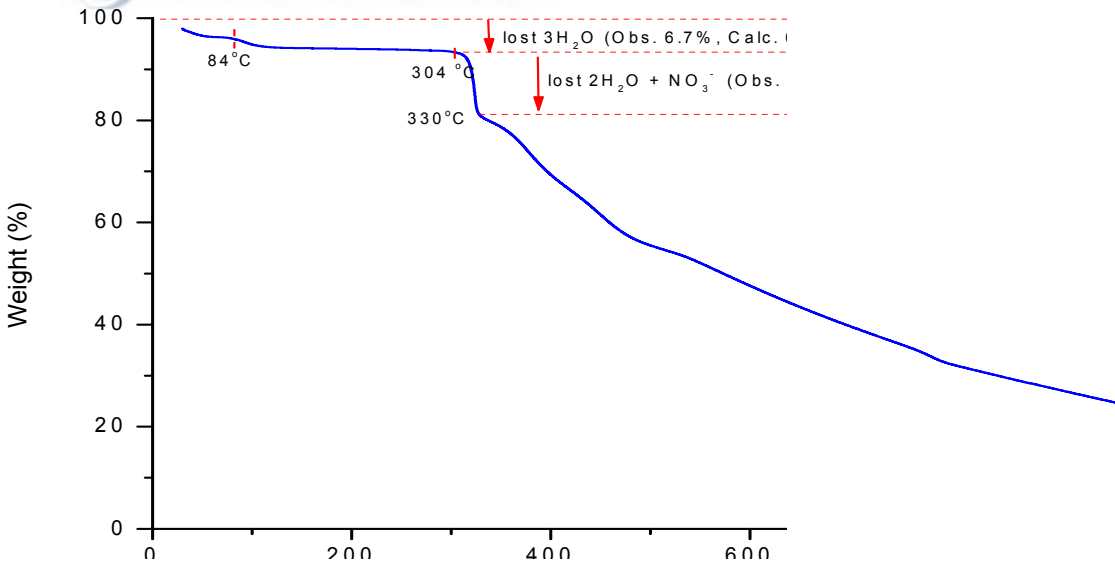

Fig. 98. TGA curve of $[Ni_2([22]\text{-HMTADO})(NO_3)(OH_2)_2]NO_3{\cdot}3H_2O$.

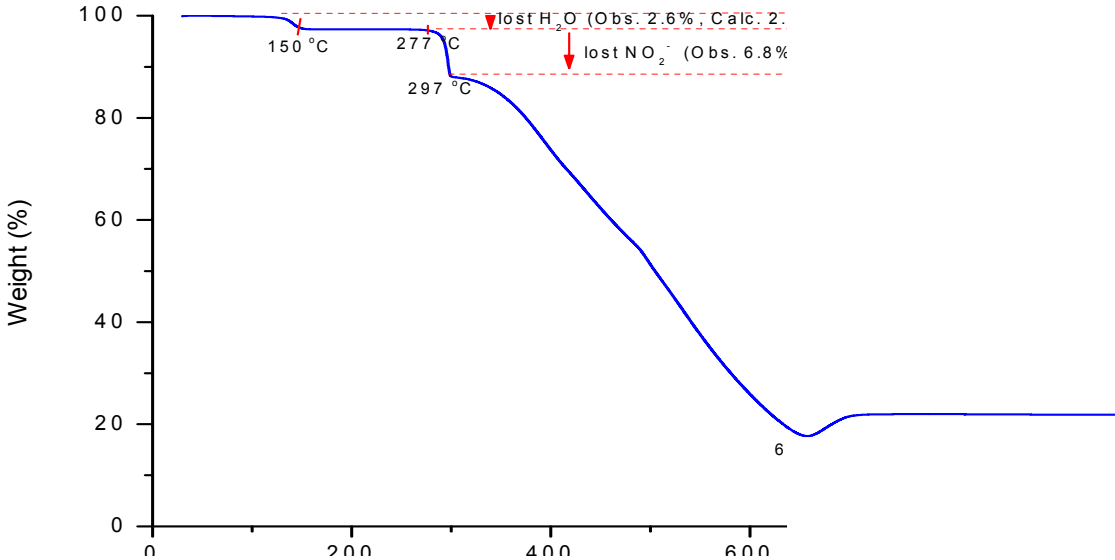

Fig. 99. TGA curve of $[Ni_2([22]\text{-HMTADO})NO_2]NO_2{\cdot}H_2O$.

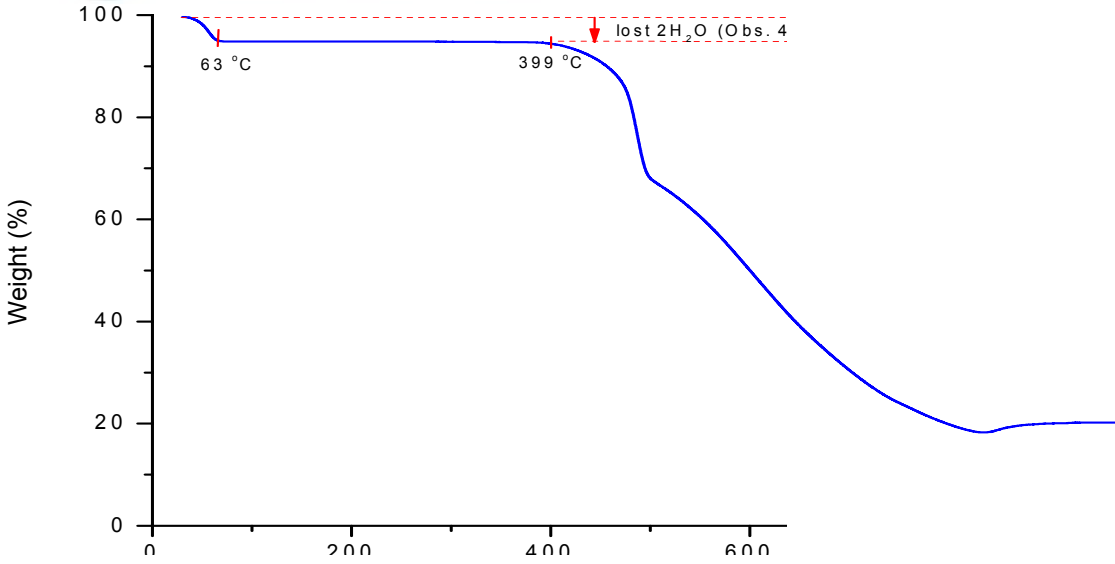

Fig. 100. TGA curve of $[Ni_2([22]\text{-HMTADO})]Br_2{\cdot}2H_2O$.

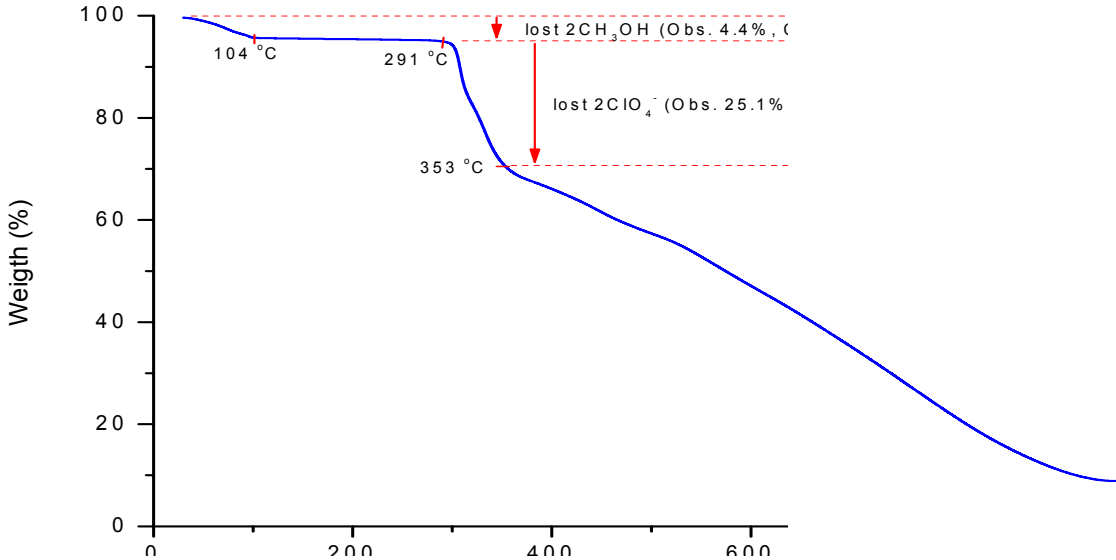

Fig. 101. TGA curve of $[Ni(H_2[22]\text{-}HMTADO)(OHCH_3)_2](ClO_4)_2$.

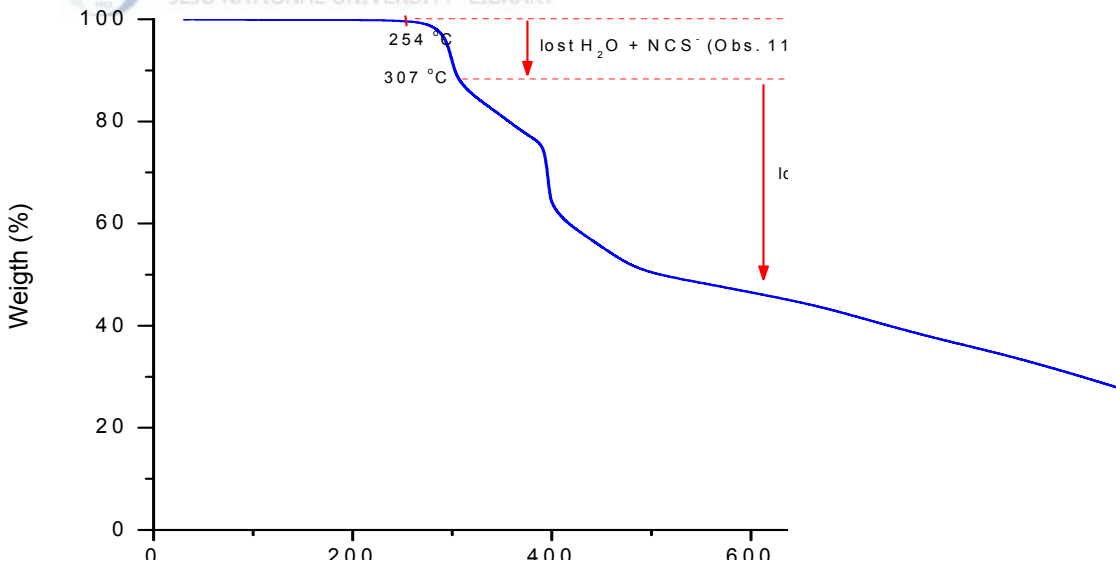

Fig. 102. TGA curve of $[Ni(H_2[22]\text{-}HMTADO)(NCS)_2]\cdot H_2O$.

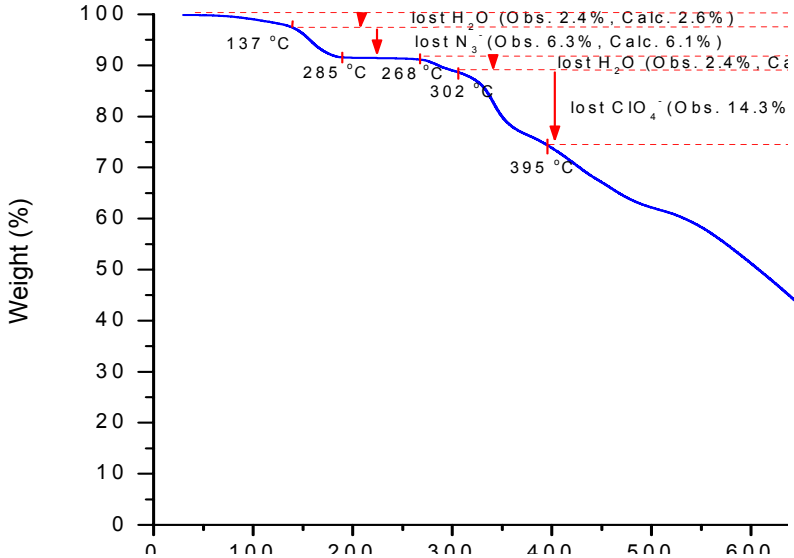

Fig. 103. TGA curve of $[Ni(H_2[22]\text{-}HMTADO)(N_3)(OH_2)]ClO_4{\cdot}H_2O$.

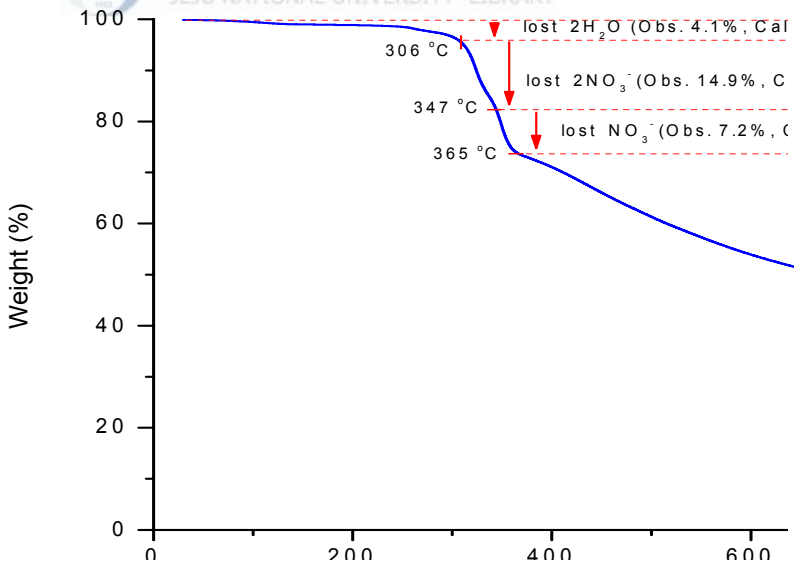

Fig. 104. TGA curve of $[Pr(H_2[22]\text{-}HMTADO)(NO_3)](NO_3)_2{\cdot}2H_2O$.

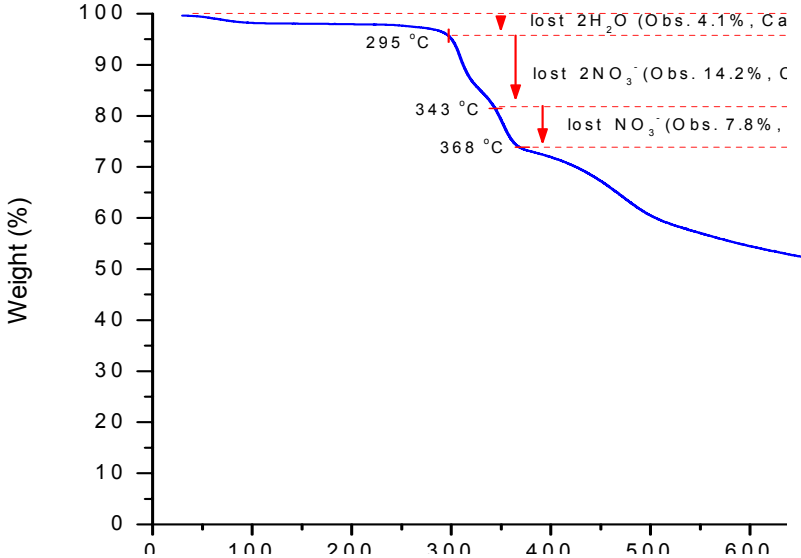

Fig. 105. TGA curve of $[Sm(H_2[22]\text{-}HMTADO)(NO_3)](NO_3)_2{\cdot}2H_2O$.

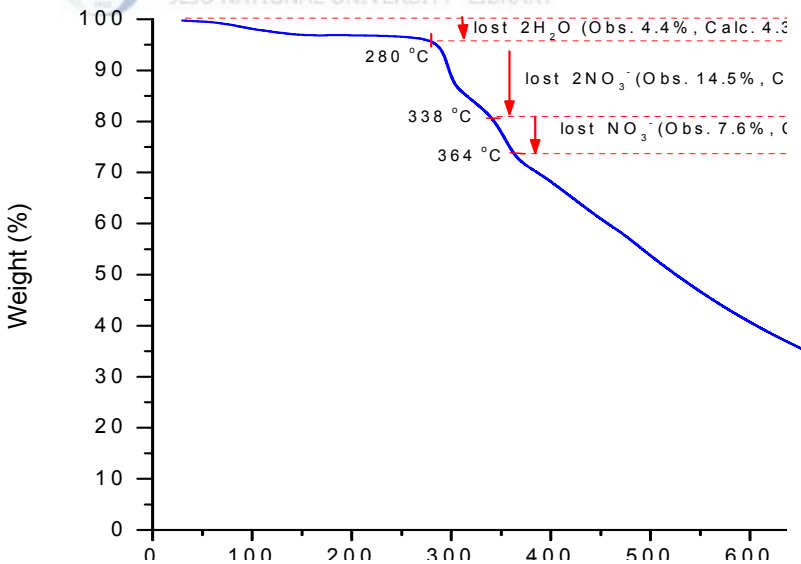

Fig. 106. TGA curve of $[Gd(H_2[22]\text{-}HMTADO)(NO_3)](NO_3)_2{\cdot}2H_2O$.

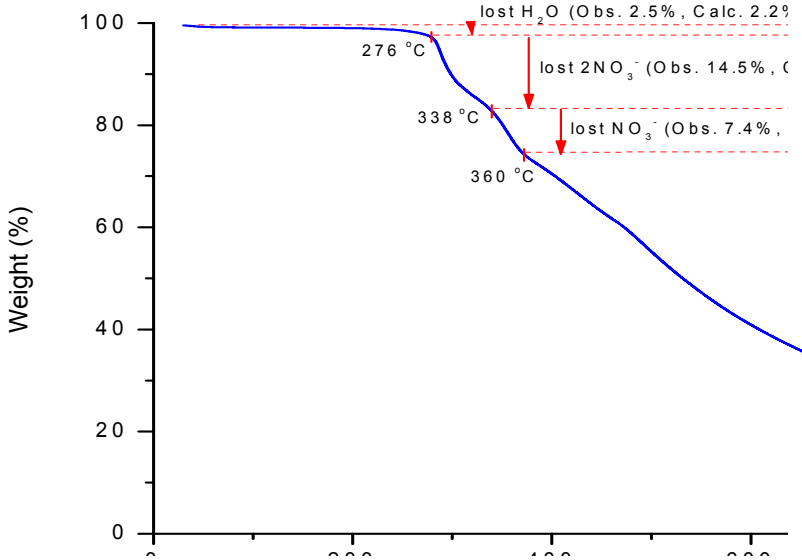

Fig. 107. TGA curve of $[Dy(H_2[22]\text{-}HMTADO)(NO_3)](NO_3)_2{\cdot}H_2O$.

6. Crystal Structures of Complexes.

1) $[Cu_2([22]\text{-HMTADO})(OH_2)_4]Cl_2 \cdot 10H_2O$

An ORTEP view of $[Cu_2([22]\text{-HMTADO})(OH_2)_4]Cl_2 \cdot 10H_2O$ is shown in Fig. 108, and bond distances and angles are summarized in Table 47 and 48. The crystal structure of this complex is composed of binuclear cation of the indicated formula and noninteracting chloride anions. These results are backed up by the molar conductivity (Λ_M = 218 $ohm^{-1}cm^2mol^{-1}$) which agreed with assignment of the structure as $[Cu_2([22]\text{-HMTADO})(OH_2)_4]Cl_2 \cdot 10H_2O$. The binuclear cation, $[Cu_2([22]\text{-HMTADO})(OH_2)_4]^{2+}$ shows two octahedral environment, where the copper(II) ions are coordinated by the two oxygen atoms of water molecules of the copper basal planes (CuN_2O_2) in trans positions, respectively.

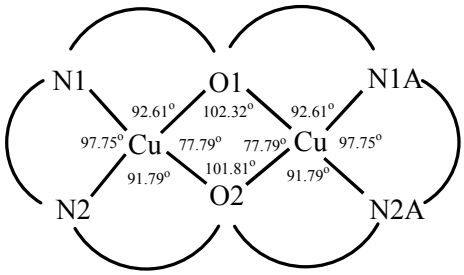

4

The macrocyclic complex adopts an essentially flat structure with the two octahedral copper centers bridged by the two phenoxide oxygen atoms, with quite large Cu-O-Cu angles (102.32(8)° and 101.81(7)°) **(4)**.

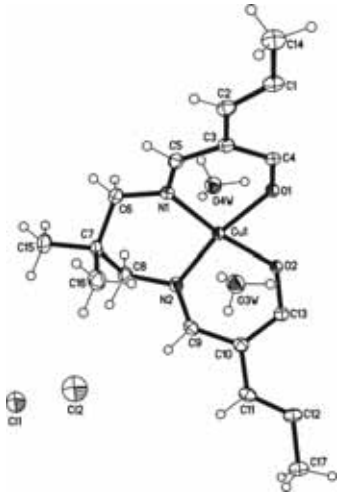

(a)

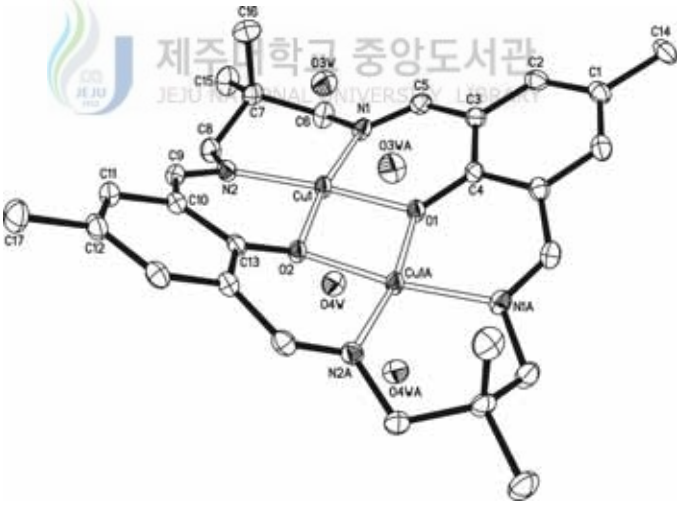

(b)

Fig. 108. Structural representation of (a) asymmetric unit and (b) core structure (top view) for the $[Cu_2([22]\text{-HMTADO})(OH_2)_4]Cl_2 \cdot 10H_2O$ complex.

Magnetostructural correlations in binuclear copper(II) complexes bridged equatorially by pairs of hydroxide groups show that the major factor controlling spin coupling between the *S*=1/2 metal centers is the Cu-O-Cu angle. The sum of angles at the phenoxide oxygens is almost exactly 360° (359.71°), indicating no square oxygen distortion. The sum of angles at the copper basal planes (CuN_2O_2) is almost exactly 360°(359.97°), indicating no plane distortion.

The copper centers are separated by 3.0482(4) Å. The Cu-N (imines) bond distances are in the range of 1.9490(15) and 1.9503(15) Å, and Cu-O (phenolic) are 1.9567(11)Å and 1.9638(11) Å. The Cu-O (aqua) bond distances are in the range of 2.4792(14) and 2.5798(14) Å. The bond angles N(2)-Cu-O(1), N(1)-Cu-O(2), and O(4W)-Cu-O(3W) are 169.15(6)°, 170.36(6)° and 172.68(5)°, respectively. In this complex Cu-N (imines) and Cu-O (phenolic) distances are shorter than Cu-O (aqua) and the angle N(2)-Cu-O(1), N(1)-Cu-O(2), and O(4W)-Cu-O(3W) are smaller than the ideal value of 180°, indicating that the donor atoms are not able to achieve the axial positions of a perfect octahedron ; this is elongated owing to the Jahn-Teller effect and steric effect.

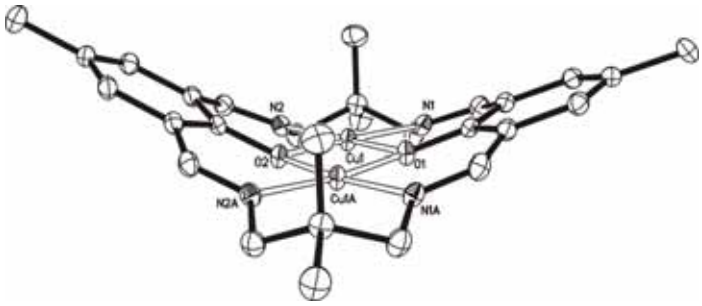

Fig. 109. Side view for the $[Cu_2([22]\text{-HMTADO})(OH_2)_4]^{2+}$ cation.

An angle of 29.61° exists between the benzene mean planes of macrocycle and the copper basal planes (Fig. 109). This is bent owing to the chair conformation effect of the six-membered ring with trimethylene chain linking the azomethine nitrogen donors and copper. The two methyl groups (C(15) and C(15A)) attached to the trimetylenes are situated eclipsed conformation.

In general, hydrogen bonding plays a principal role in the packing of the title compound. There are four types of H-bonds ; between coordinated waters, coordinated water - lattice water, chloride ion - lattice water, and between lattice waters (Table 49). These interactions result in a formation of polymeric chains (Fig. 110). This chain forms a related layer structure, but within the layers binuclear cation $[Cu_2([22]\text{-HMTADO})(OH_2)_4]^{2+}$ ions arrange zig-zag configurations.

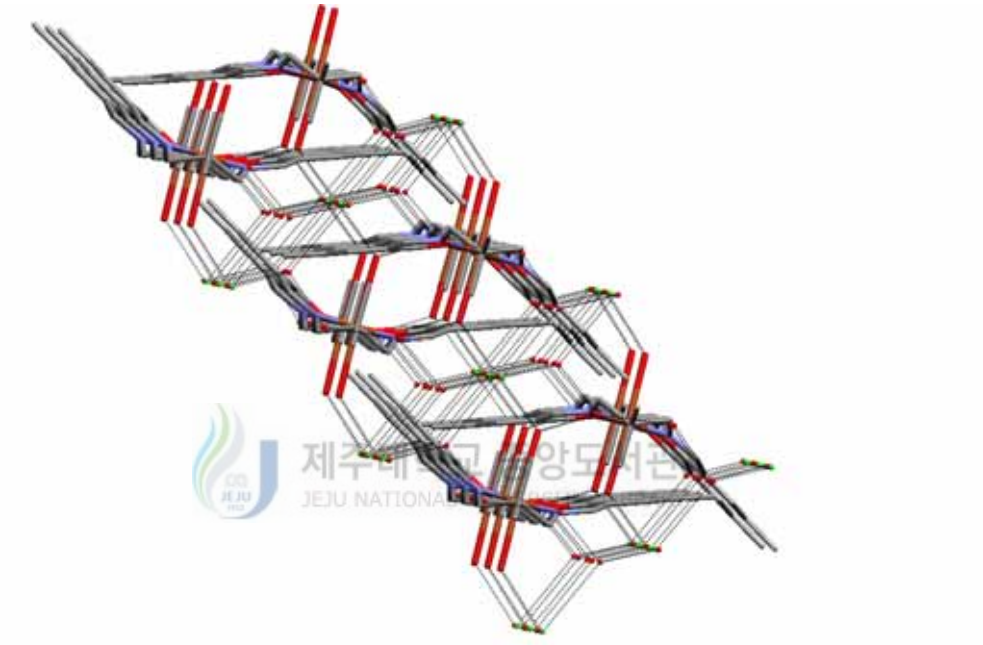

Fig. 110. The molecular packing diagram of $[Cu_2([22]\text{-HMTADO})(OH_2)_4]Cl_2 \cdot 10H_2O$. The hydrogen bonds are indicated by dotted lines.

Table 47. Bond lengths (Å) for $[Cu_2([22]\text{-HMTADO})(OH_2)_4]Cl_2 \cdot 10H_2O$

Cu(1)-N(1)	1.9490(15)	C(7)-C(8)	1.534(3)
Cu(1)-N(2)	1.9503(15)	C(8)-H(8A)	0.97
Cu(1)-O(1)	1.9567(11)	C(8)-H(8B)	0.97
Cu(1)-O(2)	1.9638(11)	C(9)-C(10)	1.456(3)
Cu(1)-O(4W)	2.4792(14)	C(9)-H(9A)	0.93
Cu(1)-O(3W)	2.5798(14)	C(10)-C(11)	1.407(2)
Cu(1)-Cu(1)#1	3.0482(4)	C(10)-C(13)	1.416(2)
O(1)-C(4)	1.325(3)	C(11)-C(12)	1.384(2)
O(1)-Cu(1)#1	1.9567(11)	C(11)-H(11A)	0.93
O(2)-C(13)	1.332(3)	C(12)-C(11)#1	1.384(2)
O(2)-Cu(1)#1	1.9638(11)	C(12)-C(17)	1.512(3)
O(3W)-H(3A)	0.7886	C(13)-C(10)#1	1.416(2)
O(3W)-H(3B)	0.7368	C(14)-H(14A)	0.96
O(3W)-H(3C)	0.8969	C(14)-H(14B)	0.96
O(4W)-H(4A)	0.7165	C(14)-H(14C)	0.96
O(4W)-H(4B)	0.7876	C(15)-H(15A)	0.96
O(4W)-H(2C)	0.9103	C(15)-H(15B)	0.96
N(1)-C(5)	1.284(2)	C(15)-H(15C)	0.96
N(1)-C(6)	1.477(2)	C(16)-H(16A)	0.96
N(2)-C(9)	1.281(2)	C(16)-H(16B)	0.96
N(2)-C(8)	1.473(2)	C(16)-H(16C)	0.96
C(1)-C(2)	1.387(2)	C(17)-H(17A)	0.96
C(1)-C(2)#1	1.387(2)	C(17)-H(17B)	0.96
C(1)-C(14)	1.509(4)	C(17)-H(17C)	0.96
C(2)-C(3)	1.405(2)	O(5W)-H(5B)	0.8689
C(2)-H(2A)	0.93	O(5W)-H(5C)	0.8185
C(3)-C(4)	1.417(2)	O(6W)-H(6C)	0.7844
C(3)-C(5)	1.456(3)	O(6W)-H(6D)	0.8445
C(4)-C(3)#1	1.417(2)	O(7W)-H(7A)	0.9649
C(5)-H(5A)	0.93	O(7W)-H(7B)	0.7347
C(6)-C(7)	1.535(2)	O(8W)-H(8C)	0.8246
C(6)-H(6A)	0.97	O(8W)-H(8D)	0.9103
C(6)-H(6B)	0.97	O(9W)-H(9B)	0.8075
C(7)-C(16)	1.527(3)	O(10W)-H(10A)	0.7835
C(7)-C(15)	1.532(3)		

Table 48. Angles [°] for $[Cu_2([22]\text{-}HMTADO)(OH_2)_4]Cl_2 \cdot 10H_2O$

N(1)-Cu(1)-N(2)	97.75(7)	Cu(1)-O(3W)-H(3C)	106.7
N(1)-Cu(1)-O(1)	92.61(6)	H(3A)-O(3W)-H(3C)	110.2
N(2)-Cu(1)-O(1)	169.15(6)	H(3B)-O(3W)-H(3C)	105.7
N(1)-Cu(1)-O(2)	170.36(6)	Cu(1)-O(4W)-H(4A)	117.1
N(2)-Cu(1)-O(2)	91.79(6)	Cu(1)-O(4W)-H(4B)	119.4
O(1)-Cu(1)-O(2)	77.79(6)	H(4A)-O(4W)-H(4B)	102.6
N(1)-Cu(1)-O(4W)	90.40(6)	Cu(1)-O(4W)-H(2C)	96.5
N(2)-Cu(1)-O(4W)	94.49(6)	H(4A)-O(4W)-H(2C)	112.3
O(1)-Cu(1)-O(4W)	88.63(6)	H(4B)-O(4W)-H(2C)	109
O(2)-Cu(1)-O(4W)	90.25(6)	C(5)-N(1)-C(6)	117.13(16)
N(1)-Cu(1)-O(3W)	92.03(6)	C(5)-N(1)-Cu(1)	122.62(13)
N(2)-Cu(1)-O(3W)	92.03(6)	C(6)-N(1)-Cu(1)	120.25(12)
O(1)-Cu(1)-O(3W)	84.36(6)	C(9)-N(2)-C(8)	117.41(15)
O(2)-Cu(1)-O(3W)	86.22(6)	C(9)-N(2)-Cu(1)	121.99(13)
O(4W)-Cu(1)-O(3W)	172.68(5)	C(8)-N(2)-Cu(1)	120.53(11)
N(1)-Cu(1)-Cu(1)#1	131.37(4)	C(2)-C(1)-C(2)#1	117.0(2)
N(2)-Cu(1)-Cu(1)#1	130.87(4)	C(2)-C(1)-C(14)	121.45(12)
O(1)-Cu(1)-Cu(1)#1	38.84(4)	C(2)#1-C(1)-C(14)	121.45(12)
O(2)-Cu(1)-Cu(1)#1	39.10(4)	C(1)-C(2)-C(3)	122.81(18)
O(4W)-Cu(1)-Cu(1)#1	86.66(3)	C(1)-C(2)-H(2A)	118.6
O(3W)-Cu(1)-Cu(1)#1	86.55(3)	C(3)-C(2)-H(2A)	118.6
C(4)-O(1)-Cu(1)	126.80(5)	C(2)-C(3)-C(4)	119.57(18)
C(4)-O(1)-Cu(1)#1	126.80(5)	C(2)-C(3)-C(5)	115.99(17)
Cu(1)-O(1)-Cu(1)#1	102.32(8)	C(4)-C(3)-C(5)	124.05(17)
C(13)-O(2)-Cu(1)#1	124.39(7)	O(1)-C(4)-C(3)	120.87(11)
C(13)-O(2)-Cu(1)	124.39(7)	O(1)-C(4)-C(3)#1	120.87(11)
Cu(1)#1-O(2)-Cu(1)	101.81(7)	C(3)-C(4)-C(3)#1	118.2(2)
Cu(1)-O(3W)-H(3A)	121	N(1)-C(5)-C(3)	127.40(17)
Cu(1)-O(3W)-H(3B)	110.9	N(1)-C(5)-H(5A)	116.3
H(3A)-O(3W)-H(3B)	101.4	C(3)-C(5)-H(5A)	116.3

N(1)-C(6)-C(7)	115.04(15)	O(2)-C(13)-C(10)	120.98(11)
N(1)-C(6)-H(6A)	108.5	O(2)-C(13)-C(10)#1	120.98(11)
C(7)-C(6)-H(6A)	108.5	C(10)-C(13)-C(10)#1	118.0(2)
N(1)-C(6)-H(6B)	108.5	C(1)-C(14)-H(14A)	109.5
C(7)-C(6)-H(6B)	108.5	C(1)-C(14)-H(14B)	109.5
H(6A)-C(6)-H(6B)	107.5	H(14A)-C(14)-H(14B)	109.5
C(16)-C(7)-C(15)	110.08(17)	C(1)-C(14)-H(14C)	109.5
C(16)-C(7)-C(8)	110.70(15)	H(14A)-C(14)-H(14C)	109.5
C(15)-C(7)-C(8)	106.83(16)	H(14B)-C(14)-H(14C)	109.5
C(16)-C(7)-C(6)	111.05(16)	C(7)-C(15)-H(15A)	109.5
C(15)-C(7)-C(6)	106.57(15)	C(7)-C(15)-H(15B)	109.5
C(8)-C(7)-C(6)	111.45(16)	H(15A)-C(15)-H(15B)	109.5
N(2)-C(8)-C(7)	114.00(15)	C(7)-C(15)-H(15C)	109.5
N(2)-C(8)-H(8A)	108.8	H(15A)-C(15)-H(15C)	109.5
C(7)-C(8)-H(8A)	108.8	H(15B)-C(15)-H(15C)	109.5
N(2)-C(8)-H(8B)	108.8	C(7)-C(16)-H(16A)	109.5
C(7)-C(8)-H(8B)	108.8	C(7)-C(16)-H(16B)	109.5
H(8A)-C(8)-H(8B)	107.6	H(16A)-C(16)-H(16B)	109.5
N(2)-C(9)-C(10)	127.12(17)	C(7)-C(16)-H(16C)	109.5
N(2)-C(9)-H(9A)	116.4	H(16A)-C(16)-H(16C)	109.5
C(10)-C(9)-H(9A)	116.4	H(16B)-C(16)-H(16C)	109.5
C(11)-C(10)-C(13)	119.49(17)	C(12)-C(17)-H(17A)	109.5
C(11)-C(10)-C(9)	116.84(16)	C(12)-C(17)-H(17B)	109.5
C(13)-C(10)-C(9)	123.37(16)	H(17A)-C(17)-H(17B)	109.5
C(12)-C(11)-C(10)	123.10(18)	C(12)-C(17)-H(17C)	109.5
C(12)-C(11)-H(11A)	118.5	H(17A)-C(17)-H(17C)	109.5
C(10)-C(11)-H(11A)	118.5	H(17B)-C(17)-H(17C)	109.5
C(11)-C(12)-C(11)#1	116.6(2)	H(5B)-O(5W)-H(5C)	127.8
C(11)-C(12)-C(17)	121.64(11)	H(6C)-O(6W)-H(6D)	105.4
C(11)#1-C(12)-C(17)	121.64(11)	H(7A)-O(7W)-H(7B)	99.7
		H(8C)-O(8W)-H(8D)	96.1

Symmetry transformations used to generate equivalent atoms: #1 ; x, -y+1, z.

Table 49. Selected bond lengths (Å) and angles(°) for hydrogen bond of $[Cu_2([22]\text{-HMTADO})(OH_2)_4]Cl_2 \cdot 10H_2O$

D-H···A	d(D-H)	d(H···A)	<DHA	d(D···A)
between coordinated waters				
O3W-H3C···O3W [x, -y+1, z]	0.897	1.876	160.45	2.738
O4W-H2C···O4W [x, -y+1, z]	0.91	1.852	174.75	2.759
coordinated water - lattice water				
O3W-H3A···O5W	0.789	2.001	165.9	2.773
O3W-H3B···O10W	0.737	2.141	157.69	2.836
O4W-H4A···O7W	0.717	2.023	162.33	2.715
O4W-H4B···O9W [-x+1/2, -y+1/2, -z+1]	0.788	2.141	161.92	2.9
O5W-H5C···O3W	0.819	1.982	162.09	2.773
chloride ion - lattice water				
O6W-H6C···Cl2	0.784	2.476	179.69	3.261
O6W-H6D···Cl1	0.845	2.423	167.38	3.252
O8W-H8C···Cl1	0.825	2.391	170.17	3.207
O8W-H8D···Cl2 [x, y, z+1]	0.91	2.311	165.92	3.202
between lattice waters				
O5W-H5B···O6W	0.869	2.094	155.5	2.907
O7W-H7A···O8W [-x+1/2, -y+1/2, -z+2]	0.965	1.909	159.73	2.834
O7W-H7B···O5W [x, y, z+1]	0.735	1.983	162.69	2.693
O9W-H9B···O8W [x, y, z-1]	0.808	2.03	172.6	2.833
O10W-H10A···O6W	0.783	2.101	166.62	2.869

2) $[Cu_2([22]\text{-HMTADO})(OClO_3)(OH_2)]ClO_4 \cdot 2CH_3OH$.

An ORTEP representation of $[Cu_2([22]\text{-HMTADO})(OClO_3)(OH_2)]ClO_4 \cdot 2CH_3OH$ with the atom labels are shown in Fig. 111, and bond distances and angles are summarized in Table 50 and 51. Unfortunately, refinement of structure was hampered due to rather inferior quality of diffraction data and severe disordering of the perchlorate anions. Nevertheless, the structural analysis has elucidated the geometric features and connectivities in the complex molecule. The binuclear cation, $[Cu_2([22]\text{-HMTADO})(OClO_3)(OH_2)]^{2+}$ shows two square pyramidal environment, where the copper(II) ions are coordinated by the two oxygen atoms of perchlorate and water molecules of the copper basal planes (CuN_2O_2) in trans axis positions, respectively.

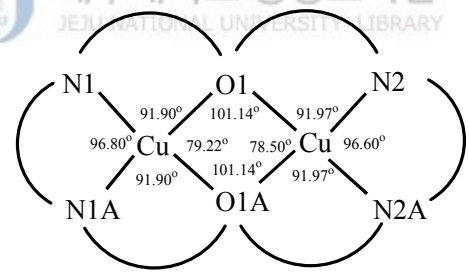

5

The macrocyclic complex adopts an essentially flat structure with the two copper centers bridged by the two phenoxide oxygen atoms, with quite large Cu-O-Cu angles (101.14(15)°) **(5)**.

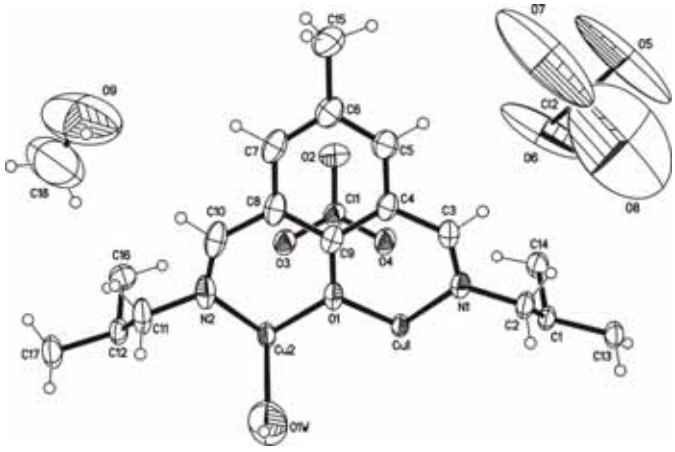

(a)

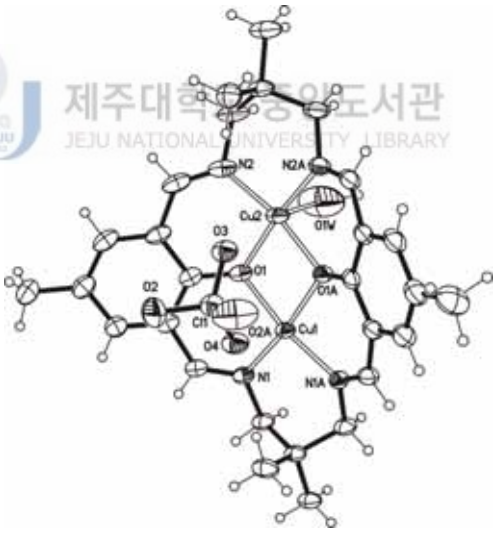

(b)

Fig. 111. Structural representation of (a) asymmetric unit and (b) core structure (top view) for the $[Cu_2([22]\text{-HMTADO})(OClO_3)(OH_2)]ClO_4 \cdot 2CH_3OH$ complex.

The sum of angles at the phenoxide oxygens is exactly 360°, indicating no square oxygen distortion.

The copper centers are separated by 3.0319(10) Å. The Cu-N (imines) bond distances are in the range of 1.945(4) and 1.951(4) Å, and Cu-O (phenolic) are 1.955(3) and 1.970(3) Å. The Cu(1)-O(4) (perchlorate) bond distance is in the range of 2.459(5) Å, and the Cu(2)-O(1w) (aqua) bond distance is in the range of 2.335(8) Å. The Cu(2)···O(3) are separated by 2.701(5) Å. The bond angles N(1)-Cu(1)-O(1A) and N(2)-Cu(2)-O(1A) are 170.73(14)° and 168.69(16)°, respectively. The bond angles O(1w)-Cu(2)-O(3) is 170.1(2)°.

An angle of 29.79° exists between the benzene mean planes of macrocycle and the copper basal planes (Fig. 112). This is bent owing to the chair conformation effect of the six-membered ring with trimethylene chain linking the azomethine nitrogen donors and copper.

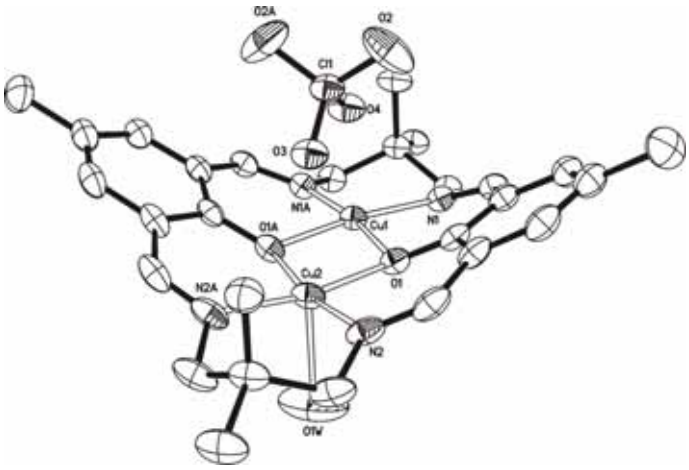

Fig. 112. Side view for the $[Cu_2([22]\text{-HMTADO})(OClO_3)(OH_2)]^+$ cation.

The two methyl groups (C(2) and C(11)) attached to the trimetylenes are situated eclipsed conformation. The another perchlorate ion and methanol molecules occupy lattice sites. Hydrogen bond not existed in the complex. The binuclear cation $[Cu_2([22]\text{-}HMTADO)(OClO_3)(OH_2)]^+$ ions arrange zig-zag configurations(Fig. 113).

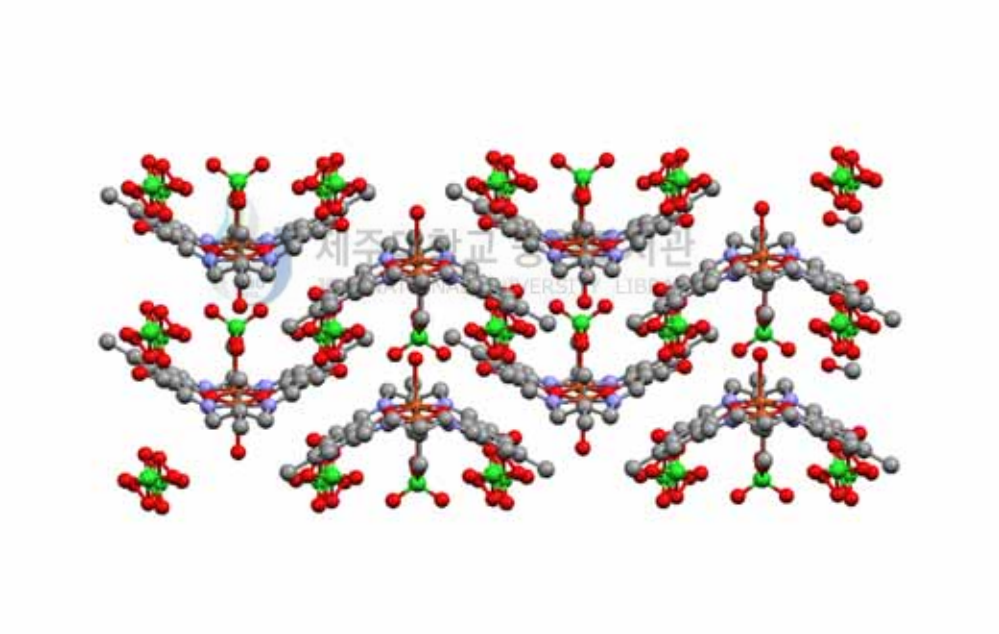

Fig. 113. The molecular packing diagram of $[Cu_2([22]\text{-}HMTADO)(OClO_3)(OH_2)]$ $-ClO_4 \cdot 2CH_3OH$.

Table 50. Bond lengths (Å) for $[Cu_2([22]\text{-HMTADO})(OClO_3)(OH_2)]ClO_4 \cdot 2CH_3OH$

Cu(1)-N(1)#1	1.945(4)	C(4)-C(9)	1.415(6)
Cu(1)-N(1)	1.945(4)	C(5)-C(6)	1.378(7)
Cu(1)-O(1)#1	1.955(3)	C(6)-C(7)	1.387(7)
Cu(1)-O(1)	1.955(3)	C(6)-C(15)	1.508(7)
Cu(1)-O(4)	2.459(5)	C(7)-C(8)	1.402(7)
Cu(1)-Cu(2)	3.0319(10)	C(8)-C(9)	1.420(6)
Cu(2)-N(2)#1	1.951(4)	C(8)-C(10)	1.447(7)
Cu(2)-N(2)	1.951(4)	C(11)-C(12)	1.526(6)
Cu(2)-O(1)	1.970(3)	C(12)-C(11)#1	1.526(6)
Cu(2)-O(1)#1	1.970(3)	C(12)-C(16)	1.532(9)
Cu(2)-O(1W)	2.335(8)	C(12)-C(17)	1.546(9)
Cu(2)-O(3)	2.701(5)	Cl(2)-O(8)#2	1.19(3)
Cl(1)-O(2)	1.433(4)	Cl(2)-Cl(2)#2	1.37(4)
Cl(1)-O(2)#1	1.433(4)	Cl(2)-O(5)	1.427(6)
Cl(1)-O(3)	1.444(5)	Cl(2)-O(8)	1.443(7)
Cl(1)-O(4)	1.449(5)	Cl(2)-O(6)	1.445(6)
O(1)-C(9)	1.335(6)	Cl(2)-O(7)	1.447(7)
N(1)-C(3)	1.285(6)	Cl(2)-O(5)#2	1.58(5)
N(1)-C(2)	1.477(5)	Cl(2)-O(6)#2	2.10(3)
N(2)-C(10)	1.284(7)	O(5)-O(8)#2	0.80(4)
N(2)-C(11)	1.472(6)	O(5)-Cl(2)#2	1.58(5)
C(1)-C(14)	1.527(9)	O(6)-O(8)#2	1.63(3)
C(1)-C(2)#1	1.533(6)	O(6)-Cl(2)#2	2.10(3)
C(1)-C(2)	1.533(6)	O(8)-O(5)#2	0.80(4)
C(1)-C(13)	1.545(8)	O(8)-Cl(2)#2	1.19(3)
C(3)-C(4)	1.462(6)	O(8)-O(6)#2	1.63(3)
C(4)-C(5)	1.389(7)	O(9)-C(18)	1.345(17)

#1 ; x, -y-1/2, z. #2 ; -x+1, -y, -z+1.

Table 51. Angles [°] for $[Cu_2([22]\text{-}HMTADO)(OClO_3)(OH_2)]ClO_4 \cdot 2CH_3OH$

N(1)#1-Cu(1)-N(1)	96.8(2)	N(2)#1-Cu(2)-Cu(1)	131.00(12)
N(1)#1-Cu(1)-O(1)#1	91.90(14)	N(2)-Cu(2)-Cu(1)	131.00(12)
N(1)-Cu(1)-O(1)#1	170.73(14)	O(1)-Cu(2)-Cu(1)	39.25(9)
N(1)#1-Cu(1)-O(1)	170.73(14)	O(1)#1-Cu(2)-Cu(1)	39.25(9)
N(1)-Cu(1)-O(1)	91.90(14)	O(1W)-Cu(2)-Cu(1)	92.6(2)
O(1)#1-Cu(1)-O(1)	79.22(18)	O(3)-Cu(2)-Cu(1)	77.55(10)
N(1)#1-Cu(1)-O(4)	94.38(13)	O(2)-Cl(1)-O(2)#1	109.9(5)
N(1)-Cu(1)-O(4)	94.38(13)	O(2)-Cl(1)-O(3)	109.6(2)
O(1)#1-Cu(1)-O(4)	88.03(12)	O(2)#1-Cl(1)-O(3)	109.6(2)
O(1)-Cu(1)-O(4)	88.03(12)	O(2)-Cl(1)-O(4)	109.1(2)
N(1)#1-Cu(1)-Cu(2)	131.43(11)	O(2)#1-Cl(1)-O(4)	109.1(2)
N(1)-Cu(1)-Cu(2)	131.43(11)	O(3)-Cl(1)-O(4)	109.5(3)
O(1)#1-Cu(1)-Cu(2)	39.61(9)	C(9)-O(1)-Cu(1)	123.1(3)
O(1)-Cu(1)-Cu(2)	39.61(9)	C(9)-O(1)-Cu(2)	124.9(3)
O(4)-Cu(1)-Cu(2)	87.82(11)	Cu(1)-O(1)-Cu(2)	101.14(15)
N(2)#1-Cu(2)-N(2)	96.8(2)	Cl(1)-O(3)-Cu(2)	133.4(3)
N(2)#1-Cu(2)-O(1)	168.69(16)	Cl(1)-O(4)-Cu(1)	131.7(3)
N(2)-Cu(2)-O(1)	91.97(15)	C(3)-N(1)-C(2)	116.1(4)
N(2)#1-Cu(2)-O(1)#1	91.97(15)	C(3)-N(1)-Cu(1)	121.2(3)
N(2)-Cu(2)-O(1)#1	168.69(16)	C(2)-N(1)-Cu(1)	122.3(3)
O(1)-Cu(2)-O(1)#1	78.50(18)	C(10)-N(2)-C(11)	117.5(4)
N(2)#1-Cu(2)-O(1W)	94.20(18)	C(10)-N(2)-Cu(2)	122.6(3)
N(2)-Cu(2)-O(1W)	94.20(18)	C(11)-N(2)-Cu(2)	119.8(4)
O(1)-Cu(2)-O(1W)	92.27(18)	C(14)-C(1)-C(2)#1	111.1(3)
O(1)#1-Cu(2)-O(1W)	92.27(18)	C(14)-C(1)-C(2)	111.1(3)
N(2)#1-Cu(2)-O(3)	92.36(14)	C(2)#1-C(1)-C(2)	110.8(5)
N(2)-Cu(2)-O(3)	92.36(14)	C(14)-C(1)-C(13)	111.2(5)
O(1)-Cu(2)-O(3)	80.10(12)	C(2)#1-C(1)-C(13)	106.2(3)
O(1)#1-Cu(2)-O(3)	80.10(12)	C(2)-C(1)-C(13)	106.2(3)
O(1W)-Cu(2)-O(3)	170.1(2)	N(1)-C(2)-C(1)	113.5(4)

N(1)-C(3)-C(4)	126.8(4)	O(8)-Cl(2)-O(6)	108.5(6)
C(5)-C(4)-C(9)	119.9(4)	O(8)#2-Cl(2)-O(7)	128(3)
C(5)-C(4)-C(3)	116.6(4)	Cl(2)#2-Cl(2)-O(7)	152.4(14)
C(9)-C(4)-C(3)	123.4(4)	O(5)-Cl(2)-O(7)	111.5(7)
C(6)-C(5)-C(4)	123.5(5)	O(8)-Cl(2)-O(7)	109.2(7)
C(5)-C(6)-C(7)	116.7(5)	O(6)-Cl(2)-O(7)	108.4(6)
C(5)-C(6)-C(15)	121.9(5)	O(8)#2-Cl(2)-O(5)#2	115(3)
C(7)-C(6)-C(15)	121.5(5)	Cl(2)#2-Cl(2)-O(5)#2	57(2)
C(6)-C(7)-C(8)	122.6(4)	O(5)-Cl(2)-O(5)#2	126.2(11)
C(7)-C(8)-C(9)	119.8(4)	O(8)-Cl(2)-O(5)#2	30.0(11)
C(7)-C(8)-C(10)	116.7(4)	O(6)-Cl(2)-O(5)#2	78.8(11)
C(9)-C(8)-C(10)	123.4(5)	O(7)-Cl(2)-O(5)#2	115.8(11)
O(1)-C(9)-C(4)	121.0(4)	O(8)#2-Cl(2)-O(6)#2	86.0(15)
O(1)-C(9)-C(8)	121.6(4)	Cl(2)#2-Cl(2)-O(6)#2	43.0(9)
C(4)-C(9)-C(8)	117.4(4)	O(5)-Cl(2)-O(6)#2	62.7(12)
N(2)-C(10)-C(8)	127.6(4)	O(8)-Cl(2)-O(6)#2	50.4(14)
N(2)-C(11)-C(12)	114.7(4)	O(6)-Cl(2)-O(6)#2	139.7(12)
C(11)#1-C(12)-C(11)	110.9(6)	O(7)-Cl(2)-O(6)#2	111.1(11)
C(11)#1-C(12)-C(16)	110.6(4)	O(5)#2-Cl(2)-O(6)#2	77.3(17)
C(11)-C(12)-C(16)	110.6(4)	O(8)#2-O(5)-Cl(2)	56(3)
C(11)#1-C(12)-C(17)	107.4(4)	O(8)#2-O(5)-Cl(2)#2	65(4)
C(11)-C(12)-C(17)	107.4(4)	Cl(2)-O(5)-Cl(2)#2	53.8(11)
C(16)-C(12)-C(17)	109.7(5)	Cl(2)-O(6)-O(8)#2	45.1(11)
O(8)#2-Cl(2)-Cl(2)#2	68.3(16)	Cl(2)-O(6)-Cl(2)#2	40.3(12)
O(8)#2-Cl(2)-O(5)	33.9(17)	O(8)#2-O(6)-Cl(2)#2	43.2(7)
Cl(2)#2-Cl(2)-O(5)	69.0(18)	O(5)#2-O(8)-Cl(2)#2	90(3)
O(8)#2-Cl(2)-O(8)	118(2)	O(5)#2-O(8)-Cl(2)	85(4)
Cl(2)#2-Cl(2)-O(8)	49.9(17)	Cl(2)#2-O(8)-Cl(2)	62(2)
O(5)-Cl(2)-O(8)	110.1(7)	O(5)#2-O(8)-O(6)#2	148(4)
O(8)#2-Cl(2)-O(6)	75.6(16)	Cl(2)#2-O(8)-O(6)#2	59.4(15)
Cl(2)#2-Cl(2)-O(6)	96.8(14)	Cl(2)-O(8)-O(6)#2	86.4(18)
O(5)-Cl(2)-O(6)	109.2(6)		

#1 ; x, -y-1/2, z. #2 ; -x+1, -y, -z+1.

3) $[Cu_2([22]\text{-HMTADO})(OH_2)_4]Br_2 \cdot 10H_2O$

An ORTEP view of $[Cu_2([22]\text{-HMTADO})(OH_2)_4]Br_2 \cdot 10H_2O$ is shown in Fig. 114, and bond distances and angles are summarized in Table 52 and 53. The crystal structure of this complex is composed of binuclear cation of the indicated formula and noninteracting bromide anions. These results are backed up by the molar conductivity (Λ_M = 160 $ohm^{-1}cm^2mol^{-1}$) which agreed with assignment of the structure as $[Cu_2([22]\text{-HMTADO})(OH_2)_4]Br_2 \cdot 10H_2O$. The binuclear cation, $[Cu_2([22]\text{-HMTADO})(OH_2)_4]^{2+}$ shows two octahedral environment, where the copper(II) ions are coordinated by the two oxygen atoms of water molecules of the copper basal planes (CuN_2O_2) in trans positions, respectively.

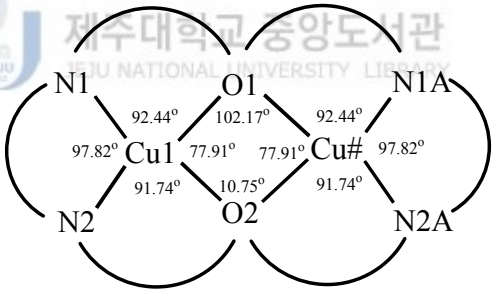

6

The macrocyclic complex adopts an essentially flat structure with the two octahedral copper centers bridged by the two phenoxide oxygen atoms, with quite large Cu-O-Cu angles (102.17(12)˚ and 101.75(12)˚) **(6)**. The sum of angles at the phenoxide oxygens is almost exactly 360˚(359.74˚), indicating no square oxygen distortion.

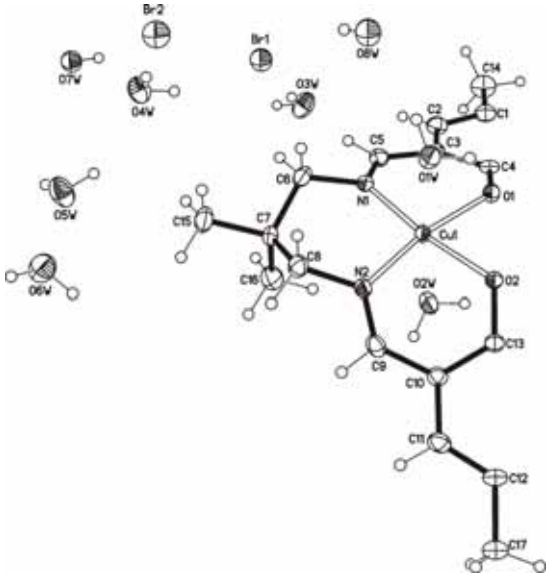

(a)

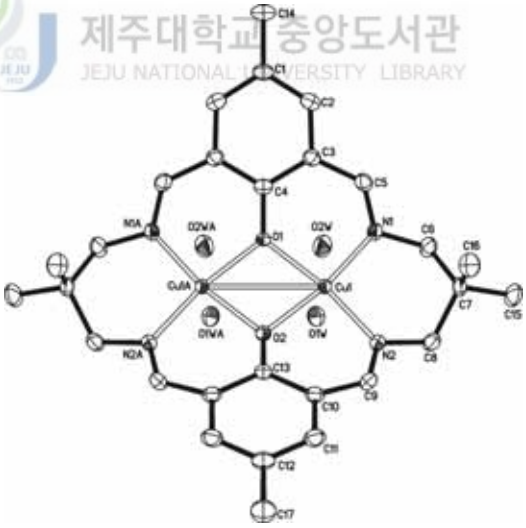

(b)

Fig. 114. Structural representation of (a) asymmetric unit and (b) core structure (top view) for the $[Cu_2([22]\text{-HMTADO})(OH_2)_4]Br_2 \cdot 10H_2O$ complex.

The sum of angles at the copper basal planes (CuN_2O_2) is almost exactly 360°(359.91°), indicating no plane distortion.

The copper centers are separated by 3.0463(8)Å and in plane copper-ligand distances fall in the range 1.944(2)-1.9635(17) Å. An angle of 21.95° exists between the benzene mean planes of macrocycle and the copper basal planes. This is bent owing to the chair conformation effect of the six-membered ring with trimethylene chain linking the azomethine nitrogen donors and copper. The two methyl groups (C(15) and C(15A)) attached to the trimetylenes are situated eclipsed conformation. Two water molecules occupy axial positions in a trans arrangement with somewhat longer contacts {Cu(1)-O(1W) ; 2.462(2) Å, Cu(1)-O(2W) ; 2.597(2) Å} ; this is elongated owing to the Jahn-Teller effect.

In general, hydrogen bonding plays a principal role in the packing of the title compound. There are four types of H-bonds ; between coordinated waters, coordinated water - lattice water, bromide ion - lattice water, and between lattice waters (Table 54). These interactions result in a formation of polymeric chains (Fig. 115). This chain forms a related layer structure, but within the layers binuclear cation $[Cu_2([22]\text{-HMTADO})(OH_2)_4]^{2+}$ ions arrange zig-zag configurations.

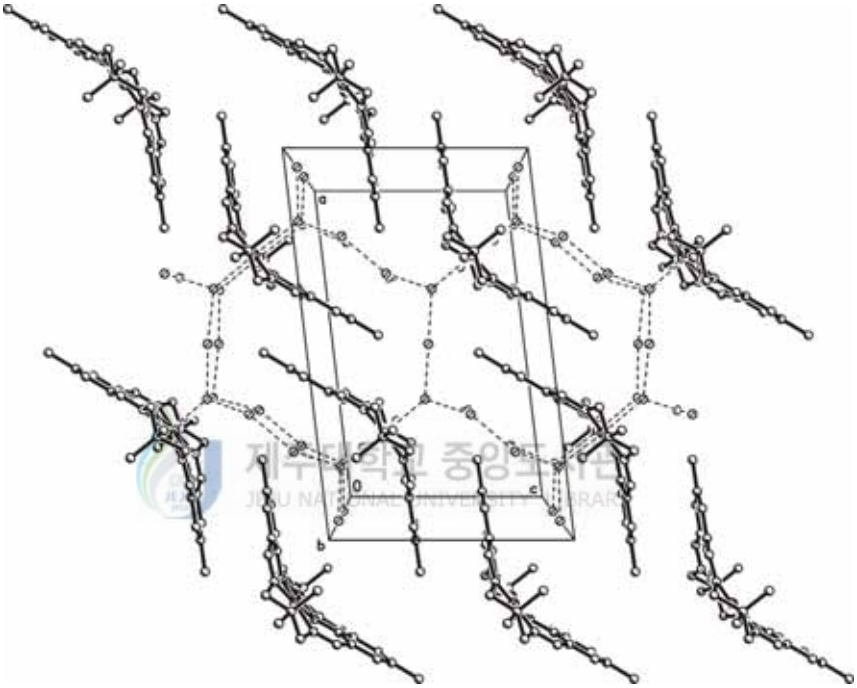

Fig. 115. The molecular packing diagram of $[Cu_2([22]\text{-HMTADO})(OH_2)_4]Br_2 \cdot 10H_2O$. The hydrogen bonds are indicated by dotted lines.

Table 52. Bond lengths (Å) for $[Cu_2([22]\text{-}HMTADO)(OH_2)_4]Br_2 \cdot 10H_2O$

Cu(1)-N(1)	1.944(2)	C(1)-C(14)	1.500(6)
Cu(1)-N(2)	1.950(2)	C(2)-C(3)	1.402(4)
Cu(1)-O(1)	1.9576(17)	C(3)-C(4)	1.413(3)
Cu(1)-O(2)	1.9635(17)	C(3)-C(5)	1.456(4)
Cu(1)-O(1W)	2.462(2)	C(4)-C(3)#1	1.413(3)
Cu(1)-O(2W)	2.597(2)	C(6)-C(7)	1.529(4)
Cu(1)-Cu(1)#1	3.0463(8)	C(7)-C(16)	1.520(4)
O(1)-C(4)	1.322(4)	C(7)-C(15)	1.529(5)
O(1)-Cu(1)#1	1.9576(17)	C(7)-C(8)	1.535(4)
O(2)-C(13)	1.339(5)	C(9)-C(10)	1.454(4)
O(2)-Cu(1)#1	1.9635(17)	C(10)-C(11)	1.408(4)
N(1)-C(5)	1.278(4)	C(10)-C(13)	1.411(4)
N(1)-C(6)	1.483(4)	C(11)-C(12)	1.375(4)
N(2)-C(9)	1.278(4)	C(12)-C(11)#1	1.375(4)
N(2)-C(8)	1.482(4)	C(12)-C(17)	1.515(6)
C(1)-C(2)#1	1.386(4)	C(13)-C(10)#1	1.411(4)
C(1)-C(2)	1.386(4)		

#1 ; x, -y, z

Table 53. Angles [°] for $[Cu_2([22]\text{-}HMTADO)(OH_2)_4]Br_2 \cdot 10H_2O$

N(1)-Cu(1)-N(2)	97.82(11)	C(8)-N(2)-Cu(1)	120.35(19)
N(1)-Cu(1)-O(1)	92.44(10)	C(2)#1-C(1)-C(2)	115.9(4)
N(2)-Cu(1)-O(1)	169.21(10)	C(2)#1-C(1)-C(14)	122.0(2)
N(1)-Cu(1)-O(2)	170.25(9)	C(2)-C(1)-C(14)	122.0(2)
N(2)-Cu(1)-O(2)	91.74(10)	C(1)-C(2)-C(3)	123.5(3)
O(1)-Cu(1)-O(2)	77.91(9)	C(2)-C(3)-C(4)	119.4(3)
N(1)-Cu(1)-O(1W)	91.32(9)	C(2)-C(3)-C(5)	116.3(3)

N(2)-Cu(1)-O(1W)	94.11(9)	C(4)-C(3)-C(5)	123.9(3)
O(1)-Cu(1)-O(1W)	88.99(10)	O(1)-C(4)-C(3)	120.89(18)
O(2)-Cu(1)-O(1W)	89.87(10)	O(1)-C(4)-C(3)#1	120.89(18)
N(1)-Cu(1)-O(2W)	90.84(9)	C(3)-C(4)-C(3)#1	118.2(4)
N(2)-Cu(1)-O(2W)	92.17(9)	N(1)-C(5)-C(3)	127.4(3)
O(1)-Cu(1)-O(2W)	84.28(10)	N(1)-C(6)-C(7)	114.9(3)
O(2)-Cu(1)-O(2W)	86.89(10)	C(16)-C(7)-C(15)	110.1(3)
O(1W)-Cu(1)-O(2W)	173.02(8)	C(16)-C(7)-C(6)	111.4(3)
N(1)-Cu(1)-Cu(1)#1	131.30(7)	C(15)-C(7)-C(6)	106.8(3)
N(2)-Cu(1)-Cu(1)#1	130.86(7)	C(16)-C(7)-C(8)	111.1(3)
O(1)-Cu(1)-Cu(1)#1	38.92(6)	C(15)-C(7)-C(8)	106.2(3)
O(2)-Cu(1)-Cu(1)#1	39.13(6)	C(6)-C(7)-C(8)	111.1(3)
O(1W)-Cu(1)-Cu(1)#1	86.80(6)	N(2)-C(8)-C(7)	113.9(2)
O(2W)-Cu(1)-Cu(1)#1	86.78(5)	N(2)-C(9)-C(10)	127.6(3)
C(4)-O(1)-Cu(1)	126.47(9)	C(11)-C(10)-C(13)	119.3(3)
C(4)-O(1)-Cu(1)#1	126.47(9)	C(11)-C(10)-C(9)	117.2(3)
Cu(1)-O(1)-Cu(1)#1	102.17(12)	C(13)-C(10)-C(9)	123.3(3)
C(13)-O(2)-Cu(1)#1	124.48(11)	C(12)-C(11)-C(10)	123.3(3)
C(13)-O(2)-Cu(1)	124.48(11)	C(11)#1-C(12)-C(11)	116.6(4)
Cu(1)#1-O(2)-Cu(1)	101.75(12)	C(11)#1-C(12)-C(17)	121.7(2)
C(5)-N(1)-C(6)	117.3(3)	C(11)-C(12)-C(17)	121.7(2)
C(5)-N(1)-Cu(1)	122.6(2)	O(2)-C(13)-C(10)	120.96(19)
C(6)-N(1)-Cu(1)	120.11(19)	O(2)-C(13)-C(10)#1	120.96(19)
C(9)-N(2)-C(8)	117.6(3)	C(10)-C(13)-C(10)#1	118.0(4)
C(9)-N(2)-Cu(1)	122.0(2)		

#1 ; x, -y, z

Table 54. Selected bond lengths (Å) and angles(°) for hydrogen bond of $[Cu_2([22]\text{-HMTADO})(OH_2)_4]Br_2 \cdot 10H_2O$

D-H···A	d(D-H)	d(H···A)	<DHA	d(D···A)
between coordinated waters				
O1W-H1WB···O1W [x, -y, z]	0.839	1.953	165.04	2.772
O2W-H2WB···O2W [x, -y, z]	0.835	1.932	168.62	2.755
coordinated water - lattice water				
O1W-H1WA···O8W	0.847	2.071	160.22	2.882
O2W-H2WA···O7W[-x+1/2, -y+1/2, -z+2]	0.840	2.025	163.33	2.840
O5W-H5WB···O2W [-x+1/2, -y+1/2, -z+2]	0.846	1.927	175.69	2.771
O6W-H6WA···O1W [-x+1/2, -y+1/2, -z+1]	0.847	1.895	174.95	2.740
lattice water - bromide ion				
O3W-H3WA···Br1	0.842	2.493	172.12	3.329
O3W-H3WB···Br2 [x, y, z+1]	0.850	2.503	163.30	3.326
O4W-H4WA···Br2	0.845	2.544	174.12	3.385
O4W-H4WB···Br1	0.845	2.568	157.29	3.363
between lattice waters				
O5W-H5WA···O4W	0.843	2.161	148.09	2.911
O6W-H6WB···O3W [-x+1/2, -y+1/2, -z+2]	0.848	2.058	153.86	2.844
O7W-H7WA···O4W [-x, y, -z+2]	0.844	2.040	167.21	2.869
O8W-H8WA···O3W [-x, y, -z+2]	0.849	1.995	167.84	2.831

4) $[Ni_2([22]\text{-}HMTADO)(OH_2)_4](ClO_4)_2 \cdot 3H_2O$.

An ORTEP view of $[Ni_2([22]\text{-}HMTADO)(OH_2)_4](ClO_4)_2 \cdot 3H_2O$ is shown in Fig. 116, and bond distances and angles are summarized in Table 55 and 56. The crystal structure of this complex is composed of binuclear cation of the indicated formula and noninteracting chloride anions. These results are backed up by the molar conductivity (Λ_M = 170 $ohm^{-1}cm^2mol^{-1}$) which agreed with assignment of the structure as $[Ni_2([22]\text{-}HMTADO)(OH_2)_4](ClO_4)_2 \cdot 3H_2O$. The di-nuclear cation, $[Ni_2([22]\text{-}HMTADO)(OH_2)_4]^{2+}$ shows two octahedral environment, where the nickel(II) ions are coordinated by the two oxygen atoms of water molecules of the nickel basal planes (NiN_2O_2) in trans positions, respectively.

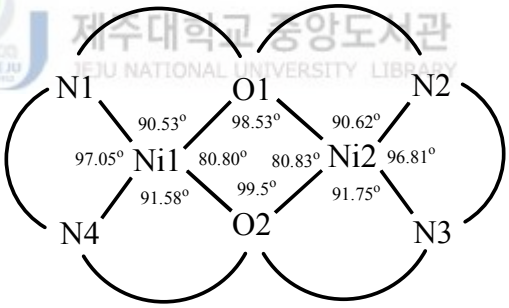

7

The macrocyclic complex adopts an essentially flat structure with the two octahedral nickel centers bridged by the two phenoxide oxygen atoms, with quite large Ni-O-Ni angles (98.53(6)° and 99.50(6)°) **(7)**. The sum of angles at the phenoxide oxygens is almost exactly 360°(359.66°), indicating no square oxygen distortion.

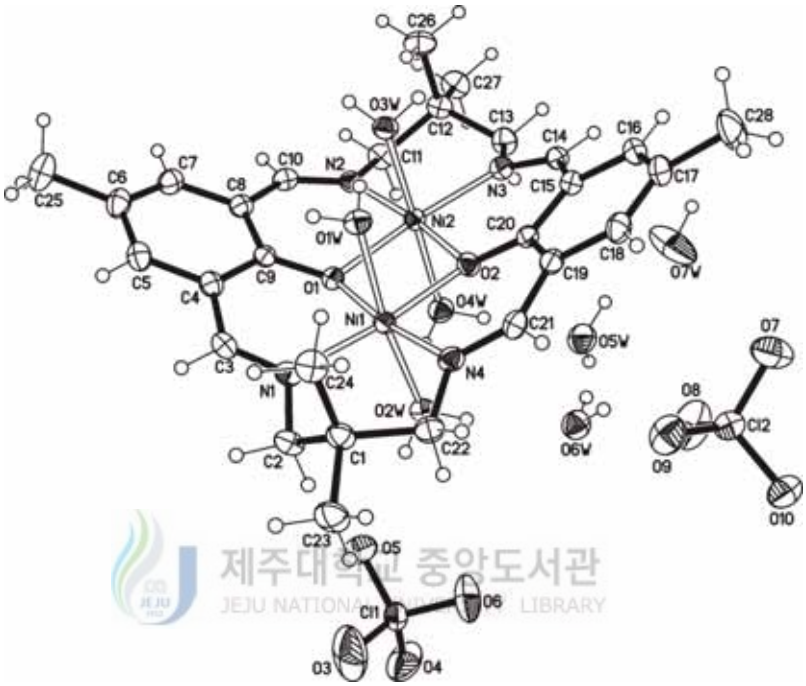

Fig. 116. Structural representation of for the $[Ni_2([22]\text{-HMTADO})(OH_2)_4](ClO_4)_2 \cdot 3H_2O$ complex.

The sum of angles at the nickel basal planes (NiN_2O_2) is almost exactly 360° (359.96° and 359.80°), indicating no plane distortion.

The nickel centers are separated by 3.0768(4) Å and in plane nickel-ligand distances fall in the range 1.9944(17)-2.0328(14) Å. An angle of 21.07° exists between the benzene mean planes of macrocycle and the nickel basal planes. This is bent owing to the chair conformation effect of the six-membered ring with trimethylene chain linking the azomethine nitrogen donors and nickel.

The two methyl groups (C(24) and C(26)) attached to the trimetylenes are situated eclipsed conformation. Four water molecules occupy axial positions in a trans arrangement with somewhat longer contacts {Ni(1)-O(1W) ; 2.1271(14) Å, Ni(1)-O(2W) ; 2.1634(14) Å, Ni(2)-O(3W) ; 2.2253(14) Å, Ni(2)-O(4W) ; 2.1209(14) Å}. The angles O_{axial}-Ni-O_{axial} {O(1W)-Ni(1)-O(2W) ; 171.81(6), O(3W)-Ni(2)-O(4W) ; 172.61(6)} are smaller than the ideal value of 180° by hydrogen bonding between coordinated water, indicating that the donor atoms are not able to achieve the axial positions of a perfect octahedron.

In general, hydrogen bonding plays a principal role in the packing of the title compound. There are five types of H-bonds ; between coordinated waters, coordinated water - lattice water, coordinated water - perchlorate ion, lattice water - perchlorate ion, and between lattice waters (Table 57). These interactions result in a formation of polymeric chains (Fig. 117). This chain forms a related layer structure, but within the layers binuclear cation $[NI_2([22]\text{-HMTADO})(OH_2)_4]^{2+}$ ions arrange zig-zag configurations.

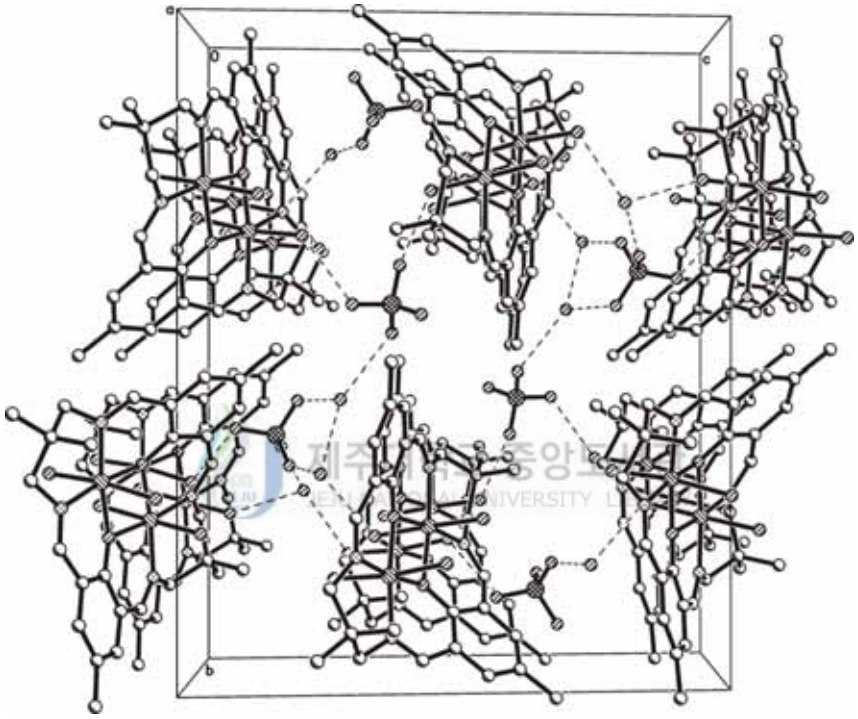

Fig. 117. The molecular packing diagram of [[Ni_2([22]-HMTADO)$(OH_2)_4$]$(ClO_4)_2$ · $3H_2O$. The hydrogen bonds are indicated by dotted lines.

Table 55. Bond lengths (Å) for $[Ni_2([22]\text{-}HMTADO)(OH_2)_4](ClO_4)_2 \cdot 3H_2O$

Ni(1)-N(1)	2.0053(17)	O(2)-C(20)	1.317(2)
Ni(1)-N(4)	2.0066(17)	N(1)-C(3)	1.279(3)
Ni(1)-O(2)	2.0101(14)	N(1)-C(2)	1.469(3)
Ni(1)-O(1)	2.0328(14)	N(2)-C(10)	1.284(3)
Ni(1)-O(1W)	2.1271(14)	N(2)-C(11)	1.468(3)
Ni(1)-O(2W)	2.1634(14)	N(3)-C(14)	1.280(3)
Ni(1)-Ni(2)	3.0768(4)	N(3)-C(13)	1.481(3)
Ni(2)-N(2)	1.9944(17)	N(4)-C(21)	1.281(3)
Ni(2)-N(3)	2.0063(17)	N(4)-C(22)	1.474(3)
Ni(2)-O(2)	2.0138(14)	C(1)-C(24)	1.528(3)
Ni(2)-O(1)	2.0277(14)	C(1)-C(23)	1.533(3)
Ni(2)-O(4W)	2.1209(14)	C(1)-C(2)	1.539(3)
Ni(2)-O(3W)	2.2253(14)	C(1)-C(22)	1.540(3)
Cl(1)-O(4)	1.4079(18)	C(2)-H(2A)	0.97
Cl(1)-O(3)	1.424(2)	C(2)-H(2B)	0.97
Cl(1)-O(6)	1.4340(18)	C(3)-C(4)	1.459(3)
Cl(1)-O(5)	1.4369(18)	C(3)-H(3A)	0.93
Cl(2)-O(8)	1.4269(18)	C(4)-C(5)	1.395(3)
Cl(2)-O(7)	1.4308(19)	C(4)-C(9)	1.426(3)
Cl(2)-O(10)	1.4368(16)	C(5)-C(6)	1.386(3)
Cl(2)-O(9)	1.4469(17)	C(5)-H(5A)	0.93
O(1W)-H(1WA)	0.834(7)	C(6)-C(7)	1.385(3)
O(1W)-H(1WB)	0.838(7)	C(6)-C(25)	1.509(3)
O(2W)-H(2WA)	0.836(7)	C(7)-C(8)	1.400(3)
O(2W)-H(2WB)	0.839(7)	C(7)-H(7A)	0.93
O(3W)-H(3WA)	0.839(7)	C(8)-C(9)	1.420(3)
O(3W)-H(3WB)	0.841(10)	C(8)-C(10)	1.468(3)
O(4W)-H(4WA)	0.836(7)	C(10)-H(10A)	0.93
O(4W)-H(4WB)	0.834(7)	C(11)-C(12)	1.540(3)
O(1)-C(9)	1.321(2)	C(11)-H(11A)	0.97

Table 56. Angles [°] for $[Ni_2([22]\text{-}HMTADO)(OH_2)_4](ClO_4)_2 \cdot 3H_2O$

N(1)-Ni(1)-N(4)	97.05(7)	O(1)-Ni(2)-O(4W)	86.19(6)
N(1)-Ni(1)-O(2)	171.19(6)	N(2)-Ni(2)-O(3W)	90.64(6)
N(4)-Ni(1)-O(2)	91.58(6)	N(3)-Ni(2)-O(3W)	90.85(6)
N(1)-Ni(1)-O(1)	90.53(6)	O(2)-Ni(2)-O(3W)	86.67(6)
N(4)-Ni(1)-O(1)	172.23(6)	O(1)-Ni(2)-O(3W)	89.11(5)
O(2)-Ni(1)-O(1)	80.80(6)	O(4W)-Ni(2)-O(3W)	172.61(6)
N(1)-Ni(1)-O(1W)	91.97(6)	N(2)-Ni(2)-Ni(1)	131.23(5)
N(4)-Ni(1)-O(1W)	89.30(6)	N(3)-Ni(2)-Ni(1)	131.80(5)
O(2)-Ni(1)-O(1W)	86.38(6)	O(2)-Ni(2)-Ni(1)	40.08(4)
O(1)-Ni(1)-O(1W)	88.71(5)	O(1)-Ni(2)-Ni(1)	40.80(4)
N(1)-Ni(1)-O(2W)	96.06(6)	O(4W)-Ni(2)-Ni(1)	87.03(4)
N(4)-Ni(1)-O(2W)	91.31(6)	O(3W)-Ni(2)-Ni(1)	85.68(4)
O(2)-Ni(1)-O(2W)	85.44(6)	O(4)-Cl(1)-O(3)	110.25(16)
O(1)-Ni(1)-O(2W)	89.59(6)	O(4)-Cl(1)-O(6)	110.21(12)
O(1W)-Ni(1)-O(2W)	171.81(6)	O(3)-Cl(1)-O(6)	109.60(14)
N(1)-Ni(1)-Ni(2)	131.09(5)	O(4)-Cl(1)-O(5)	108.79(13)
N(4)-Ni(1)-Ni(2)	131.63(5)	O(3)-Cl(1)-O(5)	108.72(14)
O(2)-Ni(1)-Ni(2)	40.17(4)	O(6)-Cl(1)-O(5)	109.24(12)
O(1)-Ni(1)-Ni(2)	40.67(4)	O(8)-Cl(2)-O(7)	110.47(14)
O(1W)-Ni(1)-Ni(2)	85.23(4)	O(8)-Cl(2)-O(10)	109.39(11)
O(2W)-Ni(1)-Ni(2)	88.26(4)	O(7)-Cl(2)-O(10)	109.78(11)
N(2)-Ni(2)-N(3)	96.81(7)	O(8)-Cl(2)-O(9)	108.64(12)
N(2)-Ni(2)-O(2)	171.07(6)	O(7)-Cl(2)-O(9)	109.42(11)
N(3)-Ni(2)-O(2)	91.75(6)	O(10)-Cl(2)-O(9)	109.11(11)
N(2)-Ni(2)-O(1)	90.62(6)	Ni(1)-O(1W)-H(1WA)	108.4(17)
N(3)-Ni(2)-O(1)	172.57(6)	Ni(1)-O(1W)-H(1WB)	119.3(17)
O(2)-Ni(2)-O(1)	80.83(6)	H(1WA)-O(1W)-H(1WB)	101(2)
N(2)-Ni(2)-O(4W)	95.10(6)	Ni(1)-O(2W)-H(2WA)	123.1(17)
N(3)-Ni(2)-O(4W)	93.08(6)	Ni(1)-O(2W)-H(2WB)	108.5(18)
O(2)-Ni(2)-O(4W)	86.95(6)	H(2WA)-O(2W)-H(2WB)	100(2)

Ni(2)-O(3W)-H(3WA)	120.3(18)	N(1)-C(2)-C(1)	114.10(16)
Ni(2)-O(3W)-H(3WB)	118.9(17)	N(1)-C(2)-H(2A)	108.7
H(3WA)-O(3W)-H(3WB)	104(2)	C(1)-C(2)-H(2A)	108.7
Ni(2)-O(4W)-H(4WA)	113.2(18)	N(1)-C(2)-H(2B)	108.7
Ni(2)-O(4W)-H(4WB)	103.7(18)	C(1)-C(2)-H(2B)	108.7
H(4WA)-O(4W)-H(4WB)	104(3)	H(2A)-C(2)-H(2B)	107.6
C(9)-O(1)-Ni(2)	123.66(12)	N(1)-C(3)-C(4)	127.52(18)
C(9)-O(1)-Ni(1)	123.00(12)	N(1)-C(3)-H(3A)	116.2
Ni(2)-O(1)-Ni(1)	98.53(6)	C(4)-C(3)-H(3A)	116.2
C(20)-O(2)-Ni(1)	126.82(12)	C(5)-C(4)-C(9)	119.80(18)
C(20)-O(2)-Ni(2)	126.03(12)	C(5)-C(4)-C(3)	115.91(18)
Ni(1)-O(2)-Ni(2)	99.75(6)	C(9)-C(4)-C(3)	124.24(17)
C(3)-N(1)-C(2)	117.88(17)	C(6)-C(5)-C(4)	123.1(2)
C(3)-N(1)-Ni(1)	121.38(14)	C(6)-C(5)-H(5A)	118.4
C(2)-N(1)-Ni(1)	120.40(13)	C(4)-C(5)-H(5A)	118.4
C(10)-N(2)-C(11)	117.33(17)	C(7)-C(6)-C(5)	116.84(18)
C(10)-N(2)-Ni(2)	122.55(14)	C(7)-C(6)-C(25)	121.7(2)
C(11)-N(2)-Ni(2)	120.12(13)	C(5)-C(6)-C(25)	121.5(2)
C(14)-N(3)-C(13)	116.46(17)	C(6)-C(7)-C(8)	122.77(19)
C(14)-N(3)-Ni(2)	122.59(14)	C(6)-C(7)-H(7A)	118.6
C(13)-N(3)-Ni(2)	120.94(13)	C(8)-C(7)-H(7A)	118.6
C(21)-N(4)-C(22)	117.13(18)	C(7)-C(8)-C(9)	120.04(18)
C(21)-N(4)-Ni(1)	122.27(14)	C(7)-C(8)-C(10)	115.91(18)
C(22)-N(4)-Ni(1)	120.59(13)	C(9)-C(8)-C(10)	124.03(17)
C(24)-C(1)-C(23)	109.71(18)	O(1)-C(9)-C(8)	121.23(17)
C(24)-C(1)-C(2)	110.20(17)	O(1)-C(9)-C(4)	121.56(17)
C(23)-C(1)-C(2)	106.43(17)	C(8)-C(9)-C(4)	117.20(17)
C(24)-C(1)-C(22)	112.02(17)	N(2)-C(10)-C(8)	127.10(18)
C(23)-C(1)-C(22)	105.31(17)	N(2)-C(10)-H(10A)	116.4
C(2)-C(1)-C(22)	112.88(17)	C(8)-C(10)-H(10A)	116.4

Table 57. Selected bond lengths (Å) and angles(°) for hydrogen bond of $[Ni_2([22]\text{-}HMTADO)(OH_2)_4]ClO_4 \cdot 3H_2O$

D-H···A	d(D-H)	d(H···A)	<DHA	d(D···A)
between coordinated waters				
O1W-H1WA···O3W	0.834	1.930	161.54	2.734
O4W-H4WB···O2W	0.834	2.145	151.39	2.905
coordinated water - lattice water				
O2W-H2WB···O6W	0.839	2.006	164.78	2.824
O3W-H3WA···O6W [x, -y+3/2, z+1/2]	0.839	1.970	167.72	2.795
O4W-H4WA···O5W	0.836	1.932	174.62	2.765
coordinated water - ClO_4^-				
O1W-H1WB···O10 [x, -y+3/2, z+1/2]	0.838	2.060	170.58	2.889
O2W-H2WA···O5	0.836	1.976	175.03	2.810
O3W-H3WB···O6 [x, -y+3/2, z+1/2]	0.841	1.953	166.36	2.777
lattice water - ClO_4^-				
O5W-H5WA···O9 [x-1, y, z]	0.838	2.043	157.32	2.834
O6W-H6WB···O8	0.791	2.151	151.69	2.872
O7W-H7WA···O3 [-x, y+1/2, -z+3/2]	0.838	1.981	173.29	2.815
O7W-H7WB···O7 [x-1, y, z]	0.834	2.115	161.23	2.918
between lattice waters				
O5W-H5WB···O7W	0.840	1.903	154.40	2.685
O6W-H6WA···O5W	0.852	1.965	165.13	2.797

5) $[Ni_2([22]\text{-}HMTADO)(OH_2)_4]Br_2 \cdot 10H_2O$.

An ORTEP view of $[Ni_2([22]\text{-}HMTADO)(OH_2)_4]Br_2 \cdot 10H_2O$ is shown in Fig. 118, and bond distances and angles are summarized in Table 58 and 59. The crystal structure of this complex is composed of binuclear cation of the indicated formula and noninteracting chloride anions. These results are backed up by the molar conductivity (Λ_M = 142 $ohm^{-1}cm^2mol^{-1}$) which agreed with assignment of the structure as $[Ni_2([22]\text{-}HMTADO)(OH_2)_4]Br_2 \cdot 10H_2O$. The binuclear cation, $[Ni_2([22]\text{-}HMTADO)(OH_2)_4]^{2+}$ shows two octahedral environment, where the nickel(II) ions are coordinated by the two oxygen atoms of water molecules of the nickel basal planes (NiN_2O_2) in trans positions, respectively.

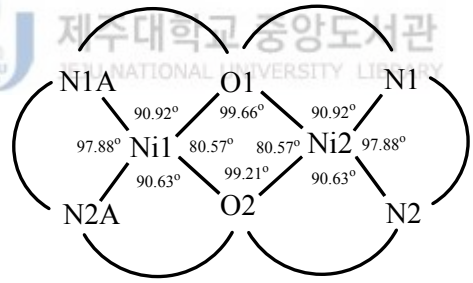

8

The macrocyclic complex adopts an essentially flat structure with the two octahedral nickel centers bridged by the two phenoxide oxygen atoms, with quite large Ni-O-Ni angles (99.66(16)˚ and 99.21(16)˚) **(8)**. The sum of angles at the phenoxide oxygens is almost exactly 360˚(360.01˚), indicating no square oxygen distortion.

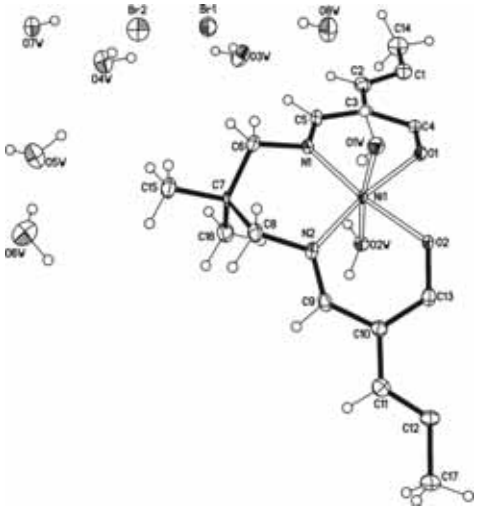

(a)

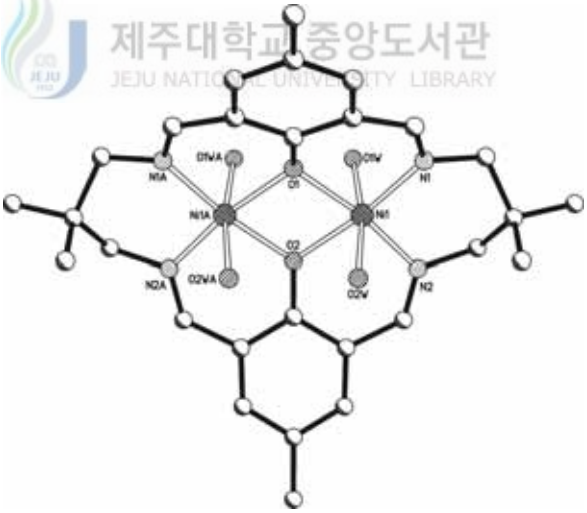

(b)

Fig. 118. Structural representation of (a) asymmetric unit and (b) core structure (top view) for the $[Ni_2([22]\text{-HMTADO})(OH_2)_4]Br_2 \cdot 10H_2O$ complex.

The sum of angles at the nickel basal planes (NiN_2O_2) is exactly 360°, indicating no plane distortion.

The nickel centers are separated by 3.060 Å and in plane nickel-ligand distances fall in the range 1.987(3)-2.009(2) Å. An angle of 23.19° exists between the benzene mean planes of macrocycle and the nickel basal planes. This is bent owing to the chair conformation effect of the six-membered ring with trimethylene chain linking the azomethine nitrogen donors and nickel.

The two methyl groups (C(24) and C(26)) attached to the trimetylenes are situated eclipsed conformation. Four water molecules occupy axial positions in a trans arrangement with somewhat longer contacts {Ni(1)-O(1W) ; 2.159(3) Å, Ni(1)-O(2W) ; 2.225(3) Å}. The angles O_{axial}-Ni-O_{axial} {O(1W)-Ni(1)-O(2W) ; 172.14(10)} are smaller than the ideal value of 180°, indicating that the donor atoms are not able to achieve the axial positions of a perfect octahedron.

In general, hydrogen bonding plays a principal role in the packing of the title compound. There are three types of H-bonds ; coordinated water - lattice water, coordinated water - bromide ion, and between lattice waters (Table 60). These interactions result in a formation of polymeric chains (Fig. 119). This chain forms a related layer structure, but within the layers binuclear cation $[NI_2([22]\text{-HMTADO})(OH_2)_4]^{2+}$ ions arrange zig-zag configurations.

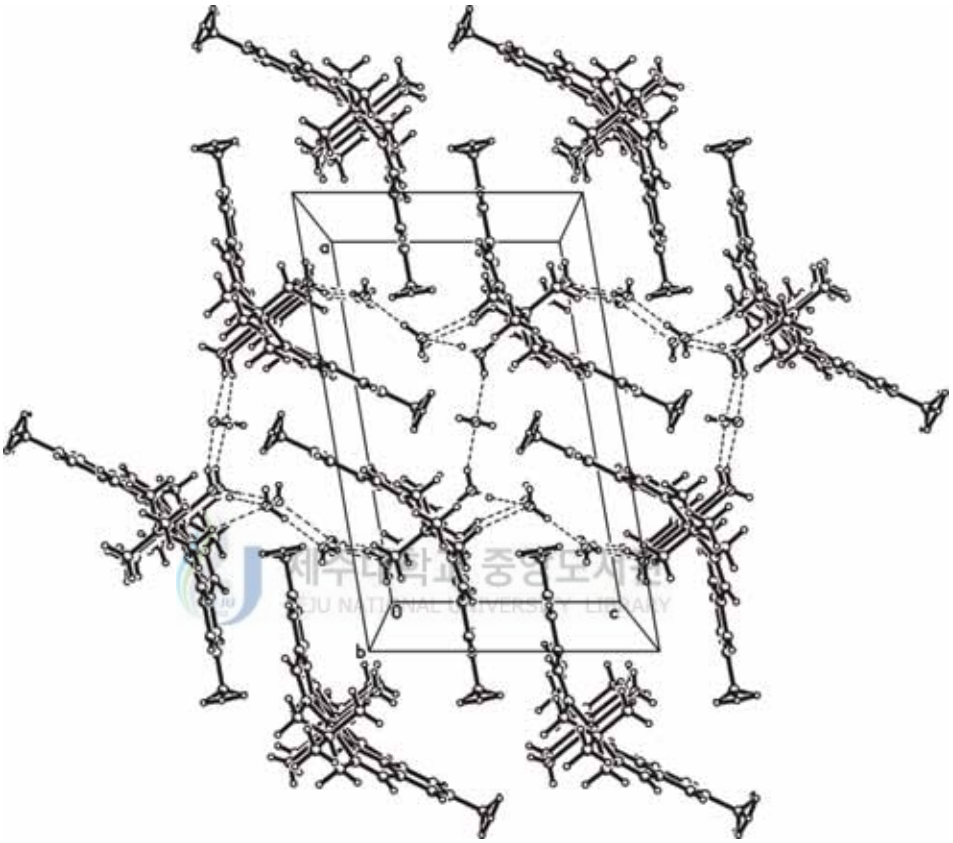

Fig. 119. The molecular packing diagram of [[Ni_2([22]-HMTADO)(OH_2)$_4$](ClO_4)$_2$ · 3H_2O. The hydrogen bonds are indicated by dotted lines.

Table 58. Bond lengths (Å) for $[Ni_2([22]\text{-}HMTADO)(OH_2)_4]Br_2 \cdot 10H_2O$

Ni(1)-N(1)	1.987(3)	C(1)-C(14)	1.489(8)
Ni(1)-N(2)	1.989(3)	C(2)-C(3)	1.397(6)
Ni(1)-O(1)	2.002(2)	C(3)-C(4)	1.424(5)
Ni(1)-O(2)	2.009(2)	C(3)-C(5)	1.470(5)
Ni(1)-O(1W)	2.159(3)	C(4)-C(3)#1	1.424(5)
Ni(1)-O(2W)	2.225(3)	C(6)-C(7)	1.535(5)
O(1)-C(4)	1.308(7)	C(7)-C(16)	1.520(6)
O(1)-Ni(1)#1	2.002(2)	C(7)-C(15)	1.523(5)
O(2)-C(13)	1.308(7)	C(7)-C(8)	1.543(6)
O(2)-Ni(1)#1	2.009(2)	C(9)-C(10)	1.475(5)
N(1)-C(5)	1.274(5)	C(10)-C(11)	1.398(6)
N(1)-C(6)	1.488(5)	C(10)-C(13)	1.423(5)
N(2)-C(9)	1.273(5)	C(11)-C(12)	1.385(5)
N(2)-C(8)	1.482(5)	C(12)-C(11)#1	1.385(5)
C(1)-C(2)#1	1.393(5)	C(12)-C(17)	1.517(8)
C(1)-C(2)	1.393(5)	C(13)-C(10)#1	1.423(5)

#1 ; x, -y, z.

Table 59. Bond angles (°) for $[Ni_2([22]\text{-}HMTADO)(OH_2)_4]Br_2 \cdot 10H_2O$

N(1)-Ni(1)-N(2)	97.88(13)	C(2)-C(1)-C(14)	122.1(3)
N(1)-Ni(1)-O(1)	90.92(12)	C(1)-C(2)-C(3)	123.7(4)
N(2)-Ni(1)-O(1)	171.07(12)	C(2)-C(3)-C(4)	119.5(4)
N(1)-Ni(1)-O(2)	171.49(12)	C(2)-C(3)-C(5)	116.6(3)
N(2)-Ni(1)-O(2)	90.63(12)	C(4)-C(3)-C(5)	123.8(4)
O(1)-Ni(1)-O(2)	80.57(11)	O(1)-C(4)-C(3)	121.1(3)
N(1)-Ni(1)-O(1W)	92.73(12)	O(1)-C(4)-C(3)#1	121.1(3)
N(2)-Ni(1)-O(1W)	93.61(12)	C(3)-C(4)-C(3)#1	117.8(5)
O(1)-Ni(1)-O(1W)	87.44(14)	N(1)-C(5)-C(3)	127.4(3)
O(2)-Ni(1)-O(1W)	86.83(13)	N(1)-C(6)-C(7)	115.1(3)
N(1)-Ni(1)-O(2W)	91.74(12)	C(16)-C(7)-C(15)	109.7(3)
N(2)-Ni(1)-O(2W)	92.18(12)	C(16)-C(7)-C(6)	110.8(3)
O(1)-Ni(1)-O(2W)	86.02(14)	C(15)-C(7)-C(6)	106.9(3)
O(2)-Ni(1)-O(2W)	87.79(13)	C(16)-C(7)-C(8)	110.6(3)
O(1W)-Ni(1)-O(2W)	172.14(10)	C(15)-C(7)-C(8)	106.4(3)
C(4)-O(1)-Ni(1)#1	126.36(14)	C(6)-C(7)-C(8)	112.3(3)
C(4)-O(1)-Ni(1)	126.36(14)	N(2)-C(8)-C(7)	114.3(3)
Ni(1)#1-O(1)-Ni(1)	99.66(16)	N(2)-C(9)-C(10)	127.2(3)
C(13)-O(2)-Ni(1)#1	124.75(16)	C(11)-C(10)-C(13)	120.0(4)
C(13)-O(2)-Ni(1)	124.75(16)	C(11)-C(10)-C(9)	116.6(3)
Ni(1)#1-O(2)-Ni(1)	99.21(16)	C(13)-C(10)-C(9)	123.1(4)
C(5)-N(1)-C(6)	117.5(3)	C(12)-C(11)-C(10)	123.2(4)
C(5)-N(1)-Ni(1)	122.9(3)	C(11)#1-C(12)-C(11)	116.4(5)
C(6)-N(1)-Ni(1)	119.6(2)	C(11)#1-C(12)-C(17)	121.8(3)
C(9)-N(2)-C(8)	117.3(3)	C(11)-C(12)-C(17)	121.8(3)
C(9)-N(2)-Ni(1)	122.6(3)	O(2)-C(13)-C(10)	121.5(3)
C(8)-N(2)-Ni(1)	120.1(3)	O(2)-C(13)-C(10)#1	121.5(3)
C(2)#1-C(1)-C(2)	115.8(5)	C(10)-C(13)-C(10)#1	116.9(5)
C(2)#1-C(1)-C(14)	122.1(3)		

#1 ; x, -y, z.

Table 60. Selected bond lengths (Å) and angles(°) for hydrogen bond of $[Ni_2([22]\text{-}HMTADO)(OH_2)_4]Br_2 \cdot 10H_2O$

D-H···A	d(D-H)	d(H···A)	<DHA	d(D···A)
coordinated water - lattice water				
O1W-H1WA···O6W [-x+1/2, -y+1/2, -z+1]	0.849	1.929	168.24	2.765
O1W-H1WB···O8W	0.847	2.123	158.63	2.929
O2W-H2WA···O5W [-x+1/2, -y+1/2, -z+2]	0.845	2.076	153.08	2.856
O2W-H2WB···O7W [-x+1/2, -y+1/2, -z+2]	0.848	2.049	165.71	2.878
O5W-H5WB···O2W [-x+1/2, -y+1/2, -z+2]	0.845	2.086	151.28	2.856
lattice water - lattice Br^-				
O3W-H3WA···Br2 [x, y, z+1]	0.848	2.488	168.98	3.325
O3W-H3WB···Br1	0.848	2.486	177.02	3.333
O4W-H4WA···Br1	0.848	2.551	168.71	3.387
O4W-H4WB···Br2	0.848	2.547	176.08	3.393
between lattice waters				
O5W-H5WA···O4W	0.848	2.103	156.37	2.900
O6W-H6WA···O3W [-x+1/2, -y+1/2, -z+2]	0.848	2.010	168.23	2.845
O6W-H6WB···O5W	0.848	1.895	169.64	2.734
O7W-H7WA···O4W [-x, y, -z+2]	0.847	2.072	167.98	2.906
O8W-H8WA···O3W [-x, y, -z+2]	0.847	2.013	168.61	2.849

6) [Ni_2([22]-HMTADO)$(N_3)_2(OH_2)$].

An ORTEP view of [Ni_2([22]-HMTADO)$(N_3)_2(OH_2)$] is shown in Fig. 120, and bond distances and angles are summarized in Table 61 and 62. The dinegative ([22]-HMTADO)$^{2-}$ accommodates two Ni(II) ions in its N_4O_2 sites in the Ni(1)···Ni(2) separation of 3.115(3) Å. The geometry about Ni(1) in the N_2O_2 site is a octahedral with a nitrogen atom of azido and a oxygen atom of aqua in trans positions. And the geometry about Ni(2) in the N_2O_2 site is a square-pyramid with a nitrogen atom of azido at the axial site. The two azido groups coordinated to the nickel centers are situated trans to each other with respect to the mean {NiN_2O_2} plane. These results are backed up by the molar conductivity (Λ_M = 13 ohm^{-1}cm^{2}mol^{-1}) which agreed with assignment of the structure as [Ni_2([22]-HMTADO)$(N_3)_2(OH_2)$].

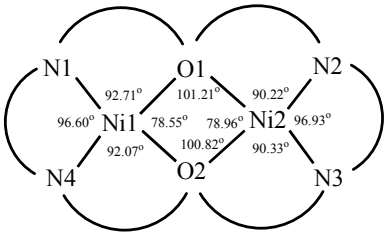

9

The macrocyclic complex adopts a non-flat structure with the an octahedral and a square-pyramidal nickel centers bridged by the two phenoxide oxygen atoms, with quite large Ni-O-Ni angles (101.21(11)˚ and 100.82(11)˚) **(9)**. The sum of angles at the phenoxide oxygens is almost 360˚ (359.54˚), indicating no square oxygen distortion.

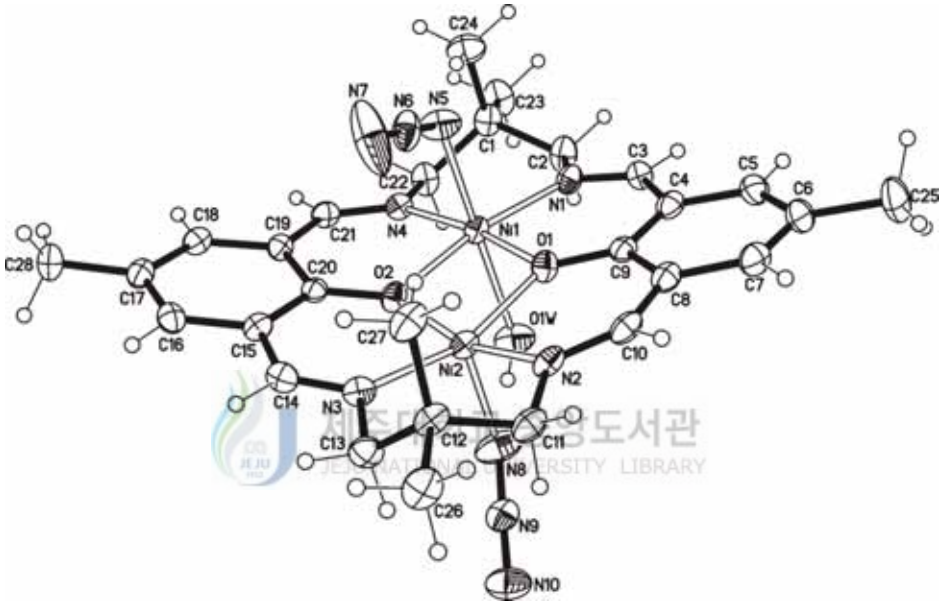

Fig. 120. Structural representation of core structure (top view) for the $[Ni_2([22]\text{-HMTADO})(N_3)_2(OH_2)]$ complex.

The sum of angles at the octahedral Ni(1) basal planes (NiN_2O_2) is exactly 360° (359.93°), indicating no plane distortion. The Ni(1)-N (imines) bond distances are in the range of 2.012(3) and 2.013(3) Å, and Ni(1)-O (phenolic) are 2.021(3) and 2.025(3) Å. The Ni(1)-N(5) (azido) and Ni(1)-O(1W) (aqua) bond distances are in the range of 2.145(3) and 2.161(3)Å, respectively. The bond angles of N(1)-Ni(1)-O(2), N(4)-Ni(1)-O(1) and N(5)-Ni(1)-O(1W) are 169.86(12)°, 170.62(12)° and 171.76(12)°, respectively. In this complex Ni(1)-N (imines) and Ni(1)-O (phenolic) distances are shorter than Ni(1)-N(5) (azido) and Ni(1)-O(1W) (aqua) distances and the angle of N(1)-Ni(1)-O(2), N(4)-Ni(1)-O(1) and N(5)-Ni(1)-O(1W) are smaller than the ideal value of 180°, indicating that the donor atoms are not able to achieve the axial positions of a perfect octahedron. The N_3 ligand keep their linearity, N-N-N bond angle is 179.1(5)°, whereas the Ni(1)-N(5)-N(6) linkage is slightly bent {120.4(3)°} towards Ni(2) {Ni(2)···N(7) 3.619 Å}. The Ni(1)-N(5)-N(6) basal least-trigonal plane are bent at basal least-trigonal plane for N(5)-Ni(1)-Ni(2) edge with a dihedral angle of 17.87° towards O(2)-phenolic group.

The sum of angles (356.44°) at the square-pyramidal Ni(2) basal planes (NiN_2O_2) is smaller than the ideal value of 360°, indicating plane distortion. The Ni(2)-N (imines) bond distances are in the range of 1.996(3) and 2.019(3) Å, and Ni(2)-O (phenolic) are 2.010(3) Å and 2.018(3) Å. The Ni(2)-N(8) (azido) bond distance {2.016(3) Å} is shorter 0.129(3) Å than octahedral Ni(1)-N(5) (azido) bond distance {2.145(3) Å}. The bond angles N(3)-Ni(2)-O(1) and N(2)-Ni(2)-O(2) are 161.58(12)° and 164.34(12)°, respectively ; indicating $Ni(2)N_2O_4$ are not able to the perfect square planer. Result, the Ni(2) is displaced by 0.320 Å from the basal N_2O_2 least-squares

plane towards N(8) (azido). The N_3 ligand keep their linearity, N-N-N bond angle is 177.8(4)°, whereas the Ni(2)-N(8)-N(9) linkage is slightly bent {121.3(3)°} towards the opposite Ni(1) by the repulsion of coordinated aqua of Ni(1). The N_3 ligand adopts the most stereochemically favorable orientation with respect to the macrocycle.

This complex is wholly asymmetric. The O(2)-phenolic groups of macrocycle is bent 18.6° with the basal Ni_2O_2 least-squares plane, whereas O(1)-phenolic groups of macrocycle is flat with the basal Ni_2O_2 least-squares plane. Hydrogen bonds are between water and azide molecules of octahedral of neighbor complexes (Fig. 121 and Table 63). And there are a weak π-π interactions by aromatic ring of neighbor complexes (Fig. 121 (a)) ; a dihedral angle and a distance between aromatic rings are 9.4(2)° and 4.1 Å, respectively.

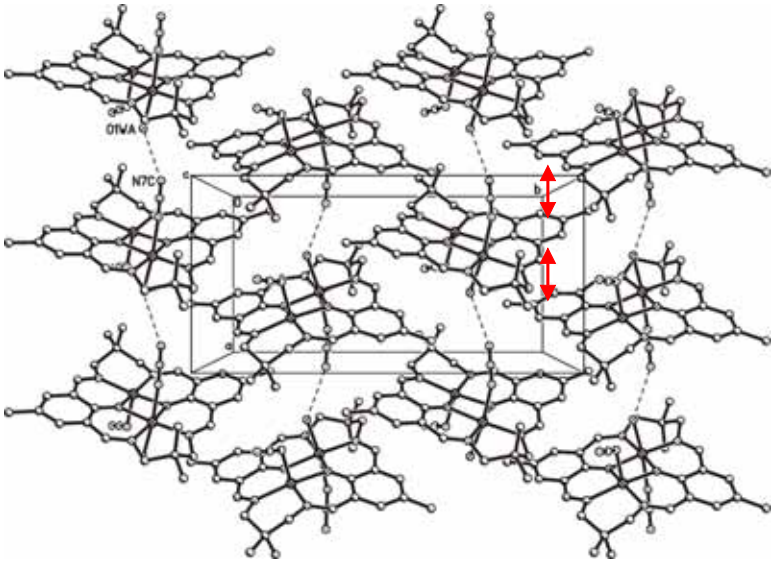

(a)

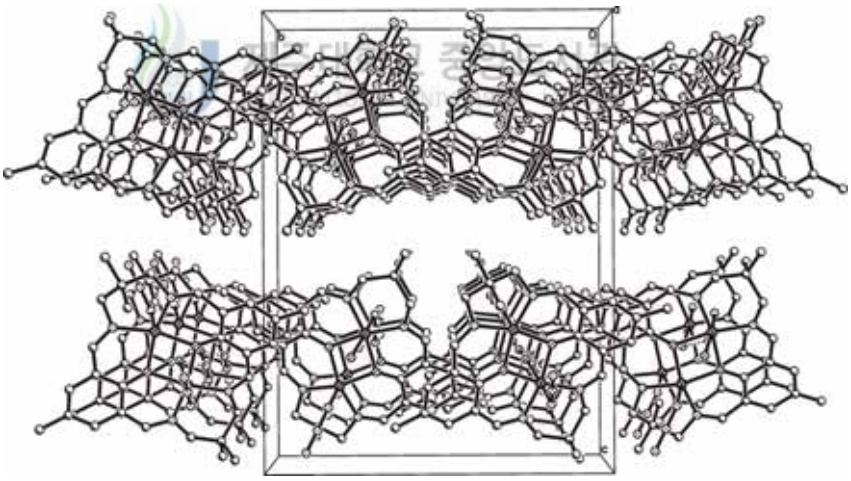

(b)

Fig. 20. The molecular packing diagram of [Ni_2([22]-HMTADO)$(N_3)_2(H_2O)$] ; (a) the hydrogen bonds and π-π interactions by aromatic ring of neighbor complexes, (b) cell packing diagram of the complex along *b* axis.

Table 61. Bond lengths (Å) for $[Ni_2([22]\text{-}HMTADO)(N_3)_2(OH_2)]$

Ni(1)-N(4)	2.012(3)	C(1)-C(23)	1.539(5)
Ni(1)-N(1)	2.013(3)	C(2)-H(2A)	0.99
Ni(1)-O(1)	2.021(3)	C(2)-H(2B)	0.99
Ni(1)-O(2)	2.025(3)	C(3)-C(4)	1.461(5)
Ni(1)-N(5)	2.145(3)	C(3)-H(3)	0.95
Ni(1)-O(1W)	2.161(3)	C(4)-C(5)	1.401(5)
Ni(2)-N(3)	1.996(3)	C(4)-C(9)	1.412(5)
Ni(2)-O(1)	2.010(3)	C(5)-C(6)	1.383(6)
Ni(2)-N(8)	2.016(4)	C(5)-H(5)	0.95
Ni(2)-O(2)	2.018(2)	C(6)-C(7)	1.382(6)
Ni(2)-N(2)	2.019(3)	C(6)-C(25)	1.516(6)
O(1)-C(9)	1.306(4)	C(7)-C(8)	1.406(5)
O(2)-C(20)	1.311(4)	C(7)-H(7)	0.95
O(1W)-H(1WA)	0.847(7)	C(8)-C(9)	1.424(5)
O(1W)-H(1WB)	0.847(7)	C(8)-C(10)	1.442(5)
N(1)-C(3)	1.288(5)	C(10)-H(10)	0.95
N(1)-C(2)	1.477(5)	C(11)-C(12)	1.524(5)
N(2)-C(10)	1.280(5)	C(11)-H(11A)	0.99
N(2)-C(11)	1.471(5)	C(11)-H(11B)	0.99
N(3)-C(14)	1.282(5)	C(12)-C(27)	1.519(5)
N(3)-C(13)	1.476(5)	C(12)-C(13)	1.538(5)
N(4)-C(21)	1.282(5)	C(12)-C(26)	1.540(5)
N(4)-C(22)	1.473(5)	C(13)-H(13A)	0.99
N(5)-N(6)	1.173(5)	C(13)-H(13B)	0.99
N(6)-N(7)	1.165(5)	C(14)-C(15)	1.466(5)
N(8)-N(9)	1.196(5)	C(14)-H(14)	0.95
N(9)-N(10)	1.158(5)	C(15)-C(16)	1.405(5)
C(1)-C(2)	1.532(6)	C(15)-C(20)	1.418(5)
C(1)-C(22)	1.533(5)	C(16)-C(17)	1.385(5)
C(1)-C(24)	1.533(6)	C(16)-H(16)	0.95
C(17)-C(18)	1.389(5)	C(24)-H(24C)	0.98
C(17)-C(28)	1.505(5)	C(25)-H(25A)	0.98
C(18)-C(19)	1.404(5)	C(25)-H(25B)	0.98
C(18)-H(18)	0.95	C(25)-H(25C)	0.98

C(19)-C(20)	1.436(5)	C(26)-H(26A)	0.98
C(19)-C(21)	1.453(5)	C(26)-H(26B)	0.98
C(21)-H(21)	0.95	C(26)-H(26C)	0.98
C(22)-H(22A)	0.99	C(27)-H(27A)	0.98
C(22)-H(22B)	0.99	C(27)-H(27B)	0.98
C(23)-H(23A)	0.98	C(27)-H(27C)	0.98
C(23)-H(23B)	0.98	C(28)-H(28A)	0.98
C(23)-H(23C)	0.98	C(28)-H(28B)	0.98
C(24)-H(24A)	0.98	C(28)-H(28C)	0.98
C(24)-H(24B)	0.98		

Table 62. Bond angles (°) for $[Ni_2([22]\text{-}HMTADO)(N_3)_2(OH_2)]$

N(4)-Ni(1)-N(1)	96.60(13)	Ni(2)-O(2)-Ni(1)	100.82(11)
N(4)-Ni(1)-O(1)	170.62(12)	Ni(1)-O(1W)-H(1WA)	127(3)
N(1)-Ni(1)-O(1)	92.71(12)	Ni(1)-O(1W)-H(1WB)	113(3)
N(4)-Ni(1)-O(2)	92.07(11)	H(1WA)-O(1W)-H(1WB)	109.4(15)
N(1)-Ni(1)-O(2)	169.86(12)	C(3)-N(1)-C(2)	114.8(3)
O(1)-Ni(1)-O(2)	78.55(10)	C(3)-N(1)-Ni(1)	122.8(3)
N(4)-Ni(1)-N(5)	92.39(13)	C(2)-N(1)-Ni(1)	121.9(2)
N(1)-Ni(1)-N(5)	96.34(13)	C(10)-N(2)-C(11)	115.2(3)
O(1)-Ni(1)-N(5)	87.75(12)	C(10)-N(2)-Ni(2)	124.1(3)
O(2)-Ni(1)-N(5)	88.51(12)	C(11)-N(2)-Ni(2)	120.5(3)
N(4)-Ni(1)-O(1W)	94.56(12)	C(14)-N(3)-C(13)	114.7(3)
N(1)-Ni(1)-O(1W)	87.24(13)	C(14)-N(3)-Ni(2)	125.6(3)
O(1)-Ni(1)-O(1W)	84.67(11)	C(13)-N(3)-Ni(2)	119.7(2)
O(2)-Ni(1)-O(1W)	86.84(11)	C(21)-N(4)-C(22)	116.1(3)
N(5)-Ni(1)-O(1W)	171.76(12)	C(21)-N(4)-Ni(1)	122.3(3)
N(3)-Ni(2)-O(1)	161.58(12)	C(22)-N(4)-Ni(1)	121.6(2)
N(3)-Ni(2)-N(8)	99.14(15)	N(6)-N(5)-Ni(1)	120.4(3)
O(1)-Ni(2)-N(8)	96.93(15)	N(7)-N(6)-N(5)	179.1(5)
N(3)-Ni(2)-O(2)	90.33(11)	N(9)-N(8)-Ni(2)	121.3(3)
O(1)-Ni(2)-O(2)	78.96(10)	N(10)-N(9)-N(8)	177.8(4)
N(8)-Ni(2)-O(2)	96.39(13)	C(2)-C(1)-C(22)	111.0(3)
N(3)-Ni(2)-N(2)	96.93(13)	C(2)-C(1)-C(24)	111.4(3)

O(1)-Ni(2)-N(2)	90.22(12)	C(22)-C(1)-C(24)	111.2(4)
N(8)-Ni(2)-N(2)	96.13(14)	C(2)-C(1)-C(23)	106.2(3)
O(2)-Ni(2)-N(2)	164.34(12)	C(22)-C(1)-C(23)	107.0(3)
C(9)-O(1)-Ni(2)	130.5(2)	C(24)-C(1)-C(23)	109.8(3)
C(9)-O(1)-Ni(1)	128.0(2)	N(1)-C(2)-C(1)	115.9(3)
Ni(2)-O(1)-Ni(1)	101.21(11)	N(1)-C(2)-H(2A)	108.3
C(20)-O(2)-Ni(2)	130.3(2)	C(1)-C(2)-H(2A)	108.3
C(20)-O(2)-Ni(1)	125.9(2)	N(1)-C(2)-H(2B)	108.3
C(1)-C(2)-H(2B)	108.3	C(12)-C(11)-H(11B)	108.7
H(2A)-C(2)-H(2B)	107.4	H(11A)-C(11)-H(11B)	107.6
N(1)-C(3)-C(4)	128.4(4)	C(27)-C(12)-C(11)	110.7(3)
N(1)-C(3)-H(3)	115.8	C(27)-C(12)-C(13)	111.4(3)
C(4)-C(3)-H(3)	115.8	C(11)-C(12)-C(13)	111.0(3)
C(5)-C(4)-C(9)	120.1(3)	C(27)-C(12)-C(26)	109.4(3)
C(5)-C(4)-C(3)	114.4(3)	C(11)-C(12)-C(26)	107.1(3)
C(9)-C(4)-C(3)	125.5(3)	C(13)-C(12)-C(26)	107.0(3)
C(6)-C(5)-C(4)	123.3(4)	N(3)-C(13)-C(12)	114.0(3)
C(6)-C(5)-H(5)	118.4	N(3)-C(13)-H(13A)	108.7
C(4)-C(5)-H(5)	118.4	C(12)-C(13)-H(13A)	108.7
C(7)-C(6)-C(5)	116.7(4)	N(3)-C(13)-H(13B)	108.7
C(7)-C(6)-C(25)	120.6(4)	C(12)-C(13)-H(13B)	108.7
C(5)-C(6)-C(25)	122.7(4)	H(13A)-C(13)-H(13B)	107.6
C(6)-C(7)-C(8)	122.6(4)	N(3)-C(14)-C(15)	127.6(4)
C(6)-C(7)-H(7)	118.7	N(3)-C(14)-H(14)	116.2
C(8)-C(7)-H(7)	118.7	C(15)-C(14)-H(14)	116.2
C(7)-C(8)-C(9)	120.4(4)	C(16)-C(15)-C(20)	120.4(3)
C(7)-C(8)-C(10)	115.3(3)	C(16)-C(15)-C(14)	115.2(3)
C(9)-C(8)-C(10)	124.4(3)	C(20)-C(15)-C(14)	124.4(3)
O(1)-C(9)-C(4)	122.3(3)	C(17)-C(16)-C(15)	122.9(4)
O(1)-C(9)-C(8)	120.7(3)	C(17)-C(16)-H(16)	118.6
C(4)-C(9)-C(8)	116.9(3)	C(15)-C(16)-H(16)	118.6
N(2)-C(10)-C(8)	128.9(3)	C(16)-C(17)-C(18)	116.8(3)
N(2)-C(10)-H(10)	115.5	C(16)-C(17)-C(28)	121.7(4)
C(8)-C(10)-H(10)	115.5	C(18)-C(17)-C(28)	121.5(3)
N(2)-C(11)-C(12)	114.4(3)	C(17)-C(18)-C(19)	123.2(3)
N(2)-C(11)-H(11A)	108.7	C(17)-C(18)-H(18)	118.4
C(12)-C(11)-H(11A)	108.7	C(19)-C(18)-H(18)	118.4
N(2)-C(11)-H(11B)	108.7	C(18)-C(19)-C(20)	119.6(3)

O(2)-C(20)-C(15)	121.1(3)	C(6)-C(25)-H(25B)	109.5
O(2)-C(20)-C(19)	121.9(3)	H(25A)-C(25)-H(25B)	109.5
C(15)-C(20)-C(19)	117.0(3)	C(6)-C(25)-H(25C)	109.5
N(4)-C(21)-C(19)	128.2(3)	H(25A)-C(25)-H(25C)	109.5
N(4)-C(21)-H(21)	115.9	H(25B)-C(25)-H(25C)	109.5
C(19)-C(21)-H(21)	115.9	C(12)-C(26)-H(26A)	109.5
N(4)-C(22)-C(1)	115.1(3)	C(12)-C(26)-H(26B)	109.5
N(4)-C(22)-H(22A)	108.5	H(26A)-C(26)-H(26B)	109.5
C(1)-C(22)-H(22A)	108.5	C(12)-C(26)-H(26C)	109.5
N(4)-C(22)-H(22B)	108.5	H(26A)-C(26)-H(26C)	109.5
C(1)-C(22)-H(22B)	108.5	H(26B)-C(26)-H(26C)	109.5
H(22A)-C(22)-H(22B)	107.5	C(12)-C(27)-H(27A)	109.5
C(1)-C(23)-H(23A)	109.5	C(12)-C(27)-H(27B)	109.5
C(1)-C(23)-H(23B)	109.5	H(27A)-C(27)-H(27B)	109.5
H(23A)-C(23)-H(23B)	109.5	C(12)-C(27)-H(27C)	109.5
C(1)-C(23)-H(23C)	109.5	H(27A)-C(27)-H(27C)	109.5
H(23A)-C(23)-H(23C)	109.5	H(27B)-C(27)-H(27C)	109.5
H(23B)-C(23)-H(23C)	109.5	C(17)-C(28)-H(28A)	109.5
C(1)-C(24)-H(24A)	109.5	C(17)-C(28)-H(28B)	109.5
C(1)-C(24)-H(24B)	109.5	H(28A)-C(28)-H(28B)	109.5
H(24A)-C(24)-H(24B)	109.5	C(17)-C(28)-H(28C)	109.5
C(1)-C(24)-H(24C)	109.5	H(28A)-C(28)-H(28C)	109.5
H(24A)-C(24)-H(24C)	109.5	H(28B)-C(28)-H(28C)	109.5

Table 63. Selected bond lengths (Å) and angles(°) for hydrogen bond of $[Ni_2([22]\text{-HMTADO})(N_3)_2(OH_2)]$

D-H···A	d(D-H)	d(H···A)	<DHA	d(D···A)
coordinated water - azide				
O1W-H1WA···N7 [x+1, y, z]	0.847	2.039	169.93	2.877
O1W-H1WB···N8	0.847	2.195	153.33	2.976

7) [Ni_2([22]-HMTADO)(μ-S_2O_3)].

An ORTEP view of [Ni_2([22]-HMTADO)(μ-S_2O_3)] is shown in Fig. 122, and bond distances and angles are summarized in Table 64 and 65. The dinegative ([22]-HMTADO)$^{2-}$ accommodates two Ni(II) ions in its N_4O_2 sites in the Ni(1)···Ni(2) separation of 3.038(2) Å. The geometry about two nickel metals in the N_2O_2 site are two square-pyramid with a sulfur atom and a oxygen atom of bridged thiosulfate in cis positions. These results are backed up by the molar conductivity (Λ_M = 3.6 ohm^{-1}cm^{2}mol^{-1}) which agreed with assignment of the structure as [Ni_2([22]-HMTADO)(μ-S_2O_3)].

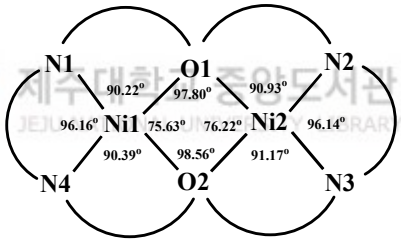

10

The macrocyclic complex adopts a non-flat structure with the square-pyramidal nickel centers bridged by the two phenoxide oxygen atoms, with quite large Ni-O-Ni angles (97.80(8)° and 98.56(9)°) **(10)**. The sum of angles at the phenoxide oxygens is 348.21°, indicating square oxygen distortion.

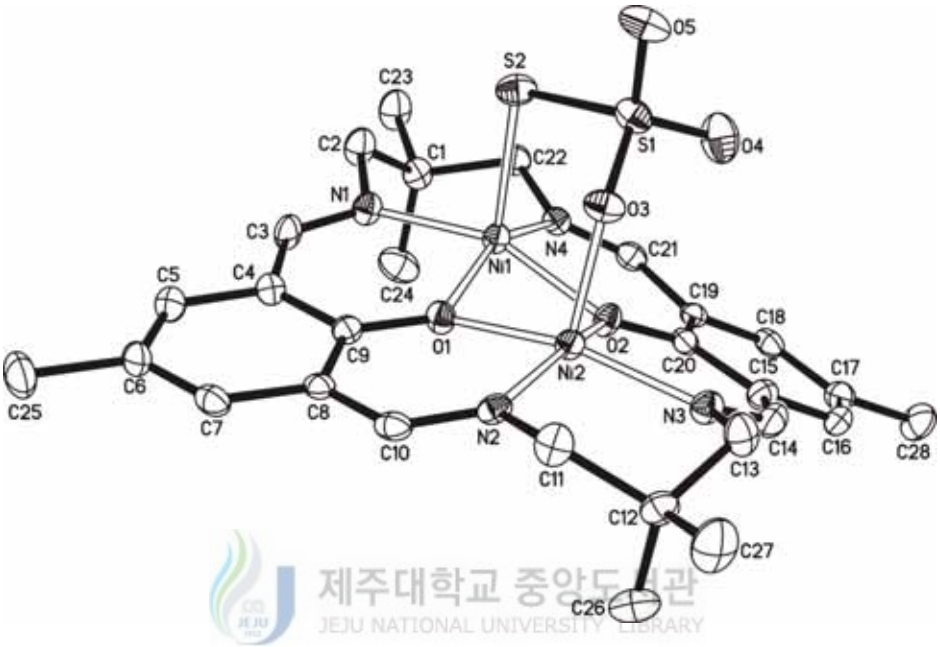

Fig. 122. Structural representation of core structure (top view) for the $[Ni_2([22]\text{-HMTADO})(\mu\text{-}S_2O_3)]$ complex.

The sum of angles at the octahedral Ni(1) basal planes (NiN_2O_2) is exactly 352.39°, indicating plane distortion. The Ni(1)-N (imines) bond distances are in the range of 2.004(2) and 2.005(2) Å, and Ni(1)-O (phenolic) are 2.0093(19) and 2.024(2) Å. The Ni(1)-S(2) (thiosulfate) bond distances is in the range of 2.3319(9) Å. The bond angles N(1)-Ni(1)-O(2) and N(4)-Ni(1)-O(1) are 157.69(9)° and 155.37(9)°, respectively. In this complex Ni(1)-N (imines) and Ni(1)-O (phenolic) distances are shorter than Ni(1)-S(2) (thiosulfate) distance and the N(1)-Ni(1)-O(2) and N(4)-Ni(1)-O(1) angles are smaller than the ideal value of 180°, indicating that the donor atoms are not able to achieve the axial positions of a perfect square-pyramidal. Result, the Ni(1) is displaced by 0.430 Å from the basal N_2O_2 least-squares plane towards S(2) (thiosulfate).

The sum of angles (354.46°) at the square-pyramidal Ni(2) basal planes (NiN_2O_2) is smaller than the ideal value of 360°, indicating plane distortion. The Ni(2)-N (imines) bond distances are in the range of 2.000(2) and 2.004(2) Å, and Ni(2)-O (phenolic) are 1.999(2) Å and 2.000(2) Å. The Ni(2)-O(3) (thiosulfate) bond distance {1.984(2) Å} is shorter 0.348 Å than octahedral Ni(1)-S(2) (thiosulfate) bond distance {2.3319(19) Å}. The bond angles N(3)-Ni(2)-O(1) and N(2)-Ni(2)-O(2) are 159.90(9)° and 159.09(9)°, respectively ; indicating $Ni(2)N_2O_4$ are not able to the perfect square planer. Result, the Ni(2) is displaced by 0.350 Å from the basal N_2O_2 least-squares plane towards O(3) (thiosulfate).

This complex is wholly asymmetric. The bridged thiosulfate, tetragonal geometry, slants toward the Ni(2) and the O(2)-phenolic groups of macrocycle.

Table 64. Bond lengths (Å) for [[Ni_2([22]-HMTADO)(μ-S_2O_3)]

Ni(1)-N(1)	2.004(2)	C(1)-C(2)	1.527(4)
Ni(1)-N(4)	2.005(2)	C(1)-C(22)	1.531(4)
Ni(1)-O(2)	2.0093(19)	C(1)-C(23)	1.540(4)
Ni(1)-O(1)	2.024(2)	C(3)-C(4)	1.452(4)
Ni(1)-S(2)	2.3319(9)	C(4)-C(5)	1.404(4)
Ni(2)-O(3)	1.984(2)	C(4)-C(9)	1.420(4)
Ni(2)-O(2)	1.999(2)	C(5)-C(6)	1.382(4)
Ni(2)-N(3)	2.000(2)	C(6)-C(7)	1.384(4)
Ni(2)-N(2)	2.003(2)	C(6)-C(25)	1.529(4)
Ni(2)-O(1)	2.008(2)	C(7)-C(8)	1.405(4)
S(1)-O(4)	1.452(2)	C(8)-C(9)	1.414(4)
S(1)-O(5)	1.453(2)	C(8)-C(10)	1.456(4)
S(1)-O(3)	1.504(2)	C(11)-C(12)	1.533(4)
S(1)-S(2)	2.0482(11)	C(12)-C(26)	1.519(4)
O(1)-C(9)	1.318(3)	C(12)-C(27)	1.541(4)
O(2)-C(20)	1.318(3)	C(12)-C(13)	1.541(4)
N(1)-C(3)	1.292(4)	C(14)-C(15)	1.451(4)
N(1)-C(2)	1.478(4)	C(15)-C(16)	1.400(4)
N(2)-C(10)	1.290(4)	C(15)-C(20)	1.428(4)
N(2)-C(11)	1.476(4)	C(16)-C(17)	1.388(4)
N(3)-C(14)	1.285(4)	C(17)-C(18)	1.386(4)
N(3)-C(13)	1.478(4)	C(17)-C(28)	1.522(4)
N(4)-C(21)	1.289(4)	C(18)-C(19)	1.409(4)
N(4)-C(22)	1.478(4)	C(19)-C(20)	1.409(4)
C(1)-C(24)	1.518(4)	C(19)-C(21)	1.457(4)

Table 65. Bond angles (°) for [Ni_2([22]-HMTADO)(μ-S_2O_3)]

N(1)-Ni(1)-N(4)	96.16(10)	C(20)-O(2)-Ni(2)	130.31(18)
N(1)-Ni(1)-O(2)	157.69(9)	C(20)-O(2)-Ni(1)	130.56(19)
N(4)-Ni(1)-O(2)	90.38(9)	Ni(2)-O(2)-Ni(1)	98.56(9)
N(1)-Ni(1)-O(1)	90.22(9)	S(1)-O(3)-Ni(2)	127.70(13)
N(4)-Ni(1)-O(1)	155.37(9)	C(3)-N(1)-C(2)	115.9(2)
O(2)-Ni(1)-O(1)	75.63(8)	C(3)-N(1)-Ni(1)	125.2(2)
N(1)-Ni(1)-S(2)	93.93(8)	C(2)-N(1)-Ni(1)	118.39(19)
N(4)-Ni(1)-S(2)	104.86(7)	C(10)-N(2)-C(11)	115.4(3)
O(2)-Ni(1)-S(2)	105.00(6)	C(10)-N(2)-Ni(2)	124.4(2)
O(1)-Ni(1)-S(2)	98.37(6)	C(11)-N(2)-Ni(2)	120.22(19)
O(3)-Ni(2)-O(2)	98.12(8)	C(14)-N(3)-C(13)	116.7(3)
O(3)-Ni(2)-N(3)	95.65(9)	C(14)-N(3)-Ni(2)	124.4(2)
O(2)-Ni(2)-N(3)	91.17(9)	C(13)-N(3)-Ni(2)	118.62(19)
O(3)-Ni(2)-N(2)	100.61(9)	C(21)-N(4)-C(22)	115.2(3)
O(2)-Ni(2)-N(2)	159.09(9)	C(21)-N(4)-Ni(1)	125.2(2)
N(3)-Ni(2)-N(2)	96.14(10)	C(22)-N(4)-Ni(1)	119.48(19)
O(3)-Ni(2)-O(1)	101.51(8)	C(24)-C(1)-C(2)	112.0(3)
O(2)-Ni(2)-O(1)	76.22(8)	C(24)-C(1)-C(22)	111.4(3)
N(3)-Ni(2)-O(1)	159.90(9)	C(2)-C(1)-C(22)	111.3(3)
N(2)-Ni(2)-O(1)	90.93(9)	C(24)-C(1)-C(23)	110.0(3)
O(4)-S(1)-O(5)	114.51(14)	C(2)-C(1)-C(23)	106.3(3)
O(4)-S(1)-O(3)	111.36(14)	C(22)-C(1)-C(23)	105.5(2)
O(5)-S(1)-O(3)	108.58(13)	N(1)-C(2)-C(1)	114.6(3)
O(4)-S(1)-S(2)	109.01(11)	N(1)-C(3)-C(4)	128.3(3)
O(5)-S(1)-S(2)	106.19(11)	C(5)-C(4)-C(9)	119.6(3)
O(3)-S(1)-S(2)	106.79(9)	C(5)-C(4)-C(3)	116.0(3)
S(1)-S(2)-Ni(1)	102.02(4)	C(9)-C(4)-C(3)	124.4(3)
C(9)-O(1)-Ni(2)	129.93(19)	C(6)-C(5)-C(4)	122.8(3)
C(9)-O(1)-Ni(1)	130.48(18)	C(5)-C(6)-C(7)	117.2(3)
Ni(2)-O(1)-Ni(1)	97.80(8)	C(5)-C(6)-C(25)	121.5(3)

C(7)-C(6)-C(25)	121.3(3)	N(3)-C(14)-C(15)	128.6(3)
C(6)-C(7)-C(8)	122.7(3)	C(16)-C(15)-C(20)	119.4(3)
C(7)-C(8)-C(9)	119.8(3)	C(16)-C(15)-C(14)	116.5(3)
C(7)-C(8)-C(10)	115.2(3)	C(20)-C(15)-C(14)	124.0(3)
C(9)-C(8)-C(10)	124.7(3)	C(17)-C(16)-C(15)	123.0(3)
O(1)-C(9)-C(8)	120.9(3)	C(18)-C(17)-C(16)	117.1(3)
O(1)-C(9)-C(4)	121.1(3)	C(18)-C(17)-C(28)	121.1(3)
C(8)-C(9)-C(4)	118.0(3)	C(16)-C(17)-C(28)	121.7(3)
N(2)-C(10)-C(8)	127.7(3)	C(17)-C(18)-C(19)	122.5(3)
N(2)-C(11)-C(12)	115.6(2)	C(20)-C(19)-C(18)	119.9(3)
C(26)-C(12)-C(11)	111.0(3)	C(20)-C(19)-C(21)	124.5(3)
C(26)-C(12)-C(27)	110.6(3)	C(18)-C(19)-C(21)	115.5(3)
C(11)-C(12)-C(27)	106.5(3)	O(2)-C(20)-C(19)	121.1(3)
C(26)-C(12)-C(13)	111.1(3)	O(2)-C(20)-C(15)	120.9(3)
C(11)-C(12)-C(13)	110.8(2)	C(19)-C(20)-C(15)	118.0(3)
C(27)-C(12)-C(13)	106.7(3)	N(4)-C(21)-C(19)	127.8(3)
N(3)-C(13)-C(12)	113.6(2)	N(4)-C(22)-C(1)	114.6(2)

8) [Ni(H_2[22]-HMTADO)($OHCH_3$)$_2$](ClO_4)$_2$.

An ORTEP view of [Ni(H_2[22]-HMTADO)($OHCH_3$)$_2$](ClO_4)$_2$ is shown in Fig. 123, and bond distances and angles are summarized in Table 66 and 67. The geometry about Ni(1) in the N_2O_2 site is a octahedral with two oxygen atom of methanol molecule in trans positions, and other N_2O_2 site is vacant.

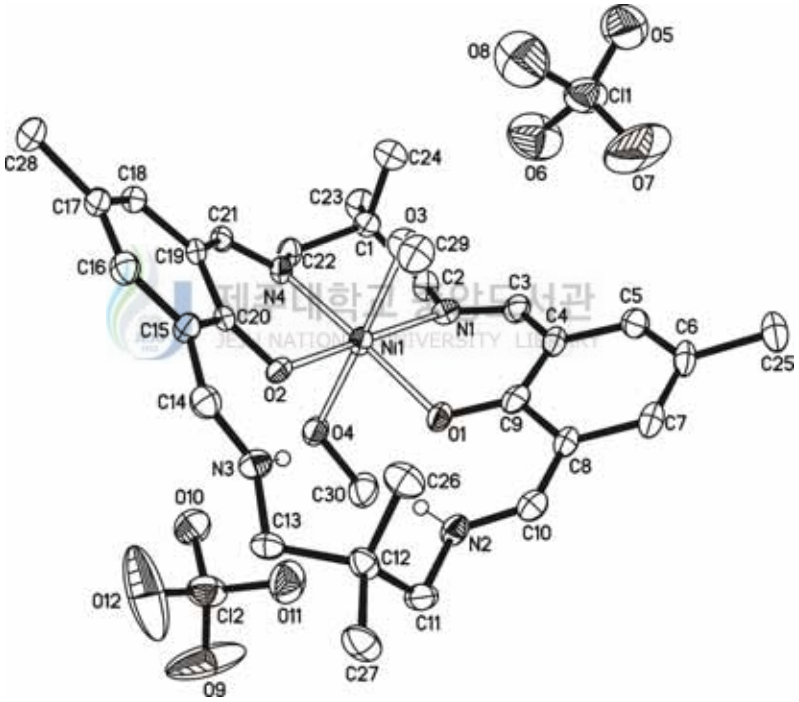

Fig. 123. Structural representation of core structure (top view) for the [Ni(H_2[22]-HMTADO)($OHCH_3$)$_2$](ClO_4)$_2$ complex.

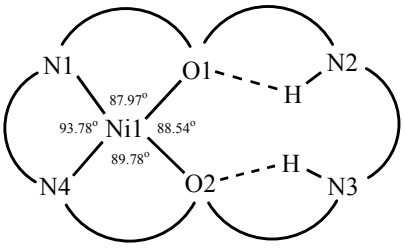

11

The macrocyclic complex adopts a flat structure with the an octahedral nickel center bridged by the two phenoxide oxygen atoms **(11)**. The sum of angles at the octahedral Ni(1) basal planes (NiN_2O_2) is exactly 360˚ (360.07 ˚), indicating no plane distortion. The Ni(1)-N (imines) bond distances are in the range of 2.035(4) and 2.052(4) Å, and Ni(1)-O (phenolic) are 2.009(3) and 2.020(3) Å. The Ni(1)-O (methanol) bond distances are in the range of 2.104(3) and 2.205(3) Å. The bond angles O(1)-Ni(1)-N(4), O(2)-Ni(1)-N(1) and O(3)-Ni(1)-O(4) are 178.05(15)˚, 174.70(15)˚ and 175.20(15)˚, respectively. In this complex Ni(1)-N (imines) and Ni(1)-O (phenolic) distances are shorter than Ni(1)-O (methanol) and the angle O(1)-Ni(1)-N(4), O(2)-Ni(1)-N(1) and O(3)-Ni(1)-O(4) are smaller than the ideal value of 180˚, indicating that the donor atoms are not able to achieve the axial positions of a perfect octahedron. The dihedral angle between the least-squares plan defined by Ni, O(3), and C(29) and the plane defined by Ni, O(4), and C(30) is 87.47˚. This complex is wholly asymmetric. The O(1)-phenolic and O(2)-phenolic groups of macrocycle are bent 35.02˚ and 28.46˚ with the basal NiN_2O_2 least-squares plane, respectively.

In general, hydrogen bonding plays a principal role in the packing of the

title compound. There are three types of H-bonds ; inner macrocycle, macrocyle - ClO_4^- ion, and coordinated methanol - ClO_4^- ion (Fig. 124 and Table 68).

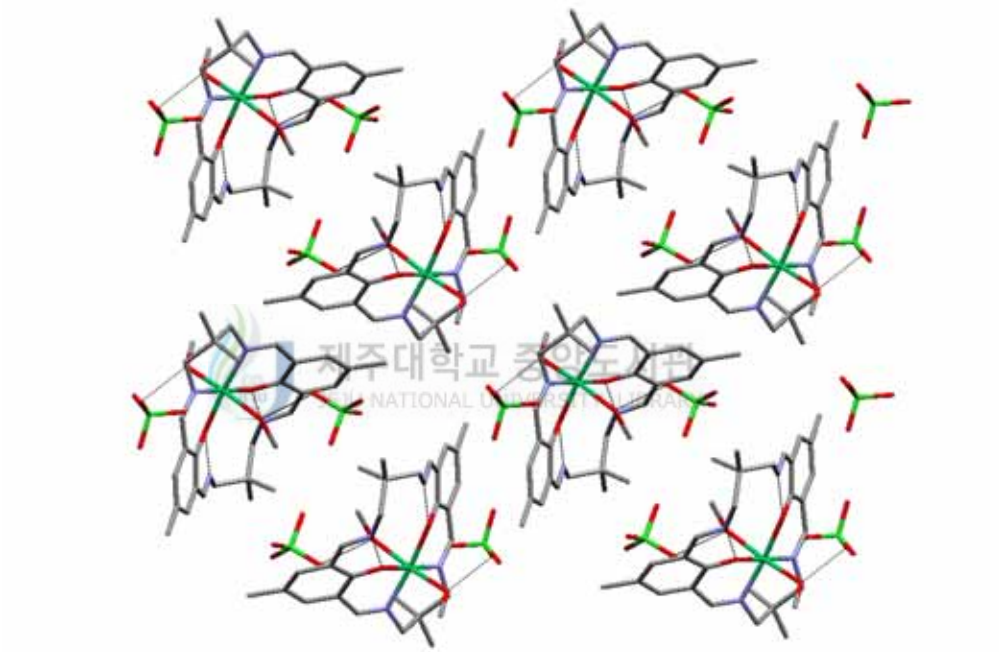

Fig. 124. The molecular packing diagram of [Ni(H_2[22]-HMTADO)($OHCH_3$)$_2$] -(ClO_4)$_2$.

Table 66. Bond lengths (Å) for $[Ni(H_2[22]\text{-}HMTADO)(OHCH_3)_2](ClO_4)_2$

Ni(1)-O(2)	2.009(3)	C(1)-C(24)	1.517(7)
Ni(1)-O(1)	2.020(3)	C(1)-C(23)	1.532(7)
Ni(1)-N(4)	2.035(4)	C(1)-C(2)	1.539(7)
Ni(1)-N(1)	2.052(4)	C(1)-C(22)	1.540(7)
Ni(1)-O(3)	2.205(3)	C(3)-C(4)	1.447(7)
Ni(1)-O(4)	2.104(3)	C(4)-C(5)	1.404(7)
Cl(1)-O(7)	1.370(5)	C(4)-C(9)	1.429(7)
Cl(1)-O(5)	1.392(5)	C(5)-C(6)	1.376(8)
Cl(1)-O(6)	1.424(5)	C(6)-C(7)	1.367(8)
Cl(1)-O(8)	1.510(6)	C(6)-C(25)	1.519(7)
Cl(2)-O(9)	1.405(6)	C(7)-C(8)	1.413(7)
Cl(2)-O(10)	1.412(5)	C(8)-C(10)	1.417(7)
Cl(2)-O(12)	1.418(6)	C(8)-C(9)	1.436(7)
Cl(2)-O(11)	1.453(4)	C(11)-C(12)	1.549(7)
O(1)-C(9)	1.297(6)	C(12)-C(26)	1.512(7)
O(2)-C(20)	1.298(6)	C(12)-C(27)	1.538(7)
O(3)-C(29)	1.435(6)	C(12)-C(13)	1.551(7)
O(4)-C(30)	1.437(6)	C(14)-C(15)	1.431(7)
N(1)-C(3)	1.272(6)	C(15)-C(16)	1.409(7)
N(1)-C(2)	1.479(6)	C(15)-C(20)	1.427(7)
N(2)-C(10)	1.288(6)	C(16)-C(17)	1.377(7)
N(2)-C(11)	1.461(6)	C(17)-C(18)	1.396(7)
N(3)-C(14)	1.283(7)	C(17)-C(28)	1.511(7)
N(3)-C(13)	1.461(6)	C(18)-C(19)	1.396(6)
N(4)-C(21)	1.282(6)	C(19)-C(20)	1.430(7)
N(4)-C(22)	1.470(6)	C(19)-C(21)	1.455(7)

Table 67. Bond angles (°) for $[Ni(H_2[22]\text{-}HMTADO)(OHCH_3)_2](ClO_4)_2$

O(2)-Ni(1)-O(1)	88.54(13)	C(9)-C(4)-C(3)	122.6(4)
O(2)-Ni(1)-N(4)	89.78(15)	C(6)-C(5)-C(4)	123.9(5)
O(1)-Ni(1)-N(4)	178.05(15)	C(7)-C(6)-C(5)	117.4(5)
O(2)-Ni(1)-N(1)	174.70(15)	C(7)-C(6)-C(25)	121.9(5)
O(1)-Ni(1)-N(1)	87.97(15)	C(5)-C(6)-C(25)	120.6(5)
N(4)-Ni(1)-N(1)	93.78(16)	C(6)-C(7)-C(8)	122.4(5)
O(7)-Cl(1)-O(5)	114.8(4)	C(7)-C(8)-C(10)	118.8(4)
O(7)-Cl(1)-O(6)	113.0(4)	C(7)-C(8)-C(9)	120.3(5)
O(5)-Cl(1)-O(6)	113.1(4)	C(10)-C(8)-C(9)	120.8(4)
O(7)-Cl(1)-O(8)	108.3(5)	O(1)-C(9)-C(4)	124.0(5)
O(5)-Cl(1)-O(8)	104.5(3)	O(1)-C(9)-C(8)	119.5(5)
O(6)-Cl(1)-O(8)	101.8(4)	C(4)-C(9)-C(8)	116.5(4)
O(9)-Cl(2)-O(10)	108.0(4)	N(2)-C(10)-C(8)	126.2(5)
O(9)-Cl(2)-O(12)	111.9(5)	N(2)-C(11)-C(12)	115.2(4)
O(10)-Cl(2)-O(12)	109.1(4)	C(26)-C(12)-C(27)	109.3(4)
O(9)-Cl(2)-O(11)	109.1(4)	C(26)-C(12)-C(11)	111.9(4)
O(10)-Cl(2)-O(11)	109.4(3)	C(27)-C(12)-C(11)	105.3(4)
O(12)-Cl(2)-O(11)	109.2(3)	C(26)-C(12)-C(13)	110.7(4)
C(9)-O(1)-Ni(1)	122.6(3)	C(27)-C(12)-C(13)	107.0(4)
C(20)-O(2)-Ni(1)	123.5(3)	C(11)-C(12)-C(13)	112.3(4)
C(3)-N(1)-C(2)	116.7(4)	N(3)-C(13)-C(12)	115.3(4)
C(3)-N(1)-Ni(1)	121.8(3)	N(3)-C(14)-C(15)	125.7(5)
C(2)-N(1)-Ni(1)	121.1(3)	C(16)-C(15)-C(20)	121.8(5)
C(10)-N(2)-C(11)	122.2(4)	C(16)-C(15)-C(14)	117.0(5)
C(14)-N(3)-C(13)	123.4(5)	C(20)-C(15)-C(14)	121.1(4)
C(21)-N(4)-C(22)	116.2(4)	C(17)-C(16)-C(15)	121.8(5)
C(21)-N(4)-Ni(1)	123.4(3)	C(16)-C(17)-C(18)	116.5(5)
C(22)-N(4)-Ni(1)	120.4(3)	C(16)-C(17)-C(28)	122.4(5)
C(24)-C(1)-C(23)	110.2(4)	C(18)-C(17)-C(28)	121.1(5)
C(24)-C(1)-C(2)	111.4(4)	C(17)-C(18)-C(19)	124.4(5)

C(23)-C(1)-C(2)	106.1(4)	C(18)-C(19)-C(20)	119.2(4)
C(24)-C(1)-C(22)	111.3(4)	C(18)-C(19)-C(21)	116.9(4)
C(23)-C(1)-C(22)	106.7(4)	C(20)-C(19)-C(21)	123.6(4)
C(2)-C(1)-C(22)	110.9(4)	O(2)-C(20)-C(15)	120.7(4)
N(1)-C(2)-C(1)	113.9(4)	O(2)-C(20)-C(19)	123.1(4)
N(1)-C(3)-C(4)	126.0(5)	C(15)-C(20)-C(19)	116.1(4)
C(5)-C(4)-C(9)	119.2(5)	N(4)-C(21)-C(19)	125.8(4)
C(5)-C(4)-C(3)	117.9(5)	N(4)-C(22)-C(1)	114.2(4)

Table 68. Selected bond lengths (Å) and angles(°) for hydrogen bond of $[Ni(H_2[22]\text{-}HMTADO)(OHCH_3)_2](ClO_4)_2$

D-H···A	d(D-H)	d(H···A)	<DHA	d(D···A)
inner macrocycle				
N2-H2···O1	0.880	1.973	130.01	2.627
N3-H3···O2	0.880	1.997	131.37	2.662
macrocyle - ClO_4^-				
N3-H3···O11	0.880	2.640	119.50	3.167
coordinated methanol - ClO_4^-				
O3-H3···O6	0.840	2.075	166.08	2.897
O4-H4···O10	0.840	1.992	162.90	2.806
O4-H4···Cl2	0.840	2.987	143.95	3.699

IV. Conclusion

The 22-membered phenol-based N_4O_2 compartmental macrocycle ligand H_2[22]-HMTADO {5,5,11,17,17,23-hexamethyl-3,7,15,19-tetraazatricyclo[19,3,1,$1^{9,13}$] -hexacosa-1(25),2,7,9,11,13(26),14,19,21,23-decane-25,26-diol} · $2HClO_4$ derived from the [2+2] cyclic condensation of 2,6-diformyl-*p*-cresol and 2,2-dimethyl -1,3-propanediamine with $HClO_4$. The macrocycle ligand has relatively high thermal stability.

Binuclear {Cu(II), Ni(II), and Mn(II)} and mononuclear {Ni(II), Pr(III), Sm(III), Gd(III), and Dy(III)} complexes with [2+2] symmetrical N_4O_2 compartmental macrocyclic ligand containing bridging phenolic oxygen atoms was synthesized by condensation of 2,6-diformyl-*p*-cresol and 2-dimethyl-1,3 -propandiamine in the metal ions.

The reaction of $[Cu_2([22]\text{-HMTADO})(OH_2)]Cl_2 \cdot H_2O$ with L_a (ClO_4^-, CN^-, NCS^-, N_3^-, NO_3^-, NO_2^-, Br^-, and $S_2O_3^{2-}$) ligands in aqueous solution formed a new $[Cu_2([22]\text{-HMTADO})(OClO_3)(OH_2)]ClO_4 \cdot 2H_2O$, $[Cu_2([22]\text{-HMTADO})(CN)_2] \cdot 0.5H_2O$, $[Cu_2([22]\text{-HMTADO})(NCS)(OH_2)]NCS \cdot 2H_2O$, $[Cu_2([22]\text{-HMTADO})\text{-}(N_3)(OH_2)]N_3 \cdot H_2O$, $[Cu_2([22]\text{-HMTADO})ONO_2]NO_3 \cdot 4H_2O$, $[Cu_2([22]\text{-HMTADO})\text{-}NO_2]NO_2 \cdot 2H_2O$, $[Cu_2([22]\text{-HMTADO})]Br_2 \cdot 1.5H_2O$, and $[Cu_2([22]\text{-HMTADO})S_2O_3] \cdot 5H_2O$ complexes.

The crystals of $[Cu_2([22]\text{-HMTADO})(OH_2)_4]Cl_2 \cdot 10H_2O$ were obtained by slow evaporation of hot aqueous solution of $[Cu_2([22]\text{-HMTADO})(OH_2)]Cl_2 \cdot H_2O$ complex at atmospheric pressure. The crystal structure of $[Cu_2([22]$

-HMTADO)$(OH_2)_4]Cl_2 \cdot 10H_2O$ is composed of binuclear cation of the indicated formula and noninteracting chloride anions. The binuclear cation, $[Cu_2([22]\text{-HMTADO})(OH_2)_4]^{2+}$ shows two octahedral environment, where the copper(II) ions are coordinated by the two oxygen atoms of water molecules of the copper basal planes (CuN_2O_2) in trans positions, respectively. The copper centers are separated by 3.0482(4) Å. An angle of 29.61° exists between the benzene mean planes of macrocycle and the copper basal planes.

The crystals of $[Cu_2([22]\text{-HMTADO})(OClO_3)(OH_2)]ClO_4 \cdot 2CH_3OH$ were obtained by slow evaporation of hot methanol solution of $[Cu_2([22]\text{-HMTADO})(OClO_3)(OH_2)]ClO_4 \cdot 2H_2O$ at atmospheric pressure. The binuclear cation, $[Cu_2([22]\text{-HMTADO})(OClO_3)(OH_2)]^{2+}$ shows two square pyramidal environment, where the copper(II) ions are coordinated by the two oxygen atoms of perchlorate and water molecules of the copper basal planes (CuN_2O_2) in axis positions, respectively. The copper centers are separated by 3.0319(10) Å. An angle of 29.79° exists between the benzene mean planes of macrocycle and the copper basal planes.

The crystals of $[Cu_2([22]\text{-HMTADO})(OH_2)_4]Br_2 \cdot 10H_2O$ were obtained by slow evaporation of hot aqueous solution of $[Cu_2([22]\text{-HMTADO})]Br_2 \cdot 1.5H_2O$ at atmospheric pressure. The crystal structure of $[Cu_2([22]\text{-HMTADO})\text{-}(OH_2)_4]Br_2 \cdot 10H_2O$ is composed of binuclear cation of the indicated formula and noninteracting bromide anions. The binuclear cation, $[Cu_2([22]\text{-HMTADO})\text{-}(OH_2)_4]^{2+}$ shows two octahedral environment, where the copper(II) ions are coordinated by the two oxygen atoms of water molecules of the copper basal planes (CuN_2O_2) in trans positions, respectively. The copper centers are separated by 3.0463(8) Å. An angle of 21.95° exists between the benzene

mean planes of macrocycle and the copper basal planes.

The reaction of $[Ni_2([22]\text{-HMTADO})(OH_2)_2]Cl_2 \cdot H_2O$ with L_a (ClO_4^-, CN^-, NCS^-, N_3^-, NO_3^-, NO_2^-, Br^-, and $S_2O_3^{2-}$) ligands in aqueous solution formed a new $[Ni_2([22]\text{-HMTADO})(OH_2)_2](ClO_4)_2 \cdot H_2O$, $[Ni_2([22]\text{-HMTADO})(CN)_2] \cdot 0.5H_2O$, $[Ni_2([22]\text{-HMTADO})(NCS)_2(OH_2)] \cdot 2H_2O$, $[Ni_2([22]\text{-HMTADO})(N_3)_2\text{-}(OH_2)]$, $[Ni_2([22]\text{-HMTADO})(ONO_2)(OH_2)_2]NO_3 \cdot 3H_2O$, $[Ni_2([22]\text{-HMTADO})\text{-}NO_2]NO_2 \cdot H_2O$, $[Ni_2([22]\text{-HMTADO})]Br_2 \cdot 2H_2O$, and $[Ni_2([22]\text{-HMTADO})(\mu\text{-}S_2O_3]$ complexes.

The crystals of $[Ni_2([22]\text{-HMTADO})(OH_2)_4](ClO_4)_2 \cdot 3H_2O$ were obtained by slow evaporation of hot aqueous solution of $[Ni_2([22]\text{-HMTADO})(OH_2)_2]\text{-}(ClO_4)_2 \cdot H_2O$ at atmospheric pressure. The crystal structure of this complex is composed of binuclear cation of the indicated formula and noninteracting chloride anions. The dinuclear cation, $[Ni_2([22]\text{-HMTADO})(OH_2)_4]^{2+}$ shows two octahedral environment, where the nickel(II) ions are coordinated by the two oxygen atoms of water molecules of the nickel basal planes (NiN_2O_2) in trans positions, respectively. The nickel centers are separated by 3.0768(4) Å. An angle of 21.07° exists between the benzene mean planes of macrocycle and the nickel basal planes.

The crystals of $[Ni_2([22]\text{-HMTADO})(OH_2)_4]Br_2 \cdot 10H_2O$ were obtained by slow evaporation of hot aqueous solution of $[Ni_2([22]\text{-HMTADO})]Br_2 \cdot 1.5H_2O$ at atmospheric pressure. The crystal structure of this complex is composed of binuclear cation of the indicated formula and noninteracting chloride anions. The binuclear cation, $[Ni_2([22]\text{-HMTADO})(OH_2)_4]^{2+}$ shows two octahedral environment, where the nickel(II) ions are coordinated by the two oxygen atoms of water molecules of the nickel basal planes (NiN_2O_2) in trans

positions, respectively. The nickel centers are separated by 3.060 Å. An angle of 23.19° exists between the benzene mean planes of macrocycle and the nickel basal planes.

The crystals of $[Ni_2([22]\text{-HMTADO})(N_3)_2(OH_2)]$ were obtained by slow evaporation of acetonitrile solution of $[Ni_2([22]\text{-HMTADO})(N_3)_2(OH_2)]$ at atmospheric pressure. The dinegative $([22]\text{-HMTADO})^{2-}$ accommodates two Ni(II) ions in its N_4O_2 sites in the Ni(1)···Ni(2) separation of 3.115(3) Å. The geometry about Ni(1) in the N_2O_2 site is a octahedral with a nitrogen atom of azido and a oxygen atom of aqua in trans positions. And the geometry about Ni(2) in the N_2O_2 site is a square-pyramid with a nitrogen atom of azido at the axial site. The two azido groups coordinated to the nickel centers are situated trans to each other with respect to the mean $\{NiN_2O_2\}$ plane. The N_3 ligand keep their linearity, N-N-N bond angle is 179.1(5)°, whereas the Ni(1)-N(5)-N(6) linkage is slightly bent {120.4(3)°} towards Ni(2) {Ni(2)···N(7) 3.619 Å}. The Ni(1)-N(5)-N(6) basal least -trigonal plane are bent at basal least-trigonal plane for N(5)-Ni(1)-Ni(2) edge with a dihedral angle of 17.87° towards O(2)-phenolic group. The Ni(2) is displaced by 0.320 Å from the basal N_2O_2 least-squares plane towards N(8) (azido). The N_3 ligand keep their linearity, N-N-N bond angle is 177.8(4)°, whereas the Ni(2)-N(8)-N(9) linkage is slightly bent {121.3(3)°} towards the opposite Ni(1) by the repulsion of coordinated aqua of Ni(1). This complex is wholly asymmetric. The O(2)-phenolic groups of macrocycle is bent 18.6° with the basal Ni_2O_2 least-squares plane, whereas O(1)-phenolic groups of macrocycle is flat with the basal Ni_2O_2 least-squares plane. Hydrogen bonds are between water and azide molecules of octahedral of neighbor complexes.

And there are a weak π-π interactions by aromatic ring of neighbor complexes ; a dihedral angle and a distance between aromatic rings are 9.4(2)° and 4.1 Å, respectively.

The crystals of $[Ni_2([22]\text{-HMTADO})(\mu\text{-}S_2O_3)]$ were obtained by slow evaporation of hot aquose solution at atmospheric pressure. The dinegative $([22]\text{-HMTADO})^{2-}$ accommodates two Ni(II) ions in its N_4O_2 sites in the Ni(1)···Ni(2) separation of 3.038(2) Å. The geometry about two nickel metals in the N_2O_2 site are two square-pyramid with a sulfur atom and a oxygen atom of bridged thiosulfate in cis positions. The macrocyclic complex adopts a non-flat structure with the square-pyramidal nickel centers bridged by the two phenoxide oxygen atoms. The Ni(1) is displaced by 0.430 Å from the basal N_2O_2 least-squares plane towards S(2) (thiosulfate). The Ni(2) is displaced by 0.350 Å from the basal N_2O_2 least-squares plane towards O(3) (thiosulfate). This complex is wholly asymmetric. The bridged thiosulfate, tetragonal geometry, slants toward the Ni(2) and the O(2)-phenolic groups of macrocycle.

The mononuclear Ni(II) complex, $[Ni(H_2[22]\text{-HMTADO})(OHCH_3)_2](ClO_4)_2$, was synthesized by condensation of 2,6-diformyl-*p*-cresol and 2-dimethyl -1,3-propandiamine in nickel perchlorate hexahydrate. The reaction of $[Ni(H_2[22]\text{-HMTADO})(OHCH_3)_2](ClO_4)_2$ with L_a (NCS^- and N_3^-) ligands in aqueous solution formed a new $[Ni(H_2[22]\text{-HMTADO})(NCS)_2]\cdot H_2O$ and $Ni(H_2[22]\text{-HMTADO})(N_3)(OH_2)]ClO_4\cdot H_2O$ complexes.

The crystals of $[Ni(H_2[22]\text{-HMTADO})(OHCH_3)_2](ClO_4)_2$ were obtained by slow evaporation of methanol solution at atmospheric pressure. The geometry about Ni(1) in the N_2O_2 site is a octahedral with two oxygen atom of

methanol molecule in trans positions, and other N_2O_2 site is vacant. The macrocyclic complex adopts a flat structure with the an octahedral nickel center bridged by the two phenoxide oxygen atoms. The two coordinated methanol molecules dihedral angle between the least-squares plan defined by Ni, O(3), and C(29) and the plane defined by Ni, O(4), and C(30) is 87.47°. This complex is wholly asymmetric. The O(1)-phenolic and O(2)-phenolic groups of macrocycle are bent 35.02° and 28.46° with the basal NiN_2O_2 least-squares plane, respectively.

The binonuclear Mn(II) complex, $[Mn_2([22]\text{-HMTADO})Cl_2] \cdot H_2O$, was synthesized by condensation of 2,6-diformyl-*p*-cresol and 2-dimethyl-1,3-propandiamine in manganese acetate tetrahydrate.

The mononuclear lanthanide complexes, $[Pr(H_2[22]\text{-HMTADO})O_2NO](NO_3)_2 \cdot 2H_2O$, $[Sm(H_2[22]\text{-HMTADO})O_2NO](NO_3)_2 \cdot 2H_2O$, $[Gd(H_2[22]\text{-HMTADO})O_2NO](NO_3)_2 \cdot 2H_2O$, and $[Dy(H_2[22]\text{-HMTADO})O_2NO](NO_3)_2 \cdot H_2O$, with [2+2] symmetrical N_4O_2 compartmental macrocyclic ligand containing bridging phenolic oxygen atoms was synthesized by condensation, in the lathanide ions, of 2,6-diformyl-*p*-cresol and 2-dimethyl-1,3-propandiamine

References

1. T. Thomas and T. Thomas, *J. Cell. Mol. Life Sci.* **2001**, 58, 244.
2. L. J. Marton and A. E. Pegg, *Annu. Rev. Pharmacol. Toxicol.* **1995**, 35, 55.
3. J. W. Sibert, A. H. Cory, and J. G. Cory, *J. Chem. Soc., Chem. Commun* **2002**, 154.
4. L. Messori, F. Abbate, G. Marcon, P. Orioli, M. Fontani, E. Mini, T. Mazzei, S. Carotti, T. O' Connel, and P. Zanello, *J. Med. Chem.* **2000**, 43, 3541.
5. D. Kong, L. Meng, J. Ding, Y. Xie, and X. Huang, *Polyhedron* **2000**, 19, 217.
6. D. Kong, L. Meng, L. Song, and Y. Xie, *Trans. Metal Chem.* **1999**, 24, 553.
7. E. De Clercq, *Biochim. Biophys. Acta* **2002**, 1587, 258
8. E. Kikuta, S. Aoki, and E. Kimura, *J. Am. Chem. Soc.* **2001**, 123, 7911
9. E. Kimura, I. Nakamura, T. Koike, M. Shionoya, Y. Kodama, T. Ikeda, and M. Shiro, *J. Am. Chem. Soc.* **1994**, 116, 4764
10. J. H. Kim, *Chem. Lett.* **2000**, 156.
11. E. L. Hegg, S. H. Mortimore, C. L. Cheung, J. E. Huyett, D. R. Powell, and J. N. Burstyn, *Inorg. Chem.* **1999**, 38, 2961.
12. K. A. Deal, A. C. Hengge, and J. N. Burstyn, *J. Am. Chem. Soc.* **1996**, 118, 1713.
13. K. A. Deal and J. N. Burstyn, *Inorg. Chem.* **1996**, 35, 2792.

14. W. H. Jr. Chapman,, and R. Breslow, *J. Am. Chem. Soc.* **1995**, 117, 5462.
15. P. Rossi, F. Felluga, P. Tecilla, F. Formaggio, M. Crisma, C. Toniolo, and P. Scrimin, *J. Am. Chem. Soc.* **1999**, 121, 6948.
16. E. L. Hegg, K. A.Deal, L. L.Kiessling, and J. N. Burstyn, *Inorg. Chem.* **1997**, 36, 1715.
17. C. Sissi, P. Rossi, F. Felluga, F. Formaggio, M. Palumbo, P. Tecilla, C. Toniolo, P. Scrimin, *J. Am. Chem. Soc.* **2001**, 123, 6948.
18. E. L. Hegg and J. N. Burstyn, *Inorg. Chem.* **1996**, 35, 7474.
19. E. L. Hegg and J. N. Burstyn, *J. Am. Chem. Soc.* **1995**, 117, 7015.
20. F. Liang, C. Wu, H. Lin, T. Li, D. Gao, Z. Li, J. Wei, C. Zheng, M. Sun, *Bioorg. Med. Chem. Lett.* **2003**, 13, 2469.
21. F. Liang, P. Wang, X. Zhou, T. Li, Z. Li, H. Lin, D. Gao, C. Zhengc, and C. Wu, *Bioorg. Med. Chem. Lett.* **2004**, 14, 1901.
22. N. H. Pilkingto and R. Robson, *Aust. J. Chem.* **1970**, 23, 2217.
23. O. Kahn, *Structure and Bonding(Berlin)* **1987**, 68, 89.
24. D. E. Feenton, H. Okawa, *Prespectives on Bioinorg. Chem.* **1993**, 2, 81.
25. N. Strater, T. Klabunde, P. Tucker, H. Witzel, and B. Krebs, *Science* **1995**, 268, 1489.
26. C. R. Kissinger, H. E. Parge, D. R. Knighton, C. T. Lewis, L. A. Pelletier, A. Tempczyk, V. J. Kalish, K. D. Tecker, R. E. Shiwalter, E. W. Moomaw, L. N. Gastinel, N. Habuka, X. Chen, F. Maldonado, J. E. Barker, R. Bacquet, and J. E. Villafranca, *Nature* **1995**, 378, 641.
27. M. P. Egloff, P. T. W. Cohen, P. Reinemer, and D. Barford, *J. Mol. Biol.* **1995**, 254, 942.

28. D. E. Fenton and H. Ōkawa, *Chem. Ber./Recueil* **1997**, 130, 433.
29. U. Casellato, P. A. Vigato, and M. Vidali, *Coord. Chem. Rev.* **1977**, 23, 31.
30. D. E. Fenton, U. Casellato, P. A. Vigato, and M. Vidali, *Inorg. Chim. Acta* **1982**, 62, 57.
31. S. F. Groh and Israel *J. Chem.* **1976**/77, 15, 277.
32. P. Zanello, S. Tanburini, P. L. Vigato, and G. A. Mazzocchin, *Coord. Chem. Rev.* **1987**, 77, 165.
33. B. F. Hoskins and G. A. Williams, *Aust. J. Chem.* **1975**, 28, 2607.
34. B. F. Hoskins, N. J. McLeod and H. A. Schaap, *Aust. J. Chem.* **1976**, 29, 515.
35. A. N. Addison, *Inorg. Nucl. Chem. Lett.* **1976**, 12, 899.
36. S. L. Lambert and D. L. Hendrickson, *Inorg. Chem.* **1979**, 18, 2683.
37. R. C. Long and D. L. Hendrickson, *J. Am. Chem. Soc.* 1983, 105, 1513.
38. H. Ōkawa and S. Kida, *Inorg. Nucl. Chem. Lett.* **1971**, 7, 751.
39. H. Ōkawa and S. Kida, *Bull. Chem. Soc. Jpn.* **1972**, 45, 1759.
40. W. D. Carlisle, D. E. Fenton, P. R. Roberts, U. Casellato, P. A. Vigato, and R. Graziani, *Trans. Mect. Chem.* **1986**, 11, 292.
41. H. Ōkawa, Y. Aratake, K. Motoda, M. Ohba, H. Sakiyama, N. Matsumoto, *Supramol. Chem.* **1996**, 6, 293.
42. A. J. Atkins, D. Black, A. J. Blake, A. Marin-Becerra, S. Parsons, L. Ruiz-Ramirez, and M. Schroder, *J. Chem. Soc., Chem. Commun.* **1996**, 457.
43. A. J. Edwards, B. F. Hoskins, E. H. Kachab, A. Markiewicz, K. S. Murray, and R. Robson, *Inorg. Chem* **1992**, 31, 3584.

44. B. F. Hoskins, R. Robson, and P. J. Smith, *J. Chem. Soc., Chem. Commun.* **1990**, 488.
45. V. McKee and S. S. Tandon, *J. Chem. Soc., Dalton Trans.* **1991**, 221.
46. S. S. Tandon, L. K. Thompson, and J. N. Beidson, *J. Chem. Soc., Chem. Commun.* **1992**, 911.
47. D. D. Perrin and W. L. F. Armarego, *Purification of Laboratory Chemicals, Pergamon,* 3rd edn., **1988**.
48. T. Shozo, *Bull. Chem. Soc. Jpn*. **1984**, 57, 2683.
49. J. C. Byun, Y. C. Park, and C. H. Han, *J. Kor. Chem. Soc.* **1999**, 43/3, 267.
50. Bruker, *SAINTPLUS NT Version 5.0. Software Reference Manual Bruker AXS: Madison*, Wisconsin, **1998**.
51. Bruker, *SHELXTL NT Version 5.16. Program for Solution and Refinement of Crystal Structures Bruker AXS*: Madison, Wisconsin, **1998**.
52. L. A. Kahwa, J. Selbin, T. C. Y. Hsieh and R. A. Laine, *Inorg. Chim. Acta* **1986**, 118, 179.
53. D. Suresh Kumar and V. Alexander, *Inorg. Chim. Acta* **1995**, 238, 63.
54. G. Socrates, *Infrared and Raman Charateristic Group Frequencies*. 3rd edn., Wiley, New York, **2001**, p. 309.
55. S. D. Kevan and D. Gixon, *Ecotoxicol. Environ. Saf.* **1996**, 35, 288.
56. A. M. Avunduk, M. C.Avunduk, C. Guven, and K. Cetinkaya, *Ophthalmological* **1997**, 211, 296.
57. M. Hiroi, M. Tajinma, T. Shimojima, and H. Sakagami, *Anticancer Res.* **1998**, 18, 1813.
58. G. Socrates, *Infrared and Raman Charateristic Group Frequencies*. 3rd

edn., Wiley, New York, **2001**, p. 320.

59. V. Mckee, M. Zvagulis, J. V. Dagdigian, M. G. Patch, and C. A. Reed, *J. Am. Chem. Soc.* **1984**, 106, 4765.
61. J. Ribas, M. Monfort, and M.Drillon, *Angew. Chem., Int. Ed. Engl.* **1996**, 35, 2520.
62. C. S. Hong and Y. Do, *Angew. Chem., Int. Ed. Engl.* **1999**, 38, 193.
63. G. Socrates, *Infrared and Raman Charateristic Group Frequencies*. 3rd edn., Wiley, New York, **2001**, p. 321.
64. P. Guerriero, U. Casellato, S. Tamburini, P. A. Vigato and R. Graziani, *Inorg. Chim. Acta* **1987**, 129, 127.
65. P. W. Crawford, M. D. Ryan, *Inorg. Chim. Acta* **2002**, 328, 13.
66. G. K. Druschel, R. J. Hamers, and J. F. Banfield, *Geochimica et Cosmochimica Acta* **2003**, 67/23, 4457.
67. K. Nakamoto, *Infrared and Raman Spectra of Inorganic and Coordination Compounds*. 3rd edn., Wiley, New York, **1997**.
68. W. Radecka-Paryzek, *Inorg. Chim. Acta* **1985**, 109, L21.
69. D. Sutton, *Electronic Spectra of Transition Metal Complexes*, McGraw -Hill, London, **1968**.

초 록

22-원 페놀 바탕 N_4O_2 칸막이형 거대고리 리간드 H_2[22]-HMTADO {5,5,11,17,17,23-hexamethyl-3,7,15,19-tetraazatricyclo[19,3,1,$1^{9,13}$]-hexacosa-1(25),2,7,9,11,13(26),14,19,21,23-decane-25,26-diol}·2$HClO_4$은 $HClO_4$ 존재 하에서 2,6-diformyl-*p*-cresol와 2,2-dimethyl-1,3-propanediamine의 [2+2] 고리 축합반응으로부터 합성하였다. 이 거대고리 리간드는 열적으로 안정함을 보였다. 2,6-diformyl-*p*-cresol와 2,2-dimethyl-1,3-propanediamine의 금속 주형 축합반응을 시켜 페놀의 산소 원가가 다리 결합을 하고 있는 이핵 {Cu(II), Ni(II), Mn(II)} 및 일핵 {Ni(II), Pr(III), Sm(III), Gd(III), Dy(III)}의 [2+2] 22-원 페놀 바탕 N_4O_2 칸막이형 거대고리 착물을 합성하였다. [Cu_2([22]-HMTADO)(OH_2)]-Cl_2·H_2O을 수용액 하에서 L_a (ClO_4^-, CN^-, NCS^-, N_3^-, NO_3^-, NO_2^-, Br^-, $S_2O_3^{2-}$)와 반응시켜 새로운 Cu(II) 이핵 착물 8 개 합성하였다. [Ni_2([22]-HMTADO)-(OH_2)$_2$]Cl_2·H_2O을 수용액 하에서 L_a (ClO_4^-, CN^-, NCS^-, N_3^-, NO_3^-, NO_2^-, Br^-, $S_2O_3^{2-}$)와 반응시켜 새로운 Ni(II) 이핵 착물 8 개를 합성하였다. $Ni(ClO_4)_2$·$6H_2O$ 존재 하에서 축합반응을 시킨 결과 일핵 Ni(II) 착물인 [Ni(H_2[22]-HMTADO)($OHCH_3$)$_2$](ClO_4)$_2$을 얻을 수 있었고, 이 착물을 L_a (NCS^-과 N_3^-) 반응시켜 새로운 Ni(II) 일핵 착물 2 개를 합성하였다. Mn(II) 착물인 경우, 이핵의 [Mn_2([22]-HMTADO)Cl_2]·H_2O 착물을 합성하였다. 란탄족 착물들은 [Ln(H_2[22]-HMTADO)O_2NO](NO_3)$_2$·$x$$H_2O$ {Pr(III), Sm(III), Gd(III), Dy(III)} 형태로 일핵 착물을 형성하였다. 이들 착물들은 원소분석, 전기전도도, UV/Vis, IR 분광법, 질량 분석법, 열중량 분석법 및 X-ray 결정 분석법 등을 이용하여 특성 및 구조적 성질을 확인·고찰하였다. 이 착물들의 구조 분석 결과, 이핵 착물들의 중심금속은 4 가지 형태의 구조 환경을

갖고 있었다 ; (1) 팔면체 - 팔면체 구조 : $[Cu_2([22]\text{-HMTADO})(OH_2)_4]Cl_2 \cdot 10H_2O$, $[Cu_2([22]\text{-HMTADO})(OH_2)_4]Br_2 \cdot 10H_2O$, $[Ni_2([22]\text{-HMTADO})(OH_2)_4](ClO_4)_2 \cdot 3H_2O$, $[Ni_2([22]\text{-HMTADO})(OH_2)_4]Br_2 \cdot 10H_2O$, (2) 팔면체 - 사각 피라미드 구조 : $[Ni_2([22]\text{-HMTADO})(N_3)_2(OH_2)]$, (3) *trans*-사각 피라미드 - 사각 피라미드 구조 : $[Cu_2([22]\text{-HMTADO})(OClO_3)(OH_2)]ClO_4 \cdot 2CH_3OH$, (4) *cis*-사각 피라미드 - 사각 피라미드 구조 : $[Ni_2([22]\text{-HMTADO})(\mu\text{-}S_2O_3)]$. 일핵 착물인 $[Ni(H_2[22]\text{-HMTADO})(OHCH_3)_2](ClO_4)_2$은 Ni(II) 중심금속이 팔면체 구조를 하고 있다. 이들 착물들의 열적 안정성 측정결과 거대고리는 대략 350℃ 이상에서 분해가 일어나 열적으로 안정함을 보였다.

감 사 의 글

본 논문을 완성하는데 도움을 주신 많은 분들께 이 지면을 통해 감사의 말씀을 드립니다.

이 논문이 완성되기까지 여러모로 부족한 저를 지금까지 이끌어 주신 변종철 교수님께 진심으로 감사드립니다. 그리고 미흡한 논문을 세심하게 다듬어주시고, 깨우침을 주신 정덕상 교수님, 김원형 교수님, 경북대학교 박유철 교수님, 부산대학교 김영인 교수님께 다시 한 번 머리 숙여 감사드립니다. 또한, 늘 격려해 주시고 용기를 북돋워 주신 한성빈 교수님, 김덕수 교수님, 강창희 교수님, 이선주 교수님, 이남호 교수님께 깊이 감사의 말씀을 드립니다. 특히 연구를 수행하는데 있어서 바쁘신 가운데에도 결정분석을 해주신 경상대학교 박기민 교수님께 감사드립니다. 그리고 박사 과정을 수행하는 동안 여러모로 도움을 주신 자연과학대학 교수님들과 선생님들께도 이 지면를 통해 감사의 말을 드립니다. 앞으로 고마운 분들 앞에서 부끄럽지 않은 모습 보여드리겠습니다.

이 매듭을 짓는데 있어서 가장 큰 도움을 준 무기화학연구실 김구철 박사님, 문대훈 선생님, 이우환 선생님, 현창식, 김기주, 양동호, 이한나, 설기선, 김보철, 이승정 학우 및 연구실을 거쳐 간 선후배님들께 감사드리고, 특히 인천에서 열심히 연구하고 있는 친동생 같은 안창훈 후배님에게도 감사의 말을 전하고 좋은 성과 거두기를 바랍니다. 또한 제주대학교 화학과 대학원 선후배님들 모두에게 각별한 감사를 드리며, 모두 건승하시길 바랍니다. 연구를 수행하면서 많은 도움을 준 물리학과, 생명과학과, 식품영양학과 및 제주대학교 대학원 학생회 선후배님들과 벗들에게도 감

사드립니다. 지금껏 살아오는 동안 여러 장소 여러 가지에 걸친 수많은 인연들을 소중하게 생각합니다. 일일이 열거하지 못한 모든 인연들 모두에게도 감사함을 전합니다.

저를 끝까지 믿어주시고 후원해주신 형, 누나, 매형, 형수님, 처남 식구들께 감사드립니다. 우리 두 공주님을 사랑으로 돌봐주시고, 항상 친아들처럼 대해주시는 장모님께 무엇보다도 감사의 말을 드립니다. 어머님, 앞으로도 훌륭한 사위가 되겠습니다.

묵묵히 옆에서 늘 믿어주고 도와준 아내와 자주 놀아주지 못해 항상 미안하기만 한 수민, 수진 우리 두 공주님, 아빠가 너희들 앞에서 당당해질 수 있어 얼마나 좋은지 모른다. 사랑한다.

평생을 자식 걱정만 하시는 부모님께 늘 마음이 무거웠습니다. 이 일이 부모님께 작은 기쁨이라도 되기를 간절히 바랍니다. 아버님, 어머님, 사랑합니다. 그리고 이 논문을 두 분께 바칩니다.